MECHANISMS OF PHASE SEPARATION FOR DISPERSIONS IN CONTINUOUS FLOW

by

HUSEYIN AVNI HITIT

A thesis submitted to the University of Aston in Birmingham for the degree of Doctor of Philosophy

DEPARTMENT OF CHEMICAL ENGINEERING
THE UNIVERSITY OF ASTON IN BIRMINGHAM

September, 1972

This research is dedicated to my family and mother for their patience. In particular I thank my small sons Mehmet and Tahir whc first demonstrated to me practical film drainage and rupture with soap bubbles, the bubbles bursting as their colour faded.

ACKNOWLEDGMENTS

The author is deeply indebted, and wishes to record his sincere thanks to:

Professor G.V. Jeffreys,

for providing facilities for research in the Department of Chemical Engineering and for his constant advice and interest.

Dr. C.J. Mumford,

in the Department of Chemical Engineering for his stimulating guidance and personal interest throughout each phase of the study.

Middle East Technical University of Ankara,

for granting me leave of absence to pursue this research.

U.N.E.S.C.O.,

for granting me a Fellowship.

The British Council,

for organisation and coordination of the Fellowship.

To the Technical Staff of the Department of Chemical Engineering and of Visual Aids Department.

To Dr. I. Onur, Research Fellow in the Production Engineering, for his suggestions.

Special thanks are extended to Mrs. S.M.Mumford for her kind helps by typing numerous pages to finalize.

Finally I acknowledge my great debt to Prof.Dr.T.G.Somer who stimulated my interest in research.

C O N T E N T S

		Page
1.	INTRODUCTION .	1
2.	COALESCENCE OF A SINGLE DROP AT A PLANE INTERFACE	2
	2.1 The process of coalescence	8
	2.1.1 Coalescence time	9
	2.1.2 Coalescence stages	18
	2.1.3 Coalescence mechanisms	21
	2.2 Factors affecting coalescence	26
	2.2.1 System properties	28
	2.2.2 Drop size	32
	2.2.3 Physical conditions	36
	a. Vibrations	36
	b. Temperature	38
	c. Temperature gradients	39
	2.2.4 Mass transfer	41
	2.2.5 Surfactants	45
	2.2.6 Impurities	47
	2.3 Shape of a drop and film thickness	52
	2.4 Single drop coalescence models	58
	2.4.1 Uniform film	58
	2.4.2 Non-uniform film	66
3.	INTERDROP COALESCENCE	75
	3.1 Introduction	75
	3.2 Experimental investigations	76
	3.3 Theoretical studies	79
4.	COALESCENCE IN A SWARM OF DROPLETS	83
	4.1 Introduction	83
	4.2 Monolayers	84
	4.3 Multilayers	90
	4.4 Coalescence Models	98

/continued ....

Page

4. COALESCENCE IN A SWARM OF DROPLETS (Cont'd)

4.4 Coalescence Models (cont'd)

4.4.1 Introduction 98

4.4.2 Unsteady state, batch 98

4.4.3 Steady state, continuous 100

a. Fluidized bed model 101

b. Idealized analysis of a horizontal wedge 106

c. Differential analysis of a wedge 114

d. A differential analysis of a vertical zone 122

4.5 Discussion of the models 125

5. COALESCENCE IN PRACTICAL EQUIPMENT 127

5.1 Horizontal and Vertical Settlers 129

5.2 Agitated Systems 131

5.3 Coalescing Aids 133

6. EXPERIMENTAL INVESTIGATION 136

6.1 Introduction 136

6.2 Design of the equipment 136

6.2.1 Arrangement for counter-current operation 138

6.2.2 Equipment for operation with a stationary continuous phase, 6 and 9-inch columns 140

6.2.3 Equipment for operation with a stationary continuous phase, 3-inch column 141

6.2.4 Design of the distributor plates 142

6.2.5 Commissioning of the equipment 143

6.2.6 Cleaning of the equipment 146

/continued ...

		Page
6.	EXPERIMENTAL INVESTIGATION (Cont'd)	
6.3	Design of the Experiments and Procedures	147
6.3.1.	Selection and purification of systems	147
6.3.2.	Drop size distribution	150
6.3.3.	Photography	150
6.3.4.	Hold-up	152
6.3.5.	Drop residence times	154
6.4	Encapsulation	156
6.4.1.	Introduction	156
6.4.2.	Procedures and trials	158
6.4.3.	Radical polymerization tests	164
7.	EXPERIMENTAL RESULTS	166
7.1	Formation of a flocculation zone	168
7.2	The formation and effect of interfacial scum	172
7.3	Distribution of inlet drop sizes	174
7.4	The effect of operating parameters on flocculation zone height	177
7.4.1.	Unsaturated systems	180
7.4.2.	Stable saturated systems	188
7.4.3.	Dispersed phase flow rate	189
7.4.4.	Mean inlet drop diameter	193
7.4.5.	Column size	195
7.4.6.	System properties	199

		Page
7.	EXPERIMENTAL RESULTS (Cont'd)	
7.5	Hold-up in the flocculation zone	201
7.5.1	Horizontal hold-up profiles	202
7.5.2	Vertical hold-up profiles	203
7.6	Change of drop size in the flocculation zone	214
7.7	Droplet residence time in the flocculation zone	216
7.7.1	Single drop rest times at a plane interface	216
7.7.2	Residence time in monolayers	220
7.7.3	Residence time in multilayers	221
7.7.4	Average velocity of drops in the multilayer	223
8.	DISCUSSION OF RESULTS	225
9.	PROPOSED MODELS FOR A FLOCCULATION ZONE	231
9.1	Introduction	231
9.2	Description of the models	232
9.2.1	Channels in the zone	234
9.2.2	Jets in the zone	235
9.2.3	Overall conduit	237
9.3	Verification of overall liquid conduit model	242
9.4	Discussion	245

Page

10. A PRELIMINARY ATTEMPT TO EVALUATE THE RESIDENCE TIME DATA BY ANALOGY WITH SEDIMENTATION AND FLUIDIZATION 247

11. CONCLUSIONS 252

12. RECOMMENDATIONS FOR FURTHER WORK 255

12.1 As an extension to this study 255

12.2 Other studies 256

APPENDICES

1. Physical properties of liquid-liquid systems
2. Rotameter calibration
3. Flocculation zone heights - Tables 1-6
4. Distributor design - Table 7
5. Typical inlet drop size distributions - Table 8-11
6. Dispersed phase hold-up - Tables 12-18
7. Residence time in the flocculation zone - Tables 19-21
8. Distribution coefficient calculations
9. Variation of drop size in the zone
10. Ia place drop diameter calculations

NOMENCLATURE

REFERENCES

MECHANISMS OF PHASE SEPARATION FOR DISPERSIONS IN CONTINUOUS FLOW

Summary

The literature pertaining to droplet hydrodynamics and coalescence affecting the separation of primary liquid-liquid dispersions has been reviewed.

The behaviour of droplets forming a flocculation zone has been studied in specially constructed 3, 6 and 9 inch diameter vertical glass gravity settlers. Characteristics of flocculation zones, namely hold-up and the variation of drop sizes and residence times, have been determined and correlated with zone heights for 4 different systems.

Difficulty was encountered initially in obtaining reproducible results due to the effects of interface scum and colloidal impurities. This was attributable to system ageing accelerated by sunlight and was minimised by blacking out the transparent sections of the equipment.

Initial experiments were performed with the system toluene-water to find the minimum practical settler diameter. Significant differences, due to wall effects, were observed in columns below 6 inches in diameter and therefore work was not pursued in the 3 inch column. The effect of countercurrent phase flow on zone height was found to be insignificant, hence

subsequent work employed a stationary continuous phase.

Experimental techniques included high speed still and normal speed cine photography and the injection of dyed droplets. A novel attempt was also made to encapsulate drops in a close packed swarm.

Flocculation zones were observed to comprise 3 distinct sections i.e. an inlet section wherein droplets form a close packed arrangement, a larger mid-section where inter-drop coalescence and droplet distortion occurs, and an exit section bounded by the interface. The differences in vertical hold-up profiles between these sections was measured. Total zone height has been correlated by equations of the form,

$$H = a.V_d^{\,b} D_p^{\,c} d_{12}^{\,e}$$

Deviations occurred with drop sizes in the lower end of the range studied, i.e. 0.7 mm to 1.0 mm.

A flocculation zone model is postulated leading to a relationship between drop residence time and hold-up which is in agreement with the experimental results. Consideration is also given to conditions under which a modified fluidised bed model is applicable.

1. INTRODUCTION

Many industrial processes, including liquid-liquid extraction and direct contact heat transfer, involve the dispersion of one liquid in another, with which it is immiscible, in order to achieve efficient mass or heat transfer. The two phases may be wholly or partially immiscible and either may contain solutes. The aim in generating such dispersions is to increase the interfacial area over which transfer occurs and to produce an even distribution throughout the continuous phase.

In the alternative, extraneous dispersions are also common in chemical and petroleum processing. The separation of these, particularly where small drops i.e. a 'secondary haze' is involved, may be costly if product contamination or effluent problems are to be avoided. Examples arise in the purification of aviation fuel (1) and in the flushing out of oil storage tanks (2).

For whatever purpose a dispersion is produced, either deliberately or incidentally, the principles involved in its separation are the same. The complete cycle may therefore be summarised as (3),

1. Dispersion formation. This may result from ejection via an orifice or from mechanical agitation.
2. Hold-up and travel or droplets through a continuum.

3. Settling. This usually occurs under the action of gravity only but in some equipments centrifugal force is utilized.
4. Flocculation.
5. Coalescence, which involves a combination of drop-interface and drop-drop interaction.
6. Phase separation.

However, although this sequence adequately describes the steps in any practical separation, the boundary of any one step may not be clearly defined. For example in a gravity settler it may be impracticable to distinguish between settling and flocculation, and flocculation and coalescence since all three of these may be occurring simultaneously in certain regions.

Investigations into steps 1 to 3 in the above cycle have been more numerous (4) than those into steps 4 and 5. Therefore the mechanisms governing the dispersion of droplets, and the manner in which they normally accelerate to a calculable terminal velocity, are well established and are not considered in detail in this work. Moreover it is restricted to a consideration of so-called 'primary dispersions', involving in fact drop-sizes of at least 1mm., except where reference is necessary to the phenomena of secondary droplet generation during the coalescence process.

The first major studies of coalescence phenomena in primary dispersions commenced about 20 years ago. Early work concentrated on the coalescence of single drops at a plane interface which is relatively easier to investigate experimentally than interdrop or multidrop-interface behaviour. These single drop studies enabled the phenomena and mechanisms of coalescence to be described, albeit under idealized conditions, and resulted in correlations quantifying the effect of physical properties of the component phases. Because of the complexity of the coalescence process in swarms, or among flocculated droplets, research in this area is of more recent origin and is limited in extent. The relevant literature is reviewed in Section 4 but it is worth noting here that the lower standards of experimentation set by some early researchers inevitably led to discrepancies in the published results.

Whilst several areas of single drop-interface phenomena merit further study, and interdrop coalescence studies are in their infancy, some work has recently been reported relating to the behaviour of dispersion bands and flocculation zones (5). In common with this, the object of the present research is to provide an understanding of the mechanisms of phase separation occurring in the dispersion band, or flocculation zone, bounded by the two phase interface and extending for a distance which varies with the physical conditions under which drop motion occurs.

Clearly results are complementary to those from single drop studies in assisting the systematic design of liquid separation equipments.

Experimental work was performed with three column sections of varying sizes, viz 3, 6 and 9 inches in diameter, the construction of which are described in Section 6.2. The flocculation zones produced with four organic liquid-aqueous systems, were studied for a range of mean inlet drop sizes as described in Sections 6 and 7. The techniques used, including high speed still and cine photography and the injection of dyed drops are fully discussed in Section 6.3; a novel encapsulation technique was also developed, as described in Section 6.4.

From the results, factors affecting the formation and volumes of flocculation zones have been correlated. A mathematical model is proposed for such zones in Section 9. Furthermore although the environment within which droplet coalescence occurs is very much more complex than that in single-drop-interface studies the basic parameters are identical; a comparison has therefore been drawn between the two. Finally the application of the results of this work to the design of gravity settlers are discussed and recommendations made for further work in this field.

2. COALESCENCE OF A SINGLE DROP AT A PLANE INTERFACE

A dictionary definition of the word coalescence is to grow, unite or come together into one body (6). Its use in phase separation terminology is encompassed by this definition i.e. a coalescence process is a series of steps which bring droplets together into a single bulk dispersed phase.

As has been emphasized in the Introduction, the efficiency of phase separation is greatly affected by the rate of coalescence processes of the dispersed phase. In this respect the size of gravity settler required for a certain volumetric throughput, and product quality is determined by coalescence rates. Therefore, a rough understanding of the coalescence mechanism in primary dispersions has been sought for the purpose of improving the efficiency.

In order for coalescence to take place a drop must approach either a second drop or an interface, or phase boundary, with another liquid. Thus the coalescence process is closely related to drop hydrodynamics.

Liquid-liquid dispersions are thermodynamically unstable. The interfacial area between the phases is one factor determining the free energies of the surfaces; if the free energy is less at the end of a process than the beginning, a change can occur spontaneously by a 'natural process'

at constant temperature and pressure. Since the coalescence of droplets amongst themselves, or with an interface, results in a decrease in surface free energy per unit area, coalescence of dispersions is from thermodynamic considerations a 'natural process'. However, as in most engineering applications, the kinetics of change are of prime concern in coalescence processes.

Hence it is the rate of coalescence which must be studied in order to utilize coalescence research in practice. Therefore, the elapsed time of the droplets at the interface, or their stability, is of prime importance in studies of coalescence rate in any phase separation process.

The time interval between the arrival of a drop at the interface and its disappearance has been designated the coalescence time.[1] This coalescence time is a function of the system properties, and the drop size, but it is not constant for any system at a fixed set of experimental conditions, having an approximately Gaussian distribution. The cause of such a distribution has been attributed to the various coalescence stages which may be involved and to the drop's behaviour at the interface; being dependent on the condition of a trapped film of continuous phase and its subsequent drainage.

Coalescence time, coalescence stages and mechanisms of

coalescence have been reviewed in Section 2.1. Following this factors affecting coalescence are discussed in Section 2.2. Many investigators have attempted to devise mathematical models based on experimental findings (1, 7 - 14). Whilst over-simplification in some of the models produced several unrealistic proposals, they aided understanding of the phenomena, and facilitated the setting up of the more complicated mathematical models, summarized in Section 2.4

Since the coalescence processes in any real situation involving a swarm of droplets are of a complex nature simplifications were made initially in an attempt to gain some understanding of coalescence. Such idealization was involved in the studies of single drop coalescence at a plane interface with extremely pure binary systems. Carefully cleaned, all glass equipment was employed under closely controlled conditions. This work, which initiated research on coalescence, is discussed in this Section.

2.1 THE PROCESS OF COALESCENCE

The first reported study of coalescence phenomena was probably that of Reynolds in 1881 (15). He observed that rain drops falling on the surface of a pond rested momentarily before their disappearance.

About half a century later, preliminary attempts were made to study and analyse coalescence phenomena (16). It was noted for example that droplets in an oil-water type dispersion did not normally coalesce spontaneously at the phase boundary with the bulk dispersed phase.

The subject received growing attention during the 1950's, the main emphasis being on studies of single drop coalescence at plane interfaces. Reviews of the literature have been given by Lawson (17), Brown and Hanson (18), Tavlarides et al (4) and more recently by Jeffreys and Davies (1).

2.1.1. Coalescence time

Coalescence, or rest times have been reported in the literature for the following cases:

i. Pure binary systems (1, 7, 13, 19, 20)

ii. Binary systems to which a third stabilizing agent was added (7, 21, 22, 23, 24, 25)

iii. Ternary systems which have attained equilibrium (26, 28)

iv. In a two phase system, wherein one phase contained unequilibriated solute, that is under conditions of mass transfer (13, 26, 28)

v. When solid powders were present with binary systems (29)

Most studies included a combination of two or more of the above cases in order to facilitate comparison.

Cockbain and McRoberts were amongst the first to report quantitative measurements of single drop rest times.[22] Coalescence times of droplets of oil in water and vice versa, were determined in the presence of different types of surface active agents e.g. various soaps, cholesterol, saponin, serum albumin, and poly vinyl, alcohol. Interfacial viscosity and interfacial tension data were obtained for some of the systems.

Their findings showed that all the water soluble stabilizers examined stabilized oil drops much more effectively than water drops, whereas the reverse was true for the oil-soluble cholesterol. They concluded that the main factor determining stability was the resistance to wetting of segments of an adsorbed film formed between the drop and the interface by the discontinuous phase. These results were in agreement with a much earlier limited study by Rehbinder and Wenstrom (30) of toluene drops at the aqueous sodium oleate-toluene interface; they found that sodium oleate stabilized oil in water emulsions more than emulsions of the opposite type. Cockbain and McRoberts (22) postulation that the wettability of the formed film governed the stability of the droplets was supported by later investigators (25, 27), but failed to explain the situation in pure systems and was therefore rejected by others (7, 19, 11).

The later investigators (7, 13, 19) used all glass equipment and implied that the one used by McRoberts and Cockbain may have contaminated the system; for example they employed a rubber bung seal.

Cockbain and McRobert's (22) real contribution was in evaluating the data in terms of a drainage and rupture theory for coalescence of a single drop at the interface. Their postulation as to film wetting being the cause of rest

time distributions has not found wide acceptance. In the author's view however it could possibly explain the behaviour of even pure systems, if more delicate experimental determinations were conducted, by similarity with the studies of factors causing stability in colloid and surface chemistry. It was indeed with this in mind that surface properties were determined in their experimental studies, but Nielsen and Wall and Adams (27) suggested that both the method of measurement and the concept require improvement. Nielsen et al further commented that pending an improved experimental method of measuring the wetting of bulk liquid by the drop before coalescence, one can only speculate on the validity of this idea.

Cockbain and McRoberts reported that the coalescence time data obtained with 30 consecutive drops gave a distribution which agreed with the following correlation(2.1) for the number of drops N not coalesced after an elapsed time of t seconds,

$$\ln N = -kt + \text{constant} \qquad (2.1)$$

The various parts of the curves obtained when the results were plotted on semilogarithmic paper were attributed to various stages in the coalescence process, viz the film drainage and

film rupture periods. This analysis was followed by all of the latter investigators, all of whom agreed that drop coalescence times produced a distribution. To demonstrate this way of data evaluation a typical plot and a histogram are shown in Fig.2.1. The time corresponding to $\frac{N}{N_o} = 0.5$ i.e. the time after which half of the total number of drops studied had coalesced has been called, $t_{\frac{1}{2}}$, half life rest time. This rest time was found to give better reproducibility of results than t_m, the mean rest time obtained from the histogram of distributions. (8, 13, 29, 27).

Watanbe and Kusui (25), who also worked with a stabilized system, agreed with the type of correlation made by Cockbain and McRoberts.[22] They claimed that a good distribution of rest times was obtainable by observing 30 drops consecutively in a set of experiments.

This approach for coalescence time analysis has been extended to studies of pure systems, and to systems in which electrolytes were present, but with better designed and temperature controlled equipment. The relation given as Equation 2.1 above was then found not to be linear but to have an exponential form.[7] Elton and Picknet[11] studied coalescence in the presence of electrolytes, and suggested a correlation of the form,

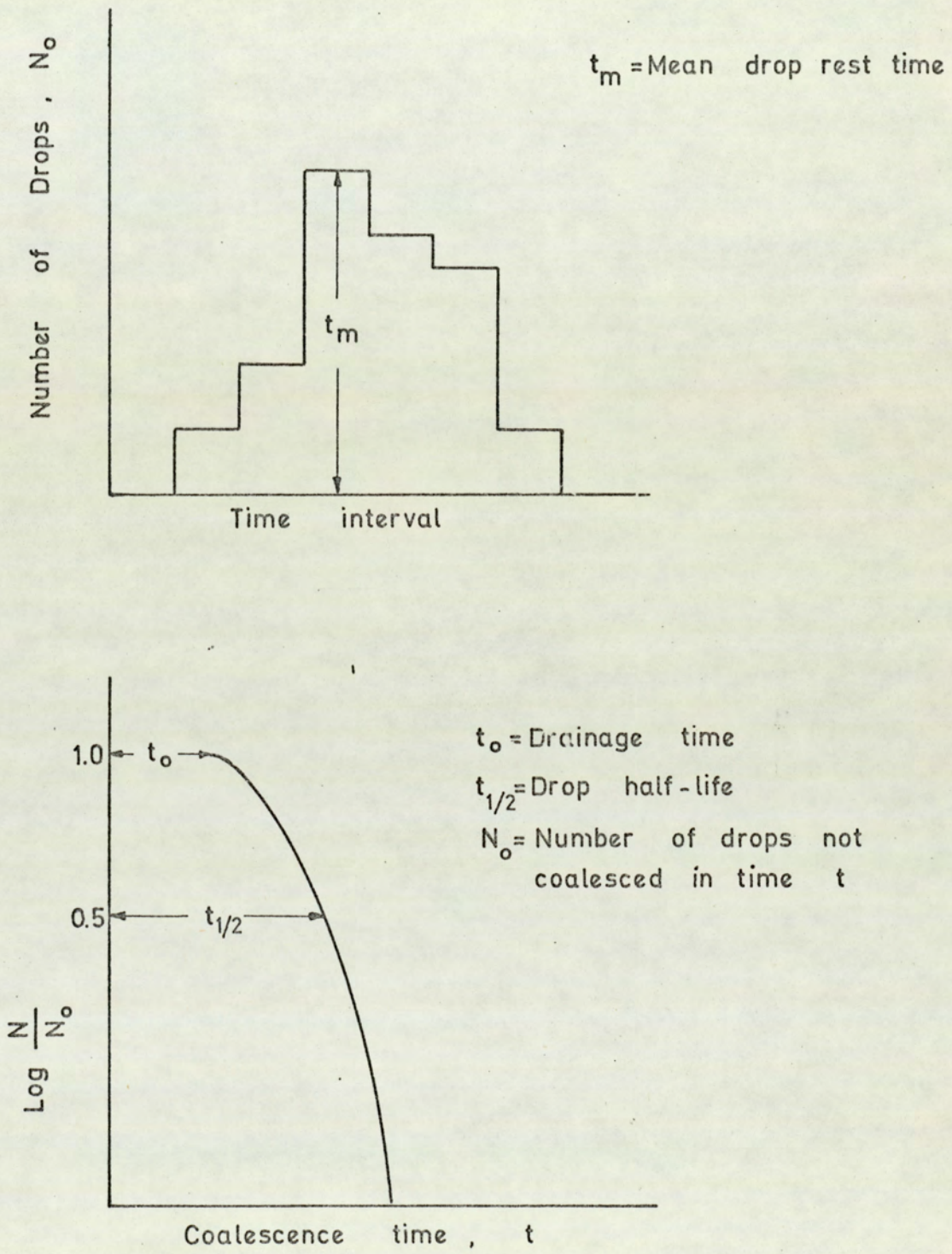

FIG. 2.1 TYPICAL REPRESENTATION OF COALESCENCE TIME DATA

References (17, 19, 22)

$$\log \frac{N}{N_o} = - ct^n \qquad (2.2)$$

where both c and n were constants. The exponent n varied with the electrolyte concentration in the system, being approximately 2 for concentrated and 3 for dilute solutions. The symbol N_o was the total number of drops assessed in the experiment and N was the number of drops not coalescing in time, t seconds.

Gillespie and Rideal[7] agreed in general with the mechanism of coalescence described by Cockbain and Mc Roberts (22) but observed that a certain time, t_o, elapsed before coalescence was possible. The following equation was proposed to correlate coalescence time,

$$\log \frac{N}{N_o} = - K (t-t_o)^{1.5} \qquad (2.3)$$

where,

$$K = f C_o A_o \left(\frac{6\sigma}{d\mu} \right)^{0.5} \qquad (2.4)$$

The product $f C_o A_o$ was independent of drop size, d, and characterized the disturbance showing the uneven drainage of the films. K was called the 'coalescence constant' which described the rate of coalescence and was related to physical properties of the system, μ, viscosity and σ, interfacial tension. The prediction of K seems difficult for practical purposes.

These investigators illustrated the proportionality

between log N/N_o and $(t - t_o)^{3/2}$ for water drops at a benzene water interface, and liquid paraffin - water interface. The variation of K with temperature was studied and in every case a linear relationship was found. Approximate values of the film thicknesses at the two stages were calculated. However, the accuracy of the data is questionable due to poor equipment design, resulting in thermal and vibrational disturbances. Gillespie and Rideal have concluded that coalescence of a drop at an oil-water interface is governed by the rate of drainage and rupture of the film between the drop and interface. Their calculated film thickness at rupture were of the order of 10^{-5} to 10^{-4} cm. Jeffreys and Hawksley (31) who employed an improved apparatus and carefully controlled conditions, found that the results for several binary systems were best correlated by equation 2.3 but the exponent of $(t - t_o)$ varied between 1 and 5 even with the same system. Correlations proposed by these and other investigators are summarized in Table 2.1.

In general it has been concluded that for the majority of cases Equation 2.3 gave the best correlation of data for two component systems whereas Equation 2.2 was better for three component systems. In contradiction to this, however, the results of Nielsen et al[27] with stabilized oil-water systems correlated with equation 2.3. Jeffreys and Lawson[26] found that Equation 2.2. with the exponent 4 and Equation 2.3 with the exponent 2 successfully correlated the results from three

TABLE 2.1

CORRELATION OF REST TIMES OR COALESCENCE TIME

Investigator and Reference		Equation	Conditions
Cockbain and McRoberts	(22)	$\log N/N_o = kt + C$	Stabilized systems; with 30 drops
Watanabe et al.	(25)	"	" " " "
Elton and Picknett	(11)	$\log N/N_o = -ct^{\beta}$	Addition of electrolytes
		where, $\beta = 2$	for low electrolyte concentration
		$\beta = 3$	high electrolyte concentration
Nielsen et al.	(27)	$t_{12} = MC^n$; $\ln \frac{N}{N_o} = k(t-t_o)^r$	With addition of stabilizers; 30 to 100 drops
		where, C = concentration of stabilizer $0.45 > n > 0.3$	
Gillespie and Rideal	(7)	$\log N/N_o = -K\,(t-t_o)^{1.5}$	pure binary systems; 100-200 drops
		where, $K = fC_oA_o\left[\frac{60}{(d\mu)}\right]^{0.5}$	

TABLE 2.1 (continued)

Investigator and reference		Equation	Conditions
Jeffreys and Hawksley	(31)	$\log N/N_o = -k(t-t_o)^r$ where, r = 1 to 5	Binary systems, 70-100 drops Overall time is measured
Jeffreys and Lawson	(26)	$\log N/N_o = ct^q$ where, $q = 4$	For binary systems, and three component systems with mass transfer
" " "		$\log N/N_o = -k(t-t_o)^r$ where r = 2	" " "
Davies, Jeffreys and Smith	(20)	$\log N/N_o = kt^n$ where $3 > n > 1$	For pure binary systems
Könnecke	(32)	$\log N/N_o = -ct^n$	
Shedulko	(33)	$\log N/N_o = 1-A^{-Bh^2}$ where, h = film thickness, A and B system characteristics	

component mass transfer studies.

Davies, Jeffreys and Smith (20) have correlated 5 different binary systems with Equation 2.2 and found that the power varied between 1 and 3.

In conclusion rest time data have been correlated with either of Equations 2.2 and 2.3 given above for two or three component systems but agreement has not been reached on the precise value of the exponent. It varied according to the system, the investigator, and the experimental conditions.

It has been established that the continuous phase film is, in fact, non-uniform with its thickest part beneath the vertical mid-axis of the drop. A mechanism was postulated to describe the experimental distributions of coalescence times suggesting that the drop may approach the interface during the drainage process with its mid-axis tilted (13) as shown in Figure 2.2.a. However, several idealized drop interface profiles have been used in the setting up mathematical models to describe the continuous phase film drainage processes shown in Figure 2.2.b, and are described in detail in Section 2.4.

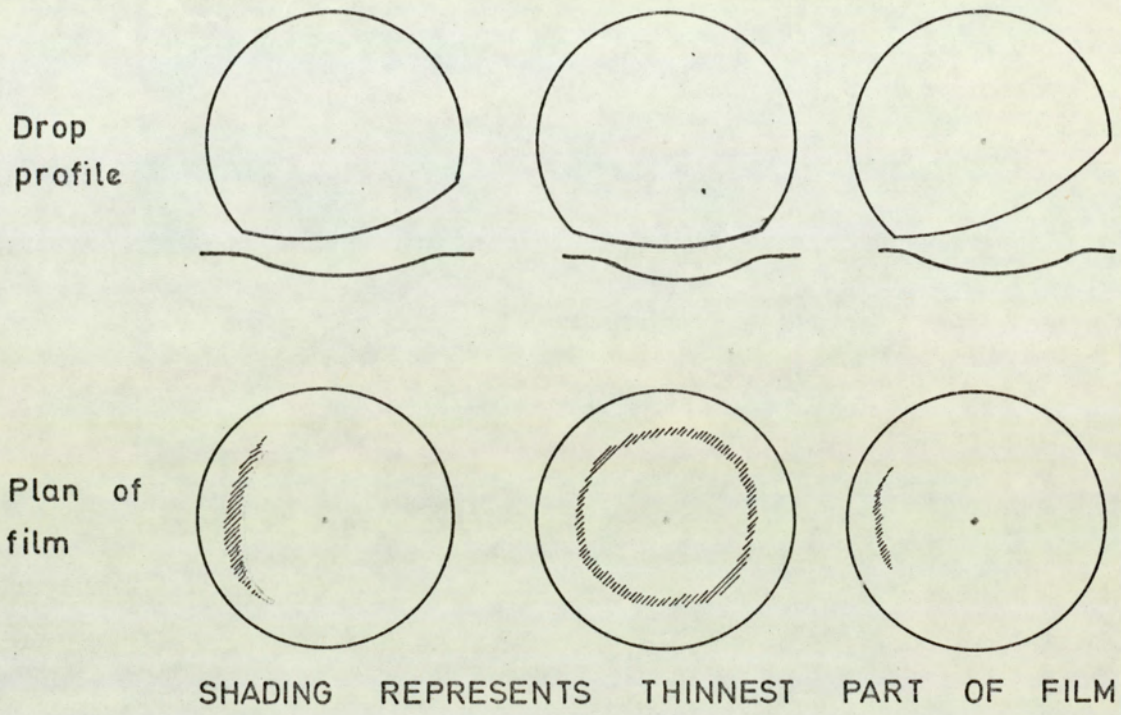

FIG.2.2.a. POSSIBLE MODEL OF DROP APPROACH (17)

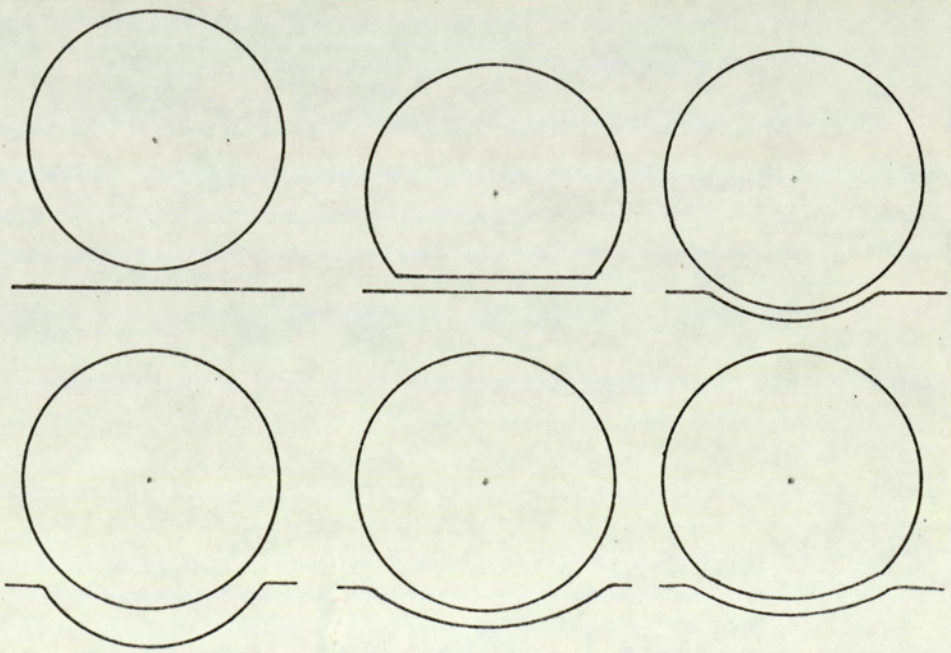

FIG.2.2.b. IDEALIZED DROP AND INTERFACE PROFILES (17)

2.1.2 The coalescence stages

The coalescence process experienced by a single drop at a plane interface, occupying a total 'coalescence time' between the drop's arrival and its complete disappearance, involves various intermediate stages. Lawson,[17] and more recently Jeffreys and Davies[1] concluded that the coalescence process takes place via five consecutive stages viz:

(i) The approach of the drop to the interface. This stage commences with the drop's arrival at the interface and terminates with the creation of deformations on the drop and interface. This time is not measurable by means of a stop-watch.

(ii) Damping of the oscillations of the drop. This commences after deformation of the drop and interface, and ends when oscillations cease. The time interval is also very small, even the sum of the times for this and the previous stage (i) which is called the 'pre-drainage time' is immeasurable by means of a stop-watch.

(iii) The formation of a continuous phase film between the drop and its bulk phase. The stage commences after oscillations have been damped out and continues during film thinning by a drainage process until a

rupture occurs. The duration of this stage is called the 'drainage time' and the sum of all three stages, i, ii and iii, is termed 'rest time'.

(iv) Removal of the continuous phase film. This starts when a rupture occurs in the continuous phase film, continues with the expansion of the hole size and ends when the film has been completely removed. This is termed the 'film removal time'.

(v) Deposition of the drop contents. This covers the time period during which drop contents are transferred. It is called the deposition time and is of the order of only 0.05 second. (1)

From this classification of the stages it is evident that it is impossible to measure the time of each stage by means of a stop-watch.

Commencement of the first stage, by impact of the drop at the interface, is sharply defined and it is possible in practice to measure the time between this and the end of the coalescence process, i.e. the end of stage (v), using a stop-watch. This requires a sufficient coalescence time however to absorb the response of the stop-watch measurement technique which is around $\pm$ 0.1 second.(19) The fifth stage itself or coalescence process proper, which starts with the rupture of

the continuous phase film and lasts for the period of transference of the drop contents, can only be detected and measured by high speed photographs synchronized with a timing device.[8] It has been found to occupy about 0.04 - 0.08 seconds for water droplets of about 0.3 to 0.4 cm. diameter in benzene (8, 19)
The time required for damping out of the oscillations of the drop, which has been defined 'predrainage time' is also reported to occupy a relatively short period viz, 0.1 seconds. (1) .

As implied in stages (iii) and (iv), a film of continuous phase is present at any instant between the time of oscillations ceasing and a rupture hole being initiated, and drainage of this continuous phase continues during this period. This is defined as the actual film drainage time. Since in all the research the coalescence time has been measured using a stop-watch, it is not possible to differentiate between the first two stages and the final stage. The duration of these stages is for many systems within the accuracy of the stop-watch determination.[19] Nevertheless, it has been indicated in some investigations that measurements were made after the oscillations had ceased. Therefore, the reported coalescence times are actually the rest times as defined above.

2.1.3 Coalescence Mechanisms

a. General

The approach of a drop to a plane interface, viz the stages reviewed in Section 2.1.2, followed by the drop resting there for a period of time before combining with the bulk dispersed phase is the generally accepted mechanism for drop-interface coalescence. Disregarding the differences between the quantitative results obtained by the various investigators, the actual process of film drainage and rupture may be summarised as follows:

i. Drop coalescence necessitates the drainage of a continuous phase film trapped between the surfaces of the drop and bulk dispersed phase and subsequent rupture of this film.

ii. Drainage and rupture of the film is governed by the physical properties of the system, drop size and physical conditions as well as by the nature and concentration of any other substances present in either phase.

iii. Non-uniform thickness of the continuous phase film, which is thinnest at the outer edges, and the fact that it may acquire a tilt during film drainage, are factors affecting both drainage and rupture.

It has been observed that some primary drops, after following the above cycle, do not coalesce completely with the interface but leave behind one or more small 'daughter' droplets. These smaller drops then follow a similar coalescence mechanism and may themselves leave behind even smaller daughter drops. In this 'step-wise' coalescence process successively smaller drops are produced until the original primary drop disappears completely. This process was described by Charles and Mason (34) and termed 'partial coalescence'. Subsequently partial coalescence has been observed by other investigators up to 7-8 steps.(19, 22, 26, 31)

To distinguish between the two different types of coalescence, the mode of coalescence in which a primary drop coalesces completely within the first step at the interface is called 'first coalescence' (1). If coalescence of the primary drop involves more than one step, leaving behind smaller drops as described in the previous paragraph the mode is termed 'partial' or 'step-wise coalescence' (34). Although in partial coalescence each subsequent step has been found to follow the same basic coalescence mechanism the total rest time is clearly dependent on the mode involved. Therefore in reporting rest time data it is always necessary to specify the conditions under which they have been determined.

b. Stepwise coalescence

Wark and Cox (35) observed the stepwise coalescence of droplets during flotation experiments. Cockbain and McRoberts (22) and Linton and Sutherland (36) also reported occasional observations of the phenomena. The first extensive study of the process was by Charles and Mason who recorded the phenomena using high speed cine photography and proposed the mechanism for it (34). Their systematic study with various systems, covered a number of drop to continuous phase viscosity ratios, p, and resulted in different secondary to primary drop ratios. No secondary drops were formed in the range of $p < 0.02$ and $p > 11$. The secondary to primary drop ratio varied in the range $0.02 < p < 11$ and reached a maximum at a value of $p \simeq 1$.

These limits were confirmed by Jeffreys and Hawksley (31) later, who also reported that the introduction of temperature changes into a system exhibiting single stage coalescence could result in a change to the stepwise mode.

The mechanism of stepwise coalescence has been described as follows.(34) After rupture of the continuous phase film, the drop is deflated by an excess internal pressure until a cylindrical column of the drop liquid is formed, having a height equivalent to the original drop diameter. The radius

of this column, at the end highest from the bulk dispersed phase, starts to decrease until its circumference becomes less than its height. A Rayleigh disturbance, which concentrates at the base of the column, then grows and the column starts 'necking down'. Deflation of the drop contents and the necking down process continue simultaneously. Thus competition between these two processes governs whether or not the coalescence will be stepwise and the size of any secondary drops formed. This is illustrated in Figure 2.3.

Wark and Cox,[35] who were the original reporters of this phenomenon, and Jeffreys and Hawskley[31] and Lawson,[19] from high speed photographic observations, described an upward reaction force that propelled the drop contents away from the interface. It was observed that daughter drops were pushed away a distance of about 0.3 cm from the interface. Moreover, it was demonstrated that following coalescence of a colourless drop with a coloured bulk dispersed phase, the daughter drop contained dye at the end of the process confirming that dispersed bulk phase transport occurs towards the drop. A certain degree of mixing is then possible. This has been verified further by collection of daughter drops with a hypodermic needle and analysis of the contents.[19] Later this mixing effect was measured by Brown and Hanson.[37] Thus the mechanism proposed by Charles and Mason[34] has only partly been accepted by the other

investigators(13,19).

That the drop contents are deposited into the bulk phase in the form of a vortex which is stable for several centimeters has been confirmed by Watanabe and Kusui (25) using coloured drops. This vortex which is illustrated in Figure 2.4 was more sharply defined with smaller primary drop sizes.

Occasionally the formation of twin daughter droplets has been observed (19, 31, 34). This has been explained by the formation of two simultaneous Rayleigh disturbances (34) and by the presence of temperature gradients (19, 31).

The addition of high concentrations of surfactants, or the presence of an electrostatic field was found to favor first coalescence (34).

Jackson (38) has commented upon the importance of eliminating secondary droplets in industrial settlers. Clearly small droplets have lower settling velocities and in the absence of coalescing aids are prone to carry over by entrainment in the bulk continuous phase. Thus an understanding of the factors leading to stepwise coalescence is of practical importance. Recently Jeffreys et al (39) have reported results from a 2½inch laboratory spray column in which stepwise coalescence occured and these are discussed in Section 4.

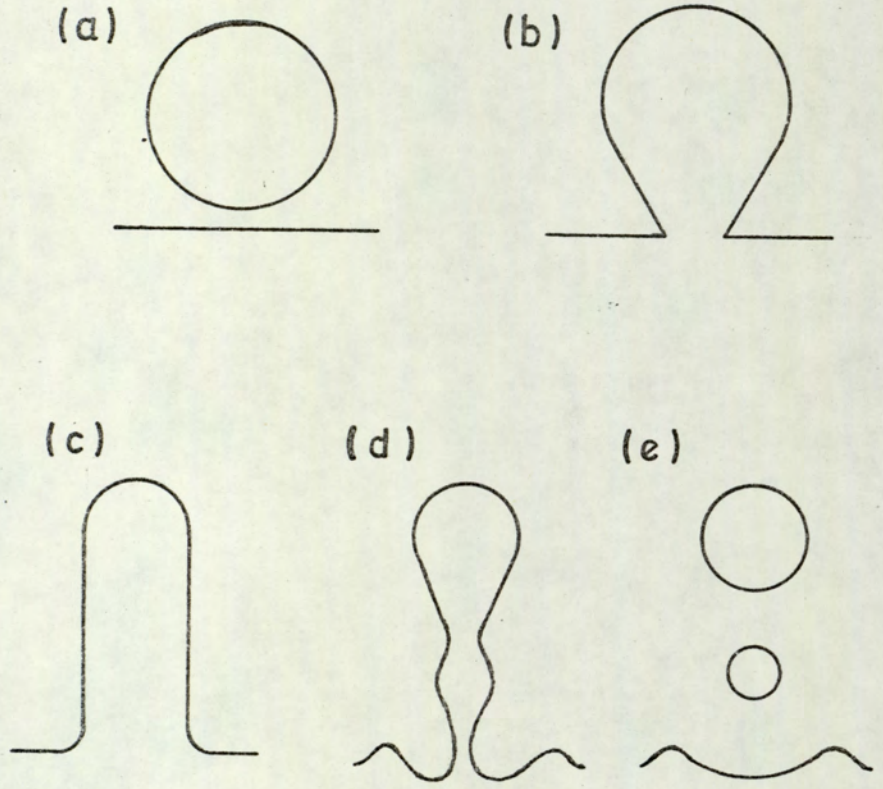

FIG. 2. 3. SIMULTANEOUS FORMATION OF TWO SECONDARY DROPS DURING PARTIAL COALESCENCE (Schematic) (34)

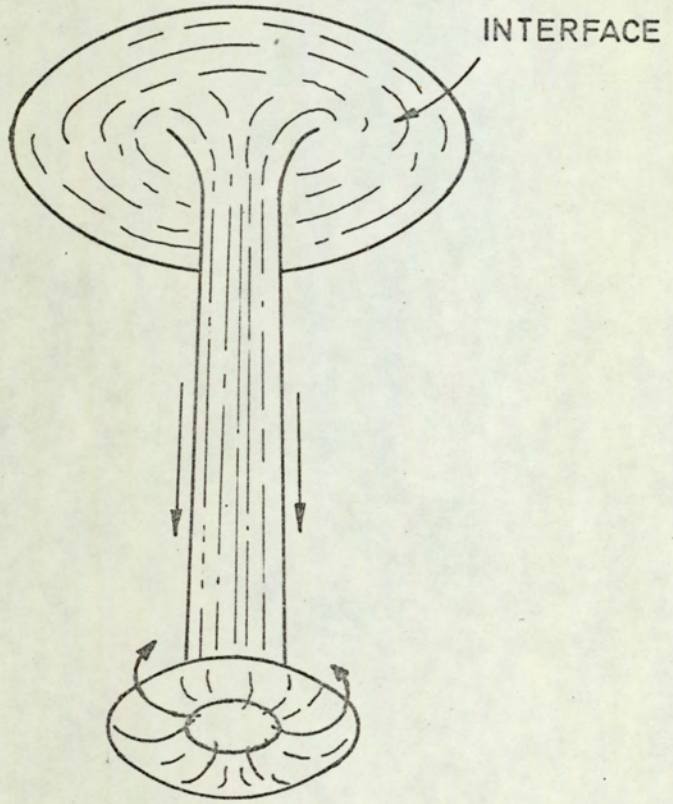

FIG. 2. 4 VORTEX RING FORMED DURING THE PARTIAL COALESCENCE OF A COLOURED DROP VIEWED FROM BELOW (19,25)

2.2 Factors affecting coalescence

It is clear from the literature, that many factors affect the coalescence of a single drop. A review by Lawson (17) included a list of these parameters and their general effect on coalescence time; subsequently Jeffreys and Davies (1) have also discussed the many factors. Current knowledge regarding the effect of most factors is summarized in the following subsections, but firstly mention must be made of curvature of the interface, distance of drop fall and electrical effects.

With regard to curvature of the interface, two investigations have shown that stability of the drop is increased when the curvature is concave to the drop (1). This result is to be expected from a consideration of the geometry and continuous phase drainage.

The effect of distance of drop fall on coalescence time is included in the general correlations shown in Table 2.2, Section 2.2.1. These investigators found that the stability of a drop increased proportional to L, the distance of fall. This may be expressed as,

$$t \propto L^n \qquad (2.5)$$

where n is a constant dependent upon drop size (19),

or

$$n = 11 \times 10^{-5} \left(\frac{\sigma^2}{\rho_c^{0.5}} \right)^{0.91}$$

In contradiction to these results, Nielsen et al (27) reported that coalescence time was independent of the distance travelled by a drop before coming to rest at the interface.

Jeffreys and Davies (1) explained this contradiction in terms of the dimensions of the apparatus. Further it is possible that reflection of disturbances off the walls of the retaining cup caused variations in the mean coalescence times.

Electrical effects cannot be adequately described in a subsection because of the extensive literature on the subject. The effects are of some practical importance in the field of coalescing aids - Section 5.4. Application of electrical fields promotes coalescence since an applied force several hundred times that of gravity can be produced by an applied d.c. electric field (8). The efficiencies of electrostatic coalescers is dependent on this fact. The investigations of Mason and his coworkers (8, 40), Brown and Hanson (37) may be cited as an introduction to this area of study.

2.2.1 System properties

The rate of film drainage, which has been established as being of prime importance, will also be affected by the system properties. Thus to determine the effect of each individual property of each of the two phases would require a number of investigations based upon factorial design of experimentation.

Such a study was conducted by Jeffreys and Hawksley and resulted in a correlation (13). Lawson (19) has also correlated the effect of system properties using dimensional analysis; a similar approach has been followed by Smith (41). All these general correlations are reproduced in Table 2.2 for ease of comparison.

Studies in terms of the effect of combined properties, instead of an individual property of each phase, e.g. combinations of density difference, viscosity ratio and interfacial tension have been found to be more convenient and to facilitate explanation of the phenomena involved, since the rate of film drainage and film thickness are controlled by the physical properties.

An empirical expression, relating the film drainage area to the drop volume, V_d, and physical properties has been

TABLE 2.2

EQUATIONS FOR THE CORRELATION OF COALESCENCE TIME OF A SINGLE DROP AT A PLANE INTERFACE WITH SYSTEM PROPERTIES

Symbols are given in the nomenclature

Investigators and Reference		Equation
Jeffreys and Hawskley	(13)	$t_{12} = 4.53 \times 10^5 \cdot \frac{\mu_c^{0.5}\ \Delta\rho^{1.2}}{\sigma^{1.2}} \cdot \left(\frac{T}{25}\right)^x \cdot d^y \cdot L^z$ where, $x = 0.71\ \mu_c^{0.5}$; $y = 0.02 \left(\frac{\sigma^2}{\mu_c^{0.5}}\right)$; $z = 11 \times 10^{-5}\left(\frac{\sigma^2}{\mu_c^{0.5}}\right)^{0.9}$
Lawson	(19)	$\frac{\sigma t}{\mu_c} = 1.32 \times 10^5 \cdot \left(\frac{L}{d}\right)^{0.18} \left(\frac{d^2 g\ \Delta\rho}{\sigma}\right)^{0.32}$
Smith	(41)	$\frac{\sigma t}{\mu_c^d} \propto \left(\frac{d^2 g\ \Delta\rho}{\sigma}\right)^{0.25}$

given by Hartland (42),

$$A = k\,(v_d)^{\frac{2}{3}(n+1)} \left(\frac{g\,\Delta\rho}{\sigma}\right)^{n} \qquad (2.6)$$

where, for a deformable interface;

$k = 0.5$

$n = 0.6$

and for a rigid plane interface;

$k = 0.25$

$n = 0.75$

This demonstrates the opposing effects of density difference and interfacial tension on the film drainage area and thus on the drainage rate. Moreover, the film thinning rate is proportional to the force exerted by the approaching drop at the interface which obviously depends on the density difference of the system material. Reynolds' equation, describing the drainage between two parallel discs, in differential form states (12),

$$-\frac{dh}{dt} = \frac{2\pi F}{3\mu_c A^2}\, h^3, \qquad (2.7)$$

where h = distance between the discs;

t = time;

μ_c = viscosity of the draining fluid;

F = Force pressing one disc to the other;

A = Area of the discs.

Variation in uniform film thickness with time beneath a liquid

drop is given by (8, 42),

$$t \propto \frac{\mu_c A^2}{F} \qquad (2.8)$$

Thus both force and film area which are dependent on the density difference will affect the coalescence time. However, the balance of these two opposing effects seems to fall on the area, since experimental analysis has shown that rest times increase with phase density difference(13, 19).

Examination of the correlated equations in Table 2.2 shows that the influence of density difference on the rest time varies as the 1.2, 0.32 and 0.25 power in the three equations (13), (19), and (41) respectively. With regard to the effect of interfacial tension the deviation between the three equations is less significant.

A high value of interfacial tension results in a very small deformation of the drop at the interface. Thus rapid coalescence occurs since the force causing drainage acts on a small area, and thus the effective pressure is increased. However, Lang and Wilke (21) have shown that an increase in interfacial tension also increases the strength of the film so that rupture is resisted. Again this physical property produces two opposing effects (1).

2.2.2 Drop size

The effect of drop size on coalescence time has been the subject of numerous investigations the results of which are summarized in Table 2.3.

A variety of experimental conditions and systems were studied. Some measurements were incidental to studies of the effect of a solute, or the addition of stabilizers and electrolytes, to mutually saturated binary or ternary systems. Further, studies of partial coalescence yielded smaller size daughter droplets from the original one and thus facilitated observation of the behaviour of different size droplets at the interface. Quantitative results and correlations have been reported from these studies (18, 13, 19). Comparison of the various researches is rendered difficult by the differences between the experimental conditions and because attempts have not always been made to correlate the results. From the majority of the qualitative results and the correlations listed in Table 2.3, it is concluded that any increase in drop diameter results in an increase in coalescence time. Exceptions to this have been encountered in stepwise coalescence processes however in that smaller size daughter droplets have been observed to have a larger life at the interface than the original large drop (8, 13, 26). When a stabilizing, or a third, component has been added the effect of variation in the

drop size was reduced.

The correlations for pure binary and stabilized systems yielded the following proportionality between the rest time and drop diameter, d,

$$t_{12} \propto d^{n} \qquad (2.9)$$

Where n varied with the conditions.

For pure binary systems, n was generally higher than for stabilized systems under the same experimental conditions in any individual investigation. On the other hand as is clear from Table 2.3, neither the magnitude of n, nor the difference between pure and stabilized systems, were in agreement among various investigators. Further, work using essentially the same equipment and procedure, with slight modifications, gave an entirely different correlation.

In summary the dependency of rest time on drop diameter has been variously reported in general as being directly proportional raised to a power. Some investigators claim that their results were obtained without any contamination present, but others probably had some degree of contamination. Certainly some sort of contamination would appear to be the most probable cause of error in measuring rest times. It is logical to conclude that contamination, superceded the effect of drop size in certain work so that contradictory results have been reported (19).

TABLE 2.3

EFFECT OF DROP SIZE ON COALESCENCE TIME

Investigator and Reference	The power on correlated drop diameter n	Condition and remarks
Charles and Mason (8)	3.15	Binary systems. Benzene, CCl_4, heptane; each with water
Lawson (19)	1.54	Binary system. Benzene-water.
Smith (59)	1.50	
Jeffreys and Hawksley (13)	1.02	Two-component. Two-phase systems, first step
Jeffreys and Hawksley (13)	0.96	Overall times
Linton and Sutherland (36)	0.78	
Komasova and Otake (58)	0.70	Benzene-water
Komasova and Otake (58)	0	Benzene-water stabilized
Lang and Wilke (21)	Inconsistent	Numerous systems
Jeffreys, Davies and Smith (20)	-1.28	Binary systems
(22), (11),	Small drops more stable with stabilized systems	

Referring now to the leading work in the literature, Cockbain and McRoberts (22) have studied stabilized benzene-water systems and found an approximately constant coalescence time for the drop sizes in the range 0.2 to 0.92 cm diameter. Jeffreys and Hawksley (13) and Lawson (19) found a definite dependence on drop size as $d^{1.02}$ and $d^{1.54}$ for pure binary systems respectively. Charles and Mason (8) empirically correlated coalescence time as proportional to $d^{3.15}$ compared with a theoretical approach which yielded d^3 as shown in Section 2.4.

Lang's studies (44,45) indicated that coalescence time was independent of drop size. His recent work (21) illustrated no consistent variation with the drop-size; it varied from system to system i.e. for certain systems there was an increase in rest time, and with others a decrease, as the drop size was increased.

The dependency on drop size has been explained with reference to the drainage and rupture of the film formed between the drop and interface (8, 13, 19, 46, 47). Conversely a theoretical explanation of the lack of dependency on drop size has been given by Lang and Wilke (21) with reference to their own coalescence model.

2.2.3 Physical Conditions

a. Vibrations

Cockbain and McRoberts (22) and Lawson (19) observed the coalescence of groups of drops at an interface and reported that relatively large disturbances, propogated by the coalescence of one of the drops, did not tend to induce coalescence in the others. On the contrary extra stability was conferred on the surviving drops. Nielsen et al (27) observed that room vibrations and mild agitation had only a slight effect on the rate of coalescence. However, in his generalized conclusions it has been stated that any factor which disturbs the interface on a molecular scale decreases the stability of drops. Lang and Wilke (21) found that subsonic disturbances promoted coalescence, induced sonic disturbances had no great effect, and disturbances of an ultra-sonic nature stabilized the drops. These findings contradicted his own postulation regarding the effects resulting in random variations in the coalescence time. Lang and Wilke (21), stated that in every significant case, the sonic disturbance decreased the rest time of the drops. They mentioned that it is also possible for a sonic disturbance up and down thus increasing the film thickness.

On the basis of experimentation using high energy A.C. fields of varying frequencies, Brown and Hanson (37) concluded

that coalescence time was virtually independent of the frequency of vibration.

Workers in nearly all the drop-interface coalescence studies recognised disturbances and considered that distribution of rest times might result from vibrational effects. Hence, without performing a systematic study, they considered the best course was to attempt to eliminate vibrations in their experimentations. Nevertheless, Jeffreys and Hawksley (13) state that in spite of great care taken to exclude vibrations from their apparatus a distribution of coalescence times persisted. Lang and Wilke (21) made the most extensive experimental study of vibrational effects. Besides studying the various types of vibration induced in a drop at the interface, they also investigated natural sonic disturbances. Unfortunately their results were inconclusive and there is a need for more detailed study. Davies et al (20), Topliss (76) have studied the effect of disturbances at the interface created by the arrival/coalescence of neighbouring drops; this will be discussed in Section 4.2.

In conclusion, for a single drop at an interface, whilst contradictory results have been reported regarding vibrational effects on coalescence, the general view is that such disturbances tend to stabilize the droplet at the interface resulting in longer rest times because of repeated renewal of the continuous phase film.

b. Temperature

Physical properties are temperature dependent so that the effect of temperature variation upon the coalescence process can be inferred from the controlling properties, viz interfacial tension, density and viscosity, of the system materials as correlated (13, 19, 41) in the Equations given in Section 2.1.1 Table 2.2.

Decrease of continuous phase viscosity with temperature would be expected to accelerate film drainage resulting in lower rest times for the drop. In fact mean rest times showed a decrease with an increase of temperature in all of the investigators results (22, 7, 13, 25).

Charles and Mason (8) found the effect of temperature on film thickness to be variable with carbon-tetrachloride and water drops in water-carbontetrachloride and benzene water systems respectively. These researchers checked the validity of the Equation shown below, proposed by Sheludko (33),

$$f = A\, e^{-Bh^2} \qquad (2.10)$$

where,

A and B are constants, characteristic of the system,

f is fraction of coalescence occurring above a film thickness h.

This Equation is claimed to show statistical temperature

fluctuations but Charles and Mason's (8) results were in poor agreement with it. However, their results do not necessarily invalidate Sheludko's Equation.

Jeffreys and Hawksley (13) correlated rest time with temperature of the medium and found,

$$t_{12} \propto \left(\frac{T}{25}\right)^{-0.7} \mu_d^{0.5} \qquad (2.11)$$

The overall coalescence time, however, as distinct from first step time, may on occasions show an increase with temperature because of a transition from single step to stepwise coalescence.

c. Temperature gradients

Gillespie and Rideal (7) observed the striking effect of temperature gradients upon the coalescence time by inserting their equipment, which was already provided with water-jacket temperature control, into an air-bath. They found that a difference of 300 per cent existed between coalescence times with and without an air-bath; the stability of the droplets being increased in the air-bath. They concluded that this profound effect was created by disturbances. To explain this phenomena Gillespie and Rideal (7) utilized the approach of Hershley (49) who showed that very small temperature differences may considerably distort a thin film of liquid. Moreover, the effect is larger the thinner the film and the

larger $\frac{d\sigma}{dT}$, i.e. the change of interfacial tension with temperature. They showed that there was far more scatter of experimental results if an air-bath was not used in investigations conducted between $0^{o}C$ to $80^{o}C$ for benzene-water and paraffin-water systems. Nielsen, Wall and Adams (27) explained the temperature dependence in terms of ΔH^{*}, the energy of activation of the coalescence process using the relationship,

$$\frac{d \ln k}{dt} = \frac{\Delta H^{*}}{RT^{2}} \qquad (2.12)$$

where

$\log k = 0.279 - 1.013 \log (t_{12} - t_{min})$

k is the coalescence constant,

t_{12} is the drop half life,

t_{min} is the minimum life of drop.

The value of k was obtained by a statistical analysis of numerous drops for many systems. However, the effect was reported to have been small with the stabilized systems used and polyvinyl alcohol stabilized drops were not affected at all.

Both Jeffreys and Hawksley (13), and Lawson (19) demonstrated that the presence of temperature gradients caused the formation of twin-secondary drops.

2.2.4 Mass transfer

A number of investigations have been carried out to determine the effect of mass transfer on the rest times of single drops at a plane interface (13,26,28). Their results are generally in accordance with the earlier explanation of Groothuis and Zuiderweg (50) i.e. that the coalescence time may either increase or decrease dependent upon the direction of solute transfer. Coalescence is promoted if mass transfer occurs from the drop to the continuous phase but is inhibited when transfer is in the reverse direction. This is due to Marangoni effects, viz gradients of interfacial tension resulting from concentration gradients along the surface in the region between the approaching drops. This explanation of the significance of the direction of solute transfer proved useful in interpreting earlier findings in industrial mass transfer equipment. For example drop sizes in spray extraction towers were considerably larger when diffusion occurred from the drops. Similarly, flooding rates and drop sizes were higher in rotating disc columns with solute transfer into the continuous phase (52). Smith et al. (53) confirmed the hypothesis of Groothius and Zuiderweg, using a model spray column, and extended it to the case of mass transfer between unsaturated binary systems.

Jeffreys and Lawson (26) studied a ternary system of benzene-water-acetone. A selection of their results are summarized in Table 2.4. These illustrate that the coalescence times of water droplets changed with the direction of acetone diffusion in accordance with the theory of Groothius and Zuiderweg (*50*), viz acetone diffusion from the drop accelerated coalescence and vice versa. The magnitude of this effect is also illustrated in Table 2.4 using the findings of Sawistowski (51) with a water-diethyl carbonate system in which propionic acid was used as solute. No quantitative treatment of the solute concentration effect has yet been reported. Jeffreys and Lawson's results (26) showed that coalescence times were almost independent of the concentration of solute, only the primary coalescence step being affected for transfer from drops. This however is quite different in the case of transfer to the drop. A progressive increase in stability was reported when rates of mass transfer increased into the drop.

McCoy and Mason (28), who measured thickness of the film trapped between the drop and interface and its thinning rate by an interferometric method, were able to confirm that mass transfer changed the rate of film thinning but not the film thickness at rupture.

Heertjes and de Nie (54) have recently reported some

experimental results on coalescence with mass transfer for a binary and for a ternary system, viz isobutanol drops in a continuous phase and acetone diffusing from water into benzene drops respectively. They concluded that the dependence of the rate of coalescence of drops on mass transfer in binary systems cannot be explained entirely by interfacial phenomena. For the ternary system their findings did not permit a final quantitative conclusion. Brown and Hanson (18) accept in part the explanation of mass transfer effects on coalescence of drops at the interface being due to Marangoni effects alone. They believe however that additional factors may be involved, such as the release of heat of solution and changes in the viscosity of the film.

A theoretical treatment of the Marangoni effect, has been provided by Sternling and Scriven (55). Their analysis showed how it is possible for some systems to be unstable with solute transfer in one direction yet stable with transfer in the opposite direction, and for other systems to be unstable with either direction of transfer.

In conclusion, the effect of mass transfer on coalescence requires further work, to explain the phenomena more clearly, and in particular to apply it to practical situations.

TABLE 2.4

EFFECT OF MASS TRANSFER ON COALESCENCE AT A PLANE INTERFACE.

Dispersed phase	Continuous phase	Average rest time sec
Sawistowski (51)		
Diethyl carbonate	water	16
0.5 N propionic acid in diethyl carbonate	water	0.2
Diethyl carbonate	1.5 N propionic acid in water	66
Water	diethyl carbonate	4.8
0.5 N acetic acid in water	diethyl carbonate	1.0
0.5 N propionic acid in water	diethyl carbonate	0.5
Jeffreys and Lawson (26)		
Benzene	water	7.10
Benzene + 0.5% Acetone	water	1.67
Benzene + 1.0% Acetone	water	1.22
Benzene + 2.0% Acetone	water	0.76
Benzene + 3.0% Acetone	water	0.46
Benzene + 5.0% Acetone	water	Instantaneous
Benzene	Water + 1% acetone	11.2
Benzene	Water + 2% acetone	13.2

2.2.5 Surfactants

It is well established that surface active materials retard the coalescence of a drop at a plane interface. No contradictory results have been encountered in the literature.

Investigations of coalescence times cited in Section 2.1 are all in agreement with this result. A quantitative correlation, however, has been proposed only by Nielsen et al (27) with the following relation,

$$t_m \propto C^n \qquad (2.13)$$

where t_m = mean coalescence time;

C = surfactant concentration;

n = a constant variable between 0.45 and 0.3.

Gillespie and Rideal (7), postulated that the surface concentration and hence interfacial tension, vary so that film drainage is inhibited. As the film area is increased, tangential stresses are taken up by the interfacial tension resulting in a deceleration of the drainage rate. Cockbain and McRoberts (22) explained this stabilization in terms of the changed wetting properties of the surface segments.

Surface active agents increase the interfacial viscosity

and lower the interfacial tension. This reduces the drainage of the film. Hartland's (56) explanation of this was that, as the surface active molecules collect on the bulk interface but not on the drop interface the film has one immobile and one mobile boundary; the drop therefore sinks into the bulk interface more than with pure binary systems thus retarding the drainage process.

2.2.6 Effect of impurities

The effect of addition of a third component or solute on coalescence times in binary systems has been reviewed in Sections 2.2.5 and 2.2.4 respectively. Addition of more than one compound to a binary system would greatly increase the number of experimental variables and hence make the study more complex. No such study, involving numerous additive compounds in one particular set of experiments with pure systems, has been encountered in the literature. However this is a practical problem; for example, in oil-water separation the change in coalescence behaviour of dispersions accompanying minor changes in the small amounts of salts makes it difficult to properly meter in flocculating agents.

In general the actual impurities have been considered not to have any significant effect, or were not studied at all. It is clear from this survey of the literature that this point is of considerable importance and merits further studies, although these will prove difficult in practice.

The term impurities is taken to mean any group of compounds, either homogeneous or heterogeneous, present in either or both phases in varying and unpredictable amounts. They may, or may not, be uniformly distributed and may comprise small pieces of grease, dust, etc. Within this concept are

materials, present in minute amounts after even the best practical purification process, so that the effect of impurities is a problem for which a systematic correlation is practically impossible. However, many investigators have observed the effect of a large range of impurities in a qualitative manner and reported surprising results from their presence. For example, all the researchers without exception, found it necessary to clean the interface, otherwise, reproducible results were unobtainable and the coalescence time varied widely in an unpredictable way. Therefore, a common objective was to remove all the impurities, and their potential sources, as far as possible.

On the basis of reports in the literature, and observations made in the present work, it is considered that impurities have a far more significant effect on coalescence time than any of the factors discussed previously. (Tests and conclusions from experimentation are given later in Section 7).

Without an understanding of the effect of impurities, coalescence research cannot be meaningful and extrapolation of the data to commercial coalescence processes must be difficult without quantitative results with impurities. Without this, empirical scale-up procedures cannot be replaced

as envisaged by all researchers in this field and the coalescence investigations will have only an academic value. Therefore all the possible sources of impurities, their probable causes, and observed effects which have been reported in the literature are summarised below.

The relationship of coalescence phenomena to the effects of impurities were first noted when Wark and Cox (35) reported on the phenomena of water droplets floating, and exhibiting a significant stability, on water surfaces covered with dust or grease particles. Katalinic (57) showed that even trace amounts of such a material on water surfaces reduced the stability of water droplets. The presence of dust particles at the air-liquid interface in the equipment reduced the life-time of the droplets in a coalescence study by Mahajan (16). Solid impurities have produced a similar effect to deliberate solids addition at the interface, that is to reduce the coalescence time (8, 29).

Jeffreys and Lawson (26) emphasized the necessity for cleanliness of the glass in coalescence apparatus and described a detailed and lengthy procedure for washing/drying. This consisted of washing in acetone, flushing with hot running water, and then steam scouring for about one hour; the cell assembly was then completely filled with fresh chromic acid and left for at least 24 hours. After draining the

acid, the glassware was rinsed with hot distilled water for a prolonged period after which it was dried in an oven. After washing, care was taken to prevent the inside of the apparatus from being contaminated by touch with the fingers. The above procedure has been detailed in full to illustrate the importance of eliminating minute amounts of impurities or contamination, and because it is typical of the procedures now followed in coalescence time studies. The materials used were of Analar quality and were redistilled in a Vigreux fractionating column. There is no doubt that this represents the greatest care which is feasible having regard to both time and expense. In these circumstances even touching the inside of the glass with a finger would lead to contamination of the interface and the distillation product of the Vigreous column should then be considered to contain a significant amount of impurities. Evidently the procedure described was arrived at after numerous other trials by these investigators who found that a previous procedure (22) was not adequate. Since such a great care is required it must be conceded that, in spite of redistillation, complete absence of impurities from any system cannot be guaranteed. Thus minute amounts of compounds, in the range of ten to a hundred ppm in the system materials will contaminate the interface. Furthermore, Jeffreys and Lawson (26) found that after observing 50 drops in the coalescence cell with binary systems,

concentrations of the solutions in the cell changed considerably. These changes were attributable to either carbon dioxide absorption from the air or to trace amounts of impurities. Since such small amounts of impurities were able to produce a great difference in coalescence behaviour it seems probable that at least part of the differences between the coalescence time results of two different investigators is due to impurities, despite purification by distillation.

The writer's contention is that minute amounts of impurities in a system-material may undergo a polymerization reaction at the interface yielding a colloidal product or, dependent on the nature of the impurities, a short chain polymer under the activation of sunlight. Lawson (19) has referred to Hodgson and Lee's findings that rest time was dependent on the age of the interface after cleaning. Immediately after the cleaning process, coalescence was very rapid, drops of 0.3 mm. diameter coalescing within a second, whereas after several minutes, stability of over 2 minutes was observed when using sodium benzoate as a contaminant in the toluene-water system. Similar results were reported for the system pure toluene-water. Lawson found this result strange and attributed it to the presence of Teflon in the equipment.

2.3. Shape of a drop and film thickness

As summarized in Sections 2.1 and 2.2 a continuous phase film, formed upon the approach of a drop to a phase interface commences to drain but, upon the drop's further approach, a part of this film is trapped between an area of the two surfaces, i.e drop and interface. Subsequent thinning of this trapped film, and finally its rupture and transference of the drop contents into the bulk disperse phase, constitutes the coalescence mechanism. Clearly therefore the properties of the film and its geometry are rate determining factors. Since, in the case of pure binary systems, the film consists of pure continuous phase material, its drainage, thinning and rupture are dependent on the system properties as has already been reviewed. With three phase systems, when a surface active agent was present in either drop or continuous phase, differences in drop shape were reported in comparison to pure system materials (48). On the other hand variations occur in the geometry and thickness of the continuous phase film dependent upon the shape of those portions of surface on either side of it. The shape of a drop at a plane interface and film thickness are therefore equally important factors affecting the coalescence process. Therefore the shape and thickness have been the subject of study in several researches (12,42, 43,60). Measurement of the film thickness has also

attracted many researchers (28, 43, 46, 48, 56, 63).

In this section the shape of a drop at an interface and the magnitude of the film thickness are discussed. This serves to assist understanding of the approaches to formulate the coalescence process mathematically, reviewed in Section 2.4.

(a) Shape of a drop

The shape of a drop at a plane interface was formulated and some values tabulated by Bashford and Adams (61). Later Princen (12) and Hartland (42) calculated the dimensions by means of a force balance around the free surface of the drop and bottom surface of the draining film or 'spherical cap'. These models were verified by the experimental work. Hartland (42) concluded that the film thickness varies, although the overall shape of the film is spherical, since the individual surfaces may diverge slightly from the radius of curvature. The theoretical equilibrium dimensions of a drop having the same value of the expression,

$$\frac{g \Delta\rho}{\sigma} = \left(\frac{3}{4} \frac{V_d}{\pi}\right)^{\frac{2}{3}} \qquad (2.14)$$

were compared with the experimental results and found to be in good agreement. Viscous materials, e.g. golden syrup and glycerine, were employed in this work in order to decelerate the process and so enable it to be followed accurately; pairs of liquids having nearly the same refractive index were selected

to overcome optical distortion.

The profile of a water drop resting upon a benzene-water interface has been investigated by Jeffreys and Hawksley (13) by projecting a high speed cine film onto squared paper. This provided measurements of the two principal radii of curvature of the drop at 22 points on the surface and subsequently enabled the pressure drop to be predicted. The film was found to be thinnest at the periphery and the drop profile was represented by,

$$H = h - \psi r^2 \qquad (2.15)$$

where h = the drainage film thickness

r = radius to a point in the drainage film

H = perpendicular film thickness at radius r

ψr^2 = a composite parameter dependent upon size of the drop and physical properties.

Hartland showed in a series of researches that the shape of the drop remains substantially constant throughout the drainage period during the approach of a drop to a plane (42) and also deformable interface (43). Further this has been illustrated theoretically (43, 62). The area of the draining film between a fluid drop and an interface was reported (42) as an approximate expression.

(b) Film thickness

Three main methods of film thickness measurement have been described, in the literature,

i. An interference method (28).

ii. By photographs (13,46).

iii. A capacitance method (46).

Gillespie and Rideal (7) calculated the film thickness at the start of coalescence and at rupture by using the theoretical approach given in Section 2.4. Their calculated film thickness at rupture was of the order of 10^{-4} to 10^{-5}cm.

Allan, Charles and Mason (63) used an interference technique to measure the 'barrier ring' with small nitrogen bubbles and found that it was formed at film thicknesses in the range of 0.3 to 1.2 micron. The film thickness was uniform at a film thickness of 1500°A. Ruptures generally occurred below 900°A. McCdy and Mason (28) explained the increased rate of drainage of the film below 2000°A as being due to the movement of surfaces and the existence of tangential stresses. They measured film thicknesses at rupture of less than 500°A. Hartland (46) has measured film thicknesses by photographic and capacitance methods at different times in the drainage process. Viscous liquids and large drop sizes were used. The film

thicknesses were larger than the values of Charles and Mason, being 10^{-3}cm at rupture. This was probably due to the large drop sizes investigated. The film profiles obtained by the capacitance method and enlargement of photographs confirmed that the thinnest part of the film occurs at the outer edge or around the periphery of the film. A secondary minimum was observed at the centre as was variation of film thickness with time from drop to drop. Similar observations were reported by Lawson from high speed cine-photographic studies (19). Hartland's results (46) showed that at any given time the average film thickness was always less for smaller drops of 0.1 ml. compared with 0.5 ml.; the coalescence times for smaller droplets were longer than for larger sizes. Some film profiles were observed to be asymmetrical about the centre; this was evidently caused by the tilt of the drop axis. The effect of this tilt was more noticeable with small film thicknesses.

Brown and Hanson (37) found rupture thicknesses to be of the order of 10^{-4} - 10^{-5} cm. in their coalescence studies with applied electrical fields. Finally van den Tempel (64) measured the thickness of water films separating two oil drops down to 100°A. He confirmed that thinning rate increased below 1000°A.

In summary, definite film thicknesses at which the

drainage and rupture stages start and end have not been determined conclusively. However, the nature of the drainage process occurring between the two approaching surfaces has been well illustrated. The film thickness is generally not uniform, showing minimum thickness points, nor is it necessarily symmetrical about the mid axis perpendicular to the surfaces. Tilting of a drop may lead to an uneven thickness in the profile.

2.4. Single drop coalescence models

The drainage times for the continuous phase film trapped between a drop and an interface were similar to the rest times measured in the work reviewed in the previous sections. Therefore, many investigators (7 - 14) have attempted to compare their results with theoretical models based upon drainage of this continuous phase film.

Drainage rate of the continuous phase is dependent upon the film thickness and the shape of the drop, as well as upon the physical properties of the systems and the forces involved. Therefore, studies have been made to determine actual film profiles from experimental results and to express them in mathematical relations in order to verify the models. In these theoretical studies either a constant or varying film thickness was envisaged dependent upon the shape of the two boundary surfaces of the film. For the purpose of this review, studies may be divided into two groups, viz. uniform and non-uniform film models.

a. Uniform film models

Model 1. ; Deformable drop-Rigid interface

The film trapped between the interface and a deformed drop is shown, in an idealised way, in Figure 2.5 - 1.a. During the drainage process the two surfaces resemble two

parallel discs approaching one another. Gillespie and Rideal (7), proposed that the radius of the film, r_f, could be considered identical to the 'Barrier ring', the expression for which has been derived for small air bubbles at an interface by Derjaguin and Kusakov (65). As an approximation,

$$r_f = a^2 \left(\frac{2 \Delta \rho g}{\sigma} \right)^{0.5} \qquad (2.16)$$

Using Reynolds' expression for the rate of drainage between approaching parallel flat plates, the film thickness, h, at any time, t, is given by,

$$\frac{1}{h_1} = \left(\frac{1}{h_o}^2 + \frac{4 \sigma^2 t}{\mu_c \Delta \rho g a^5} \right)^{0.5} \qquad (2.17)$$

where h_o is the thickness of the film at zero time.

a is the radius of the drop.

Hence, the drainage time of a film from a thickness h_o to the rupture thickness, h, will be,

$$t = \frac{\mu_c g a^5 \Delta \rho}{4 \sigma^2} \left(\frac{1}{h_1}^2 - \frac{1}{h_o}^2 \right) \qquad (2.18)$$

Charles and Mason (8) derived an equation for the rate of thinning of a film of generalized profile applicable to the two models illustrated in Figures 2.5 - 1.a and 2.5 - 2.a. They considered a rigid surface which was rotationally symmetrical about the z-axis approaching a flat stationary plane from above

1. a

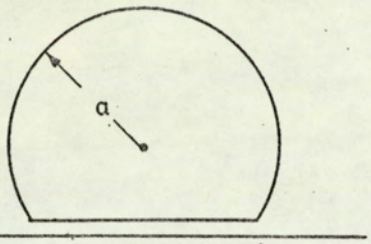

Deformable drop, R_i
Rigid interface,
Uniform film,

2.a

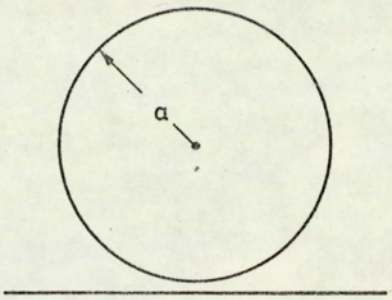

Rigid drop,
Rigid interface,
Non-uniform film,

1. b

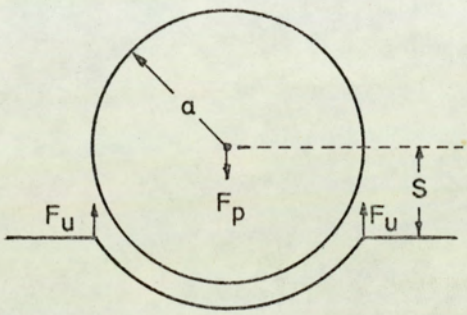

Rigid drop,
Deformable interface,
Uniform film,

2.b

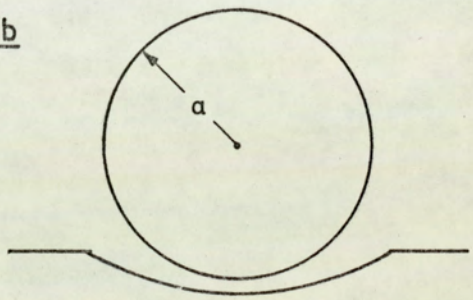

Rigid drop,
Deformable interface,
Non-uniform film,

1.c

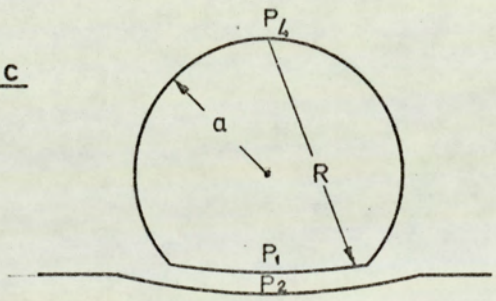

Deformable drop,
Deformable interface,
Uniform film,

2.c

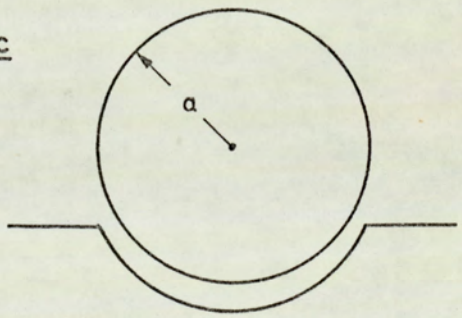

Rigid drop,
Deformable interface,
Non uniform film,

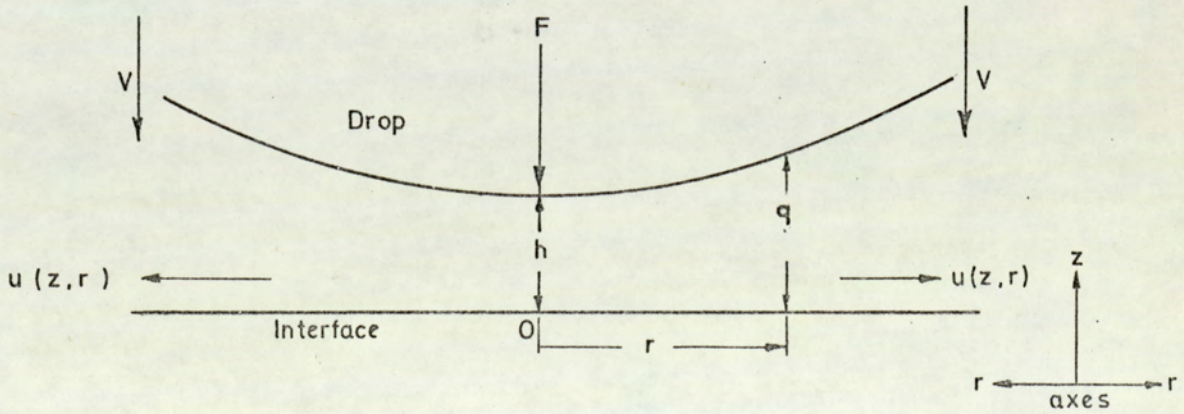

FIG. 2.5 IDEALISED DROP & INTERFACE MODELS

under the action of a force F in a liquid of viscosity, μ_c. The separation of the two surfaces was considered to be q at any distance r, where,

$$q = f(r)$$

and $q = h$ at $r = 0$

as shown in Figure 2.5-g.

The flow velocity, u, of the thinning film was assumed to be a function of r, and the velocity profile in the z-direction was assumed to be parabolic. Thus, the rate of approach of the surface to the plane was found by equating the work done by the force, F, to the energy dissipated by viscosity such that

$$V = -\frac{dh}{dt} = \frac{F}{6\,\mu_c \int_0^r \frac{r^3}{q^3}\,dr} \qquad (2.19)$$

This represents the basic equation from which a number of models have been developed to find the coalescence time. For the case of the parallel disc model, i.e. deformable drop-rigid interface, the film thickness will be,

$$q = \text{constant} = h \qquad (2.19.a)$$

$$r = r_f = \text{Barrier ring} \qquad (2.19.b)$$

Hence, upon simplification Equation 2.19 will yield,

$$\frac{dh}{dt} = \frac{2F}{3\pi r_f^4 \mu_c} h^3 \qquad (2.20)$$

Upon integration between the limits of film thickness h_o and h_1 at times of t = o and t respectively,

$$t = \frac{3\pi \mu_c r_f^4}{4F} \left(\frac{1}{h_1^2} - \frac{1}{h_o^2} \right) \qquad (2.21)$$

As pointed out by Charles and Mason (8) Equation 2.21 was first derived by other workers to explain the force necessary to close together, or draw apart, two circular discs immersed in a viscous medium (66, 67).

If the drop's approach to the interface is solely due to its own weight, i.e. gravity approach,

$$F = \frac{4}{3} \pi a^3 g \Delta\rho \qquad (2.22)$$

Further, for small deformations,

$$r_f = a^2 \left(\frac{2g \Delta\rho}{3\sigma} \right)^{0.5} \qquad (2.23)$$

Substitution of Equations 2.22 and 2.23 into Equation 2.21 yields,

$$t = \frac{u_c}{4} \cdot \frac{g \Delta\rho a^5}{\sigma^2} \cdot \left[\frac{1}{h_1^2} - \frac{1}{h_o^2} \right] \qquad (2.24)$$

When $h_o \gg h_1$, this Equation 2.24 reduces to,

$$t = \frac{\mu_c \Delta\rho g a^5}{4\sigma^2} \cdot \frac{1}{h_1^2} \qquad (2.25)$$

Equation 2.24 is similar to the one derived by Gillespie and Rideal (7) to determine the film thicknesses at rupture. Limitations are placed upon these equations,

a. Because of the assumption of rigidity of both surfaces;

and

b. Because of the neglect of tangential stresses, the existence of which may create internal circulations within the drops.

They are however applicable for small drops which can be considered to behave as rigid spheres (1).

Model 2. ; Rigid drop- deformable interface

This model is illustrated in Figure 2.5 - 1.b and the equations for it are given by Chappelear (9) based upon the derivation by Nielsen.

The fact that part of the drop lies below the interface complicates the derivation. A force balance between the upward force F_u, due to interfacial tension and the downward force F_d, equal to the weight of that part of the drop above the interface, are expressed as,

$$F_u = \frac{2\pi(a^2-s^2)\sigma}{a} \qquad (2.26)$$

$$F_d = \frac{4}{3}\pi a^3 \Delta\rho g - \pi\left[\frac{2}{3}a^3 - a^2 s + \frac{s^3}{3}\right] g\Delta\rho \qquad (2.27)$$

where s = the distance from the centre of the drop to the plane interface

a = radius of the drop

Equating these forces yields,

$$s\left(1 + \frac{2\sigma s}{\Delta\rho\, g a^3} - \frac{s^2}{3a^2}\right) = \frac{2}{\Delta\rho\, g a} - \frac{2a}{3} \qquad (2.28)$$

The time required to thin to a given film thickness h_2, based on parallel discs of area equal to the spherical segments is given by,

$$t = \frac{3\mu a^2 (a - s)^2}{(2a^3 + 3a^2 s - s^3)\Delta\rho g h_2^2} \qquad (2.29)$$

Equations 2.27 and 2.28 must be solved simultaneously and this was done numerically. It was reported (9) that for small deformations, the results approached those from Model 1.

Model 3. ; Deformable drop- deformable interface

This is illustrated in Figure 2.5 - 1.c. and would appear to be more realistic than the uniform film models. If an arbitrary radius of curvature, R, is selected, the limiting cases of,

R = ∞ will yield Model 1;

R = 2a will give Model 2.

Elton and Picknet (11) considered the shape shown in Figure 2.5 - 1.b as the general model, and by selecting an arbitrary radius of curvature and neglecting the weight correction, they obtained the approximate equation,

$$t_{12} = \frac{\mu_c \Delta\rho\, g\, a^2}{\sigma^2 h_2^2} \qquad (2.30)$$

This Equation 2.30 and the one derived by Charles and Mason (8) and given in Model 1., Equation 2.25, are similar but for the 4 which appears in the denominator of the latter Equation.

Later Chappelear (9) also adopted this approach of selecting an arbitrary radius R and considering the other uniform film models as limiting cases. In his derivation Figure 2.5 - 1.c. was taken as a base, and the assumptions were made of small spherical deformations and equal interfacial tensions on both sides of the film,

then,

$$P_1 - P_2 = \frac{2\sigma}{R} = P_2 - P_3 \qquad (2.31)$$

where P_1 is the pressure inside the drop

P_2 is the pressure at the centre of the film

P_3 is the pressure at the bulk phase below the film.

With sufficiently small drops, hydrostatic head and pressure

drop across the flat interface were assumed to be negligible. Hence the pressure drop across the free drop surface, equal to $P_1 - P_3$, may be written,

$$P_1 - P_3 = 2\frac{2\sigma}{R} = \frac{2\sigma}{a} \qquad (2.32)$$

which reduces to,

$$R = 2a \qquad (2.33)$$

Model 4. Deformable drop - deformable interface with drop shape

Princen (12) removed the restriction on drop size in a more general treatment by computing the exact equilibrium shape of the drop surface in contact with the bulk surface. The existence of this 'equilibrium' shape presupposes the presence of some repulsive force between the drop and bulk interface to prevent coalescence.

The total system of interfaces was divided into three distinguishable parts, viz "free","in contact" and "tail".

The equations for "free" drop interface, drop and bulk interfaces "in contact" and "tail" interfaces were written by equating surface tension and gravity forces. Finally equations describing the drop shape were obtained similar to those of Bashforth and Adams (61). The differential equations were solved numerically and solutions were presented in tabular form.

These results were used to evaluate the film drainage area and the force to be used in the Stefan-Reynolds equation for film drainage described in the previous models. Finally an expression for the drainage time was obtained

$$t = \frac{3\mu_c a^3}{\sigma} \quad \frac{1}{h_2^2} \qquad (2.34)$$

The fundamental weakness of uniform film models, viz. that the film between the drop and interface simply is not uniform, has been pointed out by Chappelear (9) and others (8, 13, 12, 14). This has been verified experimentally. Therefore the application of uniform film models is limited either to very small drops or to produce an approximation.

b. Non-uniform film models

Model 5. ; Rigid drop - Rigid interface

This is illustrated in Figure 2.5 - 2.a. The approach of a sphere to an unbounded plane is considered.

Charles and Mason (8) derived the general film drainage equation by equating the work done by the approaching force to the energy of dissipation which resulted as Equation 2.19 shown in Model 1. If the approaching spherical surface is assumed to approximate in shape to a parabola, the film thickness at any radial distance will be,

$$9 = h + \frac{r^2}{2a} \qquad (2.35)$$

Substitution of the value into Equation 2.19 yields upon integration, between the limits of r = o to r = a, and h = h, to h = h_2,

$$t = \frac{6\pi a^2 \mu_c}{F} \ln \frac{h_1}{h_2} \qquad (2.36)$$

if $a \gg h$.

This equation is subject to the same criticism as those for the uniform film models that is applicable for small drops. Furthermore the presence of a dimple in the surface of the drop adjacent to the interface may cause a large difference.

As mentioned earlier the approach of a liquid drop to a flat plate has been studied by Hartland (14). Theoretical approaches to the film drainage process were also discussed in this work and equations were derived applicable to this and other models. Equation 2.36 has been derived by a different approach. In deriving the drainage time equation, most of the assumptions were similar to those made in the earlier work (8) viz,

i. The flow is laminar and symetrical about the vertical axis and in the radial direction.

ii. The interfaces are resistant to tangential stresses i.e. the velocity is zero at the interfaces.

iii. The propelling force, F, arises solely from the

buoyancy of the drop so that London - van der Waals attraction, electrostatic repulsion and electroviscous effects may be neglected.

iv. Inertial effects may be neglected .

The general form outlined by Hartland (14) in terms of the axial coordinates, r, z, θ, where r is the radius and z the height of a point in the film above the bulk interface is shown in Figure 2.5 - g. A momentum balance may be written for an element of the film rdθ, dr, dz by equating the viscous and pressure forces, to give,

$$\frac{\partial p}{\partial r} + \frac{\partial T}{\partial z} = 0 \qquad (2.37)$$

The shear stress, $T = \mu (-du/dz)$, for a Newtonian fluid, was substituted and integrated twice using the boundary conditions u = o when y = o, to give,

$$2\mu u = \frac{dp}{dr} \left(z^2 - \frac{2}{n} zh\right) \qquad (2.38)$$

where n is the number of rigid surfaces,

$\frac{dp}{dr}$ is the radial pressure gradient

The radial pressure gradient is independent of z and thus Equation 2.38 shows that the velocity profile is parabolic. The approach of the bounding surfaces with velocity V causes a rate of reduction in volume of the film within a radius r

of $\pi r^2 V$ which is equal to the total rate of flow through the periphery of the film.

Thus,

$$\pi r^2 V = 2\pi \int_0^h r u \, dz \qquad (2.39)$$

From Equations 2.38 and 2.39,

$$\frac{dp}{dr} = -\frac{3n^2}{2} \cdot \frac{u V r}{h^3} \qquad (2.40)$$

Hence, if the hydrostatic pressure on the film is constant, p becomes the excess pressure in the film due to flow. Then the pressure distribution within the film, using the boundary conditions $p = 0$ at $r = r_f$, is obtained by integrating Equation 2.40,

$$p = \frac{3n^2}{4} \cdot \frac{\mu V r_f^2}{h^3} \left(1 - \frac{r^2}{r_f^2}\right) \qquad (2.41)$$

Since p, is the flow pressure, equivalent to the difference between the total pressure and the constant hydrostatic pressure within the film, the upward force exerted on the drop is

$$F_u = 2\pi \int_0^{r_f} p \, r \, dr \qquad (2.42)$$

This is balanced by the downward force,

$$F_d = \frac{3\pi n^2}{8} \cdot \frac{\mu V r_f^4}{h^3} \qquad (2.43)$$

The approach velocity, V, is already shown previously in Model 1,

$$V = -\frac{dh}{dt} \tag{2.19}$$

and substitution of this into Equation 2.43, followed by integration with $h = h_o$ at $t = o$, yields the variation in uniform thickness h with time t, already shown in the uniform film models.

If the film thickness, q , at a radius r is expressed,

$$q = a + h - (a^2 - r^2)^{0.5} \tag{2.44}$$

where h is the minimum film thickness

i.e. $q = h$ at $r = o$

Integration of Equation 2.40 using this expression for q , and with $p = o$ at $r = a$. gives the pressure distribution in the film when $h \gg a$ as,

$$p = \frac{3 \mu V}{a h^2} \cdot (a - h)^2 \tag{2.45}$$

Equating the total vertical force to this pressure, to the force F gives,

$$F = \frac{6\pi \mu_c V a^2}{h} \tag{2.46}$$

which upon integration with $V = -\frac{dh}{dt}$ yields, previous Equation 2.36, that is

$$t = \frac{6\pi \mu_c a^2}{F} \cdot \ln \frac{ho}{h} \tag{2.36}$$

Model 6. Deformable drop- deformable interface

When a drop or bubble approaches an interface it "dimples", i.e., it acquires a reverse curvature so that a central lens of liquid is trapped by a thinner 'barrier-ring'. This requires deformability of at least one surface. Frankel and Mysels (10) have shown that this convex shape may be predicted from purely hydrodynamic considerations and stated that the dimple does not require rigidity of any of the surfaces involved provided at least one of the surfaces does not dilate, i.e. expand radially, under the stresses involved. Double layer, van der Waal's effects were neglected.

The thickness in the centre of the film (the maximum thickness) was given by,

$$h = \left[\frac{0.0096\, n^2 \mu_c\, r_f^{\,6}}{\sigma\, a\, t} \right]^{\frac{1}{4}} \qquad (2.47)$$

and the thickness z_o, at the barrier ring (the minimum thickness) by,

$$z_o = \left[\frac{0.090\, n^2 \mu_c\, r_f^{\,2}\, a}{\sigma\, t} \right]^{\frac{1}{2}} \qquad (2.48)$$

Assuming the number of non-dilating surfaces, n, is equal to 2 and $z_o = h$, Equation 2.47 agrees with that obtained from the "parallel disc" approach of Model 1. to within 2% .

The ratio of Equation 2.48 to 2.47 is,

$$\frac{z_o}{h} = 3.066 \frac{a}{r_f^2} \cdot h \qquad (2.49)$$

which indicates that the dimpling persists at all times, and becomes relatively more pronounced as the film thins.

Model 7. Rigid drop - deformable interface

Jeffreys and Hawksley(13) proposed two models on the basis of the film not being uniform due to dimpling of the droplet surfaces. The exaggerated shape of the film is illustrated in Figures 2.5 - 2b and 2c. from which it is clear that whereas both models assume a rigid drop they differ with regard to the position of the thinnest part of the film.

In Model A, the film is thinnest at the centre whereas in Model B, it is thinnest at the periphery. The distance, s, between the centre of the drop and bulk interface was obtained by a force balance as shown in Model 2.

The equation for the rate of approach of the two arbitrary surfaces derived by Charles and Mason (8) and shown as Equation 2.19 in Model 1. was used.

It was assumed that the surfaces bounding the film could be represented by parabolas having the same radii of curvature at the apex. Thus the film thickness at any radial position r from the apex was, as shown in Figure 2.5 - g,

$$q = h + \left(\frac{1}{2a} - \frac{1}{2r} \right) r^2 \qquad (2.50)$$

The equation to predict the drainage time from Equation 2.19 first required evaluation of the integral, $\left[\int_0^r \left(\frac{r}{q} \right)^3 dr \right]$ between the limits o and r, and subsequently substitution of the result into Equation 2.19. Integration over the limits h_1 and h_2 then gives,

$$t = \frac{6\pi\mu_c}{4F k^2} \left[\ln \frac{h_2}{h_1} + \ln \left(\frac{h_1 + c}{h_2 + c} \right) + \frac{c}{h_2 + c} - \frac{c}{h_1 + c} \right] \qquad (2.51)$$

where,

$$c = 2 R k (a - s) \qquad (2.51.a)$$

$$k = \frac{1}{2a} - \frac{1}{2R} \qquad (2.51.b)$$

Writing R as a multiple of drop radius, $R = \lambda a$, gives,

$$k = \frac{1}{2a} \left(1 - \frac{1}{\lambda} \right) \qquad (2.51.c)$$

and

$$c = (\lambda - 1) (a - s) \qquad (2.51.d)$$

Hence, the drainage time can be calculated for different values of λ from Equation 2.51 which is Model A, i.e. the film is thinnest at the centre.

A similar derivation for the case when the film is

thinnest at the periphery gives the drainage time equation,

$$t = \frac{6\pi \mu_c}{4 k^2 F} \left[\ln \left(\frac{h_2^1 - c}{h_1^1 - c} \right) + \ln \frac{h_1^1}{h_2^1} + \frac{c}{h_2^1} - \frac{c}{h_1^1} \right] \qquad (2.52)$$

Equations 2.51 and 2.52 were tested using experimental data; and a better fit obtained with Model B than Model A. Plots of ln a against ln t showed slight curves but could be considered straight over the range of sizes studied for water droplets at a benzene-water interface. In the relation $t \propto a^n$, the power n passed from positive to negative as the radius, a, decreased; it was considered possible that n tends to -1 as $1/\lambda$ approaches to zero, that is as λ tends to infinity, for a rigid drop at a plane interface. Similarly as λ tends to 1, the power n becomes large approaching 5 as required by the uniform film thickness model.

The approach of a rigid sphere to a deformable fluid liquid interface has been studied by Hartland (43) and later the profile of the symmetrical draining film was analysed theoretically (62). A partial differential equation was obtained governing the variation in shape with time. This was solved by a digital computer using an experimental profile of a film as the initial condition.

3. INTERDROP COALESCENCE

3.1 Introduction

Whilst intensive studies have been reported on drop-interface coalescence, as reviewed in Section 2, only a limited amount of work has been reported on drop-drop coalescence. This has been attributed to the experimental difficulties in obtaining data (1) since it is impossible to maintain two drops suspended in close horizontal contact for a sufficient time without external means of support. Therefore, it is necessary to study the coalescence of two colliding drops either resting at horizontal interfaces or on a solid surface which is not wetted by the dispersed phase. The same conditions are obviously required in order to study the approach of two drops along a vertical axis.

This experimental limitation has made it difficult to verify the application of film drainage theory to drop-drop coalescence. Nevertheless, despite the lack of experimental proof this theoretical approach is used to describe the process phenomena. However, in a dynamic situation, e.g. the collision of two or more drops in an agitated vessel, analysis is only possible by including contact time, which is an added complication. It is worth noting that the area of interdroplet coalescence is closely related to droplet coalescence in a gaseous phase and therefore, certain investigations of the latter (1, 68, 69, 70) may prove useful.

3.2. Experimental investigations

Scheele and Leng (70) have indicated the primary requirements of any experiment to study interdrop collision and coalescence under conditions similar to those encountered in turbulent dispersions. There are,

i. Freely moving drops,

ii. Variable drop size,

iii. Variable collision velocities,

iv. Freshly formed interfaces, free from ageing or other uncontrollable effects.

They described an experimental technique and apparatus, using anisole droplets formed in water from two horizontal nozzles which were adjustable through 30^{o}. Collision velocities in the range of 1,9 to 11.2 $cm.sec^{-1}$ were used, the phenomena being recorded by a photo-kinetic high speed camera. Quantitative measurements obtained directly from the film were drop diameters, absolute and relative velocities, point and time of contact, and the area-time relationship for the contact period. They reported that the drops formed were oscillating and the oscillation frequency was predicted from the equation given by Schroeder and Kintner (71),

$$w = \frac{1}{2\pi} \cdot \left[\frac{24\,\sigma\,g}{R^3\,(3\rho_d + 2\rho_c)} \right]^{0.5} \qquad (3.1)$$

where w = oscillation frequency

R = radius of larger drop

σ = interfacial tension

ρ_d and ρ_c are densities of the drops and the continuous phase respectively.

q = an amplitude dependent coefficient

From the approach velocities of the drops and the measured drop dimensions the net force acting on the drops after contact was then calculated. The results suggested that the phase angle of oscillation at the moment of contact was an important parameter. Thus with the maximum horizontal elongation of the drop set at zero degree, and the maximum vertical elongation at 180°, the phase angles between 0 and 127° resulted in coalescence and phase angles between 150° and 345° resulted in bouncing. Many low velocity coalescences and high velocity bounces were observed and there was no apparent relationship between coalescence probability and impact velocity. They concluded that the classical parallel disc, rigid interface model for describing film thinning failed and that mobility of the interfaces required inclusion in any model.

This method of studying drop-drop coalescence was well

devised. However, its extension to other systems would create some difficulty unless they had a low density difference, like anisole-water, to produce head-on collisions.

Robinson and Hartland (72) studied the approach of two or more drops towards an interface, and towards each other, in a two dimensional bed. They measured the arc lengths of the profile. Observations were also made of one drop resting at an interface and of two or more drops resting on this one in a vertical column. Presumably from the drop profiles and measured arc lengths, rate of film drainage equations will be verified in future work, as has been done for a single drop resting at a plane interface.

Another recent study to measure the coalescence time between two liquid drops was conducted in a specially designed apparatus by Sivokova and Eichler (73). One drop was situated vertically above another and they measured the time between the drops touching and resting in a special section in the absence of an interface, and when they merged into one.

McCay and Mason (28) formed a drop in an immiscible organic phase and allowed it to rest on a flat non-wettable surface of lucite. A second water drop was then allowed to fall gently onto this.

McAvoy, Weighland, Tompkins and Kintner (74) have used a similar technique.

However, it is clear that these experimental techniques require improvement, especially to cover also the case of "overtaking collisions" as distinct from 'head-on' collisions.

3.3 Theoretical studies

The coalescence mechanism between two drops involves film drainage and rupture similar to that occurring in drop-interface coalescence. Drainage of the continuous phase film between the approaching surfaces of two drops is therefore the basis of theoretical analysis of the mechanism. Thus, as before, assumptions are necessary as to whether or not the drop surfaces are rigid or deformable. Furthermore it is necessary to evaluate the forces which cause the drainage and profiles between the drops.

In this way, McAvoy et al (74) have analyzed the approach of two spheres; Figures 3.1 and 3.2 show a diagramatic sketch of droplets approach and the models.

Rigid drop surfaces of equal diameter are assumed and each droplet is considered to approach the other at velocities of V_1 and V_2 respectively. The forces acting on the drops

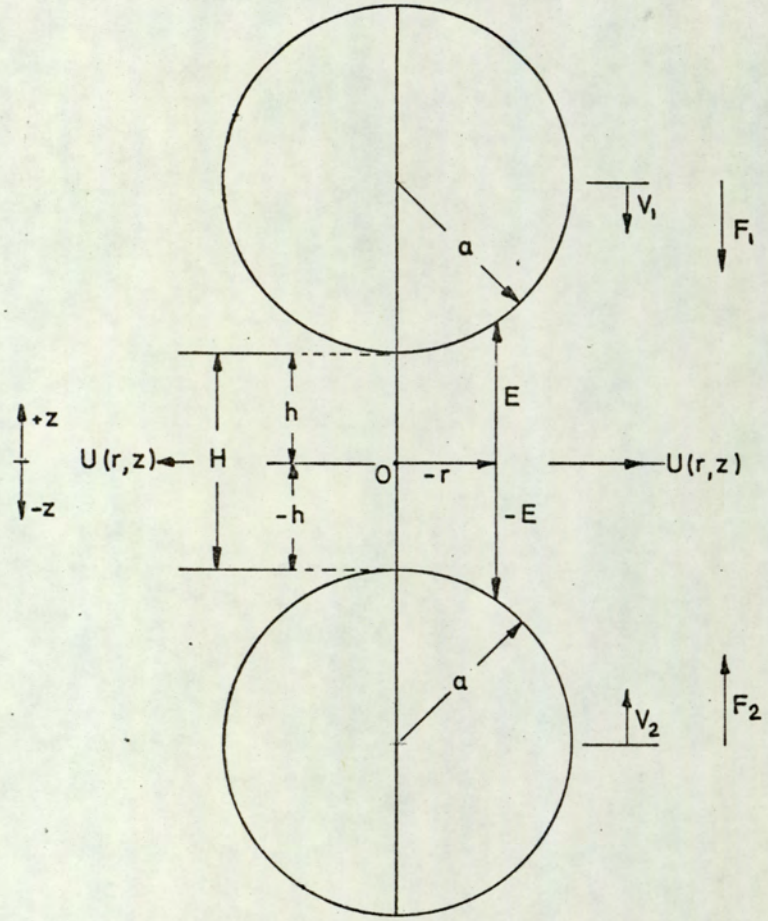

FIG. 3.1 APPROACH OF TWO SPHERES IMMERSED IN A VISCOUS FLUID (1)

	Model	Reference
1. Rigid sphere	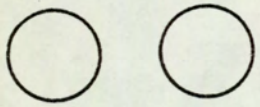	
2. Deformable spheres having parallel interfaces.	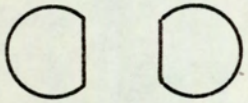	
3. Deformable spheres allowing for formation of a 'dimple'	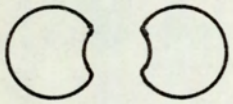	
4. Ellipsoidal drops	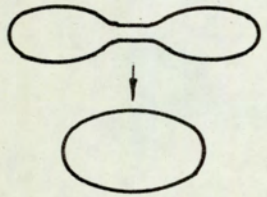	

FIG. 3.2 MODELS DEVELOPED TO SIMULATE COALESCENCE BETWEEN PAIRS OF DROPS (1)

are shown as F_1 and F_2 and the film thickness between the two spheres, H, is thinned from both sides relative to a horizontal "reference plane", mid-way between the two drops. The continuous phase attains an outward velocity of,

$$u = f(r, z) \tag{3.2}$$

Laminar flow and negligible inertia forces are assumed. As for the approach of a drop to a deformable interface, discussed in Section 2.4, a parabolic profile is assumed, with zero slip velocity at the interfaces, i.e

$$z\,u(r, z) = (z + E)(E - z)\,\psi(r) \tag{3.2 .a}$$

Where $\psi(r)$ is a function of film radius

The rate of approach of the spheres is given by

$$V = -\frac{dh}{dt} = \frac{4F}{3\pi r \mu_c \int_0^a \frac{r^3 dr}{E^3}} \tag{3.3}$$

Finally, expressing E, the film thickness at any point on the profile in terms of, droplet radius, a, and half of the minimum separation distance, h,

$$E = h + a - \sqrt{a^2 - r^2} \tag{3.4}$$

Substitution of Equation 3.4 in 3.3 yields upon integration,

$$t_2 - t_1 = \frac{3\pi r \mu_c}{4F} \left[\frac{3}{2} a (H_1 - H_2) + (\tfrac{3}{4} H_2^2 + 3H_2 a + 2a^2 \right]$$

$$x \ \ln \left(\frac{H_2 + 2a}{H}\right)(\tfrac{3}{4} H_1^2 + 3H_1 a + 2a^2)$$

$$x \ \ln \left(\frac{H_1 + 2a}{H_1} \right) \qquad (3.5)$$

where $H = 2h$

This basic Equation 3.5 can be further simplified and extended to the case of two spheres of unequal diameter. However, since the basic assumption is of rigid surfaces, it will be limited to the cases of small drops or stabilized systems.

Jeffreys and Davies (1) discussed the above Equation in more detail and suggested other approaches to the derivation such as a complete solution to the Navier - Stokes Equations. They concluded that the circulation within a drop would be an important consideration. This point has in fact been illustrated later by Murdoch and Leng (75) starting from the Navier - Stokes Equations and by comparison with data obtained by the experimental technique detailed and reported by Scheele and Leng (70) and summarized in Section 3.2.

Murdoch and Leng's derivations demonstrated that the film between two colliding drops thins most rapidly when there is an

outward radial velocity inside the drops, which tends to force the liquid away in a mobile film. If there is no such radial velocity inside the drop, the film drainage will be slower despite the existence of a mobile interface. When the interface is immobile the drainage is slowest. Thus having deduced the importance of internal circulation within a drop, they expected some correlation between coalescence probability and the droplets approach velocity. This however is not confirmed by their experimental data.

It is clear from the literature that the area of drop-drop coalescence require more further study, both experimental and theoretical, than does single drop-plane interface coalescence. The inter-connection between the two types of droplet coalescence behaviour has already been established in terms of film drainage.

4. COALESCENCE IN A SWARM OF DROPLETS

4.1 Introduction

A logical progression in the extension of single drop studies to a swarm of drops is via the intermediate condition of droplets in an incomplete layer, or monolayer (20). This can then be extended to the more complicated case of multi-layers. The monolayer studies will therefore be summarized before the multilayer investigations. However, since the mathematical models have some novelty of their own they will be taken up separately in Section 4.4; experimental findings are summarized in Section 4.3.

Some difficulty arises in comparing experimental data since the methods used for producing swarms of drops differed between one equipment to another. Even though the separation of the phases, may follow the same basic mechanisms irrespective of the way a dispersion is produced, interactions between the droplets may differ in each type of equipment. For example a dispersion produced in a mixing vessel inevitably contains a wider drop size distribution than one from a properly designed distributor plate [illegible], which affects both the packing of droplets and the ratio of interfacial area to flocculation zone volume. As in single drop coalescence studies

the results are undoubtedly influenced also by the experimental methods and the method of preparation of the liquid phases used. Moreover, since the type of contact and the flow of the phases in a particular equipment is significant, an attempt has been made to distinguish between the results of batch and continuous flow experiments.

4.2. Monolayers

Studies reported in the literature and summarized in Section 2.2.3 regarding the effect which vibrations at the interface have upon the coalescence process reveal that the droplets are stabilized resulting in longer mean rest times. The effect of adjacent drops in a monolayer upon the coalescence of a single drop is considered to arise in a similar way i.e. because of the disturbance created by the vibrations. Although qualitative observations are in accordance with this, quantitative data for single drop rest times in monolayers are insufficient to justify any conclusion as to whether or not coalescence rates are in fact invariably decreased due to stabilization of the drops.

As discussed earlier, various kinds of disturbances have been found to cause changes in single drop rest times. Even when all the conditions are fixed, disturbances may arise in all but idealised single-drop interface studies, due to

the presence of other droplets. The motion of neighbouring drops would be expected to affect the drainage and rupture of the film existing between the surfaces similar to a drop at plane interface in changing hydrodynamic conditions. The arrival or disappearance of another drop, or droplets, whilst a single drop is undergoing one of the stages of coalescence may cause a disturbance by,

i. Impingement i.e. direct collision of a second drop with the coalescing drop.

ii. Impact of a second drop with the interface inducing wave propogation and causing oscillation of the coalescing drop as well as of the interface.

iii. The disappearance of a drop, after its deflation in a short period of time (0.05 sec.) causing displacement of the continuous phase and the coalescing drop.

iv. Drop-drop coalescence.

These are possible causes of disturbance arising in a monolayer. Lawson (19) observed impingement of one drop with another at an interface resulted the coalescence times of both drops generally increased. Furthermore Jeffreys and Hawksley (13) concluded that a small tilt of the mid-axis of a single drop with an interface affected the coalescence time.

A series of investigations to determine the coalescence

characteristics of a single drop, and subsequently two or more drops as a layer at an interface have been reported by Robinson and Hartland (72). They have investigated the effect of neighbouring droplets in a two dimensional array on the arc length of the draining film between a drop approaching a bulk interface. They calculated the arc lengths from droplet profiles measurements which were obtained by projecting the photographs taken. Then these arc lengths were compared. It was reported that the arc length was least for the drop in the middle of the row and reached a minimum when there were about four drops present in investigations of one to 9 drops total in a single array. For instance, if 1, 2, 3, drops were placed on each side of a 0.1 ml. paraffin drop at paraffin golden syrup interface, making a total of 3, 5, 7 drops in a row reduced an arc lenght of 0.50 cm for a single drop to 0.42, 0.35, and 0.36 cm respectively. The arc length for a drop in the middle of a long row was about 30% less than that for a single drop for the liquid paraffin - golden syrup; and liquid paraffin glycerol systems. Aqueous glycerol-silicone system showed 12 per cent difference. Further it was observed that in a row of droplets of a volume less than 0.2 ml., the one at the middle which had the shortest arc length coalsesced first with the bulk dispersed phase. However for larger sizes drop-drop coalescence occurred before the interface.

The decrease in arc length was explained by the increase of horizontal forces exerted by the neighbouring droplets. Similar studies with drops in a vertical column and more than one row of droplets showed changes in arc lengths. It was clearly concluded that the shape of a liquid drop approaching a deformable liquid-liquid interface was affected by the presence of adjacent drops. Coalescence was slower in two dimensional beds than three dimensional beds.

Davies, Jeffreys and Smith (20) investigated the behaviour of a group of droplets at an interface, in the form of an incomplete or complete monolayer or cluster of droplets. Correlations for single drop coalescence times within the cluster of droplets were reported for both drop-interface and drop-drop coalescence. The results were obtained in a spray column of 2 inches diameter in continuous flow for various systems. The interdrop coalescence rates varied with the system employed. Measurements of coalescence times were made from the films. It has been reported that the mean coalescence time was inversely proportional to the drop size. Furthermore, if the rate of drop arrival at the interface was increased, the mean drop interface coalescence time decreased slowly. However they found that the incidence of interdroplet coalescence increased rapidly as the inlet drop sizes decreased and to a lesser extent, as the drop arrival rate decreased. Finally for drop-interface coalescence, the Equation obtained

was,

$$\frac{t\sigma}{\mu_c d} = 31 \times 10^3 \left(\frac{d^2 g \Delta\rho}{\sigma}\right)^{-1.24} \left(\frac{u_d}{u_c}\right)^{1.03} \qquad (4.1)$$

For interdrop coalescence the Equation was,

$$\frac{t\sigma}{\mu_c d} = 412 \times 10^3 \left(\frac{d^2 g \Delta\rho}{\sigma}\right)^{-0.3} (tN)^{-0.5} \left(\frac{u_d}{u_c}\right)^{0.3} \qquad (4.2)$$

However, the interdrop coalescence Equation has been reported to be inconclusive.

Topliss (76) attempted to determine the coalescence behaviour of a monolayer of regular sized droplets at a plane interface using two component systems in a specially designed all glass 6 inch diameter apparatus. High speed cine films were taken to record the behaviour and to evaluate drop sizes, drop-drop and drop-interface coalescence times. In one set of experiments droplets were formed continuously but the dispersed phase was not recycled. Fresh dispersed phase which had been saturated by 24 hours storage in bottles with occasional shaking was fed to the specially designed distributor by gravity. Temperature was closely controlled by putting a glass heat exchanger in the feed line and enclosing all equipment in air bath. For the continuous arrival of water droplets at a benzene-water interface, values of log N/N_o

were plotted versus overall drop-interface coalescence times. Similar curves were obtained to that illustrated in Figure 2.1 for single drops but of a different magnitude, the variation being dependent on the proximity of adjacent drops. No satisfactory distribution was obtained for drop-drop coalescence the incidence indeed being low for the continuous production of drops.

For the batchwise production of drops (76) most of the coalescence was observed to be drop-drop followed by a final few large drops coalescing with the interface.

4.3. Multilayers

Recent investigations (5, 41, 58, 72, 78, 80, 81) have contributed to the understanding of coalescence in droplet swarms.

These studies are summarized in this Section and in Section 2.4 together with the idealized models proposed and are clearly of major importance to the present work. Not only do they illustrate current gravity settler design fundamentals and present understanding of the phenomena involved, they also show that,with the exception of the work of Ryon et al (77), no pilot scale studies have previously been attempted. They serve, therefore, as one starting point for this research.

The analyses and experimental investigations reported in the literature may be grouped into two main sections viz, batch (unsteady state) and continuous (steady state) studies. These were conducted in either agitated-vessel type, mixer-settlers, or horizontal gravity settlers or vertical spray type columns. Binary systems were studied in the absence of mass transfer. When a third component was present it was equilibriated between the two phases merely to allow a controlled variation of a particular physical property e.g. interfacial

tension. When mass transfer is likely completely different behaviour can be anticipated.

Coalescence of droplets within a swarm necessitates firstly that they approach each other to form a close packed, heteregeneous zone between the two bulk liquid phases. In so doing the droplets high initial velocities are reduced and they move towards the interface in a close packed arrangement. Some interdrop coalescence occurs amongst the densely populated droplets before they reach the two phase-interface where they eventually undergo drop-interface coalescence. Thus coalescence within a swarm of droplets involves both modes - interdroplet and drop-interface coalescence.

Batch experiments were used by Meisner and Chertow (82) to study the effect of phase ratio. A mixture of two immiscible liquids was agitated and the time for phase separation was then determined. It was reported that large droplets separated fairly rapidly but fine droplets remained as a haze that settled extremely slowly.

Ryon, Daily and Lowrie (77) have investigated scale-up of mixer settlers. They observed that most of the coalescence occurred at the interface. However, the system employed in their investigation would seem likely to have suffered from

contamination. Therefore, their results can hardly be generalized.

Robinson and Hartland (72) have reported the arc lengths of the droplets in multi-layers in both batch and continuous experiments. Their results showed a decrease of residence time of a drop at the bulk interface as the dispersion height increased. In a comparison of the coalescence in two and three dimensional beds, the latter was reported to be higher.

Komasowa and Otake (58), in a study involving batchwise experiments, concluded that the stability of a drop layer was almost independent of the volume of drops arriving at the layer. Their results also showed that in the presence of stabilizers, especially sodium oleate, the stability of a drop layer was far less than that of a single drop, but the relation between the stability and concentration was analagous to the relation observed with single drops. They defined this stability of a drop layer as the average time that drops could remain in the layer. In the presence of sodium oleate interdroplet coalescence was negligible. However, when PVA was used as a stabilizer in benzene droplets, drop-drop coalescence occurred to such a degree that the diameter of

drops about to coalesce with the bulk phase was often 2 - 5 times larger than drops from the inlet nozzle.

Jeffreys, Davies amd Pitt (79) have reported the rate of coalescence of swarms of drops in the settler of a single stage mixer-settler. Their experimental results with kerosene dispersed in water showed that drop size increased with the distance from the inlet and was dependent upon the agitator speed and flowrate. The effect of agitator speed was most significant; the ratio of drop diameter at any position to that at the inlet increased directly with an increase in speed. This ratio varied at the top of the wedge between 2 and 5 under various conditions.

Based upon observations in a single baffled mixer-settler vessel with the systems toluene-water and diethyl carbonate-water in the pure state, and stabilized with sodium oleate, Lee and Lewis suggested a division of the separation process into two stages (78),

i. A primary stage during which most of the drops separate out

and ii. A secondary stage during which a haze of very small drops left behind in the continuous phase settle out.

This work was performed under unsteady state conditions, i.e.

agitation was stopped and observations made during the subsequent separation of the dispersed phase.

In the primary separation stage two different mechanisms were distinguishable,

a. The inter-droplet mode

and b. The interfacial mode

but both modes were both involved to some extent. When agitation had ceased, and the induced turbulence had become dissipated, the droplets began to settle and a thin film of the dispersed phase appeared forming a bulk phase boundary. An emulsion layer of higher droplet concentration than the original dispersion then developed just below the interface as a result of sedimentation.

Lee and Lewis's (78) results showed that the "clean" systems diethyl carbonate-water and toluene-water separated predominantly via the inter droplet mode and the toluene-water-sodium benzoate system via the interfacial mode. Separation times for the clean systems were relatively short. The time required for a 0.1 mm diameter drop of diethyl carbonate to reach the full distance of 7 inches from the bottom of the vessel to the surface was found to be 175 seconds at a 0.2 volume fraction of dispersed phase and 77 seconds at 0.05 volume

fraction . For the same size toluene drop the times were 65 and 29 seconds for 0.20 and 0.05 volume fractions respectively. Addition of sodium benzoate to toluene caused these times to increase.

Smith and Davies (5) have studied dispersion bands produced in a 2 inch spray column with water dispersed in five different continuous phase systems. They reported the following general correlation to predict the dispersion band height from the physical properties and inlet mean drop diameter,

$$\frac{H}{d_{12}} = 3.5 \times 10^{3} \left(\frac{V_d \mu_c}{\sigma} \right)^{0.85} \left(\frac{d_{12}\, g\, \Delta\rho}{\sigma} \right)^{-0.88} \left(\frac{\mu_d}{\mu_c} \right)^{0.77} \qquad (4.3.1)$$

An equation was also proposed for the case when the column walls were 'non-wetted' by the dispersed phase due to a coating of a silane compound,

$$\frac{H}{d_{12}} = 2.6 \times 10^{3} \left(\frac{V_d \mu_c}{\sigma} \right)^{0.82} \left(\frac{d_{12}\, g\, \Delta\rho}{\sigma} \right)^{-0.86} \left(\frac{\mu_d}{\mu_c} \right)^{0.73} \qquad (4.3.2)$$

They found that higher dispersion bands were produced when the dispersed phase wetted the column walls. Either an increase in dispersed phase velocity, or a decrease in the inlet mean drop diameter, produced an increase in band height. The

effects of the system properties were evaluated in terms of dimensionless groups as given in Equations 4.3.1 and 4.3.2. This work requires verification for inverted systems. Moreover, its validity requires to be tested in larger columns.

Gondo and Kusunoki (111) reported the thickness of dispersion bands in a 57 mm diameter column used as a settler for dispersions produced in a 170 mm diameter vessel. They found that dispersion thickness increased with any increase in superficial velocity of either the dispersed or continuous phase. They studied kerosene dispersed in water and their results showed a constant fractional hold-up of 0.55. It was observed that interdroplet coalescence did not take place in the band. A limitation arises in this work due to the sole use of the kerozene-water system. Kerozene is not a suitable material for use in such investigations and has been criticised by Kintner (112).

The most recent work to be reported in the literature is due to Allak et al (81). Droplet residence time studies were performed in dispersion bands using a flow visualisation technique by means of which droplets behaviour inside the bed could be observed and analysed. A 2 inch column was used similar to that described in reference (5). The techniques used included the addition of a special compound to the

dispersed phase, in order to render it visible in an invisible dispersion band by the application of u.v. light, and the injection of dyed droplets. It was found that dispersion band height increased with any increase in volumetric flowrate or decrease in inlet mean drop diameter. The degree of interdroplet coalescence was observed to vary between different regions.

4.4. Coalescence models

4.4.1 Introduction

The rate of coalescence of the droplets with the bulk dispersed phase governs the throughput of any gravity separator. The dimensions of the settler are also dependent upon the rate of coalescence which is of course related to the mean coalescence time of the droplets. Following observations of the behaviour of droplets within both horizontal and vertical gravity settlers, and utilizing the coalescence time studies reviewed in the previous section, mathematical models have been proposed for analysing coalescence in a swarm of droplets (41, 58, 78, 79, 80). Certain of these models have also been extended to estimate the dispersion band dimensions as a basis for gravity settler design. These models are reviewed below, firstly for primary dispersions under batch (unsteady state) in Section 4.4.2 and then under continuous (steady state) conditions in Section 4.4.3.

4.4.2 Unsteady state, batch conditions

Komasawa and Otake (58) have proposed a model based upon experimentation with and without a stabilized system in an apparatus essentially similar to a conventional coalescence cell. Drop layers were formed at the interface and measurements of time and change of height were obtained from cine-films taken

during collapse of the droplet layers. They attempted to determine the average lifetime of droplets within a drop layer and to correlate this with the drop volume and droplet dispersion height from the initial value on formation to its final disappearance following coalescence.

They defined stability of the drop layer as L so that the average time that drops could remain in the layer, became,

$$L = \frac{1}{V_o} \int_o^{Vo} t \, d\, V = \int_o^{T} \left(\frac{z}{z_o}\right) dt \qquad (4.3)$$

where V = volume of the drop at time t .

z = height of the drop layer at time t.

V_o = initial drop volume

z_o = initial height of the drop layer.

Integration of Equation 4.3 gave,

$$\frac{z}{z_o} = \exp(-kt) \qquad (4.4)$$

$$L = \int_o^{\infty} \exp(-kt)\, dt = \frac{1}{k} \qquad (4.5)$$

where k is a constant particular to each drop layer.

The use of this time in place of drop life for continuous flow conditions is of doubtful validity. However, their method

for the evaluation of k values for various systems and stabilizers may be of use to predict possible flocculation zone height for comparison purposes.

4.4.3 Steady state, continuous flow

For the continuous flow conditions at steady state the following four models were proposed:

a. A fluidization model for the interfacial mode of phase separation proposed by Lee and Lewis (78). This was subsequently verified in a simple mixer unit of 7 inch diameter cylindrical vessel which was operated as a batchwise settler.

b. An Idealised Model for a Horizontal Flocculation Zone proposed by Jeffreys et al. (79). This was verified in a continuously operated mixer-settler unit comprising a 45 x 10 cm. settler together with a 26.2 cm high and 12.8 cm in diameter cylindrical vessel.

c. A Differential Model proposed also by Jeffreys et al (80) and verified again by the same equipment in Model (b).

d. Vertical Dispersion Band Differential Model, proposed by Smith (41) and tested in a 2 inch diameter continuously operated spray column.

These are reviewed below in detail.

a. Fluidized Bed Model (78)

The basic assumption was that an emulsion layer is fluidized by the release of continuous phase which maintains a superficial drainage velocity in the opposite direction to drops coalescing at the interface.

Lee and Lewis (78) have found the mathematical analysis of the inter-droplet mode of phase separation to be difficult and they have neglected it. They considered only the interfacial mode of coalescence which was produced by stabilizing the systems with sodium benzoate. The pure binary systems underwent fast drop-drop coalescence and 2-3 cm drops formed at the interface before the interface coalescence.

They did not consider the height of flocculation zone formed. Their model is interesting in that it describes possible mechanisms of phase separation at the interface and factors affecting the rate of coalescence. The model was tested with unsteady state data, viz the time necessary for rupture of the dispersion band. Whether this verification is applicable for continuous flow is doubtful. Nevertheless, the method of derivation of the formula

does not assume an unsteady state, and therefore with improvement could be extended to a continuous operation model.

The interfacial mode of coalescence model which they have described is in fact limited in application to a single layer of droplets at the interface. Although not given for monolayer coalescence only, the absence of any inter-droplet coalescence mode renders it inapplicable for deep heterogenous zones except possibly with stabilized drops. Their proposal regarding the mechanism of phase separation and the model derivation are reviewed below.

Converting their nomenclature to that used in this work, and using hold-up in place of void volume by equating

$$\phi = 1 - \varepsilon \qquad (4.6)$$

where, ϕ is the dispersed phase hold-up, ε is void volume among the drop. Two conditions which they assumed must be satisfied simultaneously were:

a) The drops which coalesce at the interface release continuous phase which has a superficial downward velocity, V_c, relative to the drops where

$$V_c = \frac{1 - \phi}{\phi} \quad V_d \tag{4.7}$$

b) This downward velocity V_c must be sufficient to fluidize the drops beneath the interface. Provided V_c is above the minimum fluidization velocity for the drops, then the voidage, $(1 - \phi)$, of the emulsion layer will self-adjust to accommodate the flow. The relation for this condition of fluidization by Richardson and Zaki (83) viz:

$$V_c = V_t \ (1 - \phi)^n \tag{4.8}$$

is assumed to be applicable for V_t being the terminal velocity of the drops, and n is a function of the drop Reynolds number. In solids sedimentation and fluidization for the range

$$0.2 < Re < 1$$

the value of (n) is

$$n = 4.35 \ R_e^{-0.03} \tag{4.8a}$$

For $1 < R_e < 500$

$$n = 4.45 \ R_e^{-0.1} \tag{4.8b}$$

Then assuming the existence of spherical droplets, which as described in Section 4.3 are not, in fact, observed, then number of drops adjacent to the interface at any time may be written for a complete monolayer

$$N = \frac{6\emptyset}{nd^3} \qquad (4.9)$$

So that

$$m = \frac{N^{\frac{2}{3}}}{t_{\frac{1}{2}}} \qquad (4.10)$$

and

$$V_d = \frac{\pi}{6} \; d^3 m \qquad (4.11)$$

where;

N = The total number of drops per unit volume of emulsion layer

m = The number of drops released per unit time per unit area of interface

$t_{\frac{1}{2}}$ = Rest time of a drop at the interface, which is taken to include the time required for a drop to move up to the interface to occupy a vacancy created by a coalesced drop.

From Equations 4.7 and 4.8, therefore,

$$V_d = V_t \, \phi(1-\phi)^{n-1} \qquad (4.12)$$

Substituting for (m) in Equation 4.11 from Equations 4.8 and 4.11 yields

$$V_d = \left(\frac{\pi}{6}\right)^{\frac{1}{3}} \cdot d \cdot \frac{\phi^{\frac{2}{3}}}{t_{\frac{1}{2}}} \qquad (4.13)$$

Then, from Equations 4.12 and 4.13,

$$V_t \, \phi(1-\phi)^{n-1} = \left(\frac{n}{6}\right)^{\frac{1}{3}} d \, \frac{\phi^{\frac{2}{3}}}{t_{\frac{1}{2}}} \qquad (4.14)$$

that is

$$\left(\frac{6}{\pi}\right)^{\frac{1}{3}} \cdot \frac{t_{\frac{1}{2}}}{d} \cdot V_t = \frac{1}{\phi^{\frac{1}{3}} (1-\phi)^{n-1}} \qquad (4.15)$$

The final Equation 4.15 was proposed to evaluate ϕ and hence V_d and hence the total time required for phase separation, given the mean drop diameter, terminal velocity and drop rest time for any given system.

The model is of interest since it recognises the major parameters which affect coalescence in an emulsion layer or flocculation zone.

Clearly Equation 4.15 offers a more comprehensive way of deducing the coalescence rate at the interface of a flocculation zone than from single drop rest time values. Thus it may be

suitable for the comparison of relative magnitudes for various systems, although it is questionable whether absolute values may be calculated from it. Agreement between the values calculated from Equation 4.15 and experimental results, may occur if the rest time of the droplets at the interface of a flocculation zone is known and the power (n), on Equation 4.8 for hold-up or void space fraction in a bed of solid particles is applicable to distorted liquid drops or a correlation for (n) for liquid drops is available.

b. An Idealised Analysis of a Horizontal Wedge (79)

Jeffreys et al (79) have proposed a model to determine the dimensions of the wedge produced in continuous horizontal gravity settlers in liquid - liquid extraction processes and effluent treatment. This was based upon observations in a laboratory rectangular settler in which the emulsion was distributed as a heterogeneous wedge between the two phases as shown in Figure 4.1. Droplet behaviour in the wedge included drop-interface coalescence, at the bulk dispersed phase boundary and drop-drop coalescence. The residence time or life of any droplet is controlled by these two processes.

The wedge described has been drawn in three dimensional oblique sketch in Figure 4.1 to demonstrate the areas and volume

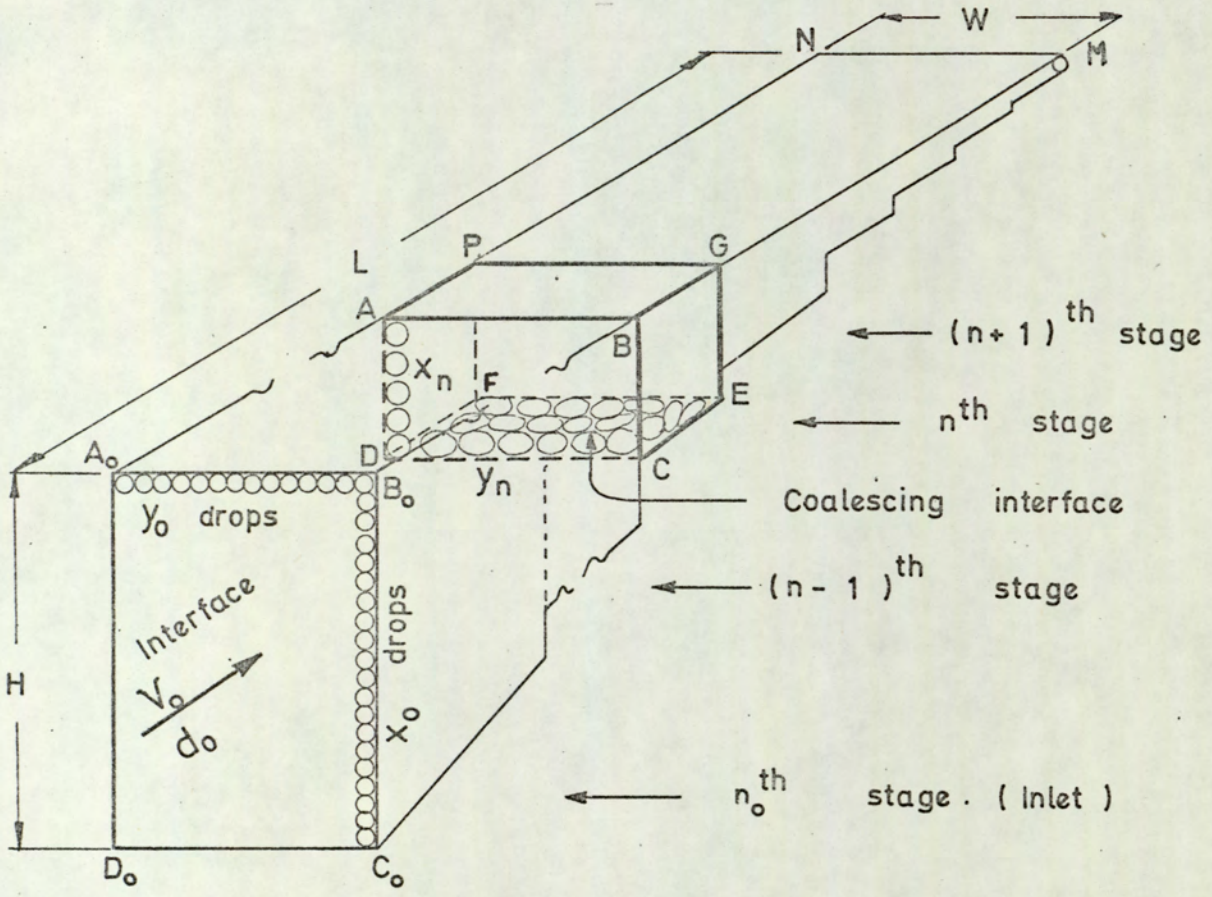

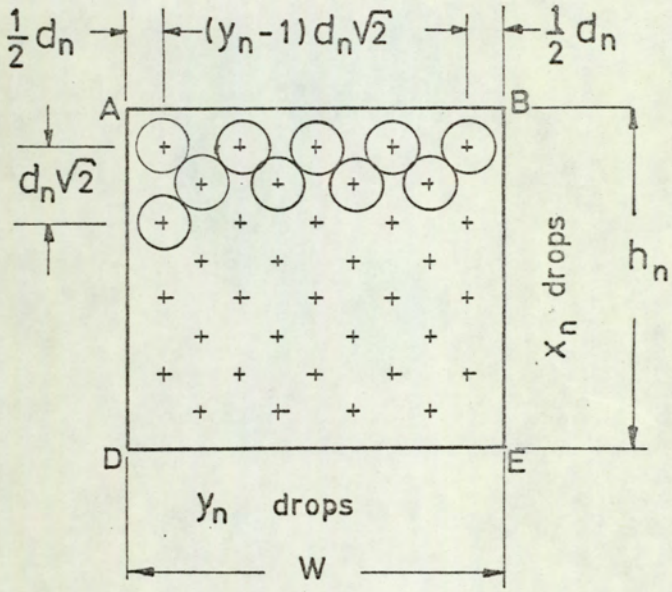

n^{th} stage cross section perpendicular to feed line and horizontal plane

FIG. 4.1 SHAPE OF AN IDEALIZED WEDGE IN A HORIZONTAL SETTLER (79)

in which the droplets behaviour is considered.

The wedge overall boundary volume is enclosed by $A_oB_oC_oD_oMN$. The top area, A_oB_oMN, of the wedge is not involved in drop interface coalescence under the assumed conditions. Because the heavy phase is dispersed this area is the boundary with the less dense phase or bulk continuous phase, corresponding to the bottom of the flocculated zone with rising drops. In other words, if the feed from the mixer was fed to the settler vertically, this area would be the droplet inlet side. In this case however it has no function since the droplets were assumed to be fed horizontally from the vertical face area of ABCD with boundary condition $A_oB_oC_oD_o$.

The upper boundary face A_oB_oNM is a horizontal surface, quite clearly distinguishable in practice, and hence easier to measure. This area of the total wedge was equal to (LW).

The lower overall surface of the wedge was C_oD_oMN. This was inclined from the horizontal at an angle of θ and all drop-interface coalescence occurred at this interface. Therefore in the elementary volume this boundary area corresponds to the area CDEF.

Drops inlet to the wedge occurred from the $A_oB_oC_oD_o$ vertical face as mentioned earlier.

The total volumetric flow V_o at the inlet contained n_o droplets at an initial diameter d_o and packing efficiency η_o.

The area $A_oB_oD_oC_o$ at the inlet was (1 x H) for a unit width of the wedge. In the elemental volume the droplet inlet area was ABCD at a distance 1 from the inlet, and was similarly equal to (1 x h) for a unit width. The droplet inlet area at the other end of the wedge (line MN) was assumed to approach to a single layer of droplets. The vertical face area for the drop will then be equal to (1 x d), i.e. (h) approaches a single drop height. The vertically projected area at which a drop coalesced with the bulk dispersed phase was (1 x d).

In the idealised analysis of a horizontal wedge, the main assumptions of Jeffreys et al (79) were that,

i. The droplets within the wedge form a hexagonal close packing or face-centred cubic configuration.

ii. The inclined edge of the coalescence wedge approximates

to a straight line.

iii. There is no distribution of coalescence time irrespective of whether coalescence is drop to drop or drop to interface.

iv. The coalescence process takes place step-wise. If one row of droplets coalesces with the interface, the remaining droplets in the adjacent rows coalesce together and their number is reduced by a half.

v. Drops are rigid and spherical.

vi. Inlet drop sizes are all equal.

The wedge shape was idealized to a general form of having a "stepped" profile in which pairs of droplets coalesce together while the droplets adjacent to the coalescing interface passed into the bulk of the dispersed phase. Each step was considered to be a coalescence stage within which the coalescence process occurred; a number balance is then performed between two consecutive stages. The assumed face centered cubic configuration of the droplets within the wedge resulted in a distance of $d\sqrt{2}$ between drops of equal diameter, resident in rows and column in each stage. The number of droplets in a row and a column of a stages were, in turn, written by this assumed packing configuration related to inlet drop diameter. Finally a first order finite difference Equation was obtained as summarized below. The number balance between two

consecutive stages was,

$$x_{n+1} \cdot y_{n+1} = \frac{x_n y_n - y_n}{2} = \frac{y_n}{2}(x_n - 1) \qquad (4.16)$$

(Assuming that at stage n, one row adjacent to the interface or y_n drops coalesce with the interface and the remainder undergo interdrop coalescence in pairs.)

The cubic face-centered droplet configuration within the wedge of width (W), is related to the number of droplets in a row, y_n, and their diameter (d_n) by,

$$y_n = \frac{W - 0.29\, d_n}{1.41\, d_n} \qquad (4.17)$$

The relation between the drop sizes of two consecutive stages was related, on the basis of each pair of droplets undergoing drop-drop coalescence, thus reducing the number to half, at each successive stage,

$$\frac{2\pi}{6} d_n^3 = \frac{\pi}{6} d_{n+1}^3 \qquad (4.18)$$

which on the inlet drop size basis will be,

$$d_n = 2^{n/3} d_o \qquad (4.18a)$$

Substituting (d_n) in Equation 4.17 gave,

$$y_n = \frac{W - 0.29(2^{n/3} d_o)}{1.41\,(2^{n/3} d_o)} \qquad (4.19)$$

A similar expression for the number of drops in a vertical column at stage n is obtained by a similar derivation yielding,

$$x_n = 1.41 \frac{h_n}{d_n} - 0.41 \qquad (4.20)$$

However, the present investigator, considering the half diameter gaps existing between the settler walls and the droplets derived alternately,

$$x_n = \frac{h_n}{1.41\ d_n} + 0.29 \qquad (4.20a)$$

Thus y_n and y_{n+1} in Equation 4.16 could be eliminated by means of Equation 4.19. Finally a first order finite difference Equation was obtained,

$$2E\left[W - 0.29\ (2^{\frac{n+1}{3}}\ d_o)\right] x_n - 2^{\frac{1}{3}}\left[W - 0.29(2^{\frac{n}{3}}\ d_o)\ x_n\right]$$

$$+2^{\frac{1}{3}}\left[W - 0.29\ (2^{n/3}d_o)\right] = 0 \qquad (4.21)$$

where,

W = The width of settler or coalescence wedge.

n = Number of the coalescence stages

d_o = Diameter of droplet in the inlet dispersed stage

x_n = Number of droplets in vertical column of stage n

E = Finite difference operator.

The complete solution of Equation 4.21 was,

$$x_n = A^1 \frac{1}{2^{\frac{n}{3}}}\left[\frac{W - 0.29(2^{\frac{n}{3}}d_o)}{W - 0.29(2^{(n+1)/3}d_o)}\right]^n - \frac{1.26W}{0.74W-0.37(2^{n/3}d_o)}$$

$$+ \frac{0.29\ (2^{n/3}d_o)}{W - 0.44(2^{n/3}d_o)} \qquad (4.22)$$

where A^1 is an arbitrary constant. Since $W \gg 0.29\ d_n$, however, this can be further simplified to

$$x_n = A\ 1.59^{-n} - 1.73 \qquad (4.23)$$

where A was the final arbitrary constant to be evaluated from the boundary conditions. At the boundary conditions, when n = o, the number of droplets in a vertical column will be x_o, then from Equation 4.23,

$$A = x_o + 1.73 \qquad (4.24)$$

Substituting this value of A into the general Equation 4.23,

$$\frac{x_o + 1.73}{x_n + 1.73} = 1.59^n \qquad (4.25)$$

Because x_n is equal to 1.0 at the tip of the coalescence wedge, the number of coalescence stages n, can be evaluated from Equation 4.25 providing an estimate is made of the number of droplets in a vertical column at the inlet stage x_o.

The authors suggested means of predicting the number of longitudinal rows of droplets, x_o, at the inlet stage given the total feed rate, V, the volume fraction of the dispersed phase in the feed to the settler, a, the inlet drop size, d_o, and the settler width.

Assuming equi-sized inlet drops, the total number fed to the settler per unit time $\frac{6aV}{nd_o^3}$ is equal to the number of

longitudinal rows of droplets formed per unit time multiplied by the total number of droplets in the first stage of a unit width of wedge. If the actual velocity of the wedge is V, then the number of droplets entering the settler per unit time is,

$$\frac{6aV}{\pi d_o^3} = x_o\, y_o\, (1.41\ \frac{v}{d_o} - 0.41) \qquad (4.26)$$

For the first stage, the number of droplets in a horizontal row across the width at right angles to the direction of flow, y_o, is from Equation 4.17,

$$y_o = \frac{W - 0.29\ d_o}{1.41\ d_o} \qquad (4.17a)$$

Substituting y_o from equation 4.17a into Equation 4.26 yields,

$$x_o = \frac{8.46\ a\ V}{\pi\ d_o\ (W-0.29\ d_o)(1.41\ v-0.41)} \qquad (4.27)$$

The number of stages, n, can hence be predicted from Equations 4.25 and 4.27 since at the tip of wedge $x_n = 1$

$$n = \frac{1}{1.59} \log \frac{8.46\ a\ V}{2.73\ n\ d_o(W-0.29\ d_o)(1.41\ v-0.41)} + \frac{1.73}{2.73} \qquad (4.2$$

The length of the coalescence section of the wedge can then be calculated from

$$L = n\ v\ T \qquad (4.29)$$

where T is the idealised coalescence time.

This model was tested by the investigators with data obtained from a laboratory mixer-settler using the system water dispersed in kerosene. The ratios of the mean droplet size at some distance from the inlet to the initial size were compared with the predicted values from the model. The best possible counts of droplets in a vertical column, obtained from photographs, were also compared with those calculated from the formulae. It was concluded that these gave reasonable agreement.

However the proposed model predicts not only the overall length of the wedge, but also the length of the coalescence section. Difficulties and discrepancies associated with the model are discussed in the original reference. They are attributed mainly to the variation in velocity and coalescence time measurements, and to the deformation and distortion of the droplets in the wedge, causing deviations from the assumed face centered cubic configuration.

c. A Differential Analysis of a Horizontal Wedge (80)

The earlier model discussed in (b) was subsequently modified by Jeffreys et al. (80). The same data were used to verify a 'differential model'.

Description of the wedge was the same as demonstrated

in Figure 4.1 and explained in coalescence stage model (Model 6). The parameters and the dimensionsused in this model are shown in Figure 4.2.

From the detailed explanations given of the behaviour of the droplets (80), the main assumptions are,

i. The droplets are spherical and rigid.

ii. The volumetric packing efficiency is constant and equal to a mean average value for the whole wedge.

iii. The surface packing efficiency is constant and equal to a mean value on the boundary of coalescing interface and bulk dispersed phase.

iv. The droplets move only axially and at constant velocity. (Horizontally in this case). The vertically downward motion is due only to drop-drop coalescence behaviour.

v. The inclination of the coalesing interface from the horizontal is so small that it can be considered zero (Sec $\theta \rightarrow 1$). Therefore, in the limit, DE distance approaches BG or for the overall dimensions D_o M approaches B_o M distance (L dimension).

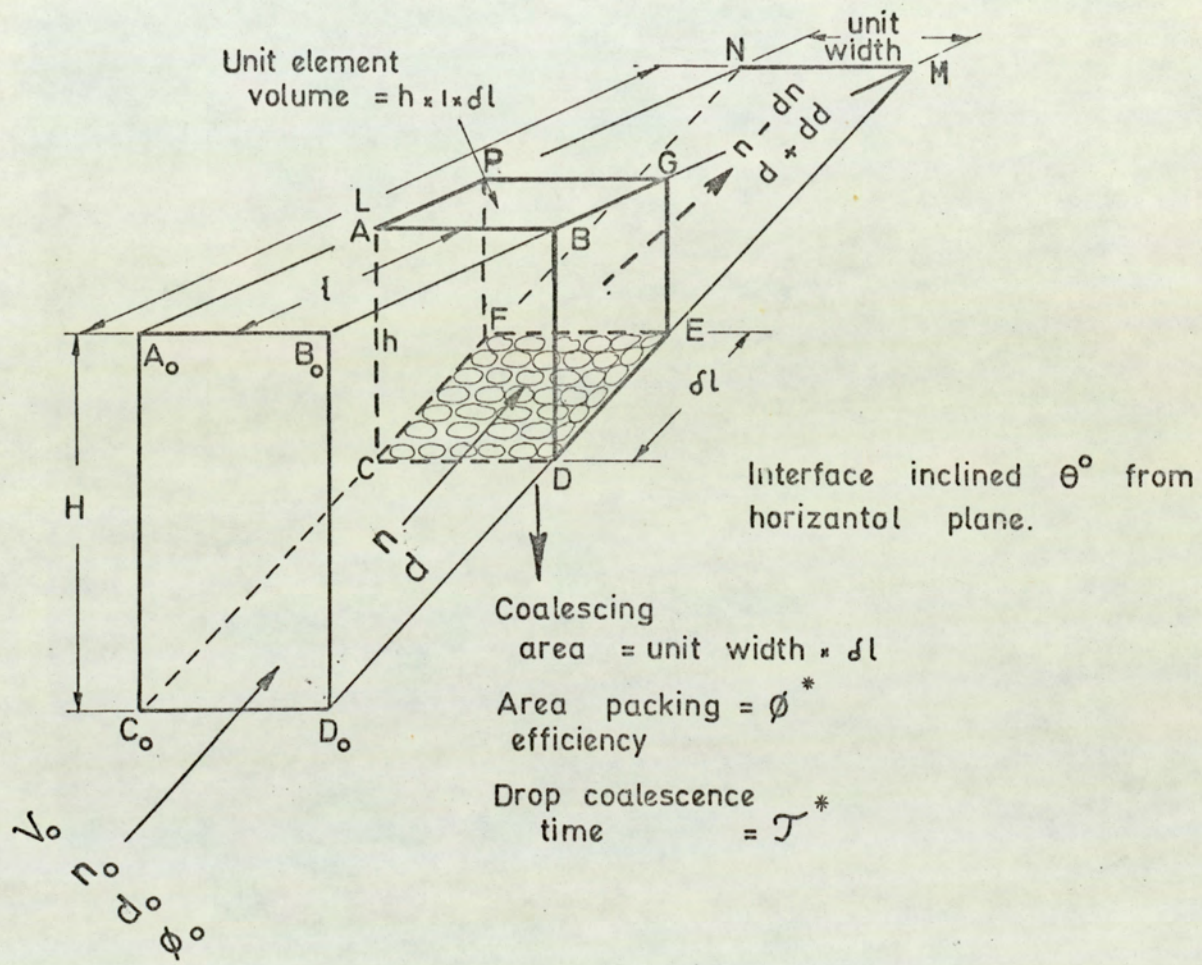

FIG. 4.2 THE WEDGE DIMENSIONS AND PARAMETERS FOR DIFFERENTIAL MODEL (80)

A small volume increment of the wedge is considered at a distance l, from the inlet along the total length, L, of the wedge, and having a unit width and height h^1.

A material balance is taken for the dispersed phase entering and leaving this small volume of element, vertical to the wedge length (ABCDEFGP). At the boundary between the bulk interface and the wedge, (CDEF) drop-interface coalescence is assumed to occur at a mean drop-interface coalescence time, T*. Further assumptions include the existence of rigid drops and a constant area packing efficiency, η^*. A differential equation expressing the drop size, d increase and inlet number, n decrease, through the element due to drop-drop coalescence was derived. After simplification and rearrangement this has the form,

$$\frac{3}{d}\frac{dd}{dl} - \frac{1}{n}\frac{dn}{dl} + \frac{4}{\pi}\frac{\eta^*}{T^*}\frac{1}{nd^2} = 0 \qquad (4.30)$$

Similarly, since the number of drops entering the element must be balanced by the number of drops leaving, plus the number of drops coalescing at the interface and half the number of drops coalescing together by a drop-drop coalescence mechanism. A drop number balance gives a second equation,

$$\frac{dn}{dl} = \frac{1}{d^2}\left(\frac{3}{n}\frac{nh^1}{Td} + \frac{\eta^*}{T^*}\right) \qquad (4.31)$$

where,

d = Inlet drop diameter, L

n = Number of drops/second/width, T^{-1} L^{-1}

T = Mean drop-drop coalescence time, T

T* = Mean drop-interface coalescence time, T

η = Volume packing efficiency of drops in wedge

η^* = Area packing efficiency of drops at the interface

l = length of wedge, L

h^1 = Height of wedge, L

These two equations were proposed to describe the general situation at steady conditions by accounting for drop-interface and drop-drop coalescence within the wedge. This assumes that,

i) Time and position average of the volume packing efficiency in the wedge,

ii) Area packing efficiency at the interface,

are acceptable.

The listed assumptions which are questioned by the authors themselves, appear to be the only inperfection in this unique treatment. Clearly these merit further study to clarify the mechanism of phase separation for primary dispersions as does any relationship between drop-drop and drop-interface coalescence time for varying drop sizes.

The discussion of authors (80) illustrates the involved mechanisms of primary phase separation phenomena. As has been pointed out by the authors, it is implicit in the assumptions that rearrangement of drops in the vicinity of a coalescence step both at the interface and within the bed is instantaneous. Intuitively this would be expected and visual observations, described later, confirm this to be so. However it is further assumed that local disturbances in the vicinity of a coalescence step do not seriously affect the coalescence mechanism. This is at variance with the single drop hydrodynamics discussed earlier.

In the event application of such an analysis is dependent upon accurate coalescence time data. Sources of such data, albeit mainly for drop-interface coalescence, are given in Sections 2 and 3 where its reliability and difficulties in extrapolation are also discussed.

Variation of the coalescence time is to expected due to the effect of neighbouring drops. Therefore, even though simple drop coalescence time correlations may help to predict the coalescence times in swarm of drops, or will indicate the general tendency, or relative magnitude for comparison, a real general correlation of coalescence times is still lacking in the literature.

Utilising the two correlations for a drop-drop and drop-interface coalescence time, surprisingly both came out equal, a final equation relating the dispersed flow rate, inlet drop size, packing efficiency and droplets residence time to the wedge length was derived as summarized in the following steps:

From a material balance for dispersed phase,

$$3\,\frac{dd}{dl} - \frac{1}{n}\,\frac{dn}{dl} + \frac{4\,\eta_c^*}{\pi T^* n\, d^2} = 0 \qquad (4.32)$$

From a drop number balance,

$$\frac{dn}{dl} = \frac{1}{d^2}\left(\frac{3nh}{\pi T d} + \frac{4\,\eta_c^*}{\pi\, T^*}\right) \qquad (4.33)$$

Substituting Equation 4.33 in 4.32,

$$\frac{dd}{dl} = \frac{n\,h}{n\,\pi\,T\,d^2} \qquad (4.34)$$

At any position of the wedge

$$n = \frac{6v\,h\,\eta}{\pi\, d^3} \qquad (4.35)$$

Substituting 4.35 in 4.34, gives,

$$\frac{dd}{dl} = \frac{d}{6v\,T} \qquad (4.36)$$

Smith (59) has correlated that,

$$T \propto f.\, d^{1.5} \qquad (4.37)$$

Lawson (19) has correlated that,

$$T^* = f. d^{1.46} \qquad (4.38)$$

Thus,

$$T \approx T^*$$

was assumed. However this seems hardly convincing.

Then from overall process and initial conditions

$$V_o = \frac{1}{3} \eta^* \int_o^L \frac{d}{T^*} \cdot dl \qquad (4.39)$$

From Equation 4.36 and with the boundary conditions, when $L = 0$, $d = d_o$; and $L = L$. $d = d$, upon integration yields,

$$V_o = 2 \eta^* V (d - d_o) \qquad (4.39a)$$

Since drop diameter d is not constant, being a function of the wedge length, drop-drop coalescence time and inlet drop size as derived in Equation 4.36, it can be evaluated for the boundary conditions of

$$l = o \qquad d = d_o$$

$$l = L \qquad d = d_n$$

Therefore, rearrangement of Equation 4.36 and substitution of 4.37 yields,

$$d = \left(d_o^{1.5} + \frac{L}{4 \pi f}\right)^{\frac{2}{3}} \qquad (4.40)$$

Finally substituting Equation 4.40 into 4.39a, gives

$$V_o = 2 \eta^* r \left(d_o^{3/2} + \frac{L}{4 r f}\right)^{\frac{2}{3}} - d_o \qquad (4.41)$$

It has been reported that this final Equation 4.41 verified the experimental data obtained (80). However, it still requires to determine drop residence time in the wedge. Therefore, further improvement seems necessary to make it more useful for practical purposes.

d. A Differential Analysis of a Vertical Zone (41)

The model proposed describes the behaviour of drops within a dispersion band formed in a vertical settler. The local average drop diameter and local rate of coalescence in the dispersion band is considered to be a function of the position in the bed. In the derivation of the model the following additional assumptions are made,

i. That the drops travel through the dispersion band towards the interface in approximately plug flow, moving relative to their neighbours only as the result of drop-drop coalescence with adjacent drops.

ii. That the incidence of drop-drop coalescence involving three or more drops simultaneously is negligible.

iii. That the rate of coalescence between drops of any given size is dependent upon their diameters.

A small incremental volume in the dispersion was considered at a distance h from the droplet entry. The dispersed phase flow rate per unit cross sectional area of the bed, V_d, was expressed as,

$$V_d = \frac{\pi}{6} n d^3 \qquad (4.42)$$

The volumetric flow rate at any cross section of the bed was assumed constant and a differential equation written as,

$$\frac{dV}{dh} = \frac{\pi}{6}\left(d^3 \frac{dn}{dh} + 3\,nd^2 \frac{dd}{dh}\right) = 0 \qquad (4.43)$$

A number balance for the droplets again led to,

$$\frac{dn}{dh} = \frac{36}{d^3} \cdot \frac{\eta}{T} + \frac{16}{\pi} \frac{\eta^*}{D_p d^2 T^*} \qquad (4.44)$$

Solutions of these differential equations with boundary conditions were derived by overall volume balances at steady state to give the general solutions. The two cases of wetting and non-wetting by the dispersed phase were considered.

For the "wetting" condition,

$$V_d = \frac{2}{3} \eta^* \frac{d}{T^*} + \frac{8}{3D_p} \eta^* \int_0^H \frac{d}{T^*}\, dh \qquad (4.45)$$

For the "non-wetting" condition,

$$V_d = \frac{2}{3} \eta^* \frac{d}{T^*} \qquad (4.46)$$

The particular solutions of these equations is dependent upon the nature of the drop-drop and drop-interface coalescence times. Various theoretical forms of the coalescence time functions were discussed, i.e.,

a. Drop-interface coalescence time is an independent constant with drop diameter,

b. Drop-interface coalescence time is a function of drop diameter.

c. Drop interface coalescence time is a function of drop diameter and the residence time in the bed.

No general conclusions were drawn regarding agreement between the model and experimental results.

4.5. Discussion of the Models

In developing the four models described in Section 4.4.4 certain, or all, of the following assumptions were made,

i. The droplets within the heteregenenous zone are spherical and rigid.

ii. The packing efficiency can be represented by a mean value.

iii. Equivalence or proportionality between single drop at a plane interface rest times and those in drop swarms.

iv. Inter-droplet and drop-interface coalescence occur independently.

The fact that after a certain bed height droplets undergo distortion, thus restricting the validity of the models, was a common observation (41, 78, 79, 80).

Furthermore, a constant packing efficiency would not normally be expected throughout a bed. If this were so, since continuous phase film thickness and drainage rate are major factors affecting coalescence rate, similar rates would exist at different points; this is contrary to the observed situation.

Assumption (iii) requires more support than that offered by Smith (41) who stated that drop coalescence times in a swarm were inversely propoertional to drop diameter to the 1.5 power. Robinson and Hartland (72) have already reported that larger film

thicknesses, and longer coalescence times, are associated with large drops. Further research, covering a range of systems and conditions, is required into this aspect.

Assumption (iv) is dependent upon the validity of assumption (iii). Clearly however, when interdroplet coalescence occurs, the drops which arrive at interface are of larger diameter; the magnitude of this increase in size will then affect the drop-interface coalescence mode. In addition the rate of coalescence at the interface determines the drop residence times and hence the incidence of interdrop coalescence. Hence there is an inter-relationship between the two modes which must be solved quantitatively.

The fluidization model (78) neglected the effects of interdroplet coalescence.

The idealized coalescence stage (79) is based upon an assumption of a constant regular packing arrangement of droplets which, as discussed earlier, is impracticable. The differential models (41, 80) are in a more advanced stage. Their improvement by the inclusion of other variables, such as packing efficiency as a function of flocculation zone height, would lead to three sets of differential equations requiring simultaneous solution. This is likely to prove very difficult.

Therefore, the use of an average hold-up and the solution of two sets of differential equations solutions may be all that is practicable.

5. COALESCENCE IN PRACTICAL EQUIPMENT

Coalescence in practical equipment may occur either as part of the main process, e.g. in efficient phase separation in a settler, or as part of an ancillary process, e.g. in mass and direct heat transfer equipment and in suspension polymerization reactors, in which it may or may not be desirable. If coalescence effects are deleterious to the main process then equipment is designed and operated so as to minimise interdrop coalescence. This may be achieved, for example, by continuous agitation. Drop-interface coalescence is also avoided unless repeated surface-renewal is required.

Whilst drop-interface coalescence can usually be eliminated from equipment, drop-drop coalescence may always persist to some extent dependent upon process conditions and system properties. However, only intentional coalescence in practical equipment will be considered in this Section. This may be achieved either in certain sections of the equipment or in ancillary equipment i.e. settlers. In either case consideration may be given to the promotion of coalescence by the use of coalescing aids, increasing the potential for interdroplet contact and providing larger areas for drop-interface interaction.

The simplest way of achieving coalescence in any equipment

is to form an interface near the dispersed phase outlet. In spray columns it is usual to provide an enlarged diameter section for this purpose to increase the area of contact between droplets and the bulk dispersed phase. Either a sudden or gradual conical enlargement may be used. Similar designs are used in the more elaborate pulsed, packed or rotary agitated extraction columns. In any application efficient coalescence at this end of the column is essential in order to avoid the wedge extending into the column proper. Drop-coalescence may also be utilized in cases where equipment operates in a stagewise fashion, such as in a cascade type mixer-settler or certain rotary agitated columns. If no separate settling section exists, however, drop-drop coalescence may be promoted in intermediate sections or calming zones, or in baffled regions remote from the agitator, in order to enhance mass transfer by repeated drop coalescence and break-up (88).

Thus coalescence in practical equipment occurs by both the interdrop and drop interface modes. In addition partial coalescence is encountered leading to the production of secondary droplets or a secondary haze. In the following subsections the coalescence phenomena involved in typical equipment designs, viz horizontal and vertical mixer-settlers and agitated systems, and the effect on performance are briefly reviewed. Practical equipment has been extensively reviewed in the literature (88,89). Finally reference is made to the effects of coalescing aids.

5.1. Horizontal and vertical settlers

A wide range of mixer settler designs are commercially available (88, 89, 90). These may be arranged vertically or horizontally with the driving force for fluid flow being either pumping or gravity and with either cocurrent or countercurrent settling. In some types individual agitators are used but in others these are fixed to a common shaft. However, despite these variations, settling or phase separation relies upon the basic processes of droplet flocculation, packing, interdrop and finally drop-interface coalescence. This applies also of course to gravity settlers for liquid-liquid process or effluent streams.

Surprisingly little attention has been given to the development of design procedures for settlers (89). In simple horizontal arrangements the dispersion is distributed from the inlet port in the form of a heteregenous wedge which may reside above or below the interface dependent upon the relative densities of the dispersed and continuous phases. The wedge should not cover the whole area but extend over only 70% of the length of the interface in order to accommodate fluctuations during normal operation or changes in throughput. The wedge dimensions are determined by the difference between the input rate of the emulsion and the rate of coalescence of droplets in the

wedge with the interface. However most of the available design procedures are based either on hydraulic balances of the two phase flows or upon empirically determined mean residence times. Hence the procedure proposed by Jeffreys et al (80) is the only one to take account of the physical processes governing separation, viz interdrop and drop-interface coalescence, using experimentally determined drop interface rest times, albeit by means of the idealised model given in Section 2.4.

The use of mechanical aids in order to promote coalescence and phase separation in settlers has long been practiced (88, 89). Thus a vertical impingement baffle is sometimes inserted adjacent to the inlet part in horizontal settlers, and horizontal baffles may serve to preserve laminar flow and to decrease settling distance (88). Baffles fitted either side of the phase inlet slot, to form a rectangular duct, have been used to reduce flow disturbances and promote up to a 30% increase in capacity in a pilot scale settler (39).

Decreased dispersion band widths, and hence increased settling velocities, are achieved in the Lurgi Multi-Tray settler by means of stacked trays to which the dispersion is evenly distributed (91). Similarly coalescing aids may be incorporated in a novel design wherein there is a complete hydraulic separation between mixer and settler (92). Settling rafts have also been proposed (93). Up to the present however no completely successful means, apart from centrifugation, has been reported

for assisting settling (94).

It is clear from the above that settling aids can be used to enhance coalescence rates. However, this is based upon reducing disturbances of flow in the settler and upon increased residence time. Thus there is some doubt as to the validity of the assumptions made in the theoretical derivation of rate Equations regarding the probability of coalescence as a function of the number of interdroplet collisions. Residence time would appear to be a more important factor than the number of collisions.

The modern tendency is to keep the settlers as simple as possible to reduce the cost (88) despite the proven advantages of settling aids.

5.2 Agitated systems

Coalescence rate is one factor affecting the efficiency of mass transfer in agitated systems. Thus a detailed design procedure published for a Rotating Disc Contactor incorporates parameters to allow for coalescence and axial mixing (95,96). The situation in agitated columns is however complex and there is potential for enhancement of mass transfer by continued droplet coalescence and break-up (97, 98). As mentioned earlier it is essential for coalescence to occur at the interface of phase

separation.

In agitated systems drop-drop coalescence may occur in the bulk of the turbulent liquid or at the column wall. Equations, either derived theoretically or empirically, for the coalescence in the bulk liquid and at the column wall are given in literature (97). These are generally based upon frequency of collisions.

The distribution of drop sizes in addition to determining the mode of solute transfer also govern the frequency of drop-drop coalescence, if present (97).

The available data on coalescence in agitated columns is limited (99). Davies et al (100) found that drop-drop coalescence was not significant in a pilot-scale R.D.C with the system kerosene-water. However this was with phase ratios of 12 to 16:1 compared with the 0.5 to 4:1 used in practice. Misek(96) assumed that a dispersion can be characterised by a hydraulic mean drop diameter, and every collision of droplets resulted in coalescence.

Mumford (97) has investigated the extent of interdrop coalescence of various systems in several agitated columns viz R.D.C, Oldshue-Rushton, Scheibel. In the R.D.C. with the three systems, at rotor speeds from 500 to 1000 r.p.m. and with varying flow rates drop-drop coalescence was found to be

insignificant until flow rates approached the flooding point. Conversely in Oldshue-Rushton column a coalescence-redispersion mechanism predominates (97, 101), and a similar effect was observed in the Scheibel column provided the agitator speed was above a minimum necessary to distribute the droplets across the column cross section. Since these findings covered a large range of interfacial tensions of the system material viz 9.7 to 55.4 dynes/cm, they clearly indicate the importance of coalescence phenomena in the design and operation of agitated columns. Thus design procedures involving the assumption of spherical uniform droplets which do not undergo coalescence are generally ill-founded.

Construction material, size of the column, impurities present and system properties and physical conditions are all reported to be important factors affecting coalescence in agitated columns (97).

5.3 Coalescing aids

As discussed in Section 5.1 various mechanical aids and equipment geometries have been found to assist coalescence, albeit for primary dispersions only. Unwanted fine dispersions commonly occur in practice and, apart from baffles, numerous methods are

employed in their separation. These include separating membranes, electrostatic coalescers and various types of packing (88). The aim in all these devices is to reduce the size, and hence the cost of the equipment. Two important phenomena are involved,

a. Coalescence of droplets on solid surfaces (1).

and b. Coalescence of droplets in an electrostatic field (1).

but a review of these is outside the scope of this work.

The utility of knitted mesh packings for the coalescence of primary dispersions was recently studied by Thomas and Mumford (102). They confirmed that for maximum efficiency the coalescer material should be preferentially wet by the dispersed phase, possess a large surface to volume ratio, have interstices small enough to cover the range of drop sizes encountered, and yet cause as low a pressure drop as possible. The common objection to the use of packings as liquid-liquid coalescing aids is that, even with voidages as high as 98 per cent, they may be prone to blockage by any solid present. However, practical results indicate that this objection may be over-ridden by the promotion of the coalescence (99, 102) . Increase in droplet sizes by drop-drop coalescence on the surfaces of the packings have been studied and confirmed by photographic analysis (1). It has been reported that no interdrop coalescence occurred in the bulk fluid (1). High separation efficiency can only be achieved if droplets can approach and adhere to a packing surface and reside

there long enough for coalescence (1).

The following design recommendations have been made (1),

i. Separation of secondary dispersions is more efficient in systems having a high interfacial tension and high density difference.

ii. Systems having a high degree of polarity are extremely difficult to separate.

iii. Packings made up of fine fibres with high surface roughness are most efficient.

iv. The efficiency increases as the fibre diameter decreases over a practical working range.

v. Generally separation increases with increasing bed depth. However in some systems of low interfacial tension redispersion can take place.

vi. Maximum superficial velocity varies with the system, type of packing and bed depth. The maximum reported value is 1.5 cm/sec.

6. EXPERIMENTAL INVESTIGATION

6.1. Introduction

The mechanism of phase separation for dispersions in continous flow has been found to involve close packing of the droplets, following flocculation, and finally coalescence (1). However, with the exception of that of Ryon and Daley (77), all the work described in the literature has been with mixer-settlers of small dimensions. A recent investigation has been reported with a 2-inch diameter spray column (5). Based on this limited work it was concluded that present investigation would be of most value if conducted in pilot scale equipment. Equipment was therefore designed and constructed as described in Section 6.2. The most important section is that containing the flocculation zone and this was studied experimentally using the techniques described in Section 6.3. In order to study the packing of droplets within the flocculation zone an attempt was made to develop an encapsulation technique so as to "freeze" the droplets for subsequent analysis. This is described in Section 6.4.

6.2. Design of the Equipment

A vertical gravity separator was preferred over a mixer-settler unit since the latter have received more attention in

literature. Moreover 'mixers' produce a very wide distribution of drop sizes (88) which may hinder fundamental analysis. Limited work in smaller columns indicated that in order to achieve consistent results wall effects must be eliminated (103). Therefore design of the equipment was based on the following criteria:

i. To construct a vertical gravity separator of the largest size considered practicable having regard to the hold-up and consumption of system materials.

ii. To produce an even distribution of droplet size variable within the range for primary dispersions.

iii. To provide for flexibility in operation and arrangement of the main column sections and ancilliaries for future use.

iv. To facilitate recirculation of the system materials to attain equilibrium and to employ the minimum amount of phase materials.

v. To allow ease of cleaning of the total equipment.

vi. To enable photographs to be taken from the top and sides of the columns.

vii. To distribute droplets as evenly as possible over the whole column cross section and hence the two phase interface.

On this basis 3, 6 and 9 inch diameter glass columns were designed and constructed, the 3-inch diameter column being separated

from the other two to allow flexibility in use e.g. for the encapsulation technique in continuous flow.

6.2.1. Arrangement for counter current operation

By rearrangement of the 6 and 9 inch columns, and slight modifications, a 6-inch column with a 9 inch settler section for operation with countercurrent phase flow was obtained. This arrangement is shown diagramatically in Figure 6.1 and illustrated in Figure 6.3.

Glass sections were preferred to provide visible operation and to facilitate photography and the thorough cleaning known to be necessary. Means were provided for mutual saturation and recirculation of the two phases. Continuous phase was pumped from the aspirator bottles, 13, through the calibrated rotameter, 22, via 3/4 inch copper pipe lines, 14. Needle, gate and quick shutting valves, 20, 21, were installed in order to adjust flow rates, to control interface level as necessary and to enable filling and drainage of the equipment for proper cleaning.

The bottom of the column was covered with a 3/8 inch brass plate, 7, which accommodated the dispersed phase inlet to the distributor, the continuous phase outlet and drains. The distributor plate, 16, was located 6 inch above the bottom of the column from which continuous phase was withdrawn for recycle. The plate type

distributor plate, 16, was located centrally at the bottom of the 9 to 6 inch reducer, 8 so that conical entry of the droplets from the distributor holes facilitated higher throughput of the dispersed phase. Droplets from the orifice holes in the plate were evenly distributed across the 6 inch diameter pipe section, 5. At the end of a 6 x 24 inch pipe section a 6 x 6 inch glass pipe, 2, projected into the 9 inch column feed, 3, to form a weir from the inlet continuous phase, via a copper ring, 28. This is shown in Figure 6.2. A 9-inch pipe section, 1, was used to contain the flocculation zone and bulk dispersed phase and siz 7/16 inch diameter holes were drilled in this, using an ultrasonic drill, to serve as pressure taps, 24, and sampling points.

A 9-inch column feed, 18 was placed on the top of 9-inch section, 1, to allow the bulk dispersed phase to overflow and maintain a constant head above the flocculation zone. This allowed better adjustment of the flow rates. The top section of the column was covered with a brass plate containing a 6-inch optically flat glass plate, 10. This enabled photographs to be taken from above the dispersion bands. Three $\frac{1}{2}$ inch outlets were provided for syringing out the samples for hold-up determination, 25, for a thermometer, 29, and vent. Dispersed phase from the top of column returned by gravity to the dispersed phase storage aspirator

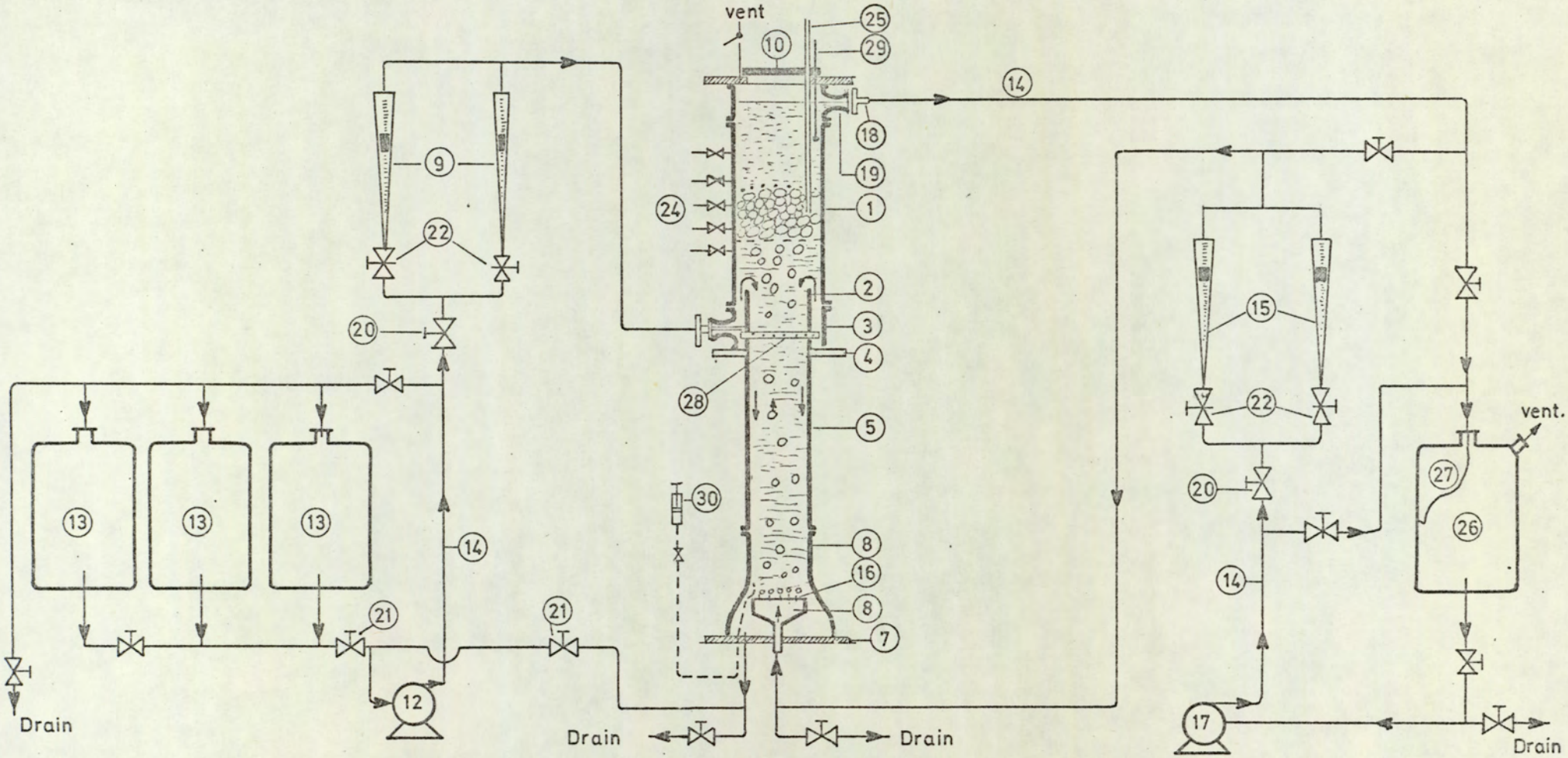

FIG. 6.1 FLOW DIAGRAM OF EQUIPMENT ARRANGEMENT FOR COUNTER CURRENT OPERATION – 6 inch column, 9 inch settler section

LEGEND FOR FIGURES 6.1 and 6.5

Number	Item
1	Glass pipe section; 9" dia. x 18", vertically spaced 3/8" ultrasonically drilled holes.
2	Glass pipe section, 6" dia. x 6".
3	Glass feed pipe, 9" dia.
4	Brass supporting plate, 14" x 14" size, 3/8" thick, seat for item 2, circular hole at the middle at 6" glass dia.
5	Glass, 6" dia. x 18".
6	Glass reducer, 9" x 9"
7	Brass supporting plate, 1" dia. hole at the centre, two $\frac{1}{2}$" holes at sides, two 3/8" holes.
8	Distributor reservoir.
9	Rotameters, Rotameter Mfg. Co. No.7 and 18, 24, replaceable floats, stainless steel.
10	Optically flat, 6" dia. circular glass.
11	Brass top cover plate, 14" x 14" size $\frac{1}{2}$" less in diameter than item 10, 3/8" and $\frac{1}{2}$" holes.
12	Centrifugal pump. ex Stuart-Turner Co., No.12, stainless steel case and impeller, all seals and gaskets replaced with p.t.f.e, 40gph capacity with 5 ft suction head, 20 ft. discharge head.
13	Glass aspirator bottles, 20 litres capacity
14	Copper pipes and brass fittings, $\frac{3}{4}$" and $\frac{1}{2}$" sizes.
15	Rotameters, as item 9.
16	Distributor plate, see Table 6.1.
17	Centrifugal pump, as item 12.
18	Brass and copper flange.
19	Quick-shut off valve, $\frac{3}{4}$" bronze, ex Crane Co.
20	As Item 19.
21	Gate valve, $\frac{3}{4}$" brass, all seals replaced with p.t.f.e. ex Crane Co.
22	Needle valves, ex Crane Co., Bronze, $\frac{3}{4}$" and $\frac{1}{2}$".
23	As Item 22.

Legend for Figure 6.1. (Continued)

Number	Item
24	Parts for manometer connections and taps 3/16" holes with $\frac{1}{4}$" taps, p.t.f.e. gaskets both sides.
25	Syringing tube, glass 9mm o.d.
26	Glass aspirator bottle, 20 litres capacity
27	Glass dip pipe, 1" dia. end bend as shown to minimise turbulence and air entrainment
28	Copper ring for continuous phase inlet, 3/8" dia. to fit between 6" and 9" glass pipe section, Item 1 and Item 2, 1/8" holes drilled outward and distributed evenly
29	Thermometer
30	Single drop introduction assembly; syringe, connection tube, tap, nozzle etc.
31	Glass, column head 6" x 1" x $1\frac{1}{2}$"
32	Glass pipe section 6" dia. drilled hole of 3/8" dia. at the middle for syringing assembly.
33	Glass pipe section 9" dia.
34	P.T.F.E Bellows, 1" dia., ex Q.V.F

NOTE: 'All glassware was of standard Q.V.F Ltd. Manufacture'.

'All glass-glass and glass-metal connections were also standard, Q.V.F. fittings with p.t.f.e. gaskets'

FIG.6.2 WEIR ASSEMBLY FOR CONTINUOUS PHASE CIRCULATION: (Not in scale)

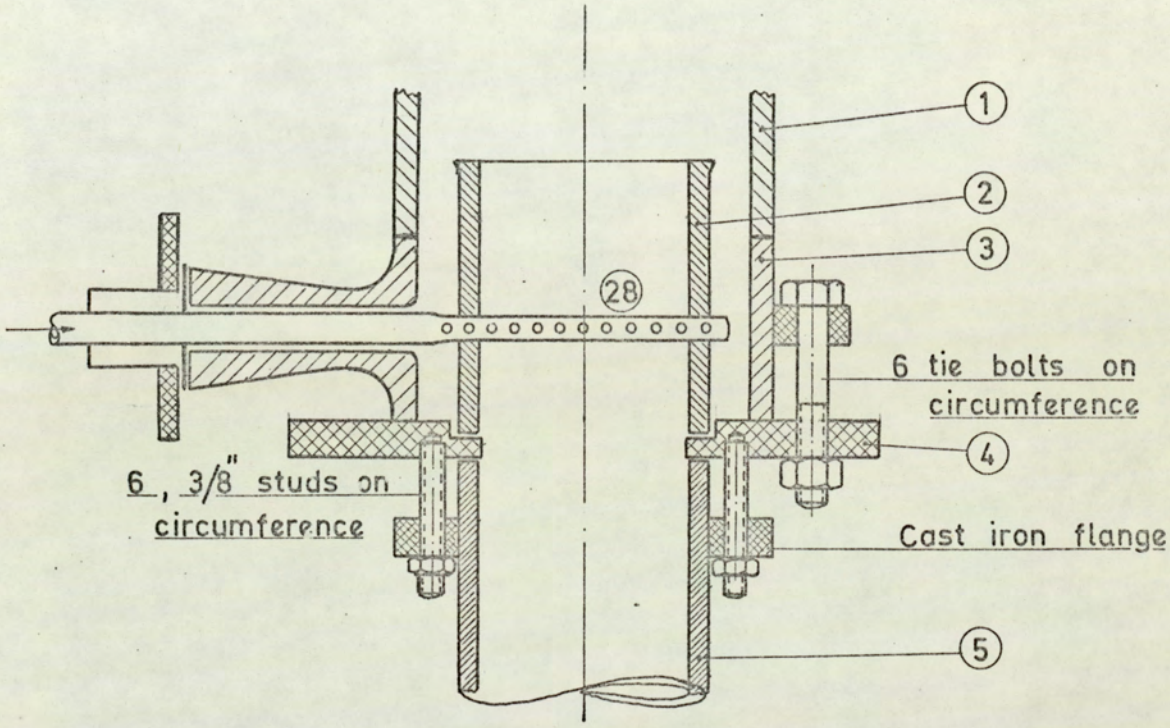

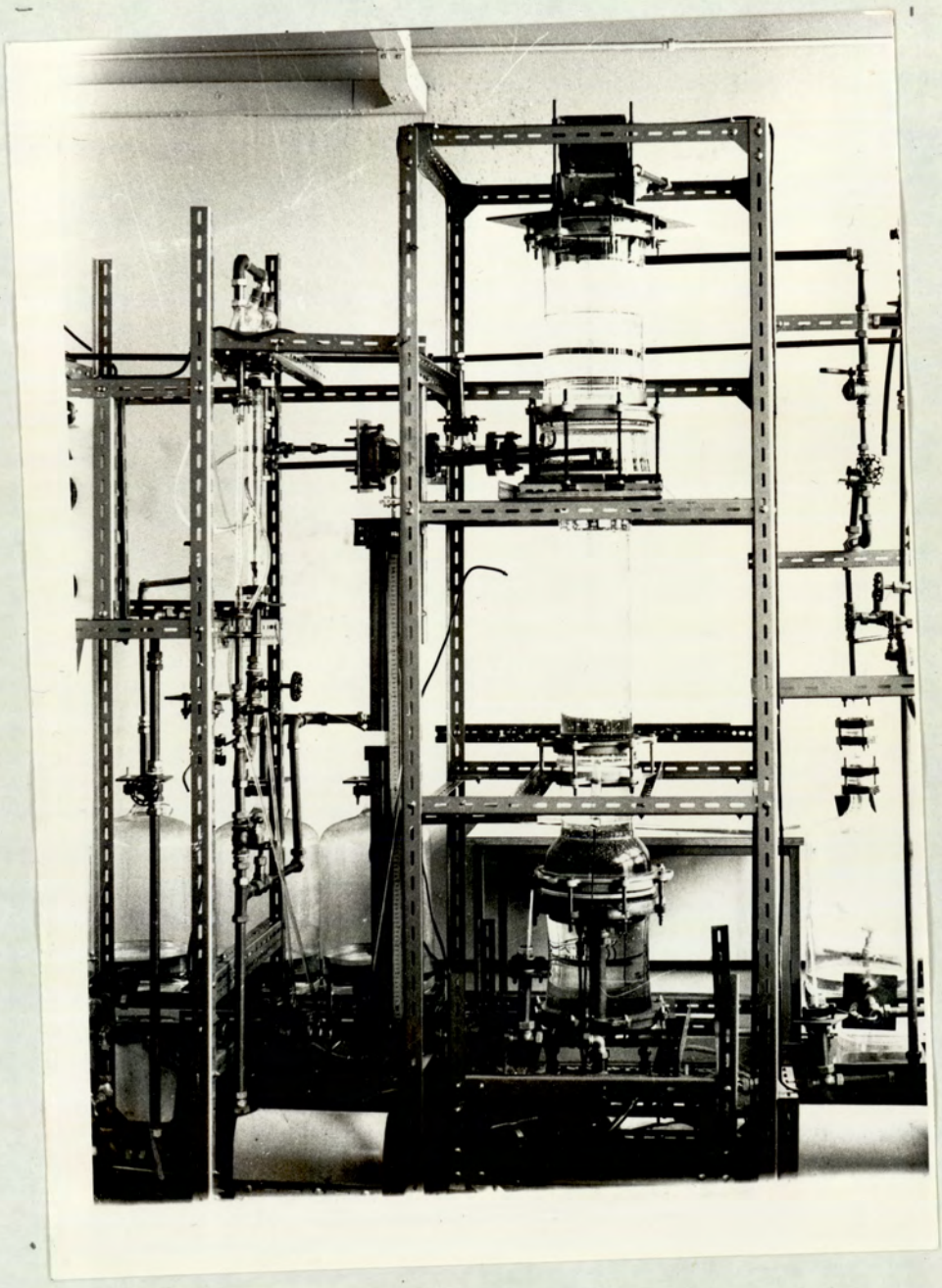

Figure 6.3 Arrangement of the equipment for countercurrent operation

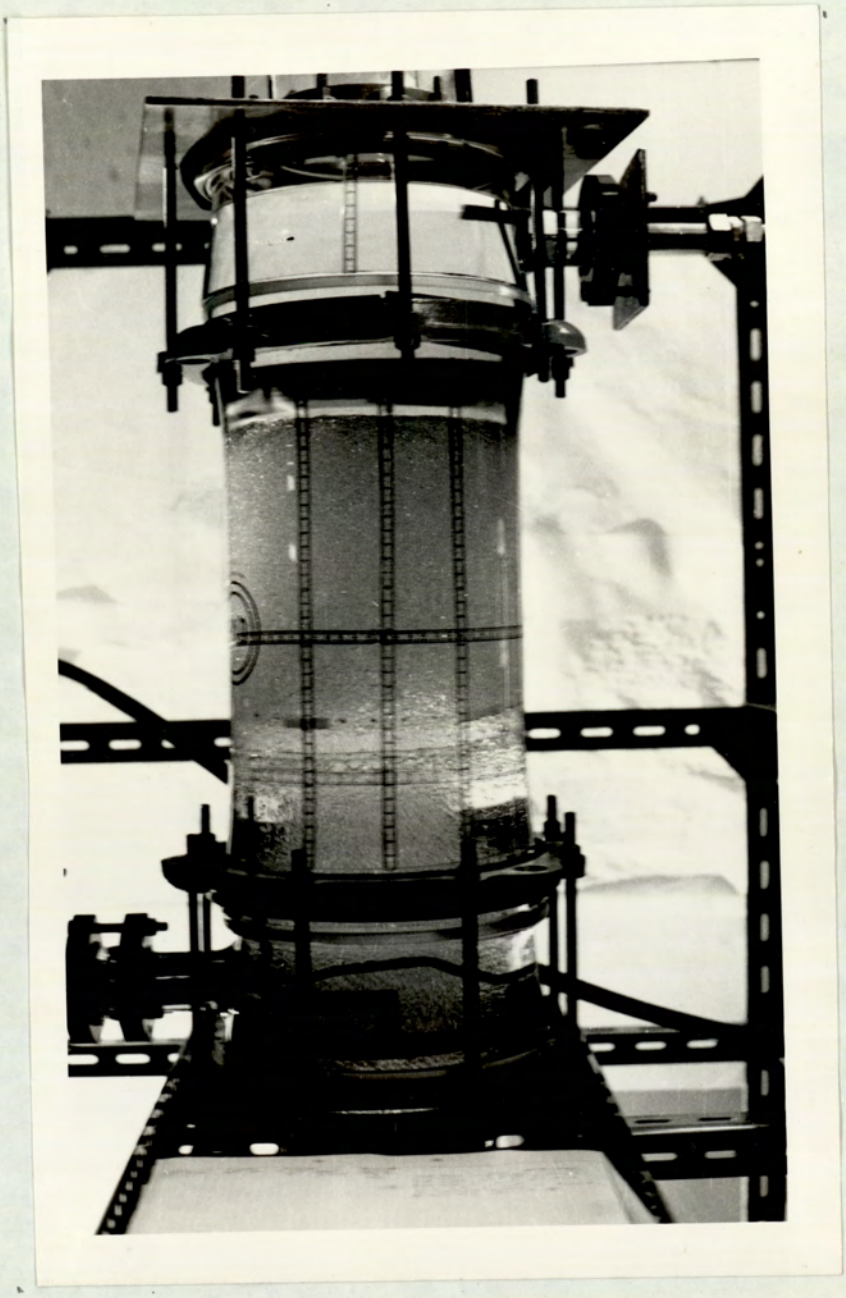

Figure 6.2.b. Weir assembly, 9 inch column, System toluene-water, d_n = 1.6 mm.

(Note: This illustrates the effect of wall contamination due to prolonged operation with toluene, described in Sections 7.2 and 7.3)

bottle, 23 and recycle was maintained by centrifugal pump, 17, to the distributor. The inlet from the pump was raised above the column level to provide a loop seal.

6.2.2. Equipment for operation with a stationary continuous phase, 6 and 9 inch columns

The arrangement is shown diagramatically in Figure 6.5 and illustrated in Figure 6.6. The recycle line for the dispersed phase and the continuous phase ancilliaries were the same as described for countercurrent operation. Continuous phase was introduced into the column from reservoir, 13, bottom by means of the pump, 12.

The main difference between 6 and 9 inch columns was in the position of the distributor plate; in the 9-inch column it was fixed onto a small reservoir, 8, but in the 6-inch column it was placed between two sections, 31 and 32. This enabled the plates to be used interchangeably. The use of a column head, 32, in the 6-inch column enabled conditions below the plate to be observed and any scum accumulated at the phase boundary was drained out from this region. This minimised scum formation at the boundary of flocculation zone and enabled the column to be operated for longer periods without contamination.

Syringing assembly for single and coloured drop was connected

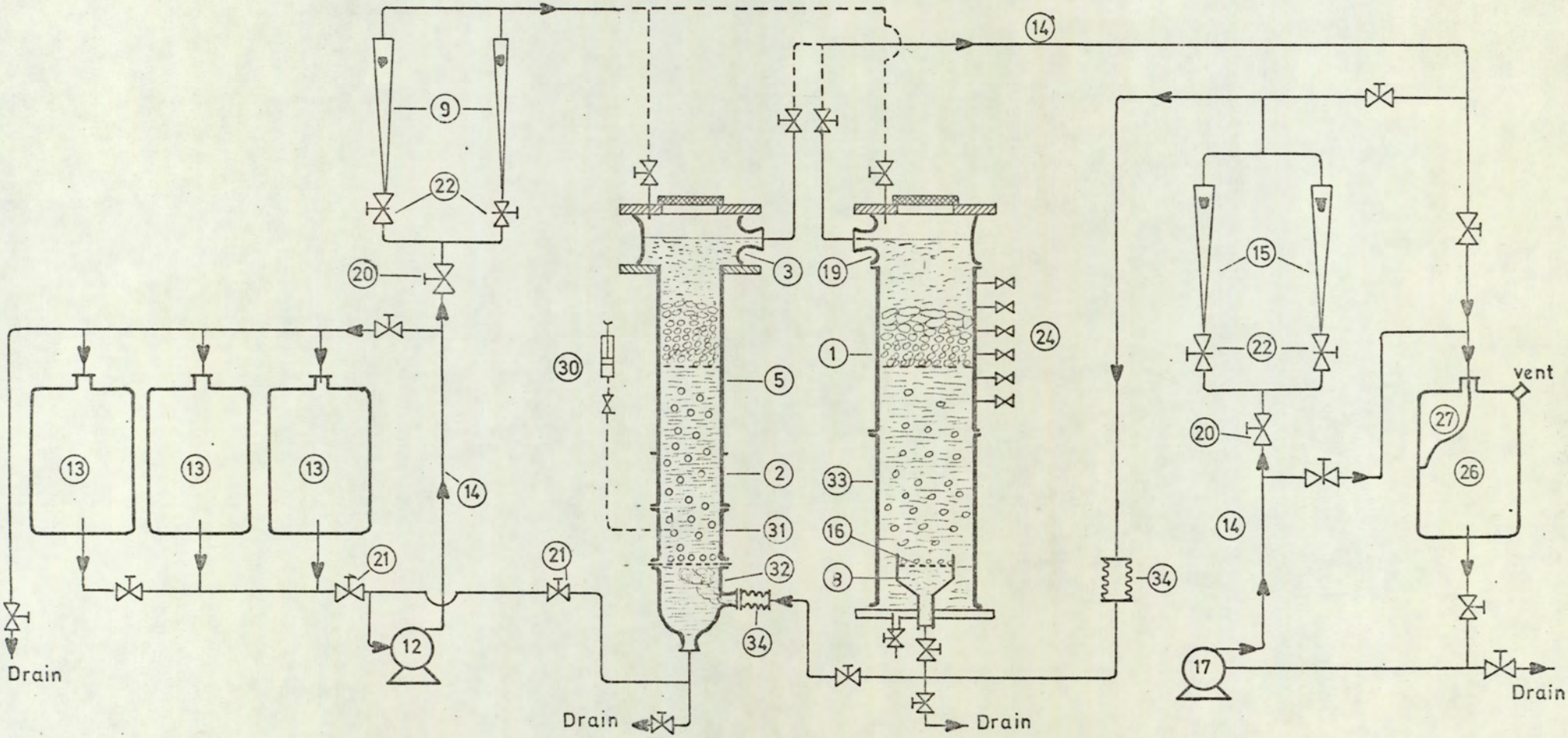

FIG. 6.5 FLOW DIAGRAM OF EQUIPMENT ARRANGEMENT FOR STATIONARY CONTINUOUS PHASE OPERATION

(6 and 9 inch columns)

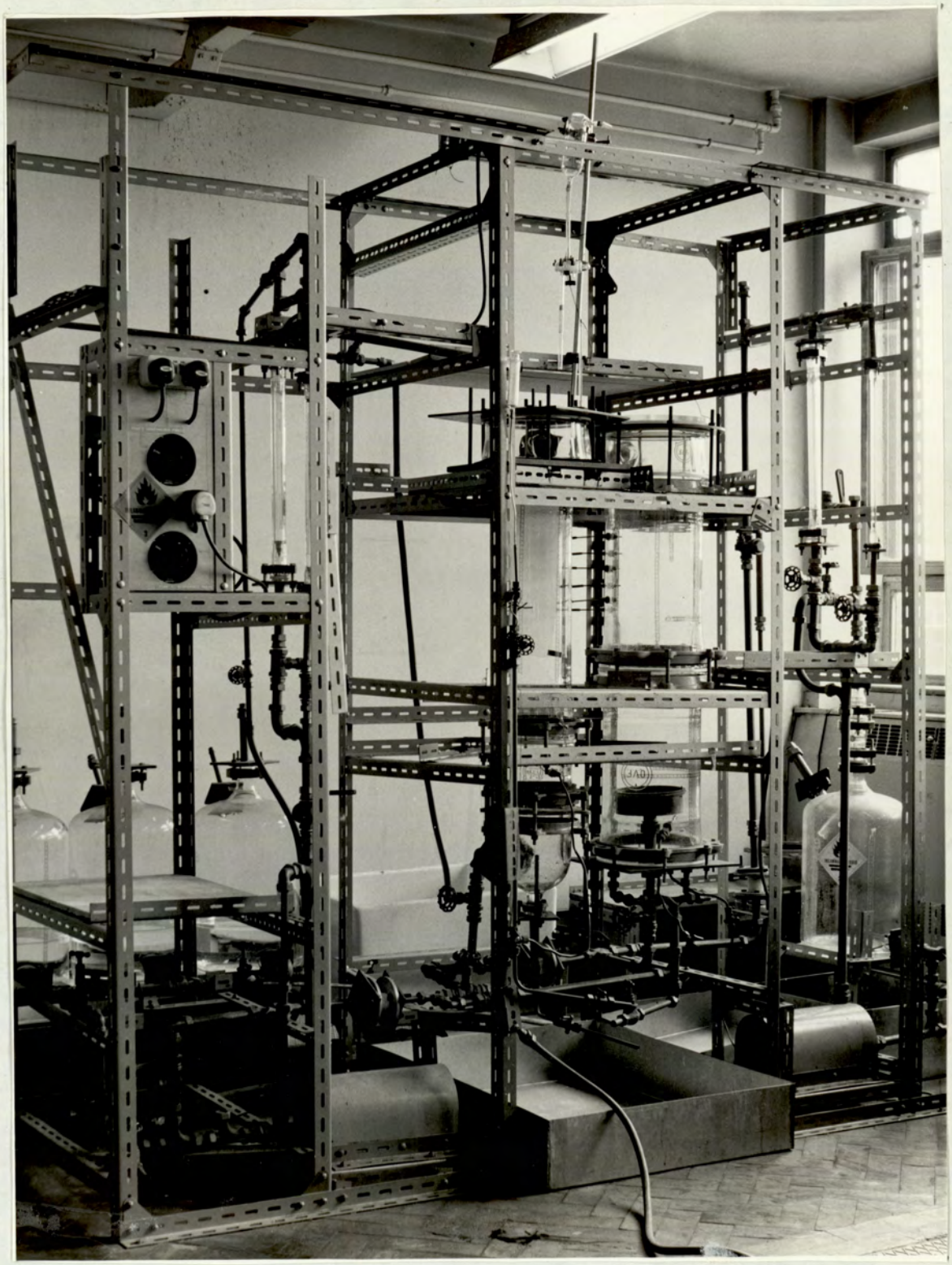

Figure 6.6 Equipment for operation with a stationary continuous phase ; 6 and 9 inch columns.

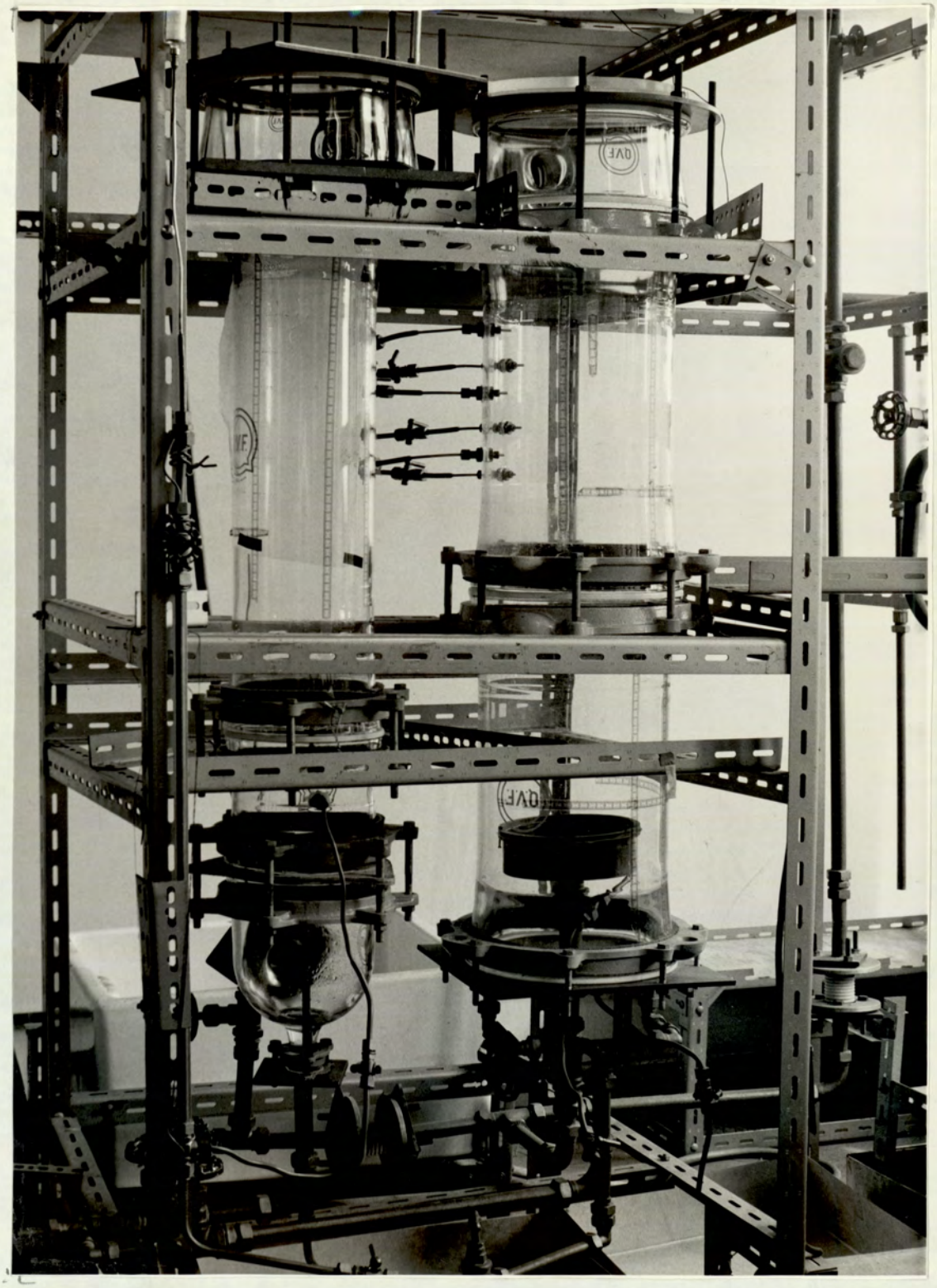

Figure 6.6 a 6 and 9 inch columns.

on 6-inch pipe section, 31, above the distributor plate. This was achieved by drilling a hole on this 6-inch pipe.

The syringing assembly simple consisted of a 50ml. glass syringe, 1/8 inch stainless steel and 3/16 inch copper tube connected to each other and finally to a stainless steel tube inside the column which was interchangeable at any bore diameter. A needle valve and tap was also placed to control the flow back and drain the contents to wash.

The seals of all the pumps and valves were replaced with p.t.f.e. The construction materials restricted to p.t.f.e., glass, copper and brass, stainless steel.

6.2.3. Equipment for operation with a stationary continuous phase, 3-inch column

The arrangement of this equipment is shown diagramatically in Figure 6.8 and illustrated in Figure 6.9. As mentioned earlier, this was separated for encapsulation work in which the introduction of the monomers into the column and the polymerization reaction subsequently required much more delicate and careful cleaning of the main column section and all pipe lines as explained in Section 6.4. Even the valves had to be dismantled and scrubbed in order to remove any polymer. Clearly therefore it would have been impracticable to introduce the monomers into the large

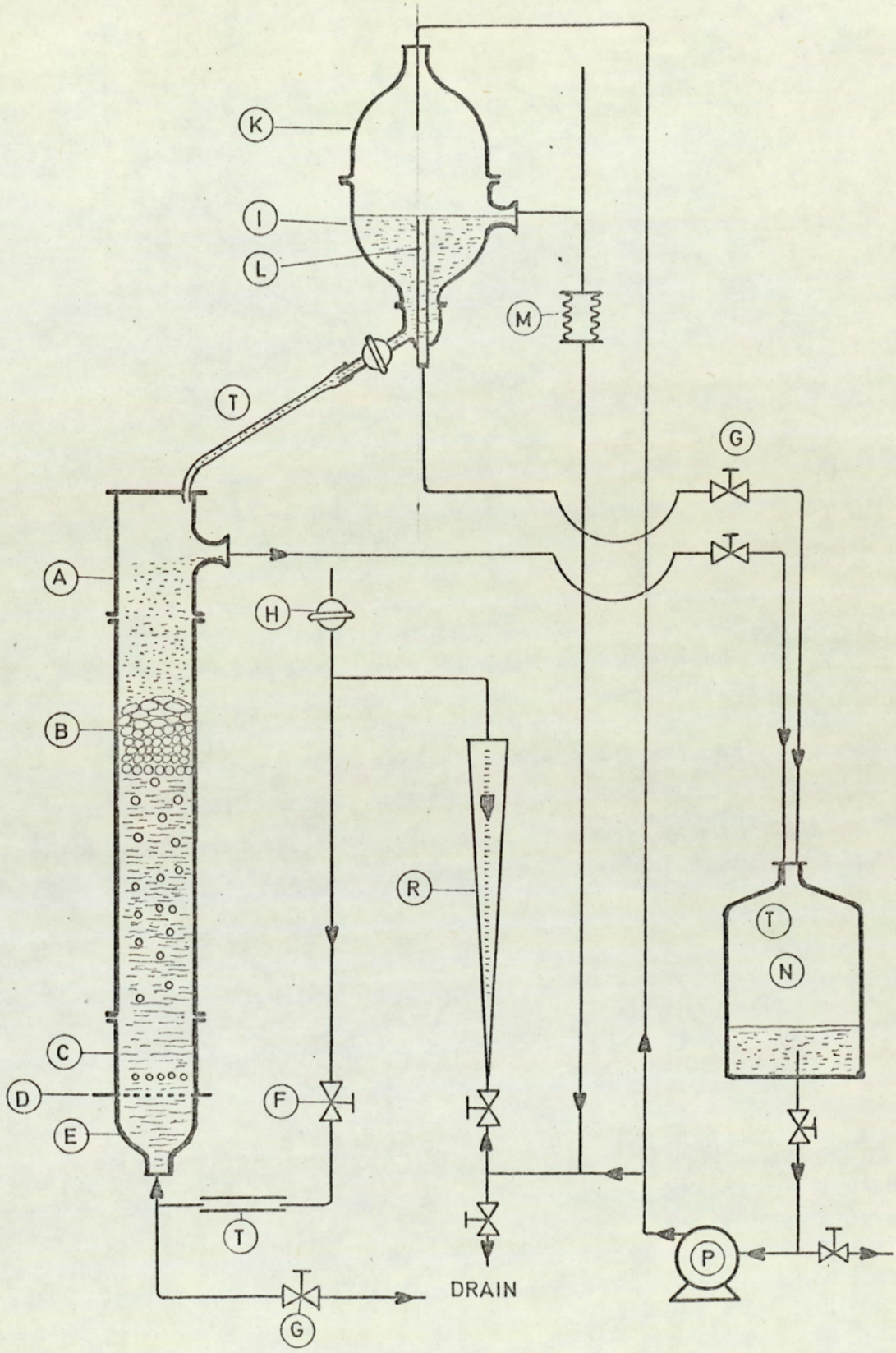

FIG. 6.8 FLOW DIAGRAM OF EQUIPMENT FOR ENCAPSULATION AND 3 - INCH COLUMN WITH STATIONARY CON - TINUOUS PHASE

LEGEND FOR FIGURE 6.8

Symbol	Item
A	Glass, Teepiece, 3" dia.
B	Glass, Pipe section, 3" dia. 24" long.
C	Glass, pipe section, 3" dia. 6" long.
D	Distributor plate, 110 orifice holes in triangular pitch, replaceable plates with orifice diameter, brass or stainless steel.
E	Glass, 3" x 1" reducer
F	Glass, and P.T.F.E valve, 5/8", modified for quick-action
G	Glass and P.T.F.E valve 5"8" standard type
H	Glass,stop-cock
I	Glass, level pipe ·
K	Glass, 6" x 1" reducer
L	Glass, column head, 6" x 1" x 1½"
M	P.T.F.E. Bellows, Q.V.F. standard flanges of 1"
N	Glass, aspirator bottle, 10 litres capacity
P	Centrifugal pump, Stuart Turner Co., stainless steel No.10 type
R	Rotameter, Rotameter Mfg. Co., No.14.
T	P.T.F.E. tube

NOTE: Connecting pipe lines and valves were mainly 5/8" diameter, Q.V.F. glass when standard Q.V.F connections with P.T.F.E seals were used.

'All glassware was of standard Q.V.F. Ltd manufacture'.

Figure 6.7. Distributor arrangement: 6 inch column.
(Note: the separation of scum at the lower phase boundary as described in Section 6.2.2).

6 and 9-inch column assembly.

The equipment consisted of two 3-inch diameter Q.V.F. glass, pipe sections, B and C, forming the main column with a 3 inch T piece, A, on the top to produce a dispersed phase outlet and a 3 x 1 inch reducer, E, on the bottom to provide an inlet. A distributor plate, D, was located between the two column sections, C and E.

Dispersed phase stored in a 10 litres capacity Q.V.F. aspirator bottle, N, was pumped either directly into the column, via rotameter, R; or to the head level reservoir formed by Q.V.F. glass pieces, K and L. Thus it was possible to recycle the dispersed phase between the head reservoir and bottom reservoir, N. The head reservoir was equipped with a dip-pipe, I, in order to maintain constant feed level.

6.2.4. Design of the distributor plates

The Hayworth-Treybal (88) Equation shown in Appendix 4 was used to estimate the orifice hole diameters required to produce five different primary drop diameters in the range of 0.1 to 0.5 cm. Initially 60 and 120 holes were provided in a 6½ inch diameter, 1/8 inch thick brass plate, but in tests with the toluene-water system this failed to produce a sufficient number of droplets to yield a flocculation zone in the 6 and 9-inch columns. The number

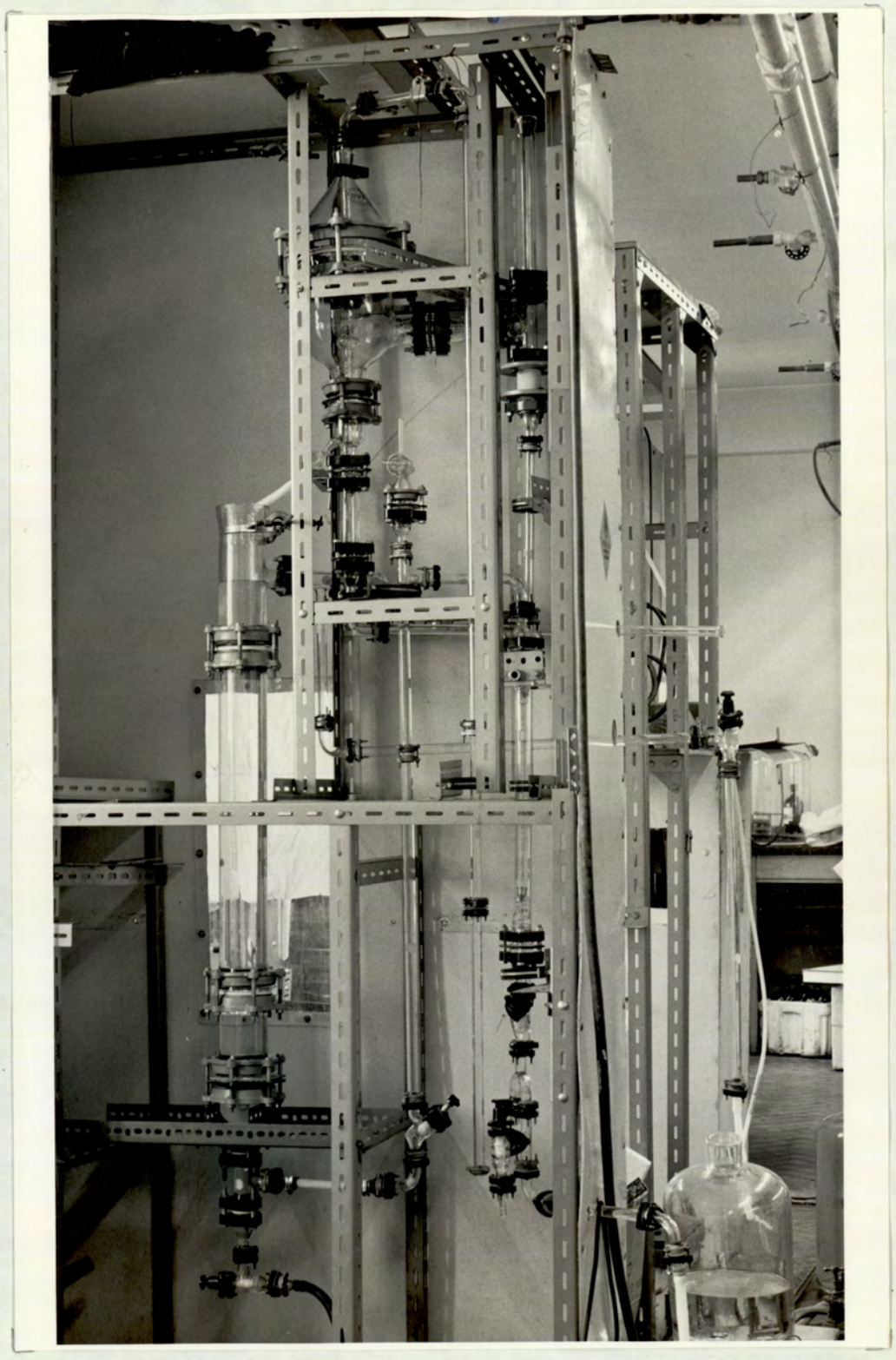

Figure 6.9 Equipment for operation with a stationary continuous phase; 3 inch diameter column.

of holes was therefore increased to 450. In the 3-inch column the number of holes was 110. Full details of the plates finally used are given in Table 6.1. Distributor plates made from copper produced evenly distributed droplets as good as brass plates. Therefore, copper plate will be useful to drill small diameter holes in further work.

6.2.5 Commissioning of the equipment

In order to start up the equipment, the column was first filled with continuous phase to within a few centimeters below the distributor plate. Sufficient dispersed phase was then pumped into the column to cause an overflow from the plate. This facilitated removal of air from the pipelines. The column was then filled with continuous phase up to the desired interface level, the dispersed phase inlet valve remaining closed. It was found necessary to keep the dispersed phase inlet line shut-off at all times when not in use to avoid back drainage of continuous phase. (If this occurred subsequent pumping of the dispersed phase produced an emulsion which separated only after 6 to 10 hours standing).

Dispersed phase wetting the plate, leading to the formation of large globules, was taken as an indication that the plate was inadequately cleaned. Since wetting precluded the

TABLE 6.1

DISTRIBUTOR PLATE SPECIFICATIONS

For 6 and 9 inch column:

Material	Orifice hole dia. mm.	Plate thickness inch	Number of holes $\frac{1}{4}$ triangular pitch
Brass	0.4	1/16	450
"	0.8	1/8	450
"	1.2	1/8	450
"	1.6	1/8	450
"	2.0	1/8	450
3 inch column			
Copper	0.4	1/8	110
"	0.8	1/8	110
"	1.2	1/8	110
"	1.6	1/8	110
"	2.0	1/8	110
Stainless Steel	1.6	1/16	110
Brass	1.6	1/8	56

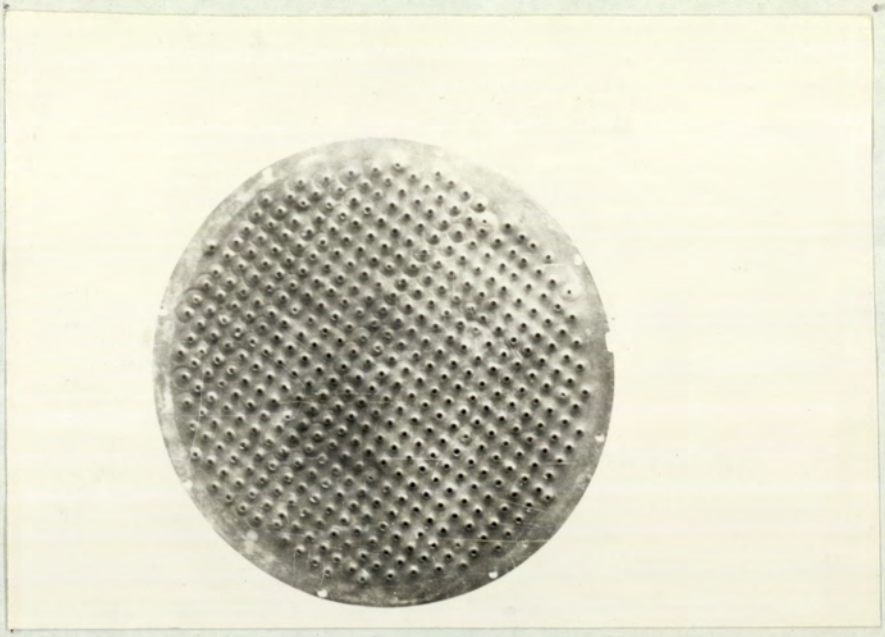

Figure 6.4. a.b. Distributor arrangement.

(a) 9 inch column

(b) Distributor plate for 6 and 9 inch columns.

proper formation of droplets. Such a plate was then recleaned. This was done by soaking it in a detergent solution for about 2-3 hours and then rinsing with tap water. The plate was then soaked in chromic acid for 4-5 seconds and rinsed with plenty of tap water. Subsequently both sides of the plate were rubbed down with fine emery paper; care being taken not to interfere with the orifice hole diameters. Finally, after washing with tap water and rinsing with acetone, the plate was left in acetone for about 15-20 minutes, washed and rinsed with distilled water and replaced in the column. Further rinsing with distilled water was performed in situ.

The vent on the top of the column was opened throughout any column filling or emptying operations and system materials had to be pumped slowly on start-up. All air had to be removed from the dispersed phase line in order to obtain a steady flow of dispersed phase after which the combined use of the voltage regulator and needle valve facilitated smooth operation of the pump. Pumps of higher capacity than required by the distributor plates were installed to allow future operation of the rig at flow rates up to 40 litres per minute.

Care was also required to remove all the air from the dispersed phase return line to the aspirator bottle, 26; this was achieved by opening the vent in the bottle and gradually

increasing the flow rate. In case of difficulty in recycling the dispersed phase from the top of the column, reduction of the flow rate was found to be safe practice. By-pass lines at the outlets were found useful on start-up, and in conjunction with voltage regulators and control valves, enabled the loading of the pumps to be adjusted.

6.2.6 Cleaning of the equipment

The utmost care was found necessary in cleaning the equipment. Prior to commissioning all glass ware was washed with tap water, detergent (Decon 75) and chromic acid; metallic parts were rinsed with acetone or kerosene. After assembly of the equipment, it was operated with Decon 75 solution for about 6 hours, followed by tap water. Use of Decon 75 at 1/3 of the concentration recommended by the manufacturer was found to be adequate. High concentrations of this detergent were found in fact to promote corrosion of brass upon long exposure i.e. $>$ 24 hours. Therefore the use of high concentrations may be deleterious.

Chromic acid washing was only practicable for individual pieces. After commissioning of the equipment, only the glass pipe section wherein the flocculation zone was formed required such treatment; detergent washing was found to be adequate for the remaining items. A detergent wash was found to be insufficient

to clean the glass after long operations e.g. if the flocculation zone section was not washed with chromic acid at the end of 2-3 weeks, a detergent wash lasted only a day before the column exhibited different behaviour. After drainage of any detergent from the equipment at least 10 hours of intermittent operation of the equipment, requiring about 3-4 tons fresh tap water was allowed. A rough test for complete removal of detergent was the observation that a strong splash of the spray on the water surface produced no bubbles other than air. Reverse cycling was achieved by adjustments of the valves.

The tap water, which was found to contain small pieces of solids from the main, was supplied via an aspirator bottle which functioned as a settler.

6.3 Design of the Experiments and Procedures

6.3.1 Selection and purification of systems

The system materials used in the experiments were selected to provide a wide variation in all physical properties except viscosity. Continuous phase viscosity was kept constant, by using distilled water, and organic phase viscosities varied over only a narrow range. A constant continuous phase viscosity was used because this was expected to affect the rate of film

drainage in a drop swarm as with single drops and it was decided in this work to avoid 'additive effect of this with density difference and interfacial tension effects. Apart from density difference and interfacial tension, the following properties were also considered,

i. Low toxicity,

ii. High flash point,

iii. Large difference in refractive index from that of water to facilitate photography,

iv. Ease of purification,

v. No tendency to hydrolyze, polymerise or oxidise,

vi. Relatively low cost.

Purification of the organic phases was performed in a standard 50cm. long, 3cm. diameter Vigreux fractionating column connected to a 1.5 litres capacity flask in an electrically heated mantel and provided with a water cooled glass condenser.

Distilled water was obtained from a standard Q.V.F. glass, 5 litres per hour capacity, electrically heated unit. The outlet from the condenser was connected to the receiver with p.t.f.e tubing since P.V.C. tubing of only about 5 feet in length was found to reduce the surface tension from 72 dyne cm^{-1} to 52-55 dyne cm^{-1}. Whilst polythene bottles appeared to have no effect on the surface tension, some doubt arose with regard to prolonged storage in them and therefore all glass aspirator bottles (Q.V.F.)

were employed throughout. Surface tension of the water was checked after each filling of the equipment. Similarly interfacial tensions were determined after placing the materials into the equipment and when saturation of the phases was completed. The Wilhelmy plate method using a standard Du Nuoy surface tension determination apparatus was employed to measure the surface and interfacial tension of the materials. Densities and viscosities were considered to be as for the pure substances.

On this basis, the selected system materials and their properties are shown in Table 6.2.

TABLE 6.2.

SYSTEM MATERIALS AND THEIR PROPERTIES (25°C)

Continuous phase : Distilled water.

System Dispersed phase	Flash point °C	Toxic limit ppm.	Interfacial Tension dyne/cm	Density difference gm/ml.	Viscosity cp	Boiling point °C
Toluene	26	300	36.1	0.136	0.58	110.8
Diethyl carbonate	25	ND	13.1	0.026	0.82	126.8
Isooctane	9	500	50.2	0.306	0.50	99.2
M.I.B.K.	15.5	1000	9.9	0.20	0.62	115.7

ND = No data

6.3.2 Drop size distribution

Photography was chosen to measure drop diameters since it also enabled size distribution to be obtained. Photographic negatives were projected onto a sheet of white paper fixed onto a smooth, light wall; this facilitated magnifications up to 27 times. The drop images were either measured directly or circled onto the paper with a pencil to allow subsequent measurement with a ruler. This was found to be quicker and more convenient than printing the negatives followed by a similar counting/measuring / marking procedure. Furthermore it was possible to encircle the images from more than one negative on the same sheet of paper and hence increase the number of drop counts to obtain an average rather than working separately on 2-3 prints. Moreover, it was found easier to join together various sections to produce a complete picture than with prints.

6.3.3 Photography

An Asahi Pentax, spotmatic camera with 45 mm, f :1.8 lens and 1 to 6 cm extension tubes, as necessary, was used for still photography. Use of a 3 cm extension tube covered a column area of about 2 x 3 cm without any significant distortion being apparent upon focussing at the centre or side. The photographs obtained in this way were found to be better than those using a telephoto lens possibly due to better measurement of the light intensity

by the lightmeter integral with the camera. For the top pictures either a smaller length of extension tube (1 cm) or no extension tube was used.

Back lighting was used as usually recommended (19) for pictures of droplet phenomena. However in the 6 and 9 inch columns back lighting comprising 3 lamps x 750 watts was inadequate to provide sufficient illumination of the flocculation zone in which droplets were densely populated. Therefore, front lighting was also tested. It was found possible to take pictures in a 2-3 cm band if the floodlights were positioned on both sides of the horizontal camera axis, and at an angle of approximately 30°, reflection of light on the column being maintained just outside the boundary of the area in focus.

Flash lighting was also used to produce successful results. However this was unsuitable for photographs over the whole range of flocculation zone heights since as the latter increased the reflection of the light varied and required adjustment of the camera aperture by trial and error.

Finally illumination from the rear and from the sides, shielding the direct light from the camera lens, was found the best practice to obtain pictures of the flocculation zone. For inlet droplets, only back lighting was necessary. Use of 500 watt lamps was considered safer than 750 watt lamps due to

rapid heating up. (In the present experiments 500 watts were used, but the use of more lamps of less power is recommended for safety.)

A speed of 1/125 sec was adequate for photography of the flocculation zone but 1/250 sec was preferred whenever sufficient lighting was employed easily. For inlet drop size photographs 1/250 sec was also necessary.

Fine grained, Kodak Pan X, ASA32 films were used throughout the investigation. ASA 400 films also proved suitable but ASA 32 film compensated better for the uneven illumination of the object area, although it required a higher level of illumination.

A Beaulieu camera, an R16 with a P3 type, 0.75 lens, was used for cine photography at 16 to 64 f.p.s. Similar lighting from the back and side was employed. This was used to obtain a movie-film of the motion of a coloured drop in the flocculation zone. Use of a Wollensak Fastax Type WF14T Camera was also attempted. Unfortunately proper lighting could not be arranged to obtain a useful cine-film at high speed between 600-6000 f.p.s.

6.3.4 Hold-up

The hold-up profiles throughout the flocculation zone were determined by syringing out samples at various locations. The

amount of each phase was measured after settling in a burette. The arrangement of the syringe assembly on the top of the column is illustrated in Figure 6.10. Before a sample was withdrawn from the flocculation zone, the liquid in the 9-mm bore glass tube was blown out using the 50 ml. syringe and 3-way stop-cock. Sufficient time was then allowed e.g. about 3-4 minutes for high zone heights, in order for steady state conditions to be re-established in the flocculation zone after the disturbance caused by the liquid and some air ejected from the tube. A 20-28 ml. sample was then drawn up steadily into the 200 ml. reservoir by syringing out over a period of 8-10 seconds. The 3-way stop-cock was closed immediately this 10 seconds had elapsed or when the plunger reached the end of the syringe. The sample in the 200 ml was finally transferred into a clean burette in which the phases were separated and their respective volumes measured. The ratio of volume of the organic phase to the total sample volume was recorded as the hold-up fraction. The following precautions were found necessary to ensure reproducibility.

i. Avoiding the addition of unsaturated organic or aqueous phase to the column, even in small amounts, in order to adjust the zone level. Only equilibriated materials from the column reservoir were therefore used.

ii. Adjusting the tip of the 9 mm bore glass tube level

in the flocculation zone rather than changing the flocculation zone levels.

iii. The samples were syringed out steadily over approximately equal time periods.

iv. The whole assembly was cleaned in the same way as the equipment before use.

Other trials to measure hold-up

Prior to syringing, attempts were made to measure hold-up in the flocculation zone by measuring the pressure difference between the two points by,

i. Measuring the static pressure between two points.

ii. Measuring the difference head by a differential manometer.

The first method failed because the static pressure at any point fluctuated between wide limits.

Use of the second method was not practicable for small differences in pressure drop found between two points less than 5 cm apart.

6.3.5 Drop residence times

A stop-watch was used to measure the residence times of single drops in the flocculation zone and their rest times at a plane interface.

An interchangeable stainless steel tube was connected to the

syringing assembly to produce a single drop at the tip. The drop from the tip was allowed to travel about 40 cm. before impinging on the plane interface. The rest time was measured between the impact of the drop at the interface and its disappearance. If partial coalescence occurred only the first coalescence was recorded.

For the measurement of the residence time of a drop in the flocculation zone, a red coloured drop dyed with 'Red Oil dye' at a concentration less than 25 mg per litre, was introduced into the column. The time between the arrival of the drop at the first layer of the zone and its complete coalescence with the interface was recorded as the residence time.

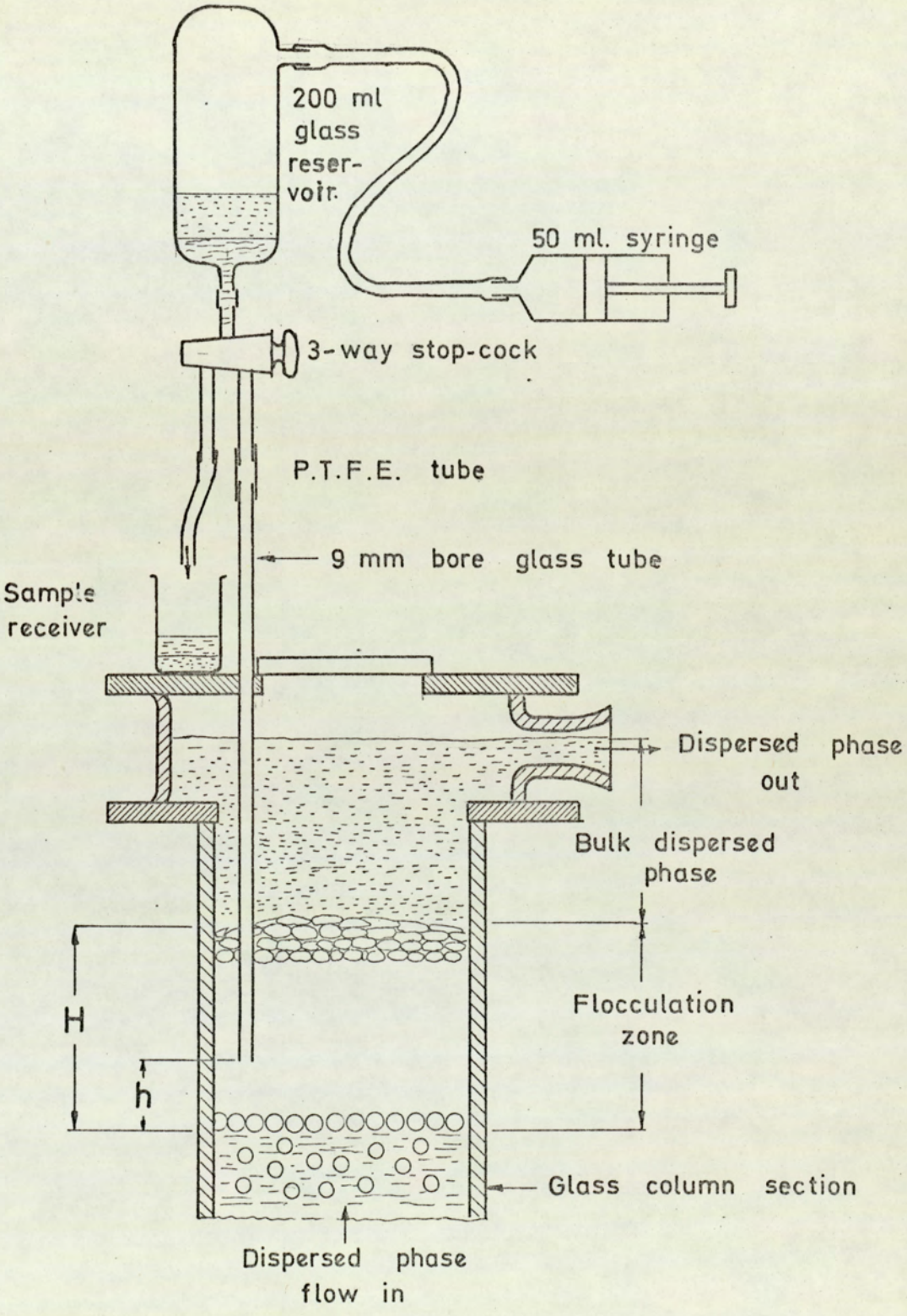

FIG. 6.10 SYRINGE ASSEMBLY ON TOP OF THE COLUMN FOR HOLD-UP MEASUREMENT

6.4 Encapsulation

6.4.1. Introduction

One method of 'freezing' the drops is to utilize a fast polymerization reaction at the surfaces of the droplets so that coalescence is terminated instantaneously. Further analysis can then be made by random sampling or photography.

The basic chemistry in the encapsulation procedure is the use of low temperature interfacial polycondensation reaction which proceeds at high rates. The best known of these reactions is that of an organic acid halide with a compound containing an active hydrogen in the functional group, such as an amine (104). This can be represented in general form, by

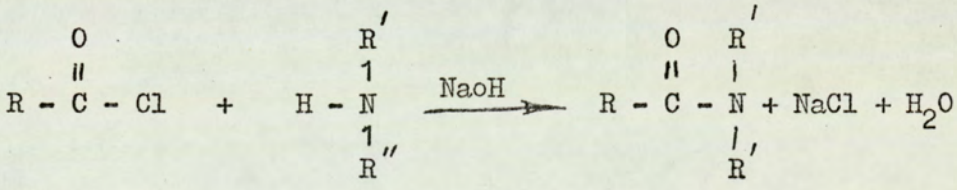

Acid halide Amine polyamide

which is also known as the Schotten-Baumann reaction.

The two intermediates, acid halide and amine, are dissolved in a pair of immiscible liquids. Amines being soluble in the aqueous phase and halides in the organic phase, the polymerization takes place at, or near, the interface.

McCoy and Madden (105) used hexamethylene diamine which is

soluble in water with sebacyl chloride, in the organic phase, to produce a polymer which is very well known as nylon 6-10,

$$H_2N\text{-}(CH_2)_6 - NH_2 + ClOC\text{-}(CH_2)_8 - COCl + NaOH =$$

Hexamethylene diamine — sebacyl chloride

$$H\left[\text{-HN-}(CH_2)_6 - HC - CO - (CH_2)_8 - CO\text{-}\right]_n Cl + n\ Na\ Cl$$

Nylon 6-10

The method McCoy and Madden employed was to add a low concentration of sebacyl chloride (1%) to tetrachloroethylene and disperse it in a baffled beaker. A small volume of water containing hexamethylene diamine and caustic soda was then added rapidly to the agitated beaker.

Resnick (106) used as monomers piperazine and terephthalic acid chloride which are soluble in water and carbon tetrachloride respectively. A 0.05 wt/% of terephthalic acid was added to carbon tetrachloride dispersed in a baffled mixing vessel containing water. A specially constructed 'trapping' device was then placed in position to withdraw samples from the vessel. By releasing the trigger on the device droplets were 'trapped' and in contact with water containing piperazine became encapsulated due to a fast polymerization reaction.

Van Heuven and Beck (107) have also reported the use of an encapsulation technique to determine the drop size distribution in a

stirred vessel with a water-benzene system but no details are provided.

The application of these techniques to encapsulate droplets in contact with each other in a densely populated dispersion, e.g. in a flocculation zone, requires further work. All the reported studies apply to agitated vessels in which droplets are invariably separated by relatively larger distances.

In the present investigation, Nylon 6-10 reaction was used to encapsulate the droplets in a flocculation zone formed in 3-inch column shown in Figure 6.8. Employing toluene-water system with d_n = 1.6mm. flocculation zone was formed

6.4.2 Procedure and trials

Sebacyl chloride was added to the toluene (dispersed phase), the amount to be added having been estimated from beaker trials. Less than 0.3% by volume failed to give sufficient strength to the droplets and $>$ 1% increased the polymerized film thickness to such an extent that flocculated droplets tended to form a bulky polymerized mass, i.e. they adhered together and made separation difficult. The amount of hexamethylene diamine had a similar effect on the degree of polymerization. A 1:1 stochiometric ratio of the two

monomers was found to be suitable. However, where a flocculation zone was formed in continuous flow in the 3-inch column, the optimum amount of sebacyl chloride to be added to the toluene was found to be 0.5 to 1.0% of the total organic recycled. The hexamethylene diamine was added rapidly from a number of holes of 1/16 to 1/32 inch diameter located around the periphery of a glass ring which was 3cm below a flocculation zone of about 6 to 7 cm. in height. The optimum amount of hexamethylene diamine was 1% of the flocculation zone volume. The requisite amount of each monomer was diluted in 50ml. of the phase material in which it was soluble. The addition of 1N NaOH solution in equal volume to the hexamethylene diamine reduced the adhesive tendency of the polymer film, but this could not be eliminated completely.

The biggest problem however was the unsuitability of the Nylon 6-10 reaction due to the hydrolysis of sebacyl chloride in contact with water. This hydrolysis was even observed following the addition of sebacyl chloride to water saturated toluene, turbidity becoming apparent after 8-10 minutes. Unsaturated toluene did not produce a similar turbidity upon the addition of sebacyl chloride.

In the column trials turbidity became apparent after

2-3 minutes of recycling and a stable flocculation zone of 6cm in height suddenly collapsed to only a monolayer. The rate of coalescence at the interface and interdroplet coalescence increased drastically after 3-4 minutes of acid halide addition. Hence the reduction in flocculation zone volume is explainable by the formation of HCl due to hydrolysis followed by its diffusion into the continuous phase. In fact continuation of recycling caused the zone to increase after 4-5 minutes but the original height was not re-established within 20 minutes.

A successful encapsulation was obtained with the system materials at 11°C and the encapsulation procedure restricted to $<$40 seconds to allow insufficient time for hydrolysis of the sebacyl chloride. This was achieved by the injection of about 10 ml. of toluene, containing 2 ml. of sebacyl chloride and Red Oil dye, at a rate to give approximately 0.5 to 1.0% of sebacyl chloride in the dispersed flow to the distributor, (i.e. by injection over 10 seconds with a flow rate of about 0.6 litre per minute). As soon as the flocculation zone turned a light red colour, H.M.D. was released to the flocculation zone and the dispersed phase flow to the column was shut off immediately. The encapsulated droplets adhered together and the mass had a jelly-like consistency. Because of this, and the tendency of the polymer to adhere to the column walls, analysis was found to be impracticable. Neither

disection nor separation of discrete drop-spheres proved possible. However, the whole mass could be displaced upwards by first cutting around the periphery with a knife and then injecting water into the bottom of the column. This may become a useful sampling technique in future work; the addition of 3% to 5% of acetone in water to the mass of encapsulated droplets, in order to reduce adhesion, may also be applicable.

In summary isolation and analysis of the encapsulated mass proved much more difficult than the encapsulation process. Because of this no quantitative data were obtained from this work and indeed in most trials only partial encapsulation was accomplished.

Subsequent cleaning of the apparatus involved a tedious procedure because the nylon 6-10 adhered to the column walls. This was removed by scrubbing and soaking in chromic acid. In addition a few drops inevitably became held-up inside the valves which had to be dismantled and cleaned after each trial.

Whilst the difficulties encountered and time consuming nature of the polymer mass removal and cleaning procedures prevented use being made of encapsulation in this investigation the technique developed, as described earlier, may be applicable in future work.

One advantage of the hexamethylene diamine-sebacyl chloride system for encapsulation work is that the amounts of each monomer do not require precise control. A major disadvantage however is the tendency for sebacyl chloride to hydrolyze as discussed earlier. This precludes anything other than encapsulation in $<$ 1 minute at temperatures below 10°C. Thus an improved method could involve the use of another dicarboxylic acid halide of a higher molecular weight e.g. terephthalic acid chloride since the higher the carbon content of the acid halides the lower is the tendency for hydrolysis (104). However to eliminate hydrolysis, or by-product formation, completely would appear more promising, and such polymerization reactions are known. One recommended by McCoy and Madden is the formation of polyureas (105). This can be put in general form,

$$-R-NH_2 + O = C = N-R^1 \longrightarrow \left[H_2N-R-O-C= N-R^1\right]_n$$

Diamine Diisocyanate Polyurea

Clearly other problems may arise in using these systems e.g. due to the toxicity of the isocyanates.

As an alternative method of eliminating hydrolysis with nylon 6-10, an attempt was made to encapsulate water drops in toluene. It was anticipated that the rapid addition of sebacyl chloride would not result in an appreciable amount

of hydrolysis. However since the polymer was formed on the organic phase side (104) thick layers around the water drops produced a bulky mass with little resemblance to an inverted dispersion.

6.4.3 Radical polymerization tests

The use of a radical polymerization for encapsulation was suggested by Scott (108). These reactions have been reviewed by Bevington (109) and of the considerable number of possible combinations one employing hydrogen peroxide as a sensitizer appeared promising.

The basis was the use of the hydrogen peroxide as a thermal sensitizer with ferrous ions to produce OH radicals which activated the monomer resulting in polymerization.

$$H_2O_2 + Fe^{++} \longrightarrow .OH + OH^- + Fe^{+++}$$

The selected monomer, methyl methacrylate, was present in the dispersed phase and the .OH radical was added rapidly to the continuous phase.

Up to 5% by volume of methyl methacrylate was added to toluene droplets in a 250 ml. beaker. Varying, dilute, concentrations of ferrous sulphate solution containing hydrogen perioxide were then added rapidly but without disturbing the droplets.

The results obtained were not promising. Few of the droplets encapsulated but the majority coalesced with the interface. However, heating the contents of the beaker to between 30-35°C and mixing the contents with the addition of a

little more hydrogen peroxide produced encapsulated droplets. Thus it would appear that activation of the methyl methacrylate was inadequate at a temperature of about 20°C and also the (OH) free radicals produced were insufficient to sensitize the monomer. This method, however, may be of use with other per oxides, which produce more radicals, and more sensitive monomers.

7. EXPERIMENTAL RESULTS

Quantitative results obtained by means of the procedures described in Section 6, or subsequently derived by calculation, will now be presented. The complete data is shown in tabular form in Appendices 3 to 10.

Phase separation of primary dispersions, in continuous flow in all three columns involved the formation of a flocculation zone of dense packed droplets before they coalesced at the interface with the bulk dispersed phase. The characteristics of this zone were observed to significantly affect phase separation. Therefore, the manner in which a flocculation zone is formed is first described qualitatively in Section 7.1.

This flocculation zone, and hence the phase separation process was found to be affected by numerous parameters; the effect of the main parameters, was investigated and quantitative results are presented in Section 7.4.

Reproducibility of the results was seriously affected by any scum formed during experimentation. The nature of this scum, factors promoting its formation and measures taken to minimise its effects are therefore described in Section 7.2.

The behaviour of droplets within the flocculation zone,

involving interdroplet coalescence and movement towards the interface was considered likely to be dependant upon the free space available, or distances between droplets. This is best characterized by the hold-up, and therefore, a comprehensive investigation of hold up is described in Section 7.5. Further droplets interaction resulted in an increase in mean drop size in the flocculation zone, and the manner in which this varied with zone height is presented in Section 7.6. Droplets remained in the flocculation zone until they reached the interface and underwent coalescence with the bulk dispersed phase. Residence time data is presented in Appendix 7 and discussed in Section 7.7.

7.1 FORMATION OF A FLOCCULATION ZONE

Drops rising axially in a column have either a zig zag, or spiral, or a straight forward motion dependant upon their diameter, shape, the presence of impurities and the physical properties of the system. (For the purpose of this discussion the dispersed phase is assumed to be the lighter phase.) That is small drops rise vertically but large drops follow unpredictable paths along their travel. A rough criteria for the deviation from solid particle behaviour has been obtained by Bond and Newton (19) by dimensional analysis,

$$\frac{d^2 g \Delta \rho}{\sigma} \simeq 0.4 \qquad (7.1)$$

The non-linear motion of the drops was in accordance with this criteria, the difference being clearly observed by comparison of the motion of isooctane and diethyl carbonate droplets e.g. even large globules of diethyl carbonate followed a straight path.

When drops arrived at the interface they rested there for a short period before undergoing coalescence. Because of this time lapse a certain number of the droplets always existed at the interface for as long as the process was continuous.

Up to a certain flow rate, which varied for each system, the number of drops at the interface did not cover the whole interface area. That is the mid-section was an

incomplete layer and the periphery 2-3 drops deep. The shape of the meniscus caused migration and formation of a queue at the column walls. Droplets which impinged on this mid-section of an 'incomplete monolayer' did not rest there but attained a radial motion towards the wall and upon coming into contact with those droplets already residing there eventually underwent interdroplet coalescence. Drop-drop coalescence seldom occurred amongst drops which arrived at the mid-section and moved radially outwards unless they collided with a drop resting near the wall or their motion slowed down considerably. Drop-drop coalescence was predominant but was of a lower order of magnitude in the two large diameter columns than in the three inch column.

Any increase in the dispersed phase flow rate in an attempt to complete the mid-section of the 'incomplete monolayer', resulted in a queue of drops, 2 or 3 droplets deep, around the periphery with increased interdroplet coalescence occurring randomly. Further increase in flow rate led to the formation of individual subgroups within the mid-section and subsequently to a complete monolayer. This is illustrated in Figures 7.1 to 7.3.

The flow rate at which the whole cross section was covered with a monolayer of the droplets varied with the mean inlet drop size and with the system employed in the range of

Figure 7.1 Incomplete monolayer
(6inch column,
System isooctane-water, d_n = 1.2mm)
(a) Plan view
(b) Side view of same layer

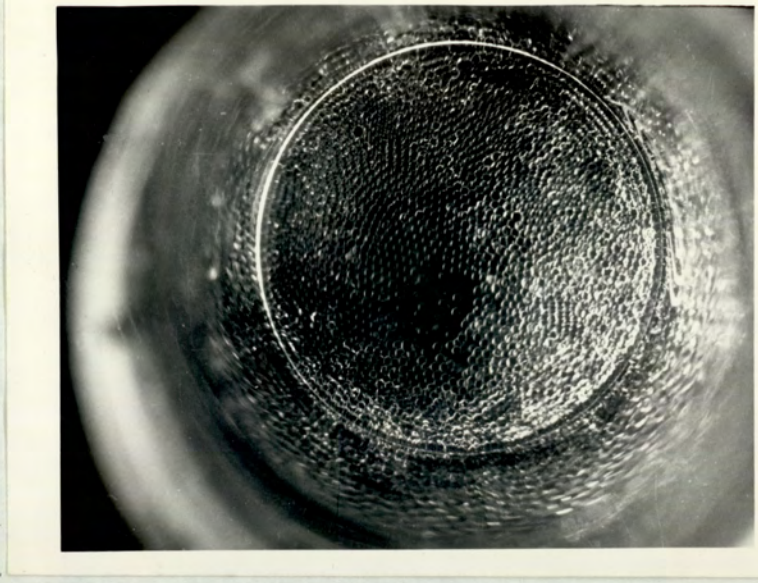

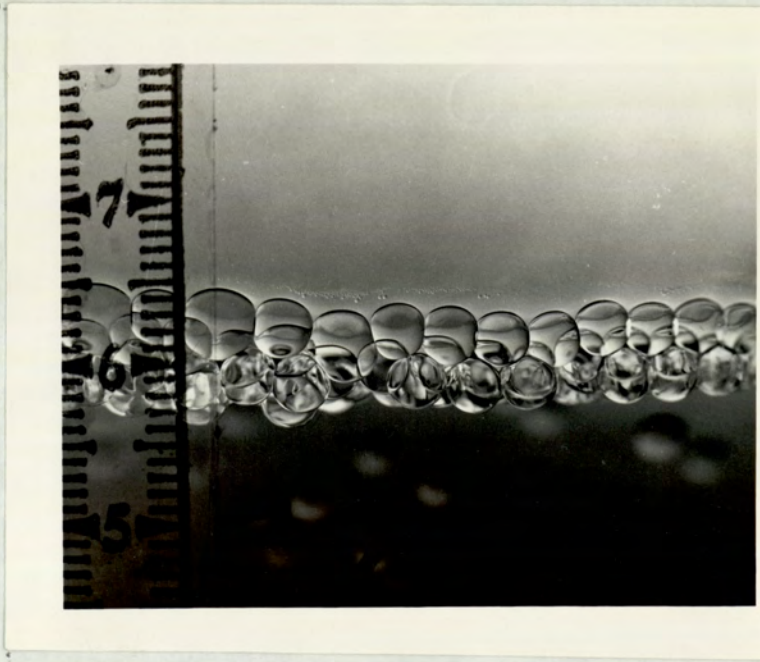

Figure7.2 Incomplete monolayer
(6 inch column,
Sysyem isooctane-water, d_n=1.2 mm.)

(a) Plan view
(b) Side view, showing droplets queueing near the periphery, mid section nearing completion)

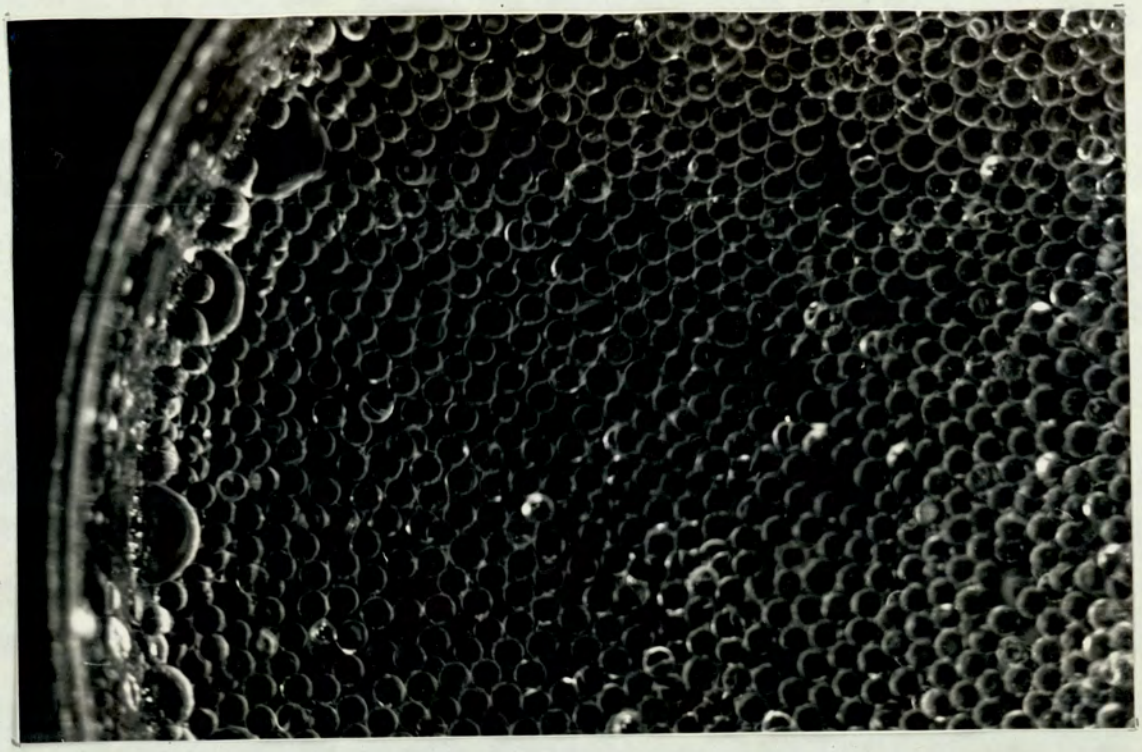

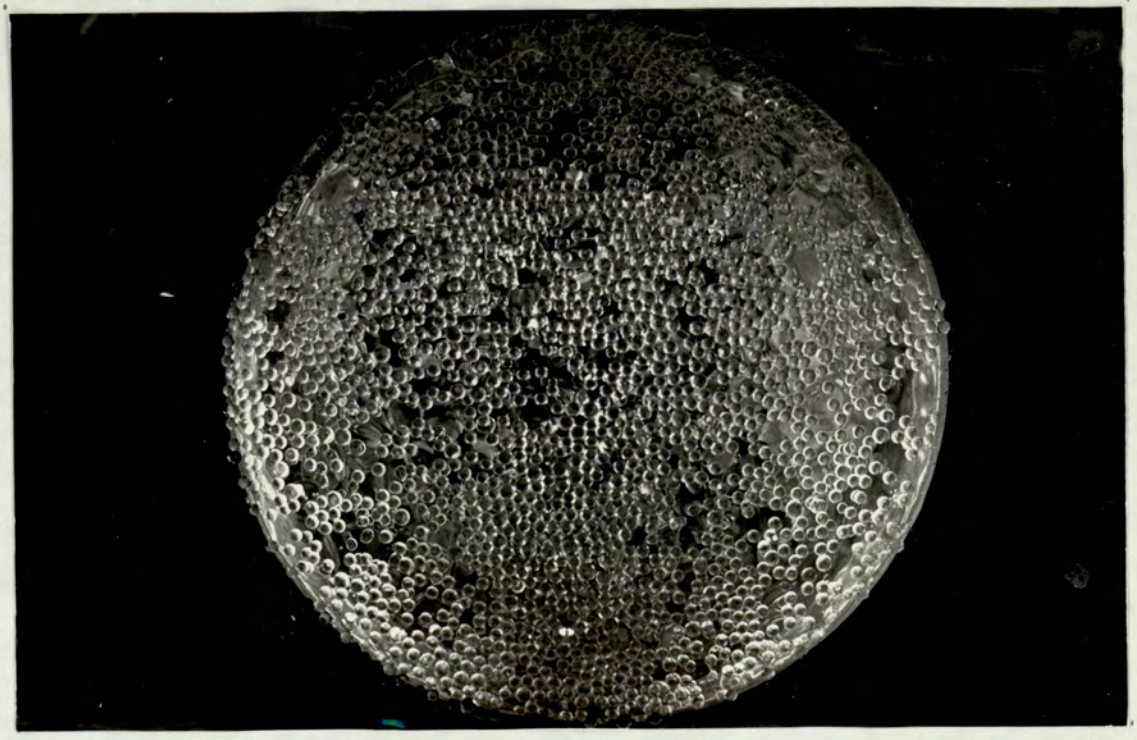

Figure 7.3 Plan views of complete monolayer
(System toluene-water)
(a) 6 inch column, d_n = 0.8 mm.
(b) 9 inch coulmn, d_n = 1.2 mm.

about 0.13 to 0.23 ml. $cm.^{-2}$ sec^{-1}. The smaller the drop size arriving at the interface the lower the dispersed phase flow rate required to form a monolayer. For an average drop size of 0.3 cm, approximately 0.16 ml. cm^{-2}. sec^{-1} dispersed phase flow was required through a distributor having 450, 1.6 mm diameter holes in order to maintain a monolayer of toluene drops in the 6 inch column.

For large drops, above 4 mm, formation of a monolayer was much more difficult.

At the mid-section the droplets were arranged on either a square or triangular pitch, albeit in a continual state of motion because of the constant disturbances created by newly arriving droplets, and by coalescence at the interface.

After the formation of a monolayer, further increase in flow rate led to a build up of other layers across the column, the rate of build up being higher at the mid-section. At this stage the larger droplets resulting from interdroplet coalescence started to appear further away from the wall and further increase in flow rate resulted in distribution of larger drops over the surface. This sequence is illustrated in the photographs on Figures 7.4 to 7.9. At this stage the profile of the boundary between the droplets and bulk dispersed phase became flat, and level. Such a condition

existed for a very small range of flow rate, covering a difference of only about 0.05 ml. cm^{-2}. sec^{-1}. for small inlet drop sizes, but slightly larger with larger drops. This stage is noticeable in the graphs of flocculation zone heights v.s. flow rate in Section 7.4.2., corresponding to a height of around 10 mm. for all systems.

Further increase in flow rate giving an increase in the number of drop layers resulted on the flat, horizontal boundary developing a curvature in the opposite direction to the normal initial meniscus. Whilst the central point of the flocculation zone - interface boundary was always higher than the level on the column walls however, the difference in height varied from system to system. The highest, observed with diethyl carbonate, was 7 mm.; M.I.B.K. exhibited a much reduced interface curvature.

The lower boundary of the droplet entry section of the flocculation zone maintained a distinct horizontal appearance over the whole range of flow rates with all the systems studied. In the absence of interface level control, increase in flowrate caused this boundary to move upwards relative to the column walls. However this was not considered to be of significance since it was obviously caused by the displacement of continuous phase by the increased dispersed phase hold-up throughout the column.

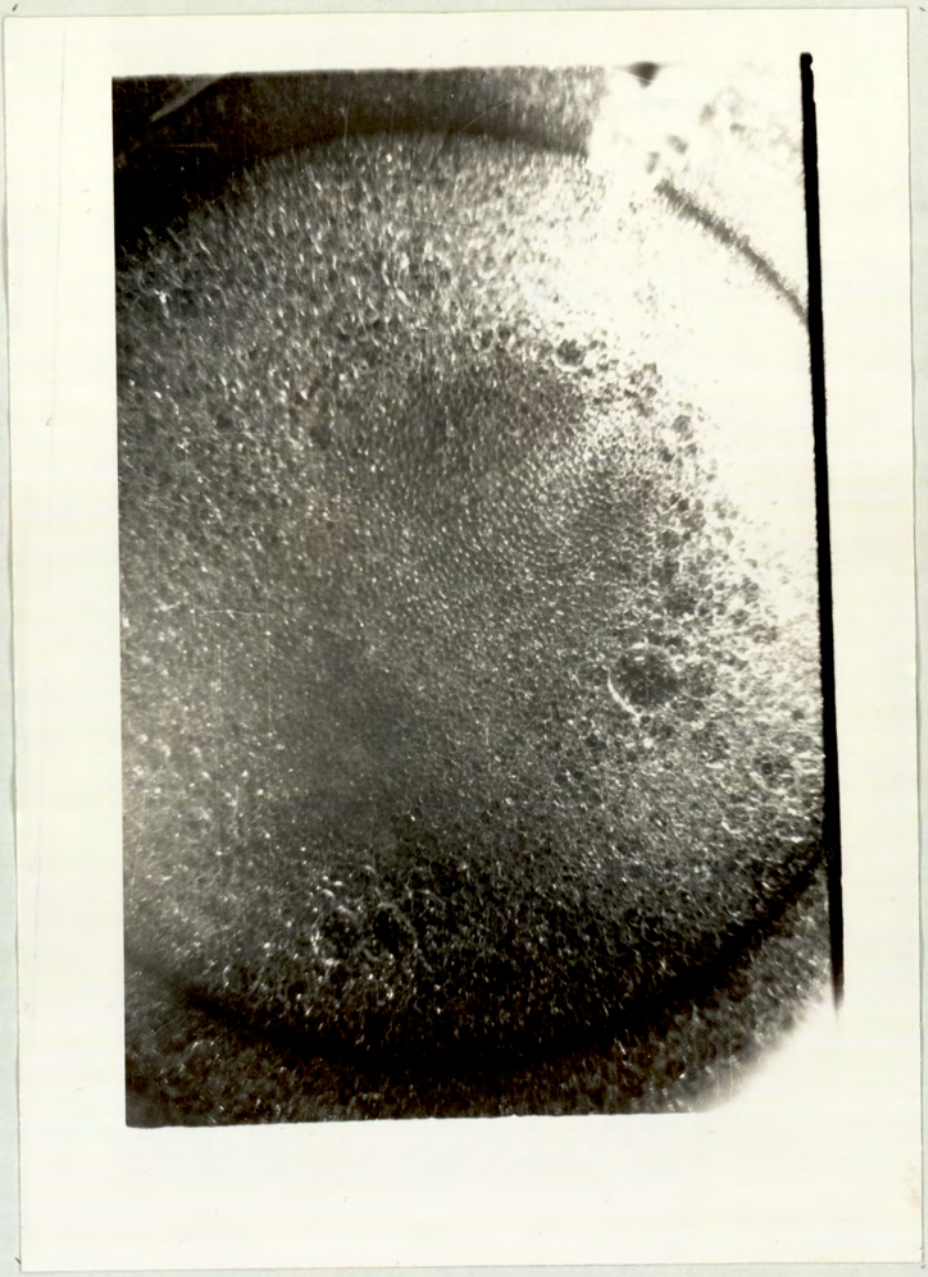

Figure 7.4 Flocculation zone starts to build-up above a monolayer.
(System: toluene-water, 6 inch column, d_n=1.6 mm. The mid-section is shallower than the periphery)

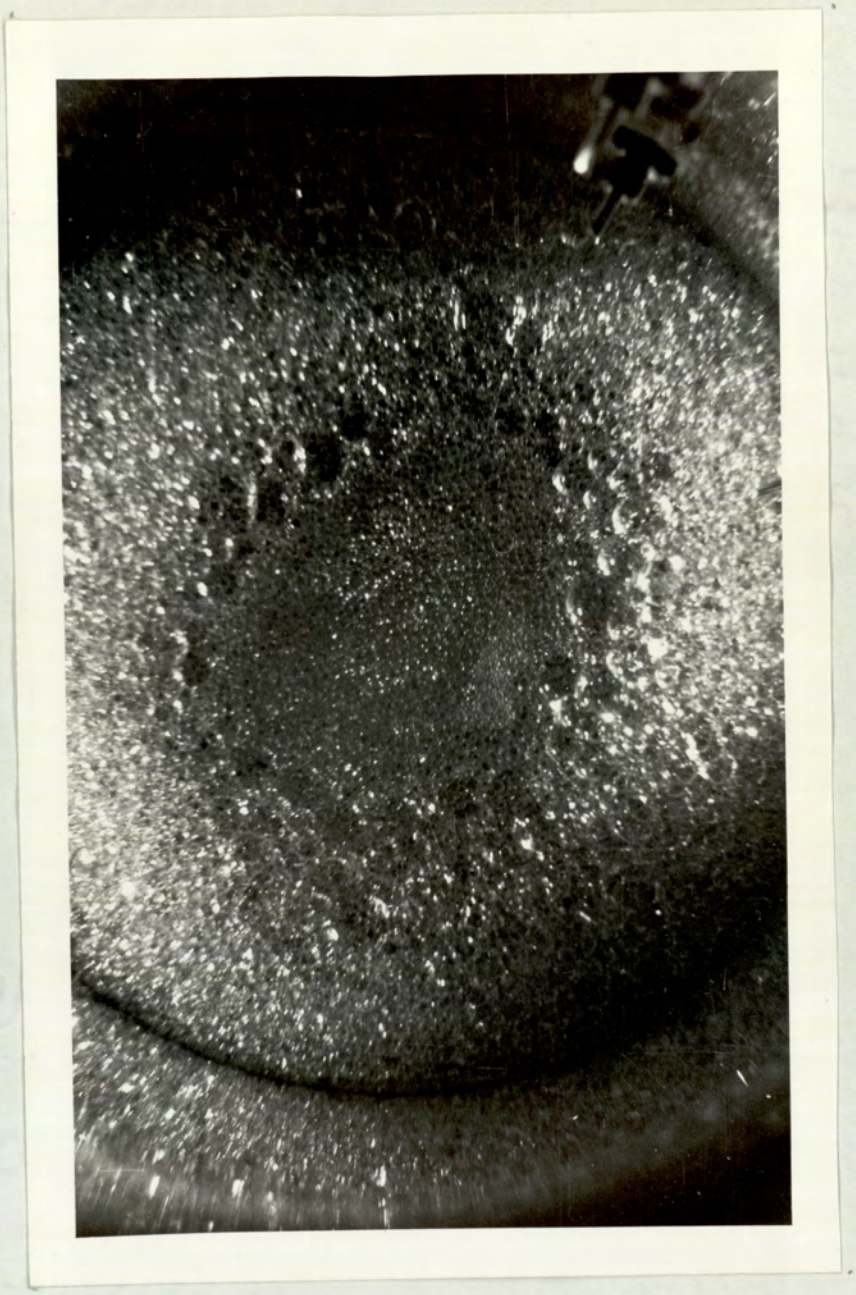

Figure 7.5 The crater at the mid-section of a shallow zone. (System: Toluene-water, 6 inch column, d_n = 1.6 mm. The height at the sides is higher than mid-section. Flow rate is higher than Figure 7.4.)

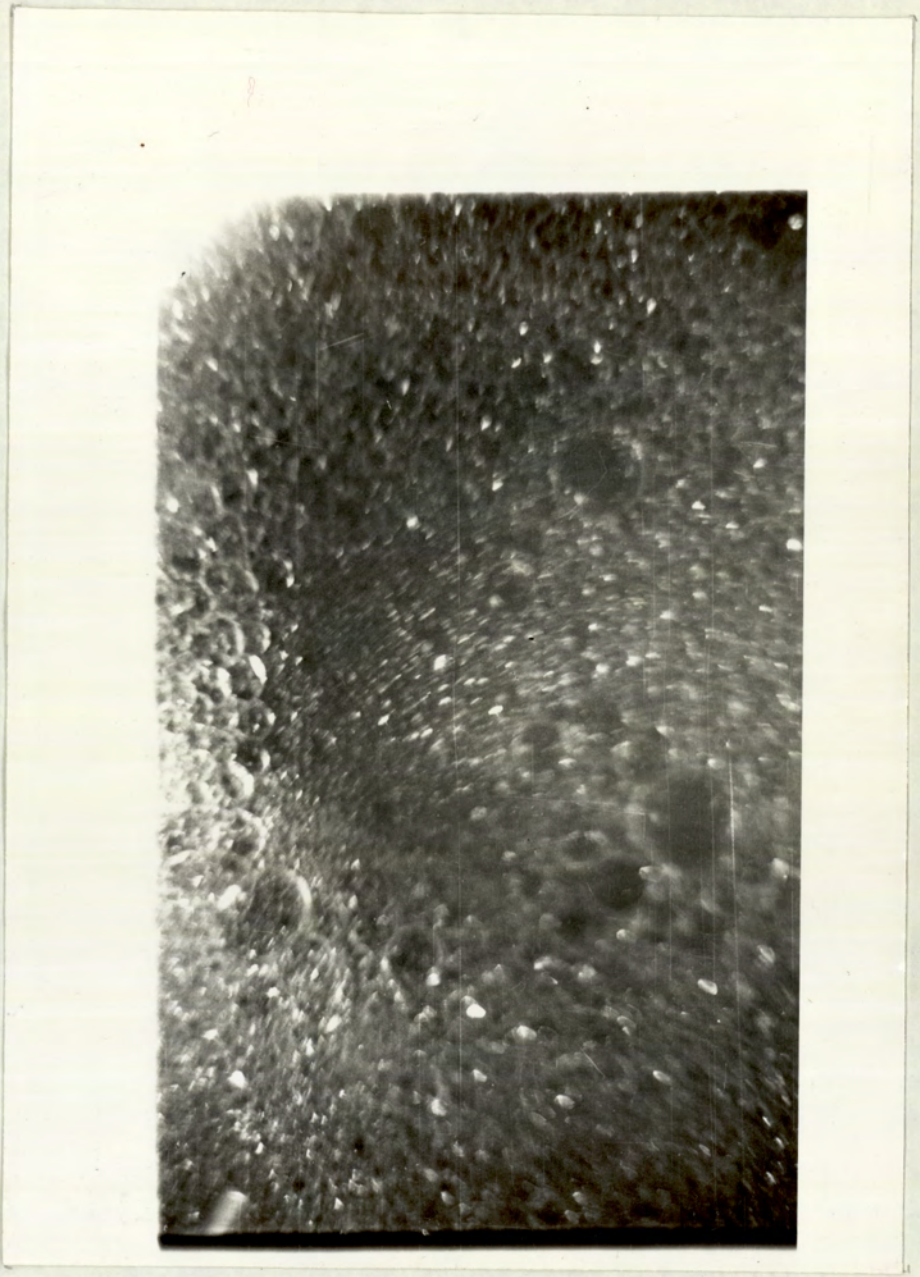

Figure 7.6 The crater formed at the mid-section starts to disappear.
(System: toluene-water, 6 inch column, d_n = 1.6 mm. Flow rate is higher than Figure 7.5.)

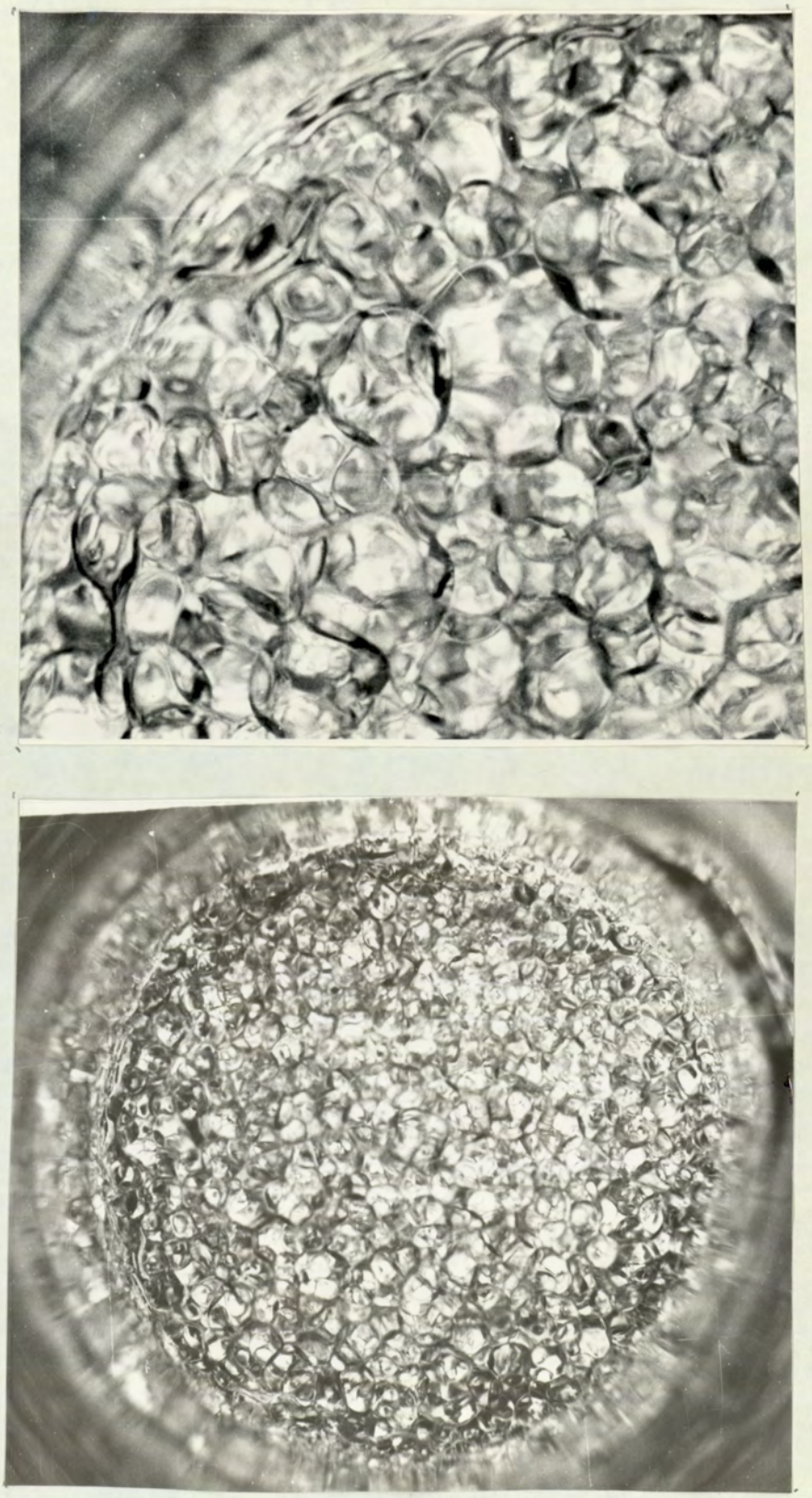

Figure 7.7 Top of a flocculation zone.
(System, toluene -water, 3.inch column, d_n = 1.2 mm)
(a) The whole cross section
(b) Enlarged part of (a).

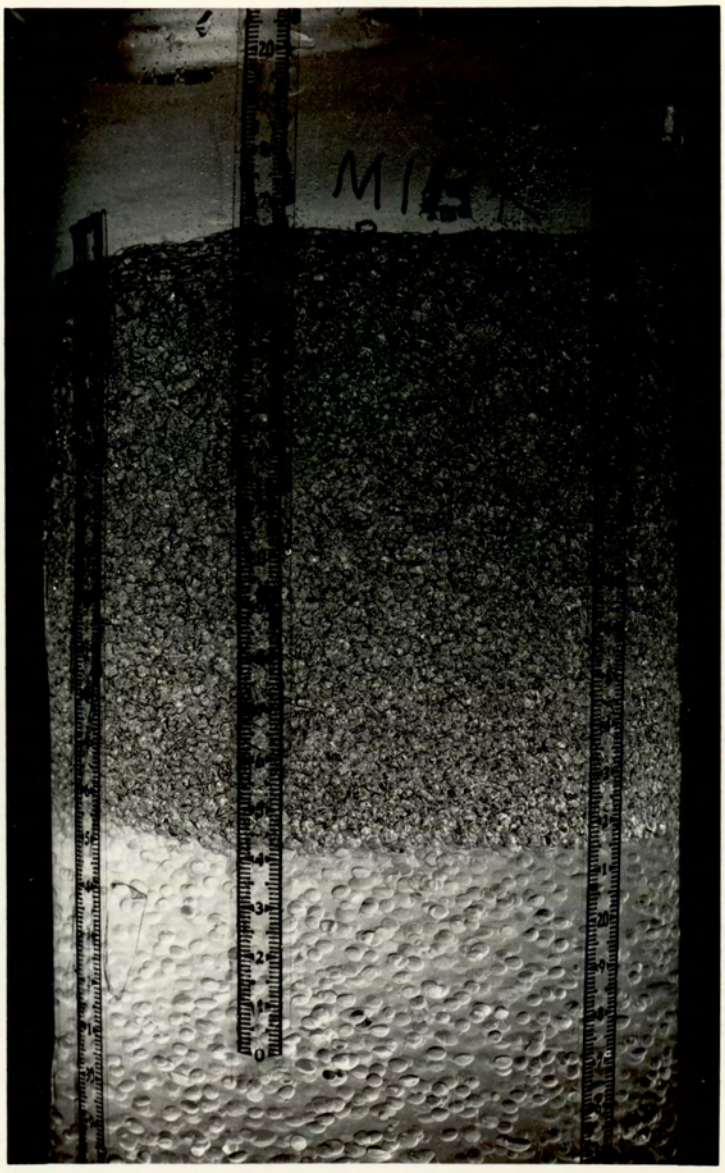

Figure 7.8 A flocculation zone.
(System: M.I.B.K.- water, 6 inch column, d_n = 1.66 mm.)

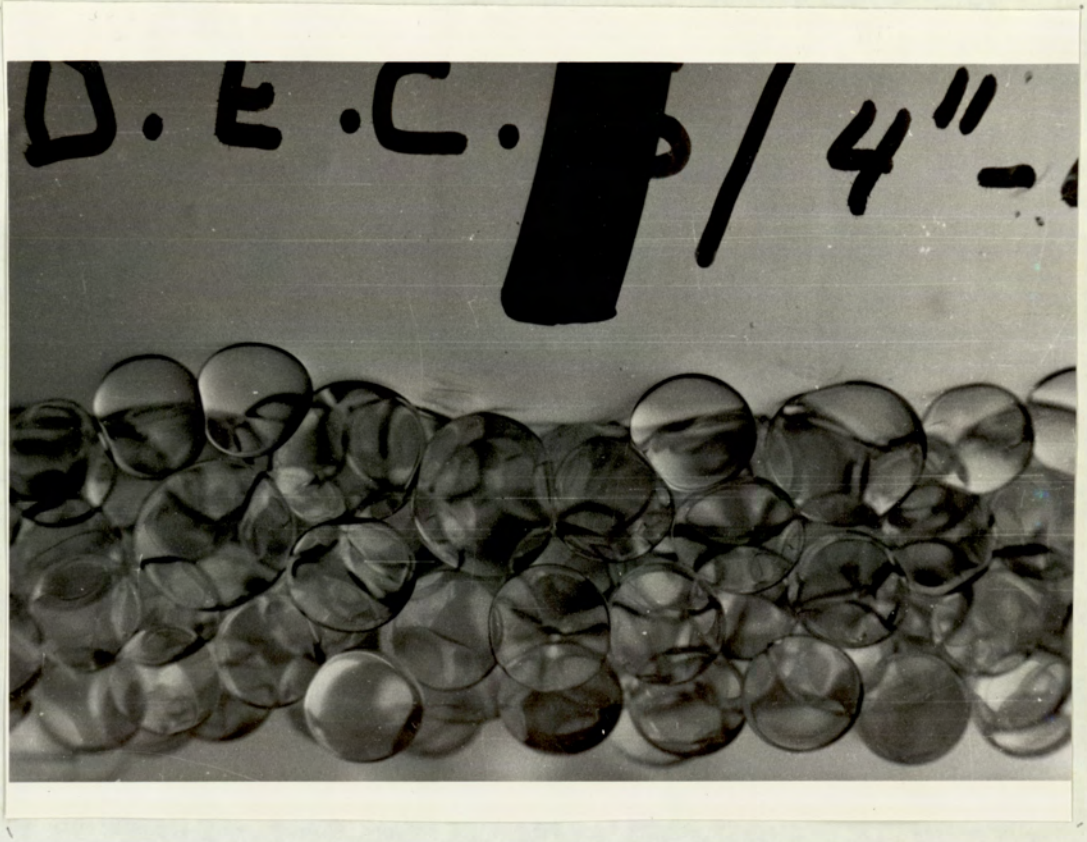

Figure 7.9 A shallow flocculation zone.
(System: Diethyl carbonate-water, d_n = 1.6 mm.)
This illustrates a flat top.)

7.2 The formation and effect of scum

Despite the use of distilled, relatively pure organic liquids and distilled water a visible scum with a jelly-like consistency was observed at the interface within 4 hours after start-up. Once this was removed, subsequent formation was reduced, and after a saturation period of 1 to 2 days no further significant amounts were formed. However the surface condition of the walls changed gradually after this time.

A sample from the toluene water was analyzed with a Mass Spectrometer and the results indicated only the presence of water, CO_2 and toluene. When it was dried on a watch-glass a thick deposit of the scum acquired the appearance of tissue paper; thin deposits had a transluscent appearance. The scum from toluene adhered to the glass walls but the scum from diethyl carbonate and isooctane was non-adhesive. No solid scum was observed with M.I.B.K. but a turbidity was noticeable in either the organic or aqueous phase.

A series of qualitative tests was conducted with the toluene-water system and the results are summarized below,

i. Technical toluene produced significantly more scum than distilled toluene.

ii. 'Solid' deposits at the interface reduced the flocculation zone height in the surrounding region; cleaning of the interface restored the zone height.

iii. Fresh deposits of scum on the column wall reduced the zone height. However, when operation was continued, after removal of these deposits but without cleaning the column walls, thin patches of scum on the column wall resulted in a progressive increase in bed height, as shown in Figure 7.10.

iv. Shielding the system materials from direct exposure to sunlight reduced the amount of scum formation and ageing effects.

Equal amounts of toluene water in a 100 ml clean flask progressively exibited distinct changes in behaviour. This was more significant after 30 days. A test sample exposed to sunlight for more than 90 days produced stabilized droplets compared with a similar sample, which was shielded throughout.

SYSTEM: TOLUENE - WATER

9" Column

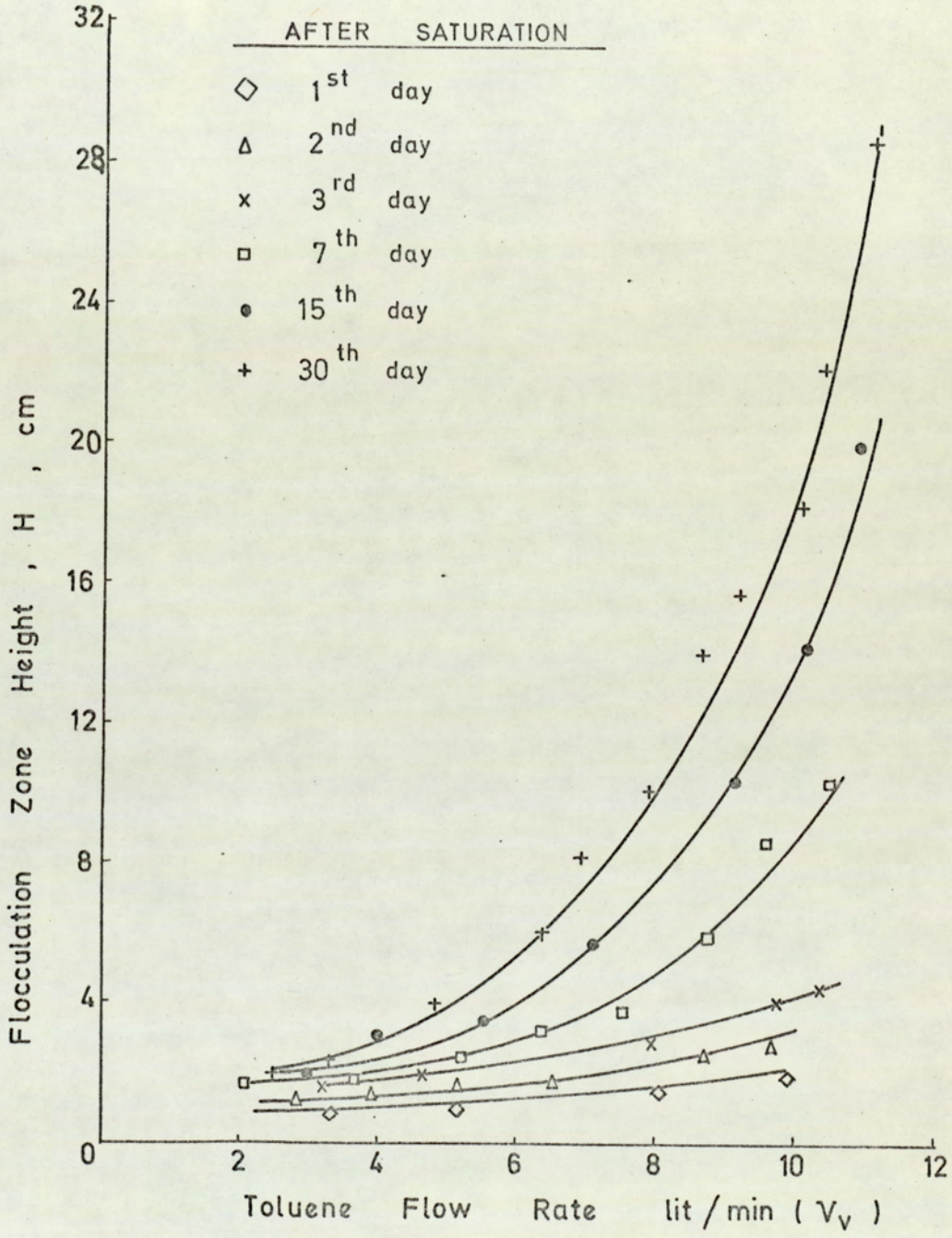

FIG. 7.10 THE EFFECT OF AGEING AND WALL CONTAMINATION ON FLOCCULATION ZONE HEIGHT (Column flushed before each operation and with the same system throughout , visible scum removed)

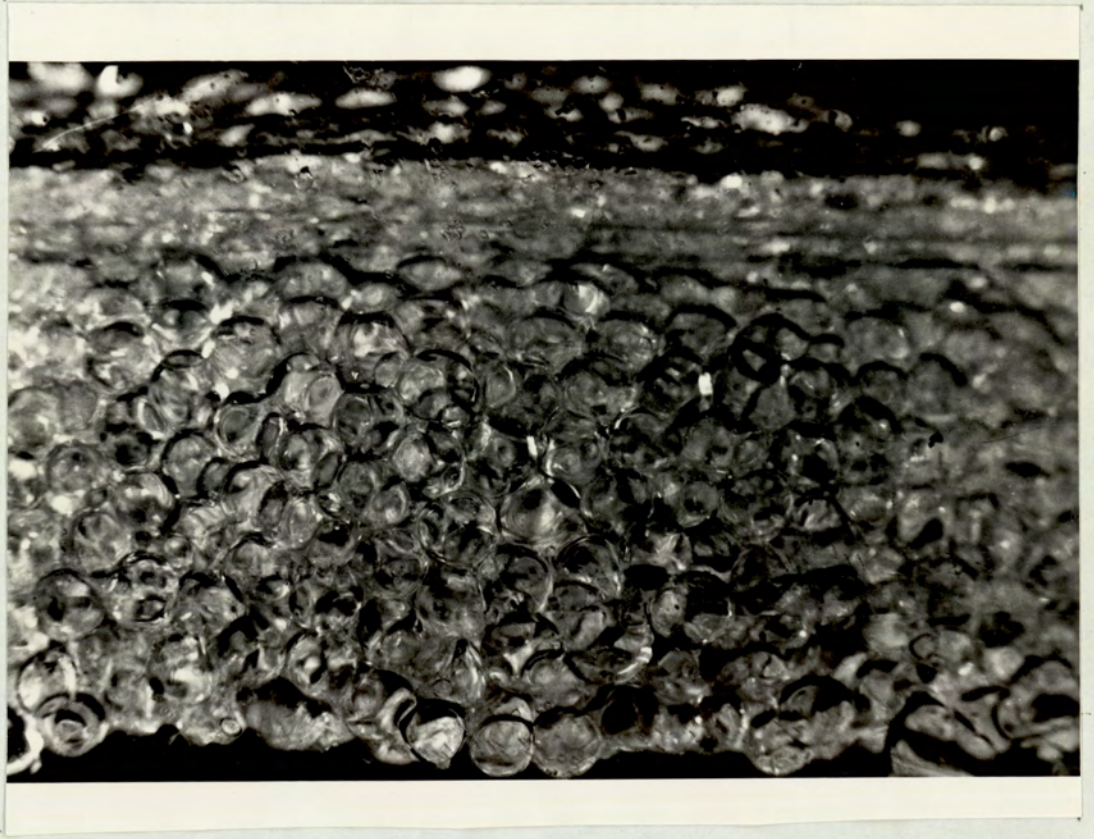

Figure 7.5.b Flocculation zone with toluene-water droplets, after operation of over 6 days in 9 inch column Very limited interdroplet coalescence.

7.3 Distribution of inlet drop sizes

Inlet drop size distributions, based upon drop counts from photographs for each system at various flow rates are given in Appendix 5.

Projection of the negatives was found to be more accurate, less expensive, quicker and more convenient than producing and then analysing prints. For small drop sizes, up to 20 times magnification could be produced. Therefore, the error introduced by the measurement of the diameters with a simple ruler was reduced below 0.1 mm, the biggest source of error being drops which deviated from sphericity.

To find the equivalent drop diameter for ellipsoidal drops, equivalence to an oblate spheroid volume gave a better approximation than use of a prolate spheroid volume. This has been found by measuring and comparing the equivalent diameter of elipsoidal drops in free motion with those resting on a plane interface which were closer to true spheres.

The approach of inlet drops of various systems to the interface, and the interface are illustrated in photographs shown in Figures 7.11 to 7.14.

For the range of dispersed phase flow rates employed assuming equal distribution of the total flow between all 450

Figure 7.11 Inlet drops from a distributor. (System toluene-water, 6 inch column, d_n=1.2 mm. ; d_{12}= 3.0 mm.)

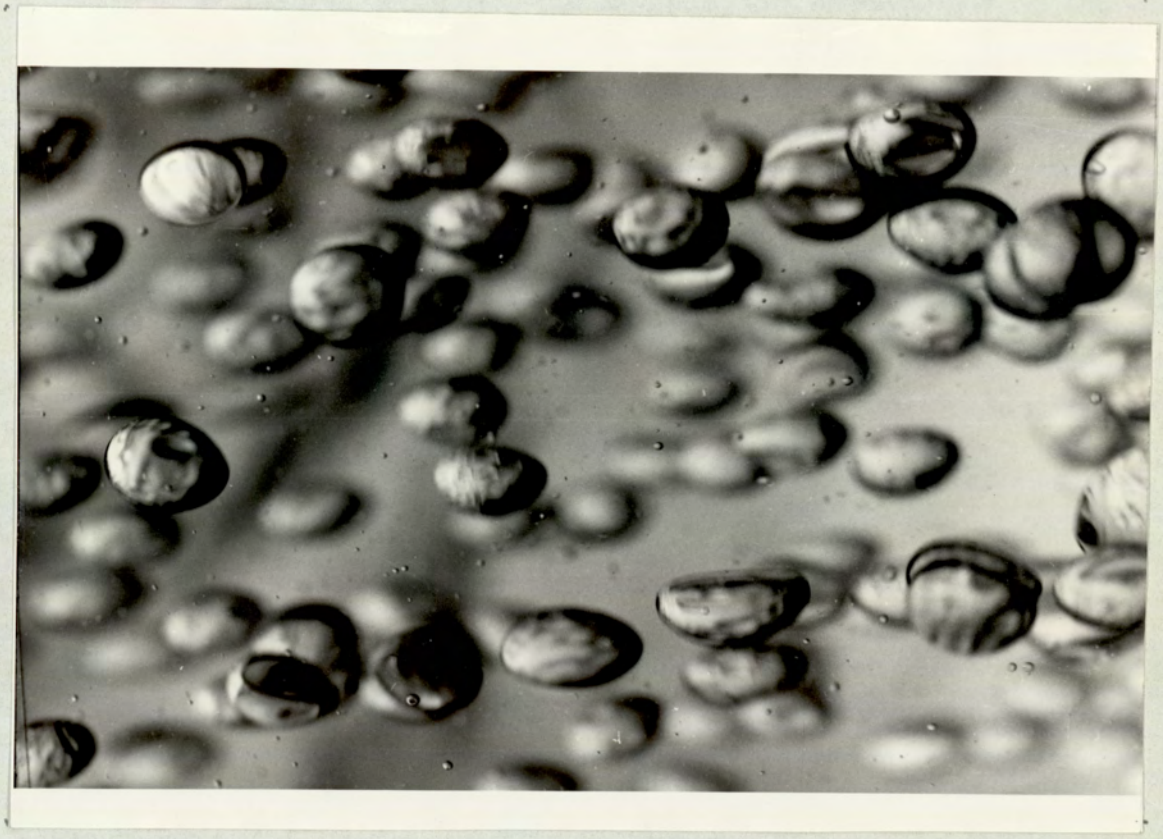

Figure 7.12 Inlet drops from distributor.
(System diethyl carbonate-water,
6 inch column , d_n = 1.6 mm)

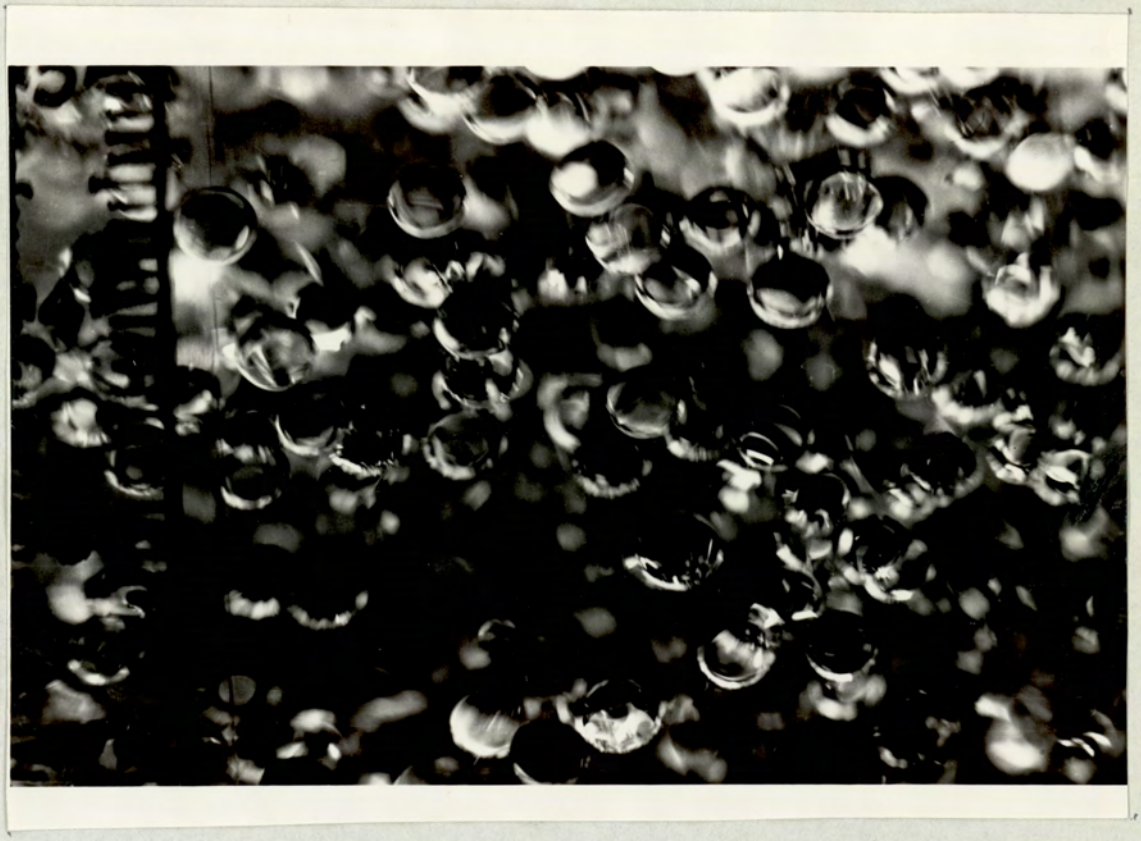

Figure 7.13 Inlet drops from a disributor.
(System Isooctane-water, 6 inch diameter column, d_n = 1.2 mm.)

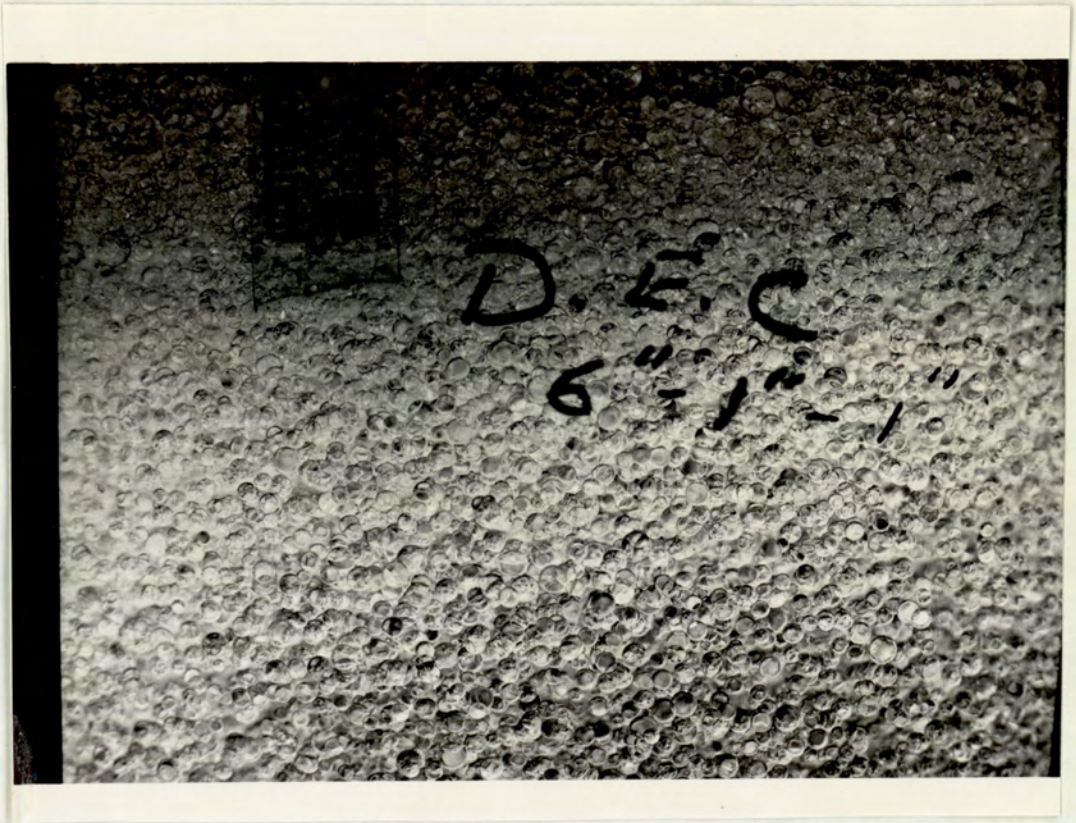

Figure 7.14 Inlet drops from a distributor.
(System: Diehtylcarbonate-water, d_n = 0.4 mm.)

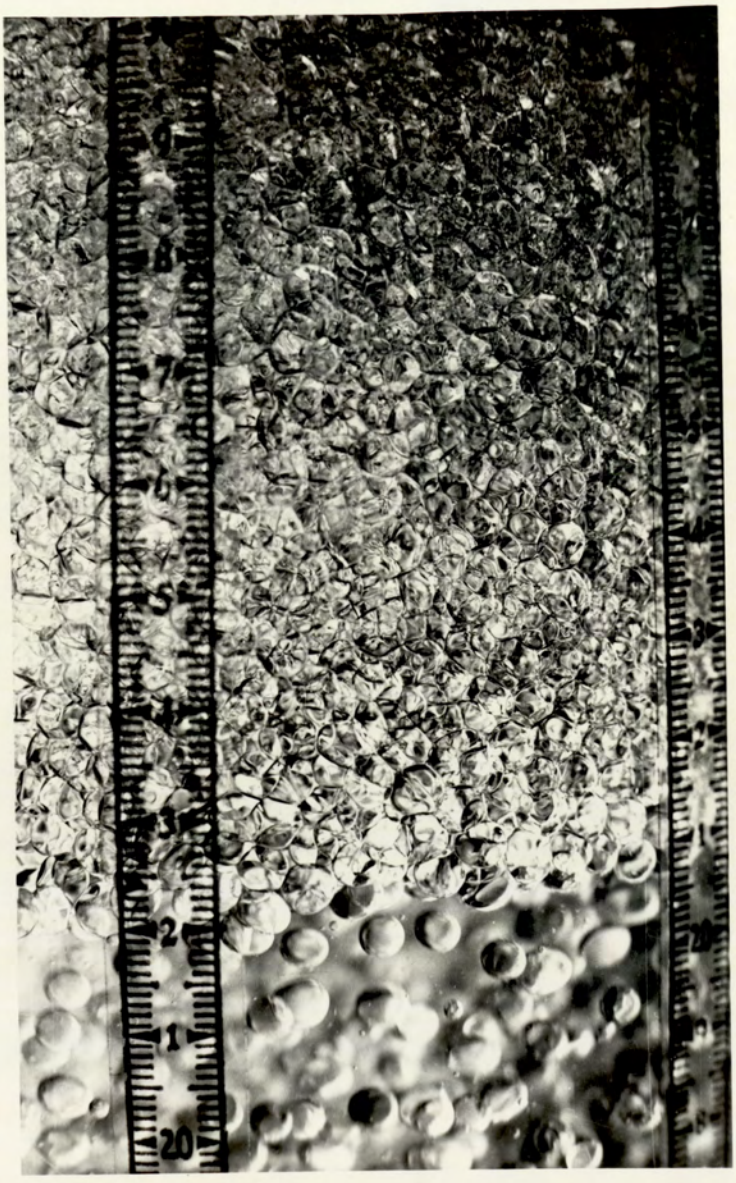

Figure 7.14.a 6 inch column.
System M.I.B.K.-water, d_n = 1.2 mm.

orifice holes, used in the 6 and 9 inch columns, drop diameters were calculated for the systems utilizing the plots given in Treybal (88). This was developed from the correlation given in English units, by Hayworth and Treybal (88),

$$v_d + 9.68(10^{-10}) \frac{v_d^{\frac{2}{3}} \rho_d V_n^2}{\Delta\rho} = 4.92\ (10^{-9}) \frac{\sigma' d_n}{\Delta\rho}$$

$$= 4.92\ (10^{-9}) \frac{\sigma' d_n}{\Delta\rho} + 4.95\ (10^{-4}) \frac{d_n^{1.12} V_n^{0.547} \mu_c^{0.279}}{\Delta\rho^{1.5}} \qquad (7.2$$

These theoretically calculated drop diameters and experimentally determined, d_{12}, mean drop diameters calculated from the drop size distribution data in Appendix 5, are plotted against the dispersed phase flow rate in Figures 7.15 to 7.18.

For low flow rates, calculated drop diameter was generally higher than the measured mean drop diameter. One reason for this was that at low flow rates drops were not produced from all the orifices. This was attributed to,

(a) the difficulty of installing an absolutely level distribution plate using a spirit level; the level was upset slightly when the bolts and nuts were tightened to join the pipe sections, and

(b) the plates having a very slight uneven curvature because, in the production of each orifice, every hole was punched and then drilled.

Thus at low flow rates the actual flow from the functional

orifices was greater than that calculated on the basis of perfect distribution between all of the orifices. For small orifice diameters, $d_n = 0.4$, the deviation was less than with the larger orifices. In fact, the measured drop size was larger than the calculated size with the smallest orifices although the reverse was true for large orifices.

The general trend of both measured and calculated drop size against flow rate curves are as expected, viz smaller size drops were produced at higher flow rates. The deviation between the two curves for any one orifice diameter varied with each system but increased with an increase in orifice hole diameter. Results with diethyl carbonate droplets were more unpredictable.

In conclusion the formula prepared by Hayworth was found unsuitable for the precise calculation of drop sizes from multi hole distributors for drop swarms. However, it was useful, in preliminary distributor design i.e. in the calculation of hole sizes to produce drops within the range to be studied.

The minimum and maximum drop sizes deviated by up to $\pm$ 15 per cent from the mean values, but about 80 per cent of the sizes fell within less than 10 per cent of the mean. Rarely an unusually large drop was produced from an accumulation of dispersed phase on the p.t.f.e. seal of the coloured drop introduction arrangement.

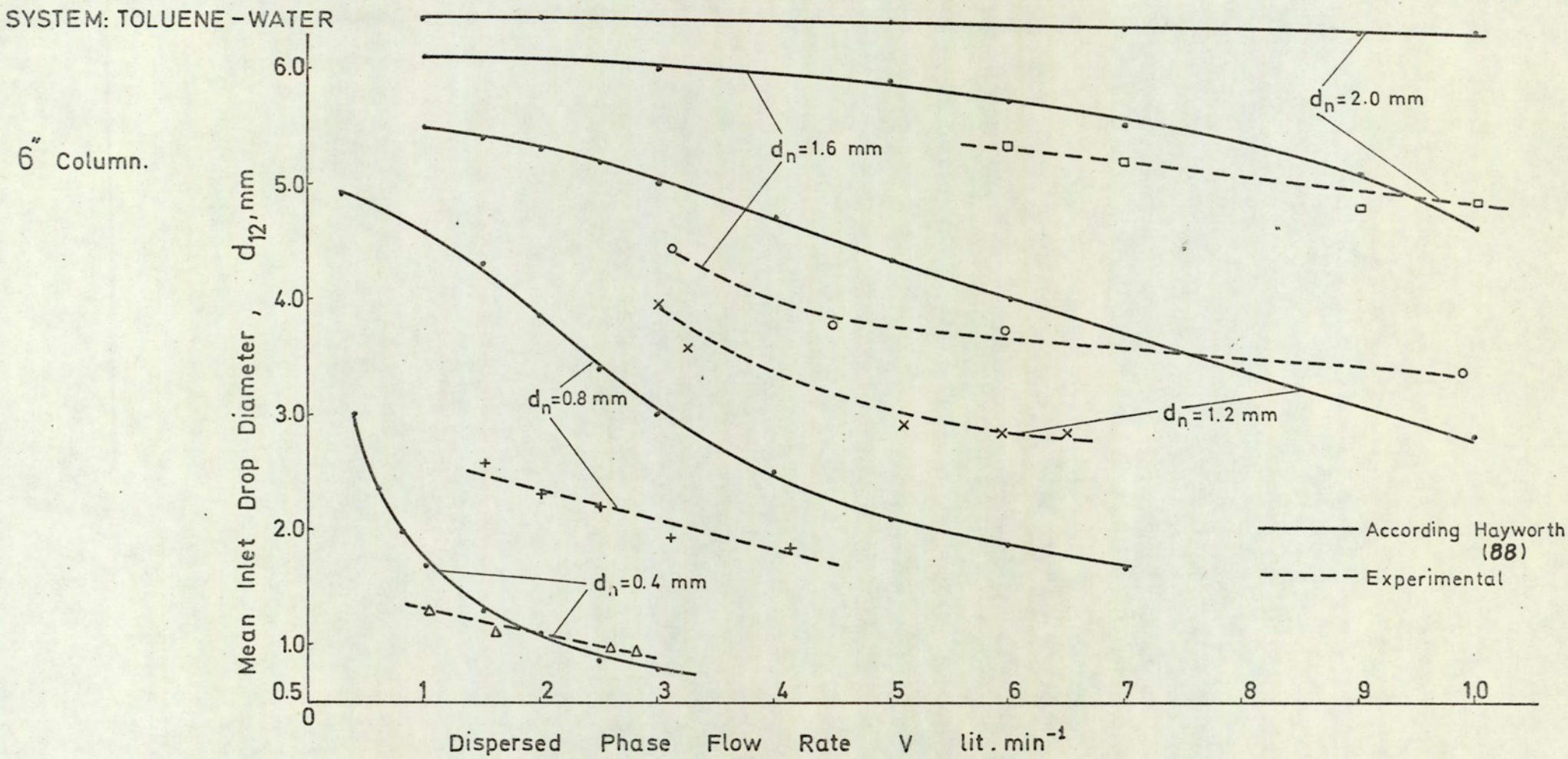

FIG. 7.15 MEAN MEASURED INLET DROP DIAMETERS AND DIAMETERS CALCULATED FROM THE HAYWORTH CORRELATION (88), VERSUS FLOW RATE.

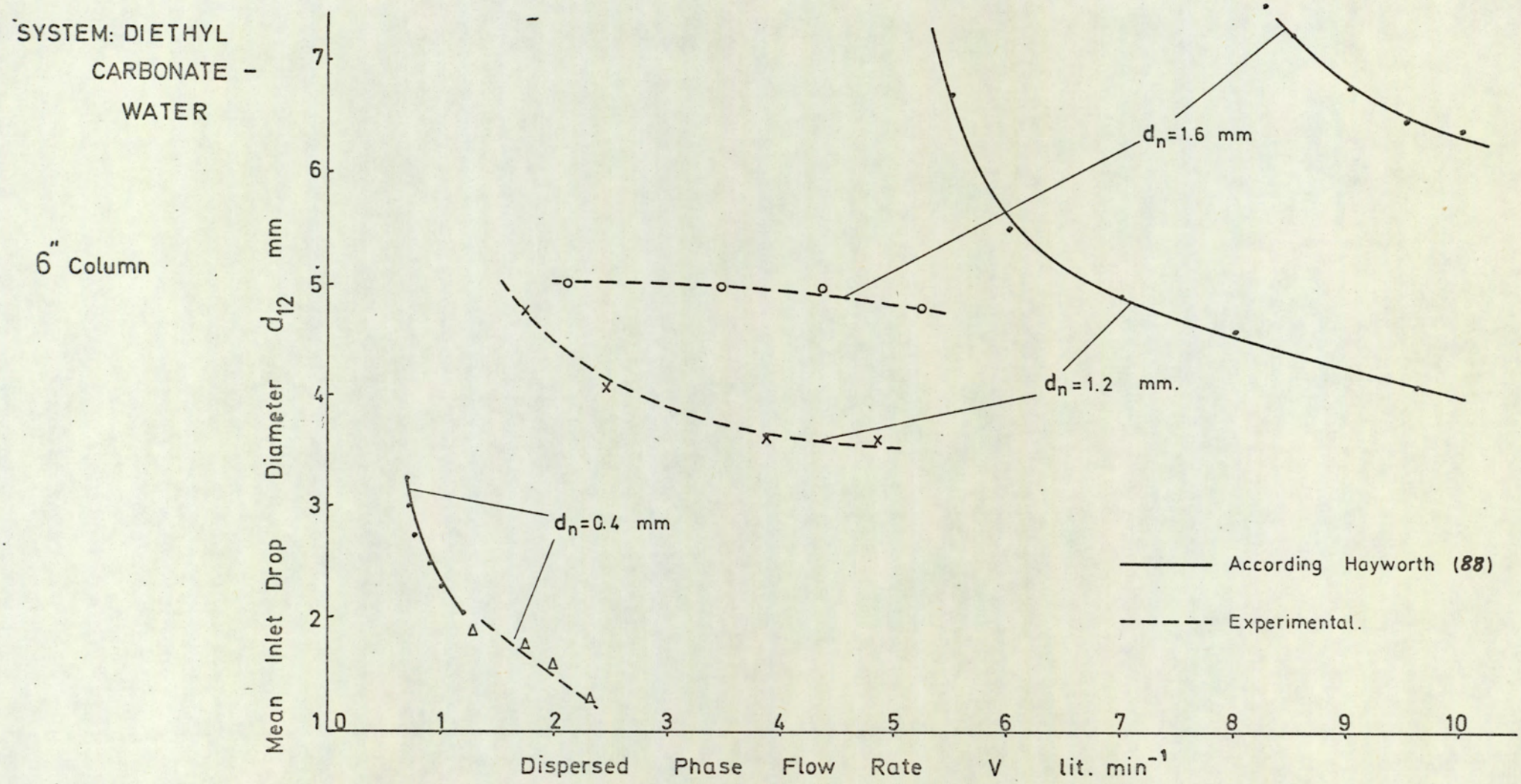

FIG. 7.16 MEAN MEASURED INLET DROP DIAMETERS AND DIAMETERS CALCULATED FROM THE HAYWORTH CORRELATION (88), VERSUS FLOW RATE.

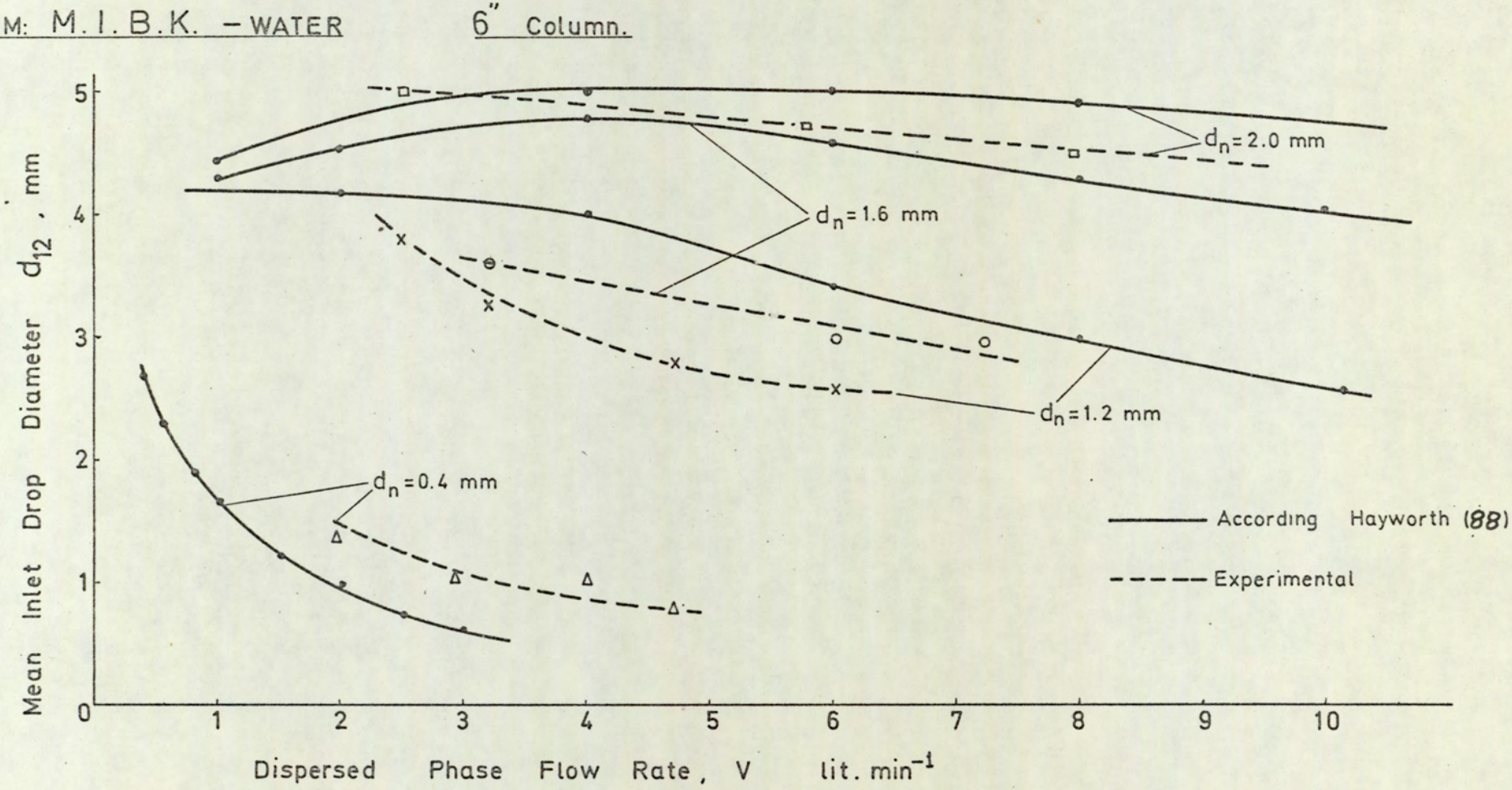

FIG. 7.17 MEAN MEASURED INLET DROP DIAMETERS AND DIAMETERS CALCULATED FROM THE HAYWORTH CORRELATION (88), VERSUS FLOW RATE

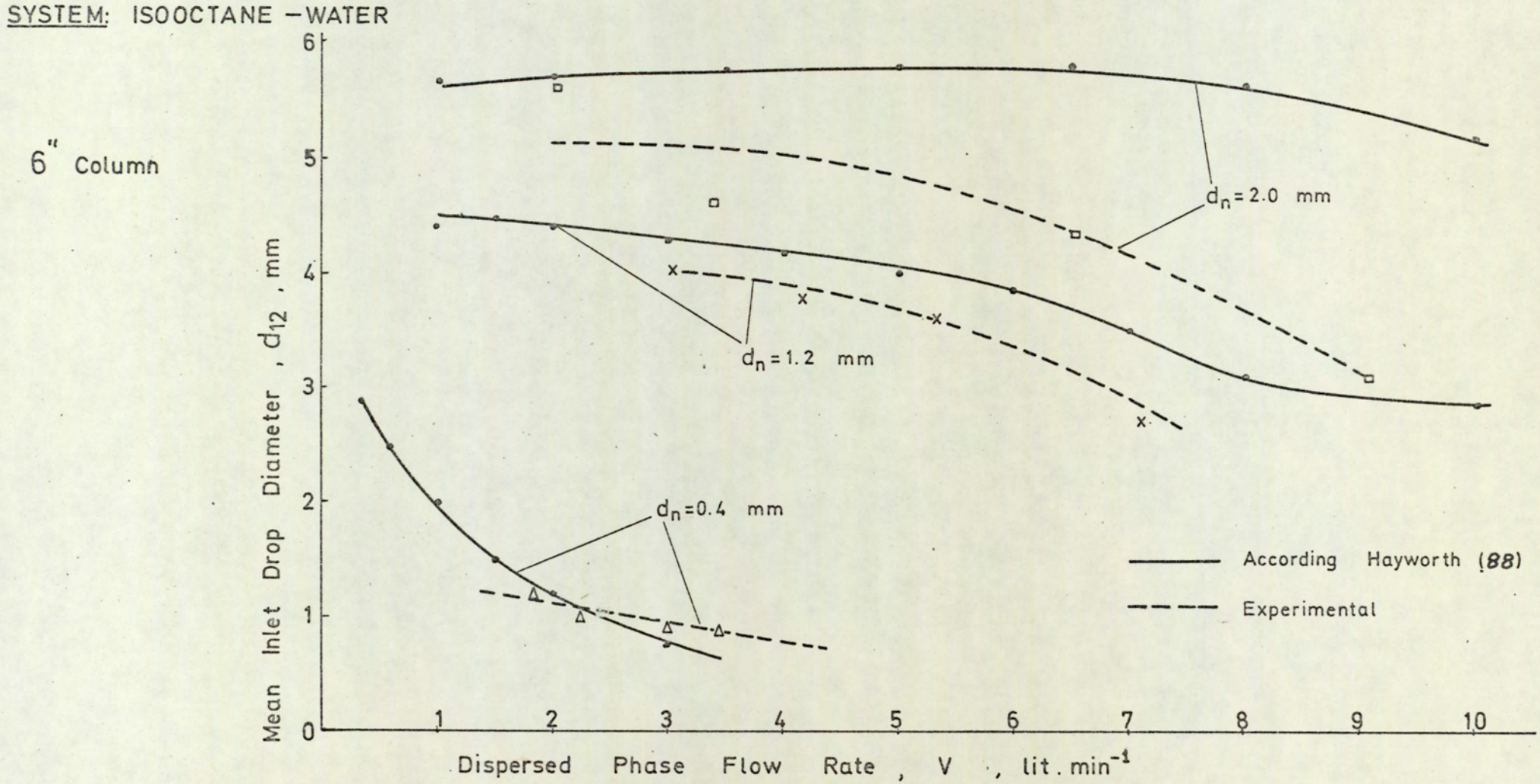

FIG. 7.18 MEAN MEASURED INLET DROP DIAMETERS AND DIAMETERS CALCULATED FROM THE HAYWORTH CORRELATION (88), VERSUS FLOW RATE

7.4 The effect of operating parameters on flocculation zone height

The results are tabulated in Appendices 3 to 7. The flocculated zone heights were measured by varying the dispersed phase flow rate after the bed reached a steady state. Distributor plates having orifice holes of known diameter were used to produce practically uniform size droplets as discussed in Section 7.3.

Counter current operation was initially investigated in an equipment arrangement, having a 6 inch column and a 9 inch settler as described in Section 6. It was found that flow of the continuous phase countercurrent to the droplets motion below the flocculation zone had no significant effect on the zone heights. Up to 1 : 1 ratio of continuous to dispersed phase flow rates this was less than 5 per cent. For phase ratios of above 1 : 1 to near 2 : 1 the difference went up to 5 to 10 per cent more than heights measured with a stationary continuous phase. The difference was not noticeable in the shallow beds produced in a clean column using the toluene-water system. With an aged toluene-water system and contaminated walls however which gave unusually high bed heights as illustrated in Section 7.2., differences in height such as 4-5 mm were observed between stationary and countercurrent operation for 1 : 1 phase ratios and a

dispersed phase flow of 6 - 8 litres per minute.

Countercurrent flow of the continuous phase influenced the motion of the droplets in the region below the flocculation zone in the usual way that is by creating more turbulence and back mixing of the droplets. In practice this back mixing affected the rate of drop formation at any given dispersed phase flow setting but for a set superficial dispersed phase velocity flocculation was unaffected. Therefore, counter - current operation was not utilized in subsequent work, the simpler operating conditions with a stationary continuous phase being preferred to obtain better control when obtaining measurements for other aspects of the investigation.

Temperature variations in the room over a whole year were recorded between 14 and 22°C, but during experimentation fluctuations were restricted to below 1°C. The results obtained in various days which were over the range 18 3 were considered acceptable. However in experiments involving the measurement of the zone height at increased flow rates the data could well be considered between 16 and 20°C. In some cases such as measurements of hold-up, for which at least a day was required to obtain a profile, fluctuations of 2-3 millimeters in total height were observed during the total time of measurement possibly due to a $> 4^{\circ}$ variation.

In a separate set of experiments the zone was cooled

outside by means of crushed pieces of ice wrapped in a cloth for a period of 2 hours; the temperature fell from 20°C. down to 15°C. Under these conditions, which produced approximately a 1°C fall in temperature in every 15 minutes, no noticeable fluctuations were observed over these individual time intervals. However, a fall of temperature between 1° and 2°C caused a measurable difference of 1 to 2 mm in height. The total 5°C temperature fall resulted in a total decrease of 4 mm in the height of a 5 cm flocculation zone of toluene.

Flocculation zone heights were measured by reference to graduations fixed to the column wall by adhesive tape. The accuracy of measurement was $\pm$ 1 mm. Readings were reproducible within less than $\pm$ 5% deviation once the systems had achieved mutual saturation i.e. within 1 to 2 mm. for bed heights of 2 - 6 cm or within 5 mm for heights up to 20 cm.

7.4.1. Unsaturated systems

Saturation was ensured by circulating the systems in the equipment for a total of 4-5 hours over a period of 24 hours; individual periods of circulation were generally for 20-30 minutes each. It was found that materials which had been 'mutually saturated' by manual shaking in 2½ litres bottles did not give reproducible results until they had been circulated in the equipment, in a similar manner to that described, over a period of 6 hours. Therefore a standard saturation procedure was adapted which involved running the phases in the equipment for 24 hours and then collecting results within the following 12 hours. All the results reported were obtained within this 'first day' period with the exception of those given in Figure 7.10 and certain hold-up data for the system toluene-water only.

The actual 24 hours during which fresh materials reached mutual saturation is called the 'saturation period'.

Repeated measurements of height with toluene-water showed that about 21 hours was necessary to produce reproducible results. Other systems took different times. The shortest time required was with the M.I.B.K.-Water system because of the higher mutual solubilities; this required about 8-10 hours to reach saturation or to achieve reproducibility.

The operating procedure outlined in Experimental Investigations Section 6, was in fact found to give essentially reproducibile results with toluene-water up to 5-6 days after saturation. After this the rate of increase of height became significant as indicated in Figure 7.10. This was attributed to the changing wall conditions and to a change in the system behaviour although there was no apparent difference in interfacial tension.

Stabilization of the flocculation zone, to produce a constant bed height, occurred within 24 hours and it was considered that the system had then reached complete mutual saturation. Any change of height after 'saturation' was considered to be due to the ageing, or contamination, of the system providing the effects of wall condition had been eliminated by proper cleaning given in Section 6.

All four systems gave less than 10 mm height with all orifice plates, i.e. in the range of 0.4 to 2.0 mm. orifice diameter, upon initial operation at the start of the saturation period. Very great fluctuations occurred in flocculation zone profile and height during the first 30 minutes due to the predominant effect of interdroplet coalescence; this clearly arose as a result of mass transfer taking place in two directions.

In the 3 inch column single drops of 3 cm diameter,

that is covering almost half the column diameter, have been observed during the first 10 minutes due to this phenomenon. The flocculation zone began to appear as the system progressed towards mutual saturation, resulting in a decreased incidence of interdroplet coalescence. This is illustrated in Figures 7.19 and 7.20.

As a point of interest it was found to be impractical to pump the unsaturated organic phases beyond certain flow rates because of the production of small droplets, leading to an uneven distribution, presumably due to mass transfer effects.

In general a minimum of about 1 hour was required from start-up with fresh liquids, during the saturation period, before a zone with distinct boundaries was established. Measurements were possible after this time although fluctuations persisted due to interdrop coalescence. Zone heights continued of course to increase up to the saturation point albeit at a decreasing rate. Within the first hour significant changes in height occurred within the time necessary to complete a set of readings covering the range of flow rates considered. This was usually about 10–15 minutes. Thus repeat results could not be obtained. It was observed that interdrop coalescence, and hence height changes, were less when one phase was saturated.

Figure 7.19 Flocculation zone with an incompletely saturated system. This illustrates the increased incidence of interdroplet coalescence.
(System Diethyle carbonate- water, 6 inch column, d_n = 1.2mm.)

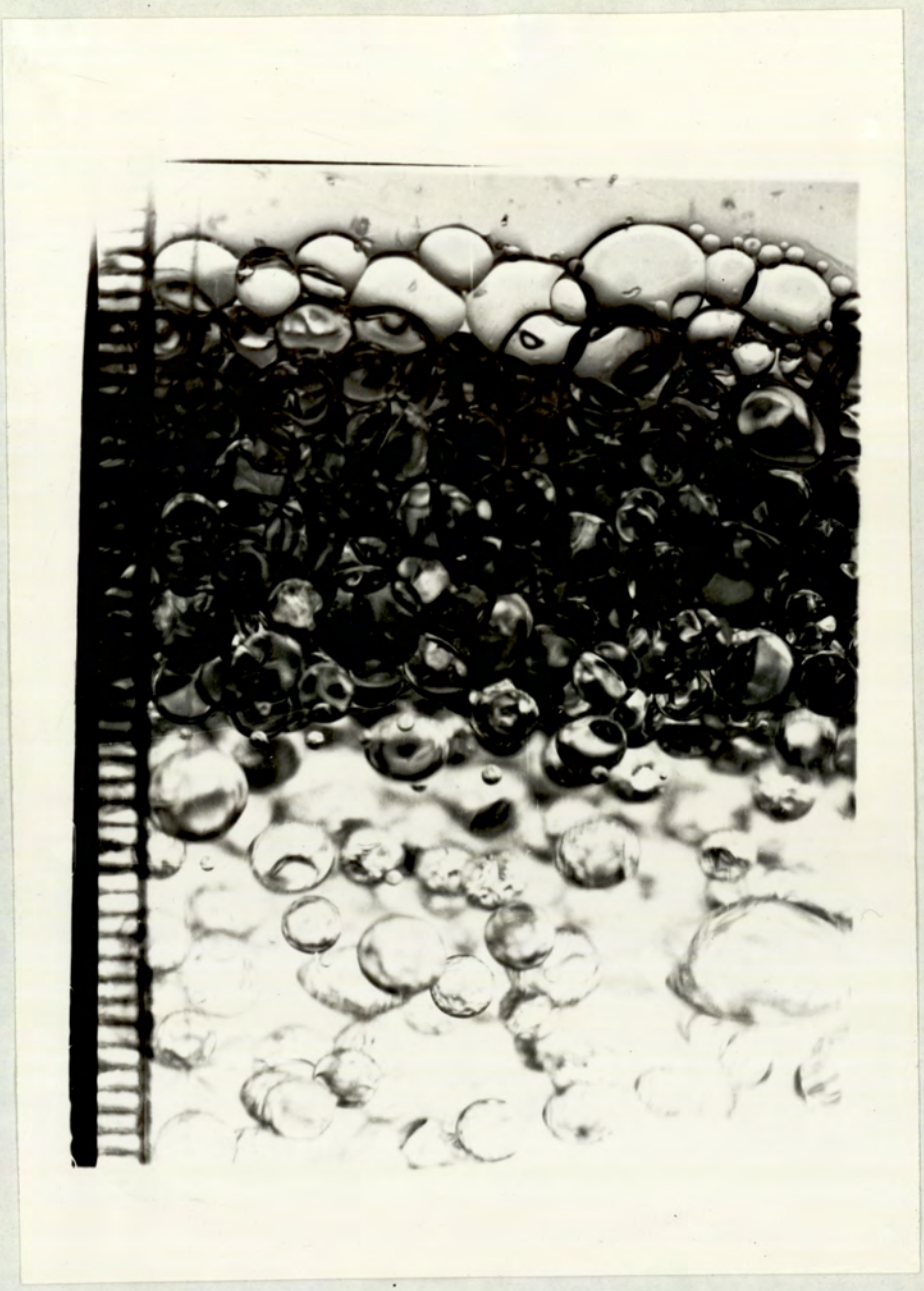

Figure 7.20 3 inch column.
System toluene water, d_n = 1.2 mm.

During the 3-4 hours following this first hour a noticeable change in bed height occurred only after periods of 15-20 minutes in comparison to the 5 minutes referred to above. This time extended to 20-30 minutes after the first 4 hours.

Attempts to determine the rate of change of bed height during the saturation period failed due to this lack of reproducibility and the difficulty of producing large amounts of system materials. To obtain such data, which may have been of doubtful value, would have required fresh system materials amounting to about 25 litres of organic and 50 litres of water for one set of results.

Results obtained in 9 inch column with the system toluene water are plotted in Figure 7.21 to provide a comparison of the change of bed height during the 'saturation period'. The results refer specifically to a column condition after 15 days normal operation, the column being washed with tap water for up to 30 minutes and then rinsed with distilled water before each run. A similar trend was observed with the column after cleaning but, since the overall heights were considerably less, these results do not illustrate the phenomena so well. The data for heights after 24 hours are however shown in Figure 7.21.

The column condition, to which Figure 7.21 is specific, is one in which a film of scum was observed adhering to the wall as a thin coat. It was found that thin scum could not be removed completely merely by flushing with water. At high flow rates bed heights were approximately 10 times larger with this column condition than in a clean, uncontaminated column. The reason for the high bed heights associated with this condition was that the film of scum enabled the walls to be wetted by the dispersed (toluene) phase. This'wetting'was observed not to occur uniformly but to be distributed randomly as patches. Davies and Smith (5) reported and Allak (81) has demonstrated that if the column walls are coated with a compound such as a 2 per cent solution of dimethyl dichlorosilane in carbon tetrachloride, so as to alter the wetting condition of the glass walls the bed heights were decreased *i.e* it was higher with the walls wetted by the dispersed phase. This may be explainable by the increased resistance to the continuous phase drainage on the walls that takes place.

In a clean column fresh toluene-water attained a bed height of about 20 mm at the maximum flow rate after 21 hours. Similar fresh toluene water in a contaminated column attained a total height of about 200 mm after 21 hours and this height was reproducible over the following 5-6 days. Any steady height attained with isooctane-water after 14 hours from the start-up remained reproducible for the following 31 hours.

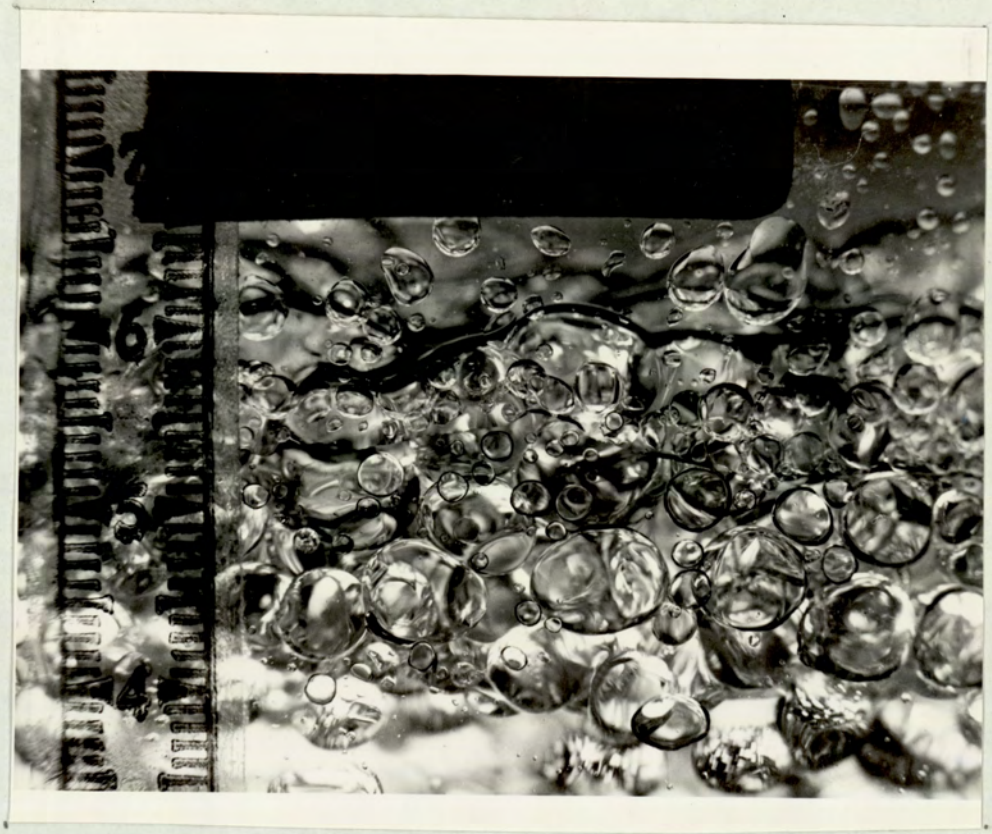

Figure 7.21.a Flocculation zone showing dispersed phase wetting of the column walls due to the contamination.(System toluene- water, 6 inch column, d_n= 2 mm)

SYSTEM: TOLUENE-WATER

9" Column

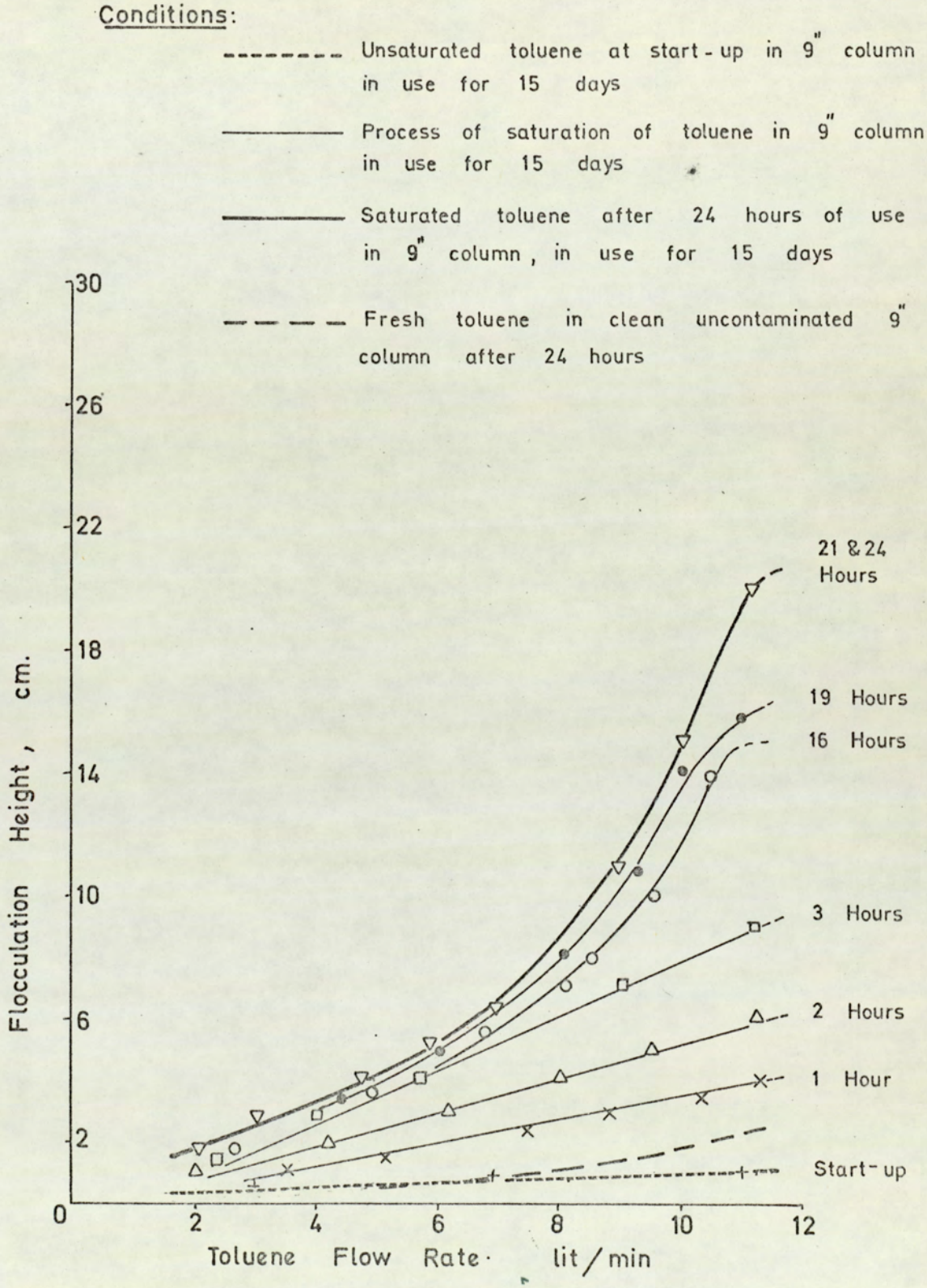

FIG. 7.21 FLOCCULATION ZONE HEIGHT versus FLOW RATE FOR TOLUENE IN 9" COLUMN AT CONDITIONS SPECIFIED

Similarly diethyl carbonate was found to be saturated within 10 hours and bed heights then remained steady for the following 32 hours. These results are tabulated in Table 7.1. On the basis of these observations, all the measurements used in this investigation were recorded during the period following the first 24 hours and up to the time given in the second column in Table 7.1. Otherwise the column was cleaned and fresh system materials were employed.

TABLE 7.1

TIME TO REACH CONSISTENT ZONE HEIGHTS AND SIGNIFICANT CHANGE AFTERWARD

System	d_n	Time to reach consistent bed height	Time after which noticeable changes in height exceeds 10% of the 'first day' height
	mm	hrs	hrs
Toluene	1.6	21	80
Isooctane	1.2	14	45
M.I.B.K.	0.4	6	31
Diethyl carbonate	1.2	10	42

The above times were not obtained with the same orifice diameters which could conceivably result in there being some variation in

the saturation time given in the first column of Table 7.1., since Treybal has indicated that a change of equilibrium saturation occurs with drop size. This effect is given quantitatively by the equation,

$$RT \ln \frac{f}{f^{o}} = \frac{4\sigma V}{d} \qquad (7.3)$$

where f = fugacity of the small particle

f^{o} = fugacity of the same substance with a float surface

d = diameter of the particle

σ = interfacial tension

T = Temperature

V = molar volume of the dispersed phase

R = constant

Fugacity ratios are proportional to the solubilities. Whilst this seems unlikely to have any significance because of the relatively narrow size range of drops employed in this work, it may be of importance in secondary haze studies.

As mentioned earlier, all the systems were allowed 24 hours to reach saturation to eliminate any possibility of measurements being taken with unsaturated phases due, for example, to changes in temperature or drop sizes. That different systems required different times within this 24 hour period to attain mutual saturation was of course due

to the different solubilities and rates of diffusion.

It is worth noting that there is a need for a practical and accurate method of testing saturation point. As mentioned in the earlier paragraphs, systems which were 'saturated' by occasional shaking in bottles over a period of 24 hours, or indeed even up to 72 hours, did not give constant bed heights upon start up. This created doubts as to whether saturation by bottle shaking is sufficient to establish equilibrium. One qualitative test that tended to confirm the inadequacy of this technique involved the addition of 2.5 litres of dispersed phase material 'saturated' in the bottle to the column contents of about 20 litres. This resulted in a reduction of more than 10% in bed height. Aqueous phase addition gave similar results. Since the column contents were uncontaminated this can only be explained on the grounds that the material from the bottles was not saturated.

In conclusion the results submitted in Subsection 7.4.2. are those from 'first day' measurements with mutually saturated systems.

7.4.2 Stable saturated systems

Flocculation zone heights are plotted against dispersed phase flow rates in the Figures 7.22 to 7.28 from the results tabulated in Appendix 3.

Flocculation zone height invariably increased with increase of the dispersed phase flow rate with all four systems investigated. Up to 0.2 $ml.cm^{-2}.sec^{-1}$. flow rate, little difference was observed between zone heights for all the systems, being $<$ 10 mm. for a mean inlet drop size of $>$ 2 mm. The smaller orifice holes in the distributor plates, i.e. 0.4 and 0.8 mm producing droplets of less than 2 mm size, generally gave substantially higher bed heights over the whole range of flow rate studied (0.15 to 0.8 $ml.sec^{-1}.\ cm^{-2}$).

Mean inlet drop diameters had a greater effect on zone height than flow rate. In general zone height was directly proportional to the dispersed phase flow rate and indirectly proportional to the inlet mean drop size. As far as system properties were concerned the only exception to this trend occurred with the system M.I.B.K-water when 1.2 and 1.6 mm nozzles gave approximately the same bed heights with only a slight tendency for the 1.2 mm nozzle to result in a higher bed height.

The relationship between bed height and flow rate over the total range studied is non-linear. However, for large drop sizes a linear relationship between the height and flow rate would give a fair representation of the data.

In order to obtain a general relationship, all the data have been plotted on log-log scales and the best straight lines drawn through them. If very low flow rates, including monolayer formation, were considered all these curves would in theory start from heights corresponding to one drop diameter, at the flow rate required to produce a complete monolayer. Unfortunately the true minima of each curve pertaining to a specific mean drop diameter could not be found because a true monolayer was impossible to produce in practice since at least 2-3 layers of droplets piled up at the column wall whilst the mid-section of the column was still an incomplete monolayer as described in Section 7.1. Therefore, the minimum consistent bed height was of the order of 5-6 mm; more reliable height measurements required at least a 10 mm bed.

7.4.3 Dispersed phase flow rate

The variation of flocculation zone height with dispersed phase flow rate was found to be best represented by the general equation,

$$H = a_o V_d^b \qquad (7.4)$$

The values of coefficient a_o and the power, b, have been evaluated by a graphical method, for all the inlet drop sizes, systems and columns investigated and are tabulated in Table 7.2.

The largest effect of flow rate was exhibited with the system isooctane-water. If the effect of the other variables is assumed to appear only in the coefficient a_o in Equation 7.4, increase of bed height with isooctane is proportional to about the cube of the flow rate in comparison to an almost linear relationship with toluene. The power terms for the other systems, diethyl carbonate and M.I.B.K are 1.88 and 1.43 respectively except for an orifice diameter of 0.04 cm.

From an inspection of the values of the power term, b, it is clear that with the 0.04 cm. orifice diameter distributor plate, which produced droplets $<$0.1 cm diameter, or with diethyl carbonate, $<$0.12 cm, the effect of flow rate on the flocculation zone height was significantly higher.

Toluene was the sole exception to this. However from an inspection of all the lines drawn through the points in Figure 7.25 it is clear that less confidence has been placed upon results for low bed heights below about 1 cm. This is

TABLE 7.2

VALUES OF POWER TERM b AND COEFFICIENT a_o IN THE EXPRESSION RELATING ZONE HEIGHTS WITH DISPERSED PHASE FLOW RATE

General equation 7.2: $H = a_o V_d^b$

System	Dp cm	d_n cm	d_{12} cm	a_o	b
Toluene-water	7.3	0.04	0.09	13.20	1.04
	7.3	0.08	0.18	7.77	1.04
	7.3	0.12	0.30	6.70	1.04
	7.3	0.16	0.36	5.62	1.04
	7.3	0.20	0.48	4.78	1.04
"	15.0	0.04	0.09	15.16	1.24
	15.0	0.08	0.18	9.91	1.24
	15.0	0.12	0.30	7.64	1.24
	15.0	0.16	0.36	5.96	1.24
	15.0	0.20	0.48	4.96	1.24
"	21.6	0.12	0.30	7.06	1.20
	21.6	0.16	0.36	5.81	1.20
	21.6	0.20	0.48	4.29	1.20
Diethyl carbonate-water	15.0	0.04	0.12	1760	2.90
	15.0	0.12	0.35	61.4	1.88
	15.0	0.16	0.47	41.0	1.88
M.I.B.K - water	15.0	0.04	0.08	66.5	1.73
	15.0	0.12	0.27	64.9	1.43
	15.0	0.16	0.31	26.0	1.43
	15.0	0.20	0.47	32.5	1.43
Isooctane-water	21.6	0.04	0.07	979	3.49
	21.6	0.12	0.28	43.5	2.75
	21.6	0.20	0.45	16.1	2.80

done since, in accordance with the mechanisms for the formation of flocculation zones described in Section 7.1, curvature of interface and piling up drops around the column wall produced significant effects at low dispersed phase flow rates, in the range of 0.1 to 0.2 $ml.cm^{-2}.sec^{-1}$, just following monolayer formation. Moreover, in shallow beds of 10 mm or less the possible measurement error of 2 mm represents a greater percentage.

Therefore, placing less reliance upon results with shallow beds, should yield a better general representation of data over the whole range. However, the solid line through the data for toluene drops from a 0.4 mm. nozzle can only be drawn by including the two points obtained at low flow rates; this then results in a line parallel with the other four and enables a general relationship to be derived. Unfortunately this leads to a poor representation of the data with this size orifice at high flow rates; if little reliance is placed on the values at low flow rates, equivalent to bed heights of only about 1 cm with 0.9 mm drops, the bulk of the results are best represented by the dashed line with a slope of 1.81. This is in agreement with the results with other systems for which drops $<$ 1 mm behaved differently to the larger sizes. Thus the correlations given here should be considered applicable only to zones in which the initial drop diameter is $>$1 mm. and zone heights $>$ 1 cm.

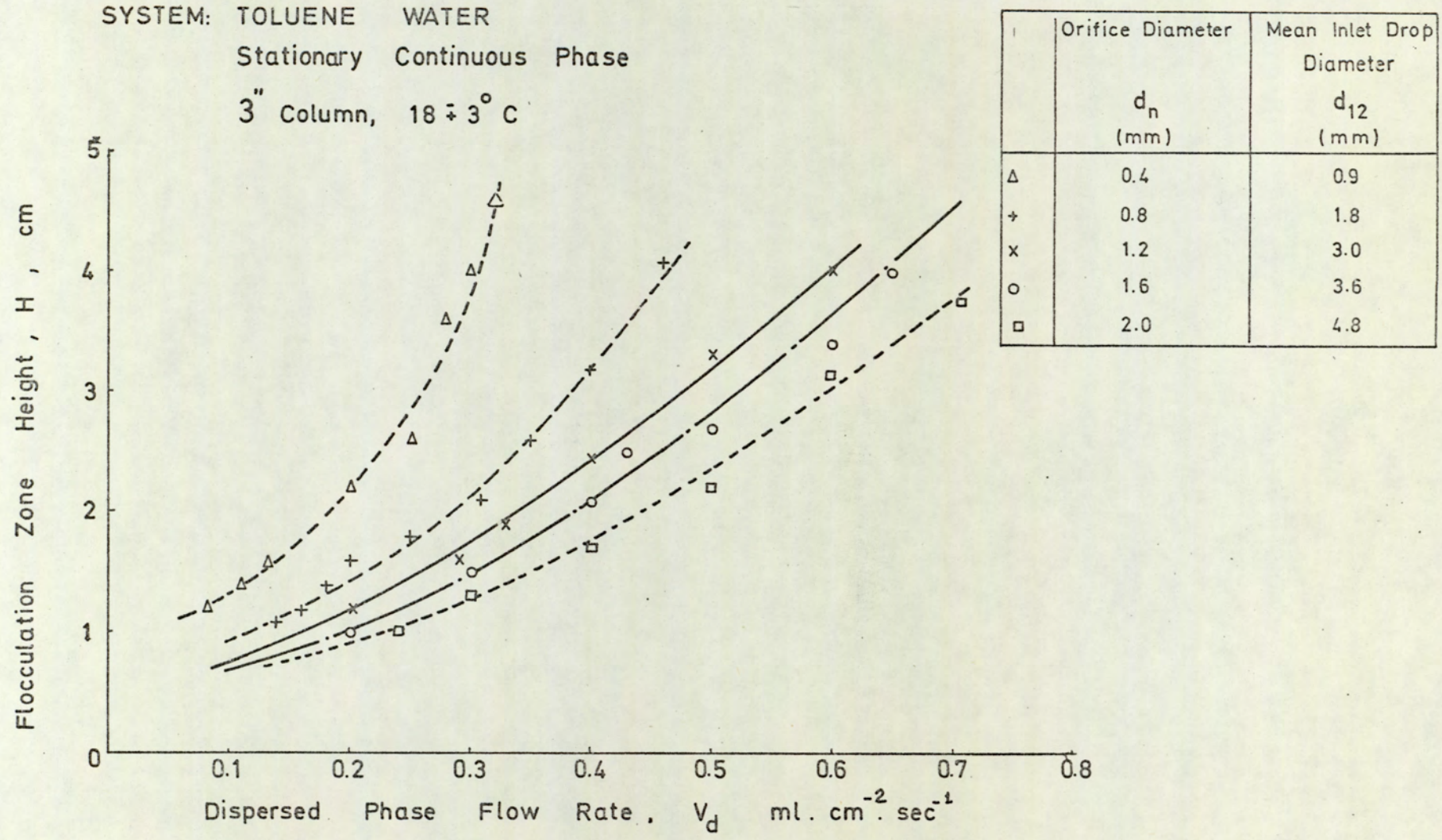

	Orifice Diameter d_n (mm)	Mean Inlet Drop Diameter d_{12} (mm)
△	0.4	0.9
+	0.8	1.8
×	1.2	3.0
○	1.6	3.6
□	2.0	4.8

FIG. 7.22 EFFECT OF DISPERSED PHASE FLOW RATE AND INLET DROP SIZE ON FLOCCULATION HEIGHT.

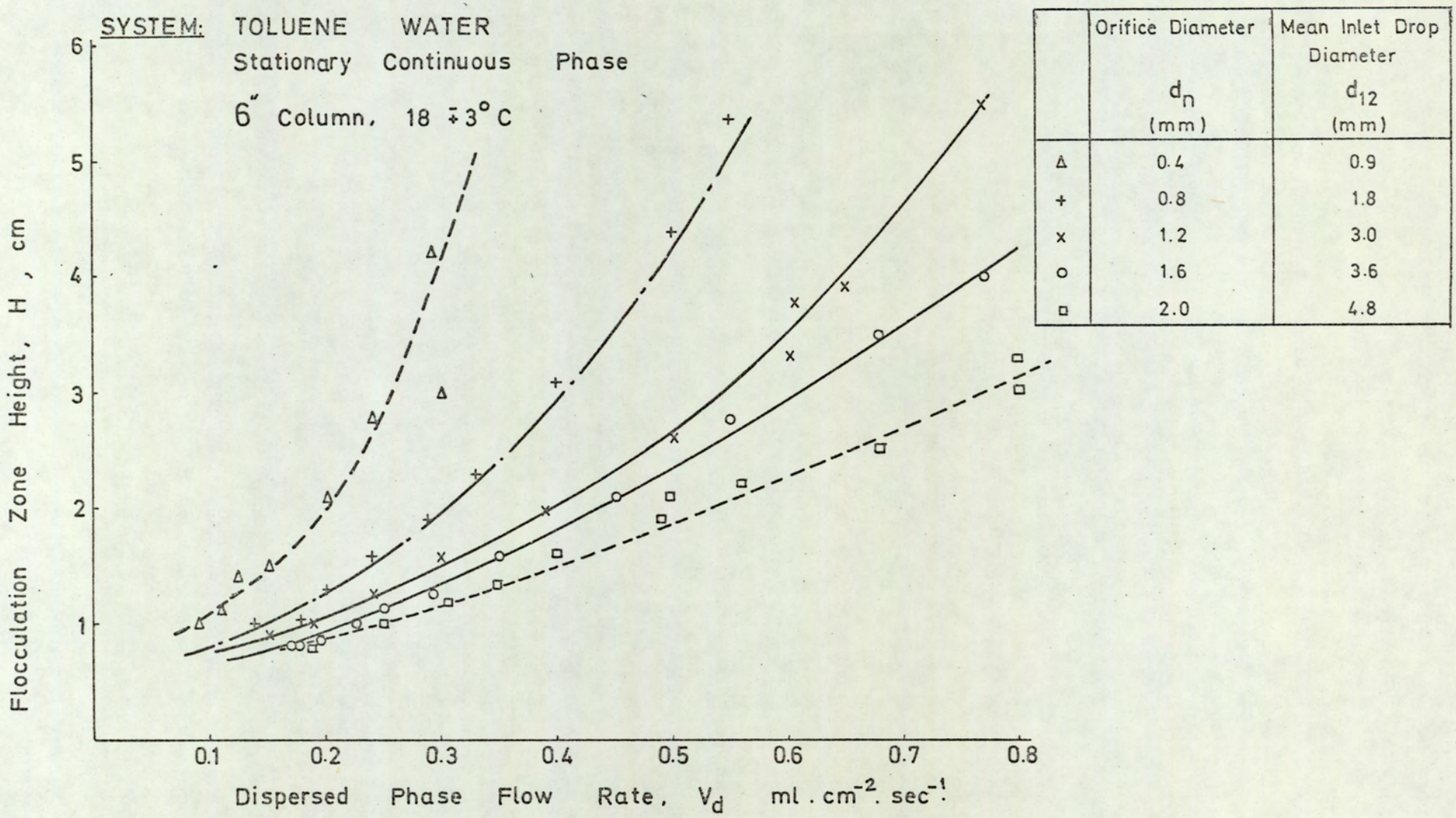

	Orifice Diameter d_n (mm)	Mean Inlet Drop Diameter d_{12} (mm)
△	0.4	0.9
+	0.8	1.8
×	1.2	3.0
○	1.6	3.6
□	2.0	4.8

FIG. 7.23 EFFECT OF DISPERSED PHASE FLOW RATE AND INLET DROP SIZE ON FLOCCULATION ZONE HEIGHT

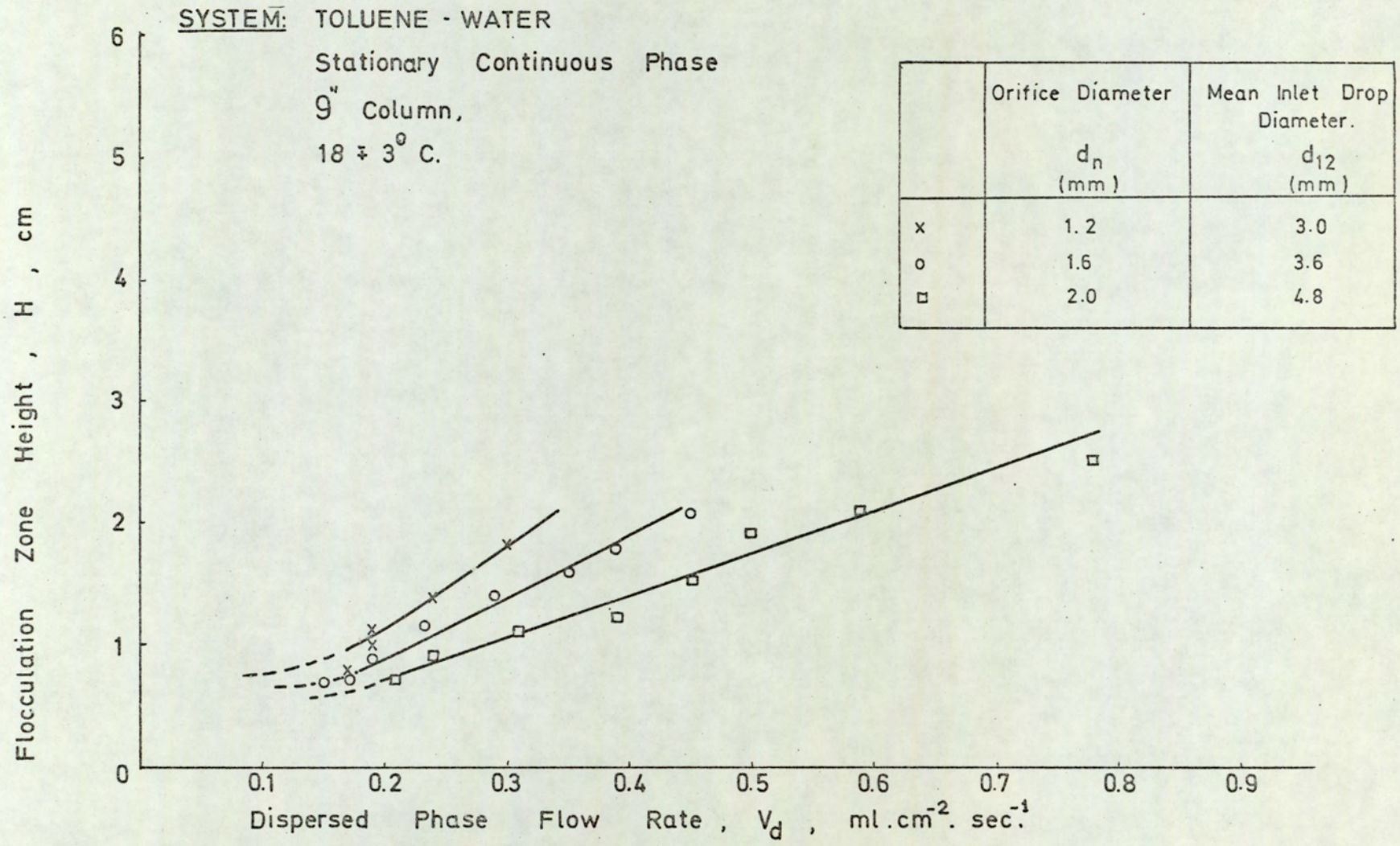

FIG. 7.24 EFFECT OF DISPERSED PHASE FLOW RATE AND INLET DROP SIZE ON FLOCCULATION HEIGHT

SYSTEM: TOLUENE - WATER

Stationary Continuous Phase

6" Column

	Orifice Diameter d_n (mm)	Mean Inlet Drop Diameter d_{12} (mm)
Δ	0.4	0.9
+	0.8	1.8
×	1.2	3.0
○	1.6	3.6
□	2.0	4.8

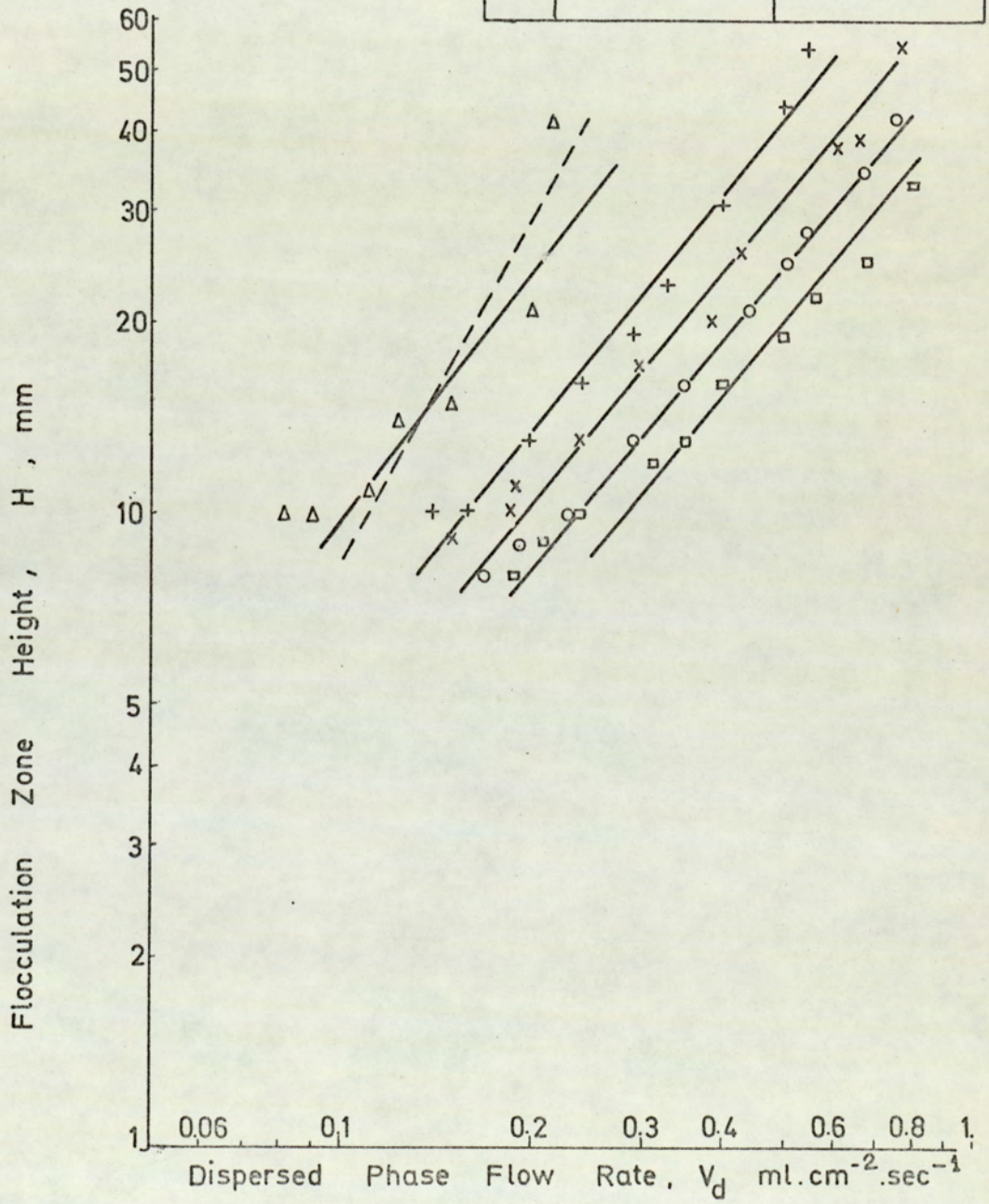

FIG. 7.25 EFFECT OF INLET DROP SIZE AND FLOW RATE UPON FLOCCULATION ZONE HEIGHT

SYSTEM: DIETHYL CARBONATE - WATER

Stationary Continuous Phase

6" Column.

	Orifice Diameter d_n (mm)	Mean Inlet Drop Diameter d_{12} (mm)
Δ	0.4	0.12
x	1.2	0.35
o	1.6	0.47

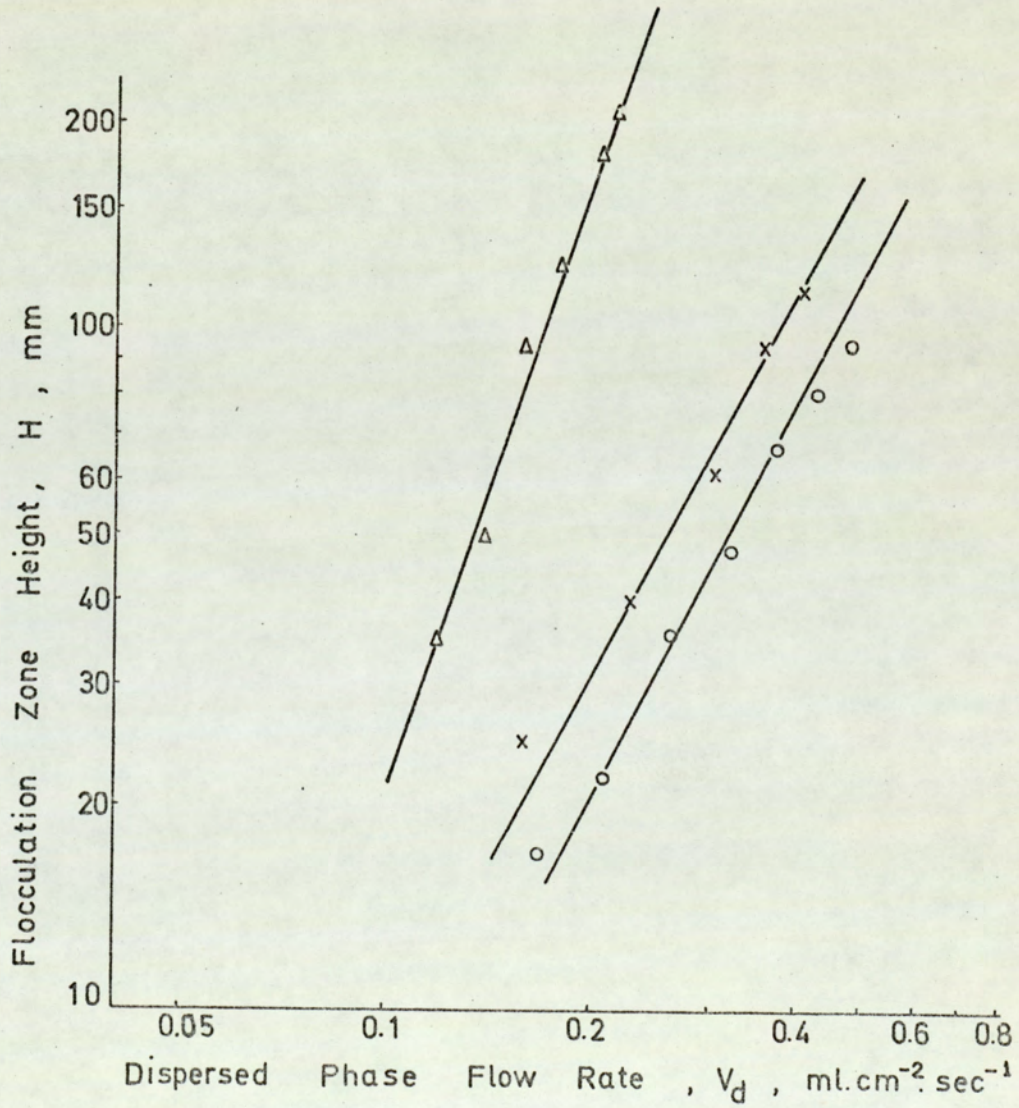

FIG. 7.26 EFFECT OF INLET DROP SIZE AND FLOW RATE UPON FLOCCULATION ZONE HEIGHT.

SYSTEM: M.I.B.K. - WATER

Stationary Continuous Phase

6" Column,

	Orifice Diameter d_n (mm)	Mean Inlet Drop Diameter d_{12} (mm)
Δ	0.4	0.8
×	1.2	2.7
○	1.6	3.1
□	2.0	4.7

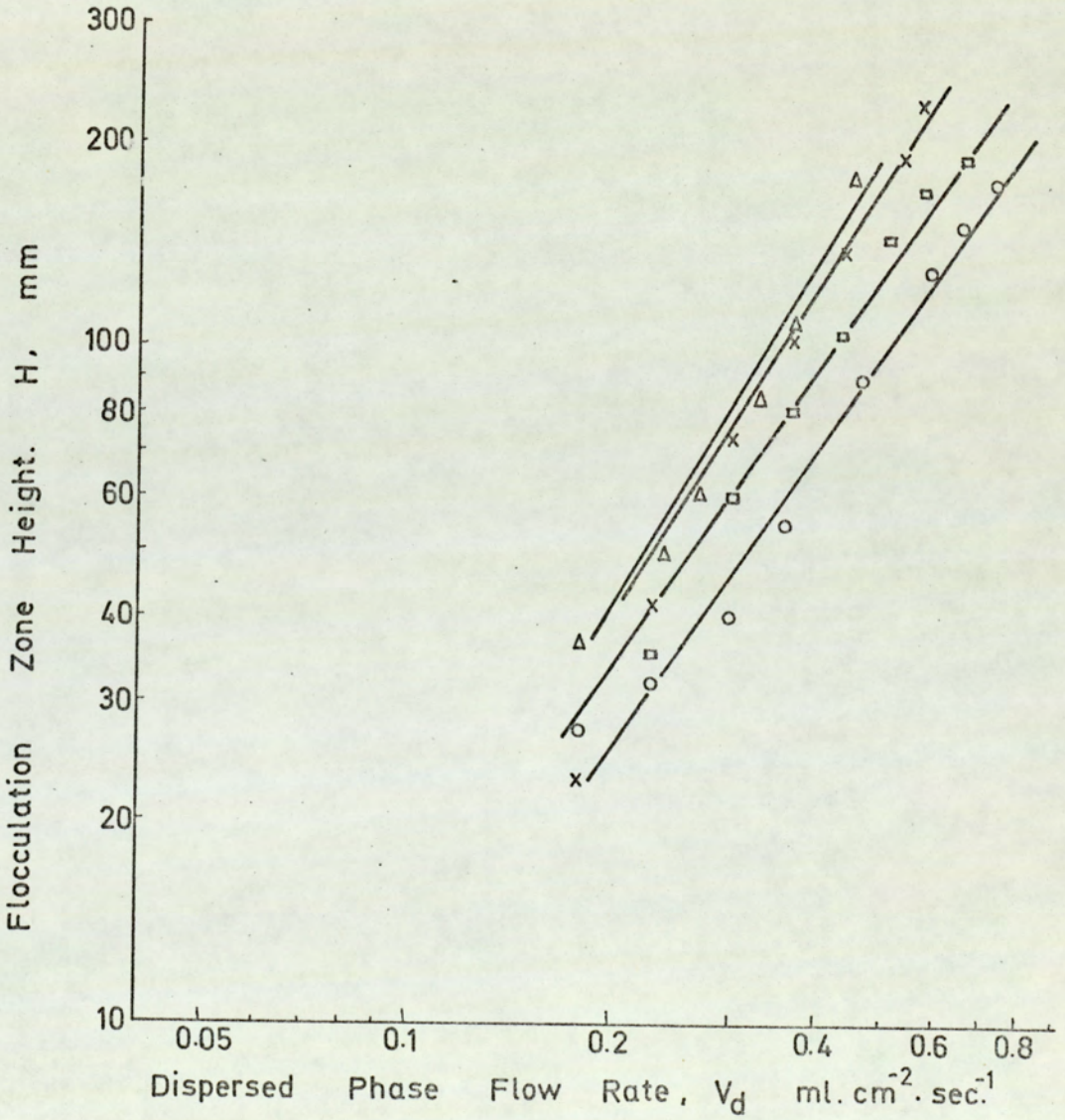

FIG. 7.27 EFFECT OF INLET DROP SIZE AND FLOW RATE UPON FLOCCULATION ZONE HEIGHT.

SYSTEM: ISO-OCTANE WATER

Stationary Continuous Phase

6" Column,

	Orifice Diameter d_n (mm)	Mean Inlet Drop Diameter d_{12} (mm)
Δ	0.4	0.7
x	1.2	2.8
□	2.0	4.5

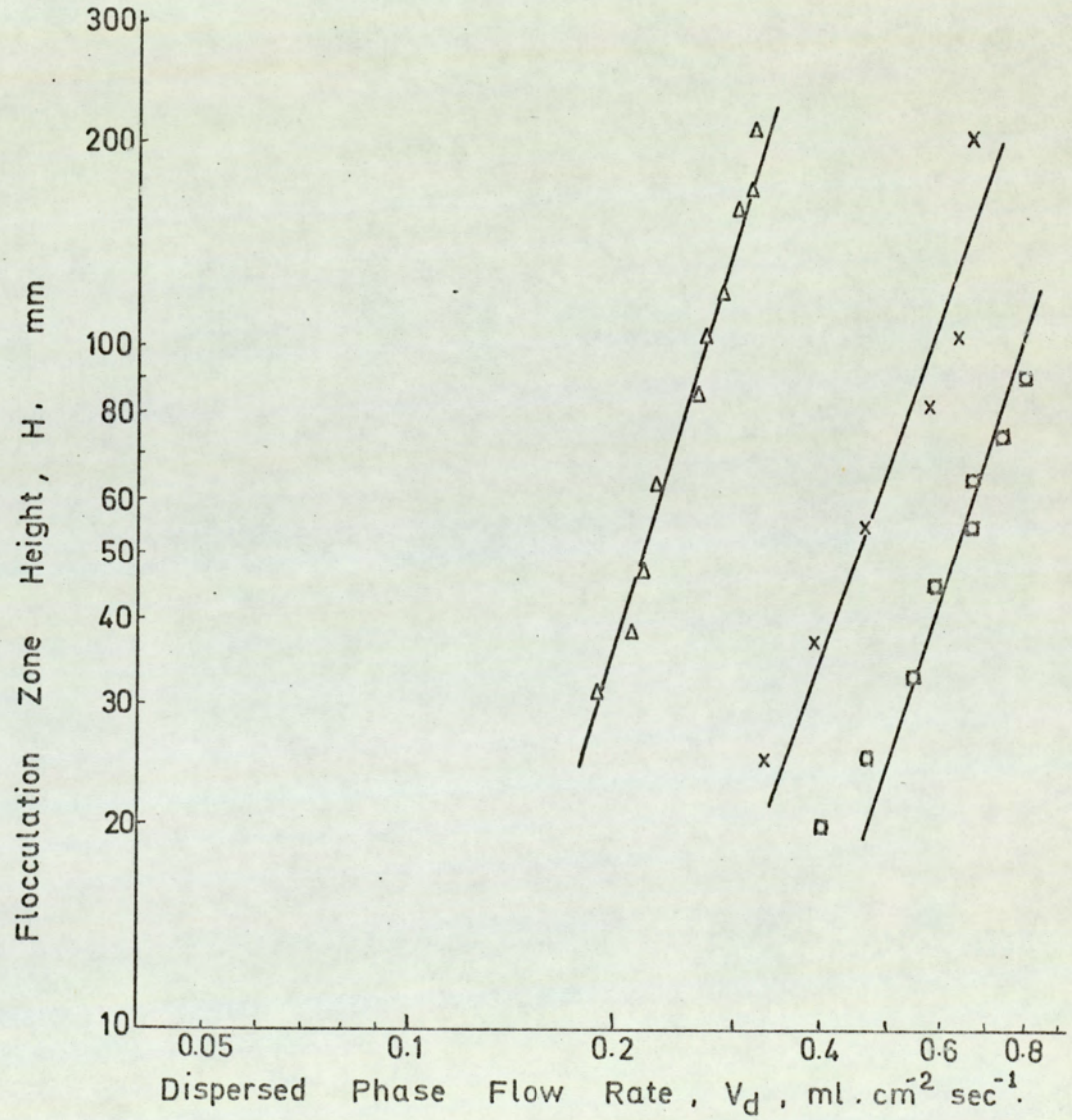

FIG. 7.28 EFFECT OF INLET DROP SIZE AND FLOW RATE UPON FLOCCULATION ZONE HEIGHT

7.4.4 Mean inlet drop diameter

At a constant dispersed phase flow rate decrease of mean inlet drop diameter, resulted in an increase in the bed height. This is demonstrated by the results plotted in Figures 7.25 to 7.28 for all systems in Section 7.4.3.

To determine the effect of mean inlet drop diameter on the flocculation zone height, measured height was plotted against mean inlet drop diameter for a constant flow rate, V_d= 0.3 ml.cm.$^{-2}$sec.$^{-1}$, using data from Figures 7.25 to 7.28 for all of the four systems dispersed in the 6 inch column. They are plotted in Figure 7.29.

The effect of drop size variation is greater with dispersed isooctane and diethyl carbonate; these exibit an almost identical rate of increase of height with decreasing drop size. The least effect was observed with M.I.B.K.; in fact a mean inlet drop diameter of 0.31 cm gave almost the same bed height as 0.47 cm droplets.

Normalized curves of bed height against the mean inlet drop diameter at a constant flow rate of 0.3 ml.cm.$^{-2}$sec^{-1} for the four systems, have slopes of c and coefficient , a_1, the values of which are as tabulated in Table 7.3.

This enables the effect of drop diameter to be isolated from the earlier expression for variation of height with volumetric flow rate.

TABLE 7.3

POWER AND COEFFICIENTS OF THE RELATIONSHIP BETWEEN ZONE HEIGHT AND DROP DIAMETER

Column : 6 inch diameter

Flow rate : 0.3 $ml.cm^{-2}.sec^{-1}$

System	Coefficient a_1	Power c
Toluene-Water	3.28	-0.62
Diethylcarbonate-Water	15.20	-1.56
M.I.B.K - Water	25.0	-0.15
Isooctane-Water	7.65	-1.54

For each of the systems studied the dependency of flocculation zone height in the 6 inch column on the two variables viz. drop diameter and dispersed phase flow rate, applicable for drop sizes above 0.2 cm in diameter and zone height greater than 1 cm may be expressed as,

For toluene,

$$H = 3.28\ d_{12}^{-0.62}\ V_d^{1.24} \qquad (7.5)$$

For diethyl carbonate,

$$H = 15.20\ d_{12}^{-1.56}\ V_d^{1.88} \qquad (7.5\ a)$$

SYSTEM: 6 inch COLUMN

V_d = 0.3 ml . cm^{-2} sec^{-1}

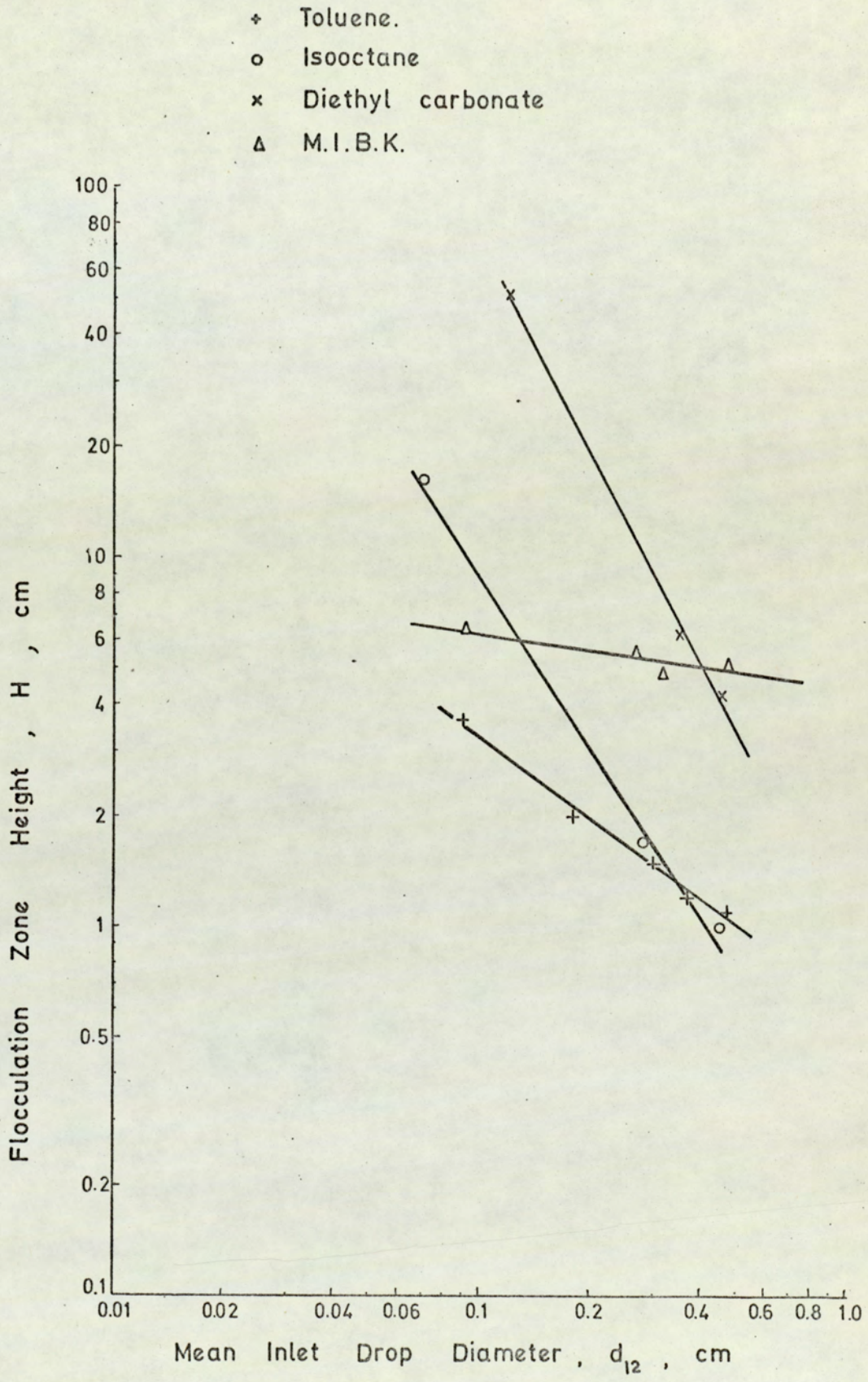

FIG. 7.29 EFFECT OF MEAN INLET DROP DIAMETERS ON FLOCCULATION ZONE HEIGHTS

For M.I.B.K,

$$H = 25.0 \; d_{12}^{-0.15} \; V_d^{1.43} \qquad (7.5\,b)$$

For Isooctane,

$$H = 7.65 \; d_{12}^{-1.54} \; V_d^{2.80} \qquad (7.5\,c)$$

7.4.5 Column size

Flocculation zone heights were measured in the three different diameter columns at different dispersed phase flow rates and varying mean inlet drop diameters with the system toluene-water only. The results are tabulated in Appendix 3 and plotted in Figures 7.25, 7.30 and 7.31. From these a similar relationship to Equation 7.5 for the toluene-water system in the 6 inch column may be derived for the 3 and 9 inch columns, viz,

For the 3 inch column,

$$H = a_1 \; d_{12}^{c} \; V_d^{1.04} \qquad (7.6)$$

For the 6 inch column,

$$H = a_1 \; d_{12}^{c} \; V_d^{1.24} \qquad (7.5)$$

For the 9 inch column,

$$H = a_1 \; d_{12}^{c} \; V_d^{1.20} \qquad (7.7)$$

The power, c, and coefficient a_1, for each column are tabulated in Table 7.4.

TABLE 7.4

POWER AND COEFFICIENTS OF THE RELATIONSHIP BETWEEN ZONE HEIGHT AND DROP DIAMETER FOR DIFFERENT COLUMN SIZE - Toluene-Water

Column diameter			
Nominal inch	Inside, D_p cm	c	a_1
3	7.3	- 0.57	2.78
6	15.0	- 0.62	3.28
9	21.8	- 0.62	3.08

The dependency of the zone height on flow rate for varying mean inlet drop diameters are listed in Table 7.2 together with the other systems. Flocculation zone heights were greater in the 3 inch diameter column than in the 6 and 9 inch columns. However, inspection of the Equations 7.5, 7.6 and 7.7 show that there was a greater dependancy on flow rate in the 6 and 9 inch columns (D_p = 7.3 and D_p = 15.0 cm), i.e. in the 6 and 9 inch columns heights vary as the 1.24 and 1.20 power of the flow rate respectively in comparison to 1.04 power in the 3 inch column. Therefore, the effect of dispersed phase volumetric flow rate per unit area of the column cross section on zone height is obviously of similar order in the 6 and 9 inch columns but slightly less in the 3 inch column. Because zone heights were larger in the 3 inch column, change in drop size would be expected

to be one parameter having a greater significance in this column.

If the same volumetric flow rate was fed to each column using a distributor plate having identical evenly distributed orifice holes, the number of droplets arriving at each unit area of the interface would be identical. Thus the packing of the droplets and their interaction would appear to be more important than the overall flow rate in the flocculation zone with a decrease in column diameter. To demonstrate the drop size effect further, toluene flocculation zone heights are plotted against drop diameter at a constant flow rate, for all three columns in Figure 7.32. The dotted line shows the effect of drop diameter in the 9 inch column and a comparison with the line for 6 inch shows that there is no distinguishable difference. On the other hand, there is a significance with the 3 inch column above 0.25 cm. mean inlet drop diameter, although data merge into that for the 6 inch column at smaller mean inlet drop sizes.

Then it can be concluded that the effect of column size on the zone height is dependant on the mean inlet drop diameter, i.e. the lower the mean inlet drop size, the less the effect of column diameter on zone height. When the

inlet drop size approaches 0.5 cm, the effect of change in column size between 6 and 9 inch starts to appear. However, for the range of drop sizes studied, column sizes of 6 and 9 do not affect the zone height greatly. This point is further demonstrated in Figure 7.33 which shows the effect of various mean inlet drop sizes for three different columns. The slope, e, and coefficient, a_2, of each line is listed in Table 7.5 for comparison purposes.

The dependancy of the flocculation zone heights upon the column diameter is related by,

$$H = a_2 D_p^{-e} \qquad (7.8)$$

TABLE 7.5

POWER AND COEFFICIENT FOR EQUATION 7.8 - Toluene-water

d_{12} cm	a_2	e
0.09	3.7	-0.12
0.18	2.4	-0.17
0.30	1.9	-0.23
0.36	1.5	-0.25
0.48	1.3	-0.29

Further, the power e, and the coefficient, a_2, are related to mean inlet drop diameter, d_{12}, by

$$e = -0.41\ d_{12} - 0.09 \qquad (7.8\ a)$$

$$a_2 = -3.33\ d_{12} + 3 \qquad (7.8\ b)$$

SYSTEM: TOLUENE - WATER

Stationary Continuous Phase

3" Column.

	Orifice Diameter d_n (mm)	Mean Inlet Drop Diameter d_{12} (mm)
Δ	0.4	0.9
+	0.8	1.8
x	1.2	3.0
o	1.6	3.6
□	2.0	4.8

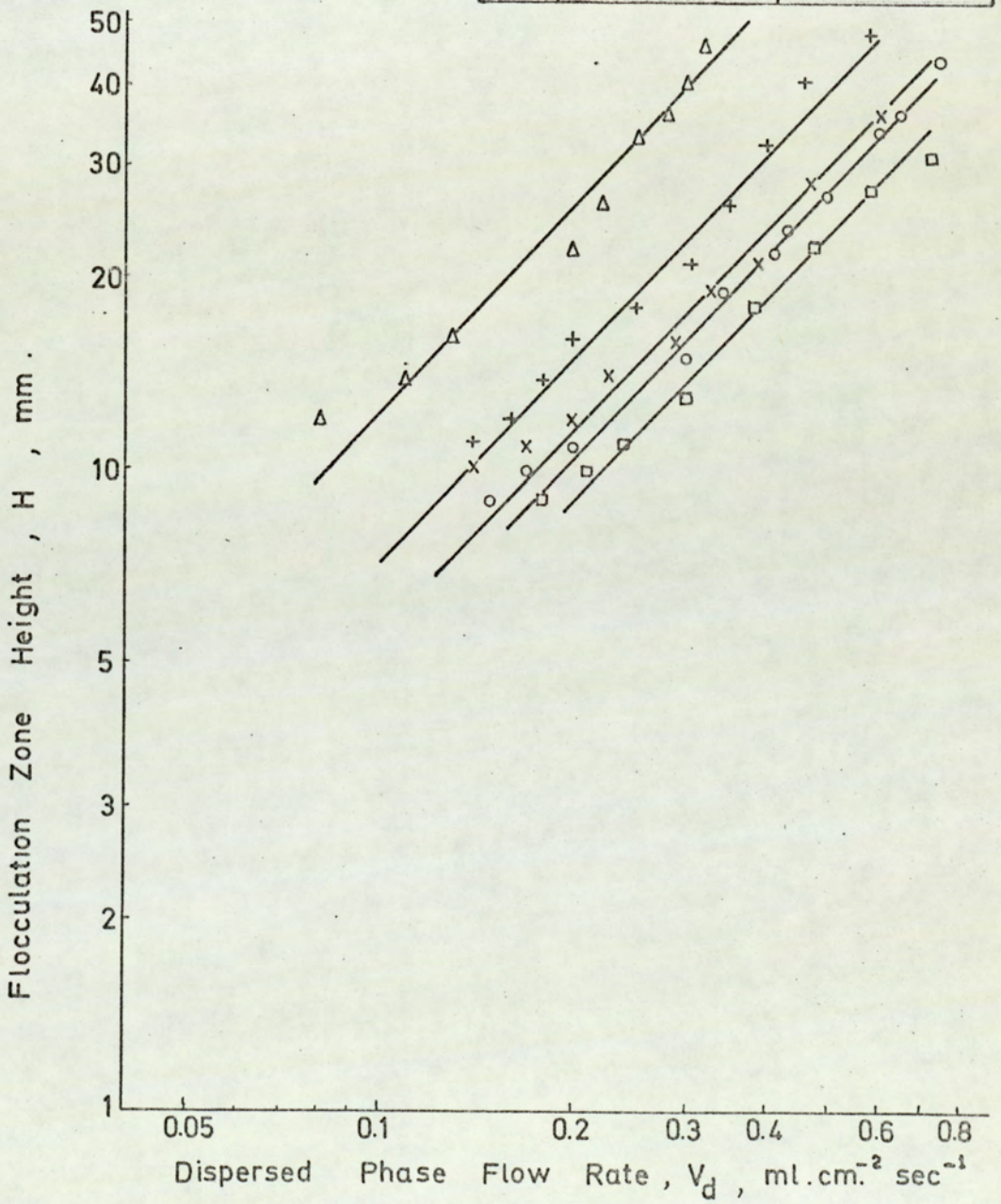

FIG. 7.30 EFFECT OF INLET DROP SIZE AND FLOW RATE UPON FLOCCULATION ZONE HEIGHT

SYSTEM: TOLUENE – WATER

Stationary Continuous Phase

9" Column.

	Orifice Diameter d_n (mm)	Mean Inlet Drop Diameter d_{12} (mm)
x	1.2	3.0
o	1.6	3.6
□	2.0	4.8

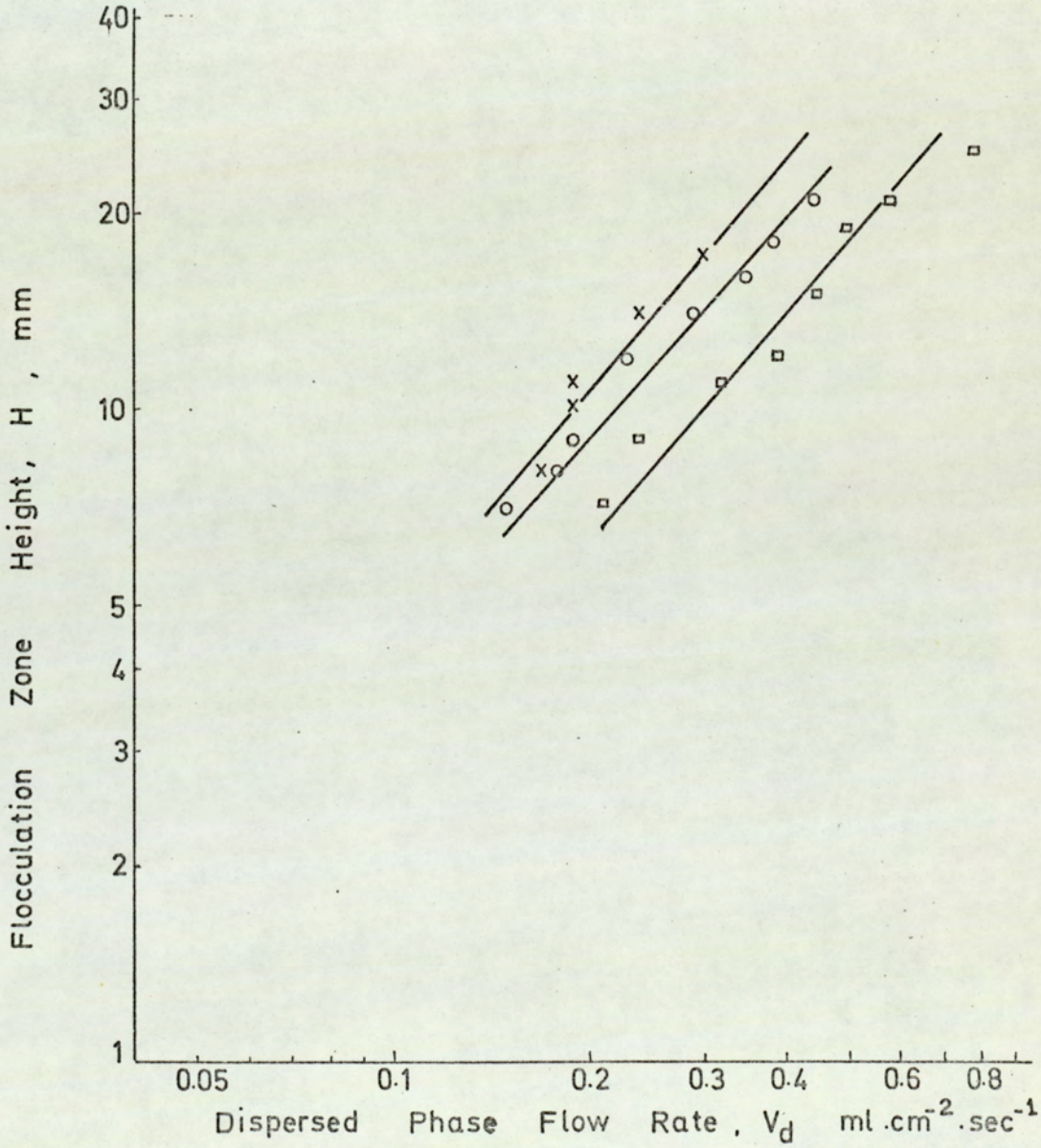

FIG. 7.31 EFFECT OF INLET DROP SIZE AND FLOW RATE UPON FLOCCULATION ZONE HEIGHT.

SYSTEM: TOLUENE - WATER

o 9 - inch column (D_p = 21.6 cm)

Δ 6 - inch column (D_p = 15.0 cm)

x 3 - inch column (D_p = 7.3 cm)

$V = 0.3 \ ml.cm^{-2}.sec^{-1}$

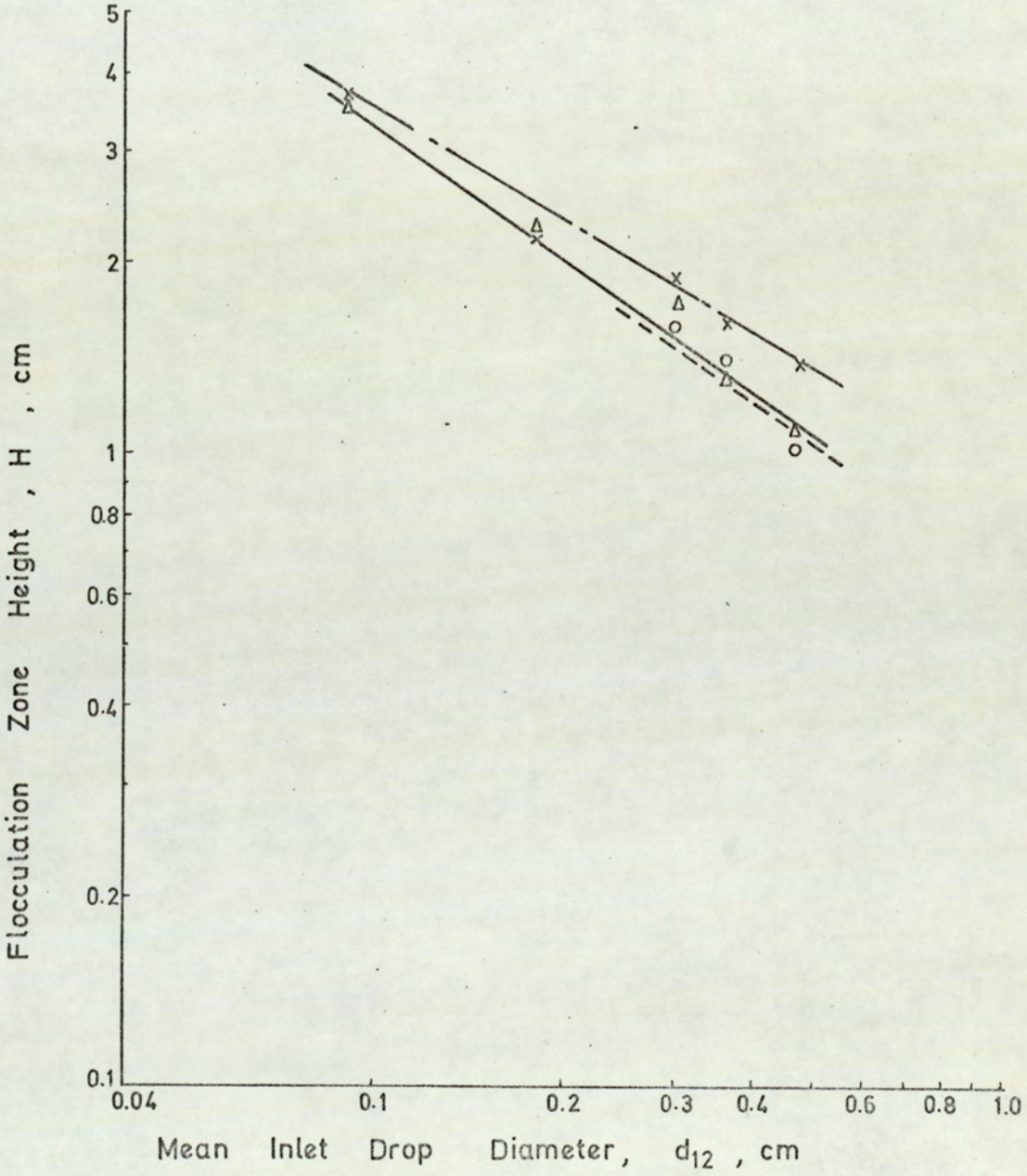

FIG.7.32 EFFECT OF MEAN INLET DROP DIAMETERS ON THE FLOCCULATION ZONE HEIGHTS FOR DIFFERENT SIZES OF COLUMNS.

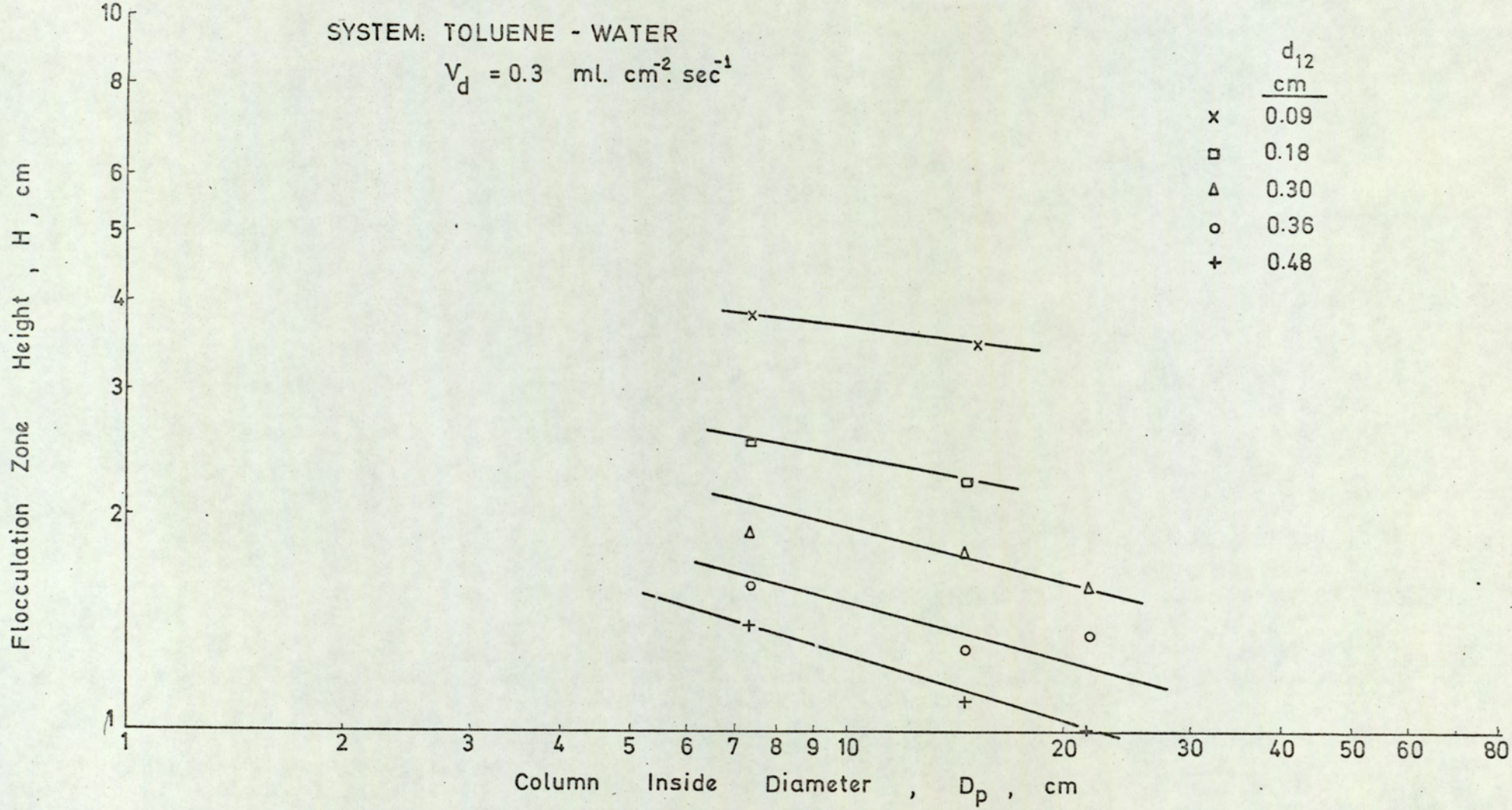

FIG. 7.33 EFFECT OF MEAN INLET DROP DIAMETERS ON FLOCCULATION ZONE HEIGHTS IN DIFFERENT DIAMETERS OF COLUMN

7.4.6. System properties

From the data given in Appendix 9 and Figure 7.34, correlations have been derived to express the effect of the main dispersed phase physical properties upon zone height. These are given in Table 7.6.

TABLE 7.6

PHYSICAL PROPERTY CORRELATIONS

Continuous phase: Water

Dispersed phase	Correlation
Toluene	$H = 1.03 \left(\frac{d_{12}^2 g \Delta\rho}{\sigma} \right)^{-0.34}$
M.I.B.K.	$H = 8.20 \left(\frac{d_{12}^2 g \Delta\rho}{\sigma} \right)^{-0.14}$
Isooctane	$H = 0.75 \left(\frac{d_{12}^2 g \Delta\rho}{\sigma} \right)^{-1}$
Diethyl carbonate	$H = 1.2 \left(\frac{d_{12}^2 g \Delta\rho}{\sigma} \right)^{-1}$

Unfortunately no approximate general correlation would appear possible by combining the equations in Table 7.6. The reason for this is not clear but the one property not included is dispersed phase viscosity. (Since distilled water was used as the continuous phase this viscosity was constant). However dispersed phase viscosities only varied over the range of 0.5 to 0.82 centipoise which is unlikely to be significant.

The correlation obtained by dimensional analysis for single drop rest times (19) indicated that in addition to Laplace drop diameter ($d_{12}^2 \, g \, \Delta\rho / \sigma$), another dimensional group of

$$\left(\frac{t_{1/2} \, \sigma}{d_{12}} \right)$$

was involved. However its inclusion does not lead to a general correlation. Therefore, some other factor than physical properties must be involved. Inspection of Figure 7.29 suggests that the range of drop dize has a more important influence than the system properties.

FIG. 7.34 VARIATION OF FLOCCULATION ZONE HEIGHT WITH LAPLACE DROP DIAMETER

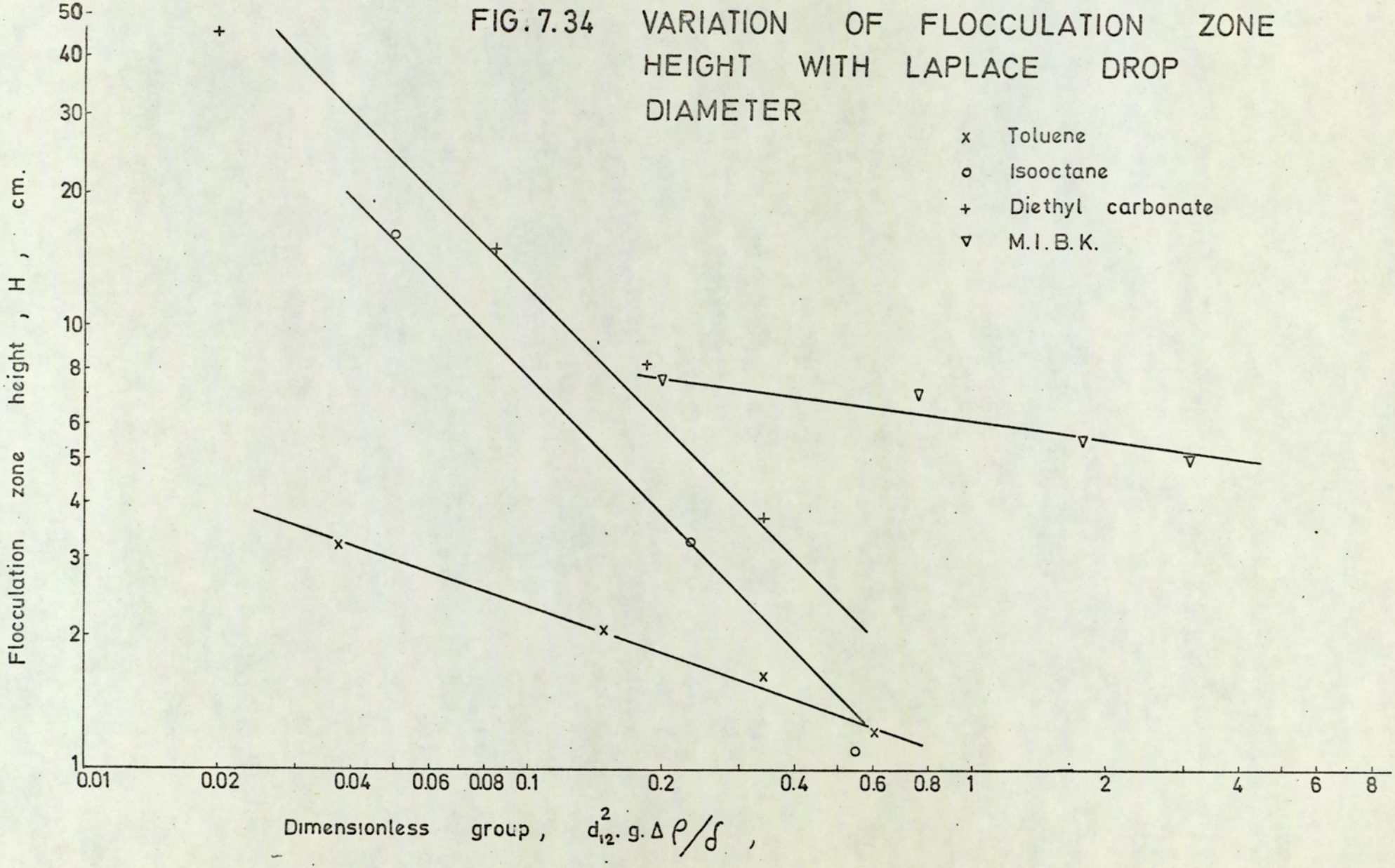

7.5. Hold-up in the Flocculation Zone

Hold-up measurement studies were made to determine the effect of column size, system properties, dispersed phase flow rates and inlet drop sizes upon horizontal and vertical hold-up profiles. The results are tabulated in Appendix 6, and, for the purpose of discussion, are plotted in Figures 7.35 to 7.40.

The method selected to measure hold-up was to steadily syringe out a 20-30 ml. sample from a position near the wall in the flocculation zone as described in Section 6.3.4. Attempts to employ other methods, i.e. static head, differential manometer and encapsulation techniques have been described in Section 6.3 also.

The syringing-out method was found to be reproducible within $\mp 2\%$, with an expected accuracy of $\mp 2\%$.

Unfortunately no means were available to check the accuracy of this method. However, the reproducibility of the results, and sensitivity of the measurements, confirm that the syringing-out method was probably the most reliable and accurate, albeit the most tedious one in the present investigation. As would be anticipated, for hold-ups of lower order, i.e. less than 60 per cent, the reproducibility was less satisfactory

with deviation increasing from ∓2% to ∓6%. For densely packed droplets, above 60% the syringing was found to be the most reliable.

7.5.1. Horizontal hold-up profile

Horizontal hold-up profiles were measured in 3, 6 and 9 inch columns with the toluene water system only. No significant difference was detectable between hold-ups at the centre and about 1-2 centimetres from the column wall in the 6 and 9 inch columns. However in the 6 inch column there was a tendency for it to increase at the column centre e.g. four measurements at each location, gave results of 80 to 84 at the wall and 82 to 86 per cent at the centre. Clearly, however, the difference between the two positions was only just within the limits of experimental error; no difference could be measured in the 9 inch column. However, a significant difference was determinable in the 3 inch column, hold-up being about 5 per cent more at the centre at the mid section of the zone height. This is illustrated with a typical result obtained in Figure 7.35. Near the droplets entry zone or near the coalescence interface, the accuracy of the method probably precluded measurement of any difference. However, at the two ends, the difference between

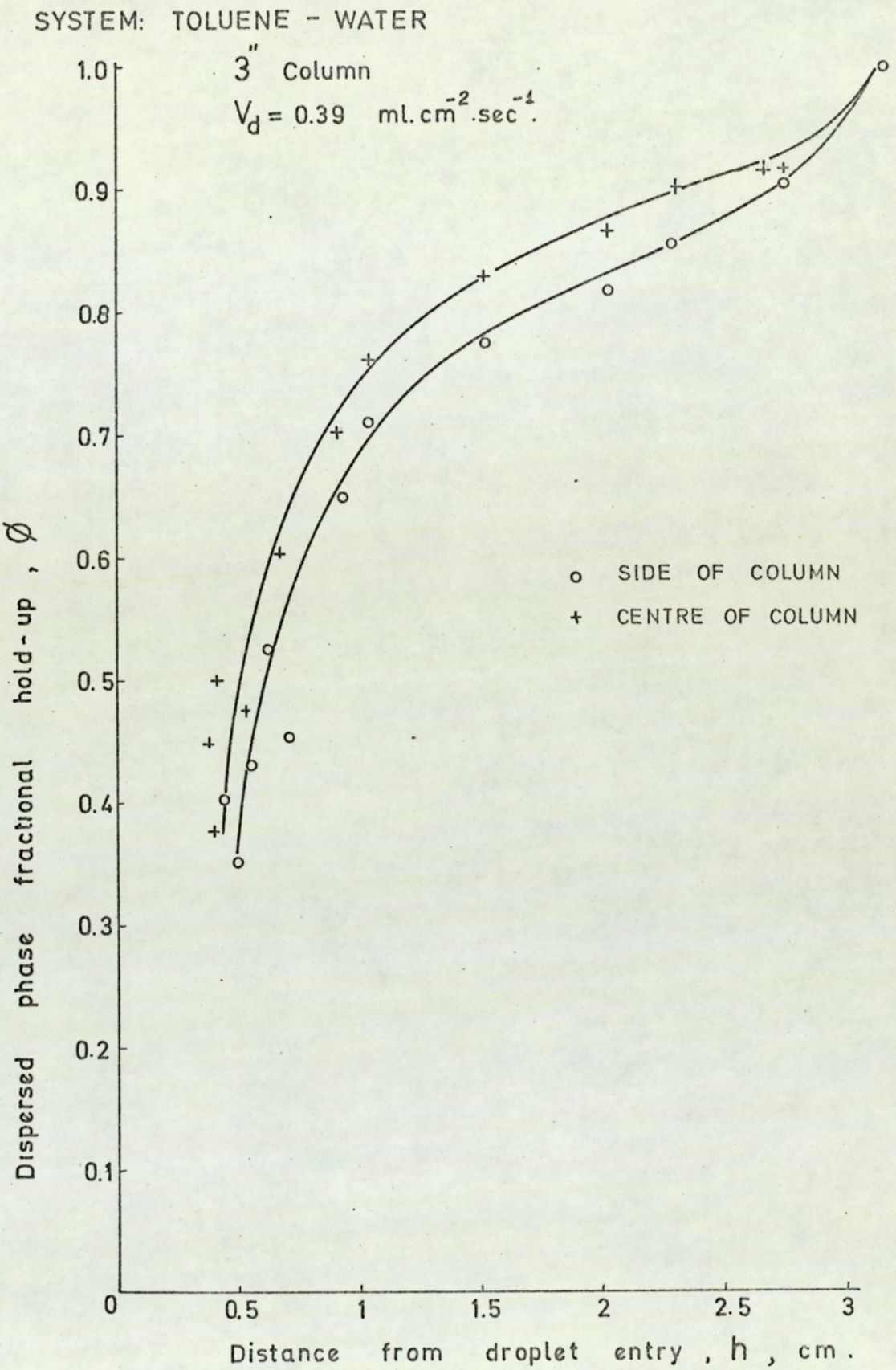

FIG. 7.35 VARIATION OF THE VERTICAL HOLD-UP PROFILE AT THE MIDDLE AND NEAR THE WALL OF COLUMN

the centre and side wall tends to be the same even in 3 inch column.

It is concluded that the horizontal hold-up profile was less than 3% in the 6 and 9 inch columns and could not be determined by the method employed.

A hold-up difference of more than 3% was however present between the centre and side of the walls of the 3 inch column indicating the wall effects.

7.5.2. Vertical hold-up profile

The vertical hold-up profiles determined in the 3, 6 and 9 inch columns with the toluene-water system at various dispersed phase flow rates and at different mean inlet drop sizes are tabulated in Appendix 6.

Profiles determined for diethyl carbonate, M.I.B.K. or isooctane droplets dispersed in water in the 6 inch column only are also included in Tables 12 -18 of Appendix 6.

In general the toluene-water system produced low bed heights of up to 5 cm in comparison with about 20 cm with the other systems. However, aged toluene, after being in the equipment more than two weeks, resulted in flocculation heights of ever 20 cm as described in Section 7.2. and 7.4.1. The hold-up profile of such an aged system is plotted in Figure 7.36.

The overall hold-up varied with different dispersed phases an increase occurring in the order diethyl carbonate, toluene, M.I.B.K and isooctane, for the same fractional bed height.

A proper comparison was not possible between the hold-up profiles of the systems for different heights because of interaction between various parameters viz flow rates and drop diameters. Hence a flocculation zone height at which the hold-up profile for any system was identical with that of another system could not be produced. Therefore, a dimensionless height, h/H, fractional height has been chosen to identify any point in a flocculation zone to facilitate comparison of the profiles at various flow rates and drop diameters.

a. The effect of operating parameters

The effect of flow rate on the hold-up is shown in Figure 7.37. Increasing flow rate, caused the bed height to increase, tending to decrease the hold-up at the same position being described by fractional height.

A sharp change of hold-up observed throughout the bed height in the direction of the coalescing interface at low flow rates with shallow beds is less pronounced with the

increased bed heights associated with high flow rates.

The bed height changes inversely with the inlet droplet size. With a zone only 3 to 4 droplets layers thick, the relationship probably approximates to a straight line since a relatively large change in hold-up (25%) occurs over a very small height (10 mm). It was, however, impractical to measure hold-up with sufficient accuracy to confirm this. It was possible to detect some difference between the very first level of droplets, where the tip of the syringe was located, and 2-3 mm. above it within a total height of 5-7 mm. However, the results were not reproducible under these conditions since fluctuations were present in such a shallow bed. When the bed reached a height of about 20 mm, comprising at least 8-12 droplet layers, the meniscus of the interface flattened, and a consistent change was measureable between small differences of height such as 2-3 mm.

In summary with 5-6 droplets layers it was not possible to obtain a profile but with 10-12 layers measurements were possible at five different levels with a reproducibility of ±6% with a flattened meniscus, a change of one milimeter in syringe tip height produced a detectable change in measured values and such a true cylindrical flocculation zone appeared to be better stabilized. With the system toluene-water,

when droplets were formed from distributor diameters of 1.2 and 1.6 mm., an undisturbed flocculation zone was consistently maintained, and the height profiles were measurable by syringing with excellent reproducibility (±3%) above 3-4 mm. from the droplet entry. With shallow beds approximating to monolayer formations, attempts at hold-up measurement gave the impression that the hold-up profile is a straight line. Unfortunately the method was not sufficiently accurate nor the layers sufficiently stable for this to be confirmed. When total bed height increases beyond 15 mm., deviations commence from the expected linear hold-up profile; a curvature appears on the profile at around 70% hold-up at 5-6 mm above the droplet entry.

Increased flow rate reduces the onset of curvature to 60%; but the gradient of the curve is then somewhat less. Up to this transition, reproducibility of the measurements is poorest i.e. consecutive point hold-ups may yield 40, 46, 36%.

The general trend is clear from inspection of the plots in Figures 7.35-7.40. This entry zone, comprising up to 70% hold-up, or up to 10 mm. distance from the droplet entry, i.e. up to 0.25 fractional height, with the toluene-water system, can best be represented by a straight line. A

sensitive measurement of the variation could not be achieved in the present investigation. However, deviations from linearity may be due not to the method of the measurement, but to the actual behaviour of the droplets in this entry section. It is concluded that droplets formed a close packed pattern within a distance of some 10 mm. from the droplet entry. This applied for flow rates in the range of 0.2 to 0.8 ml. cm^{-2}. sec^{-1} with all the systems studied over a wide range of mean inlet drop diameters in the 3 different column sizes.

It was observed that droplets in this entry section were in a state of random turbulent motion despite a distinct queue of droplets in the very first layer separating the flocculation zone. On this basis it is concluded that the droplets attempt to form a dense packed arrangement in this first 10-15 mm. Any one droplet probably touches between 3 and 10 neighbouring droplets but under dynamic conditions so that a stable arrangement is never established with respect to the neighbouring droplets. The void volume studies of Ridgway and Tarbuck (84), and others (85, 86), regarding the random packing of spheres and local voidage variations of equal-sized spheres, and in which void volume was correlated with co-ordination number (84) provides some explanation of

the variation of the hold-up in this entry section.

This co-ordination number, represents the number of contacts between one sphere and those surrounding it; this is correlated with voidage fraction (84) in Figure 7.41. All packing arrangements with a co-ordination number of < 4 are supposed to have $\leq 35\%$ voidage, but they are not stable under gravity unless some attractive force acts between the spheres. Any increase in co-ordination number results in lower voidage.

By analogy to the co-ordination number correlation, a liquid drop which is surrounded by 5 drops in the entry section would be expected to be in a state of continuous change with the co-ordination number varying between 6 and 4 due to turbulence. Having one drop less in the packing arrangement would reduce the voidage by 0.1 fraction according to Figure 7.41. Thus the variation in hold-up reported for the entry section may be due to this phenomenon.

Increase in flow rate did not affect more than the first 3-5 mm of the entry section of the flocculation zone. Similarly the effect of inlet drop size, within the range 1 mm to 5 mm, was restricted to the first 2-3 mm height. However above 4 mm drop diameter a comparatively greater distance was required to reach a close packed arrangement of 70 per cent. This distance was in the range of 3 to 4 mm.

Significant differences were observed between the

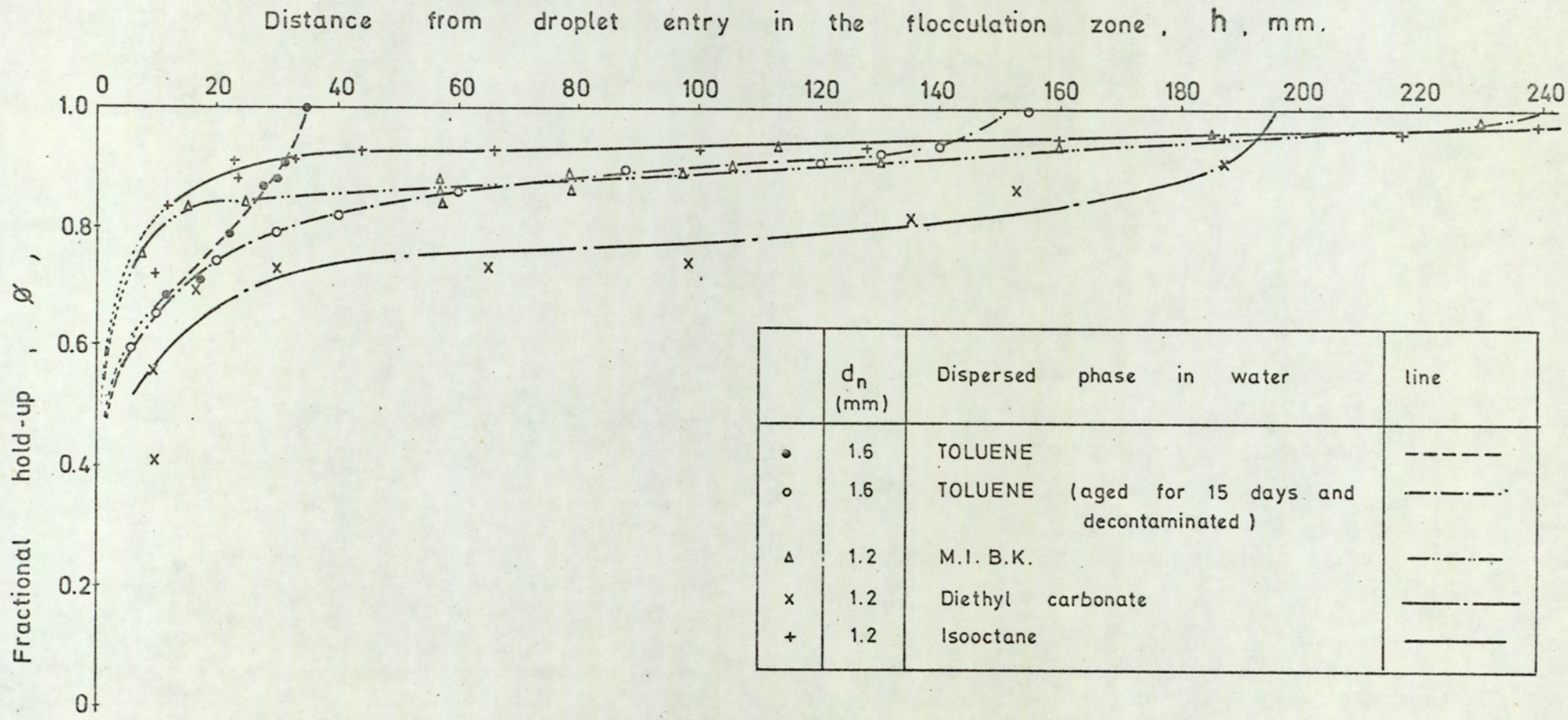

	d_n (mm)	Dispersed phase in water	line
●	1.6	TOLUENE	– – – –
o	1.6	TOLUENE (aged for 15 days and decontaminated)	—·—·—·
Δ	1.2	M.I. B.K.	—·—·—
x	1.2	Diethyl carbonate	——·——
+	1.2	Isooctane	———

FIG. 7.36 VERTICAL PROFILE OF DISPERSED PHASE HOLD-UP (6" Column)

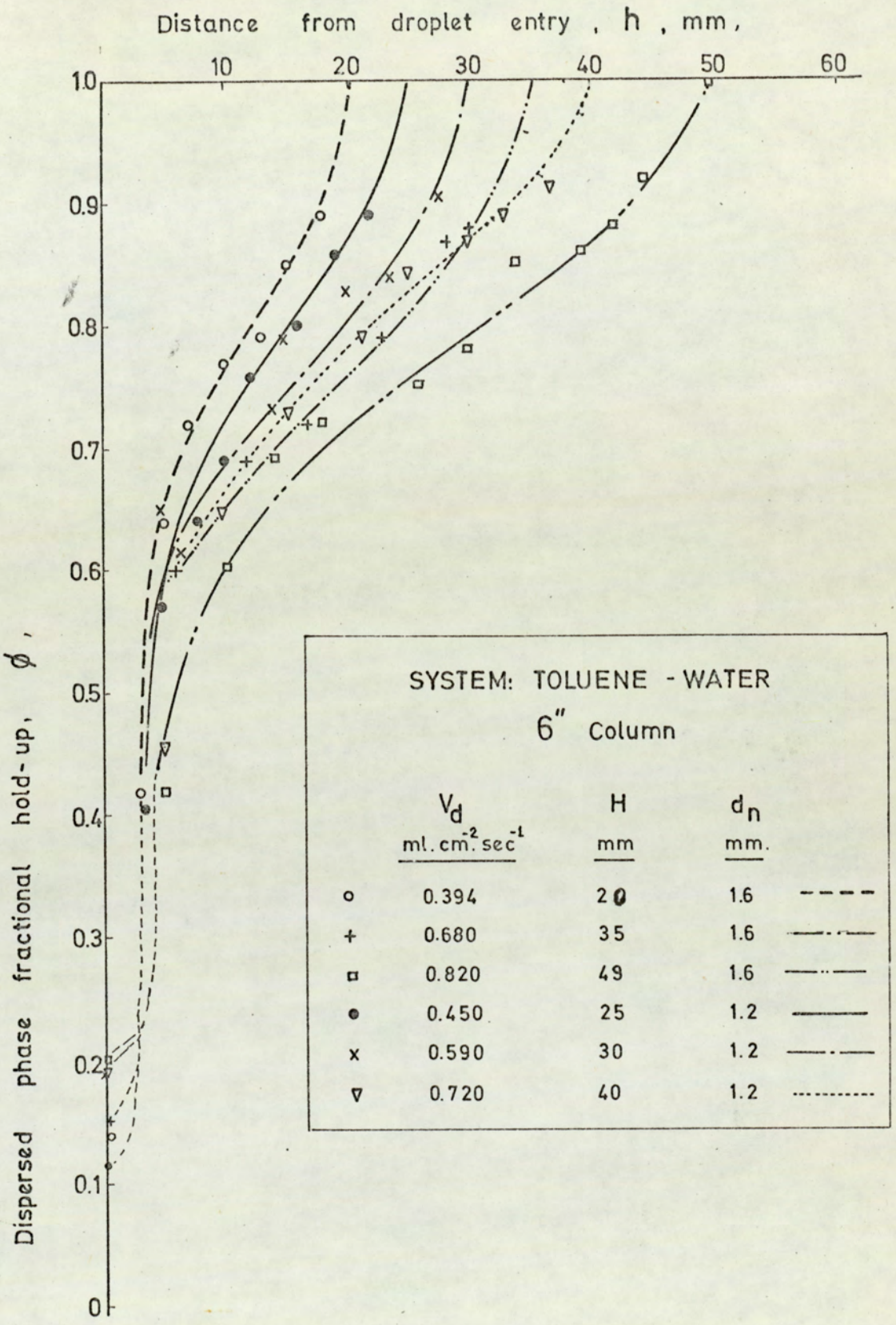

FIG. 7.37 EFFECT OF FLOW RATE ON VERTICAL HOLD-UP PROFILE

SYSTEM: TOLUENE - WATER — 6" Column

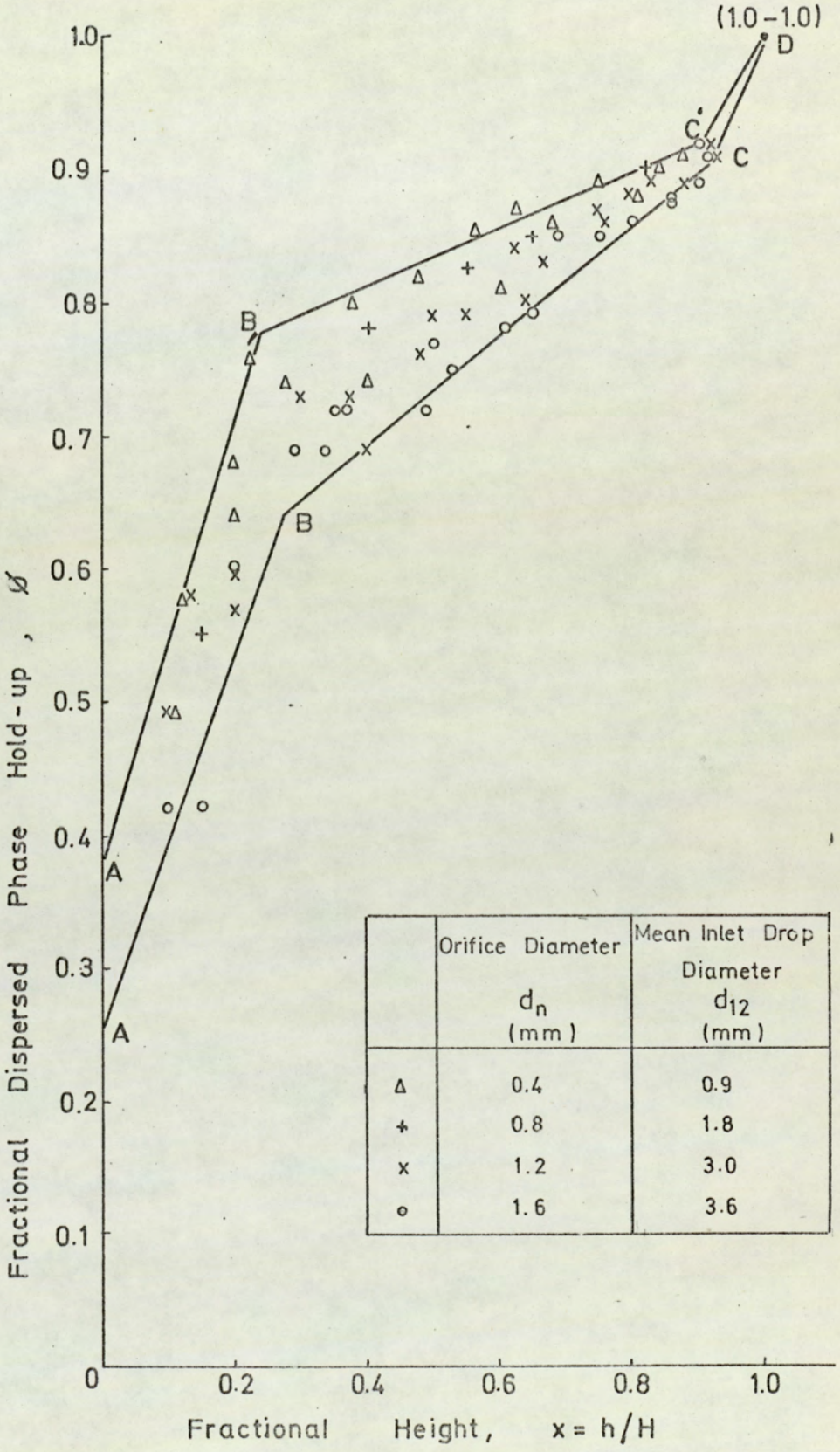

FIG. 7.38 VARIATION OF FRACTIONAL HOLD-UP WITH HEIGHT AT DIFFERENT MEAN INLET DROP DIAMETERS.

SYSTEM: TOLUENE - WATER 3" Column

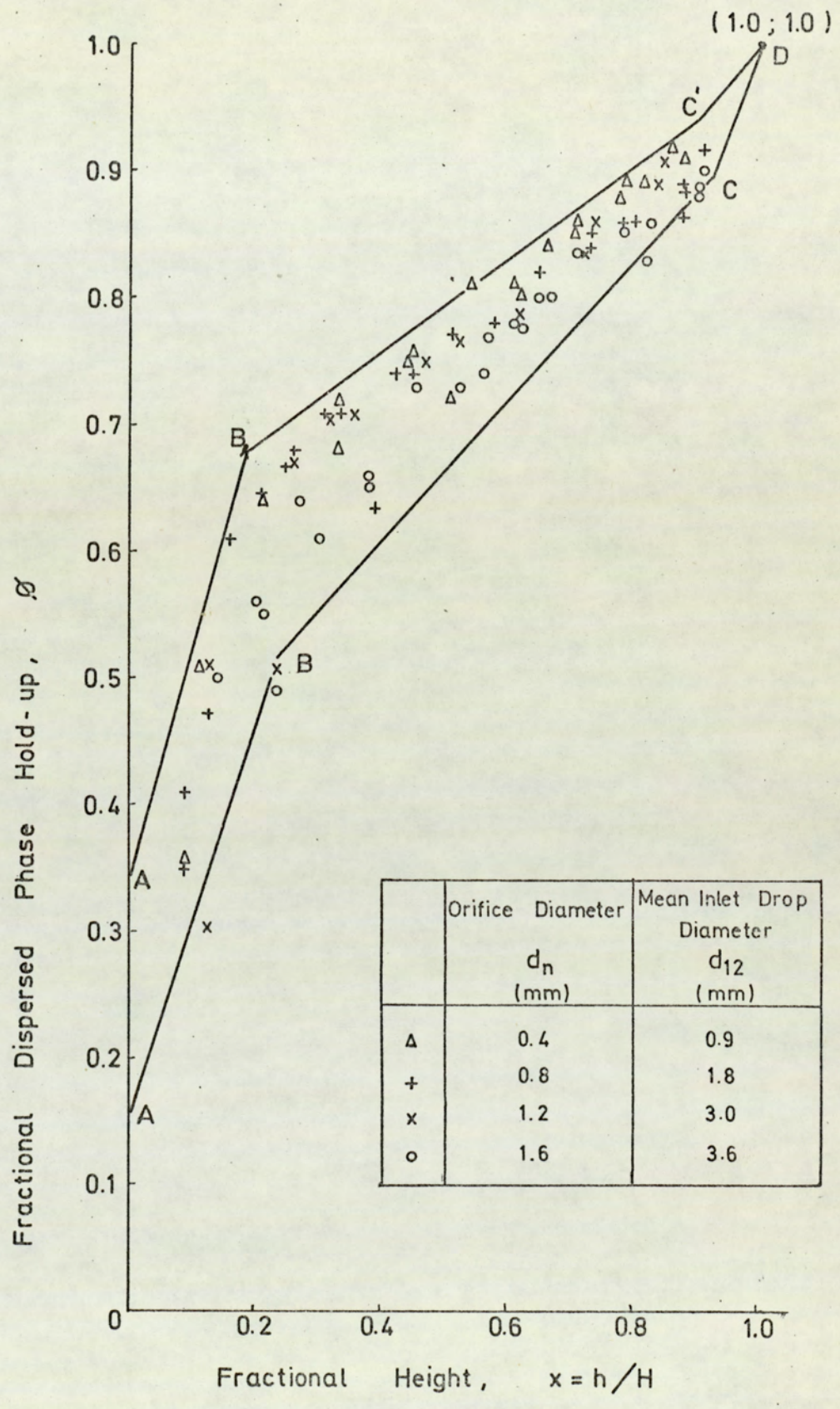

FIG. 7.39 VARIATION OF FRACTIONAL HOLD-UP WITH HEIGHT AT DIFFERENT MEAN INLET DROP DIAMETERS

SYSTEM: Indicated in table below 6" Column

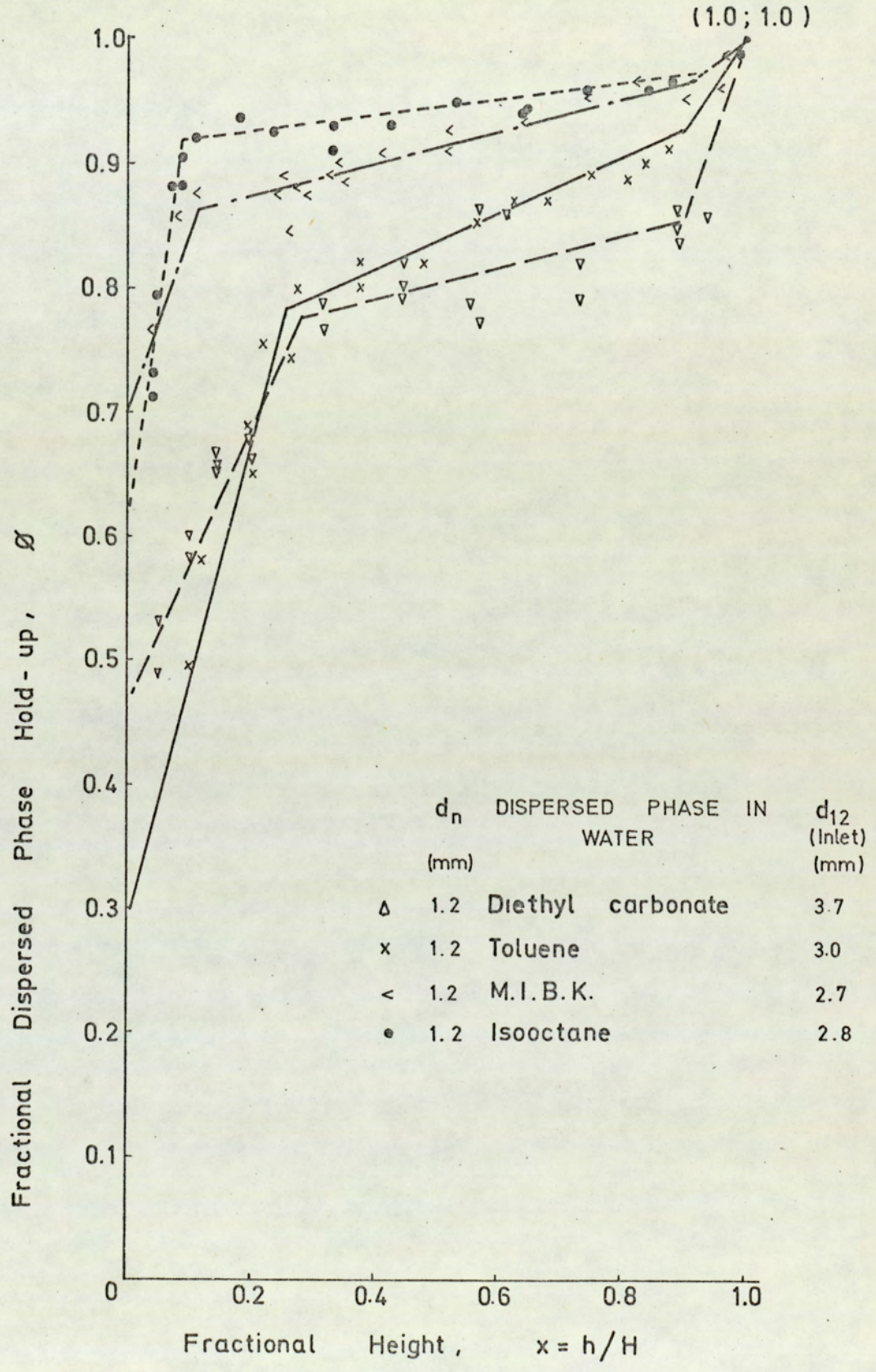

FIG. 7.40 VARIATION OF FRACTIONAL HOLD-UP WITH HEIGHT IN FLOCCULATION ZONE

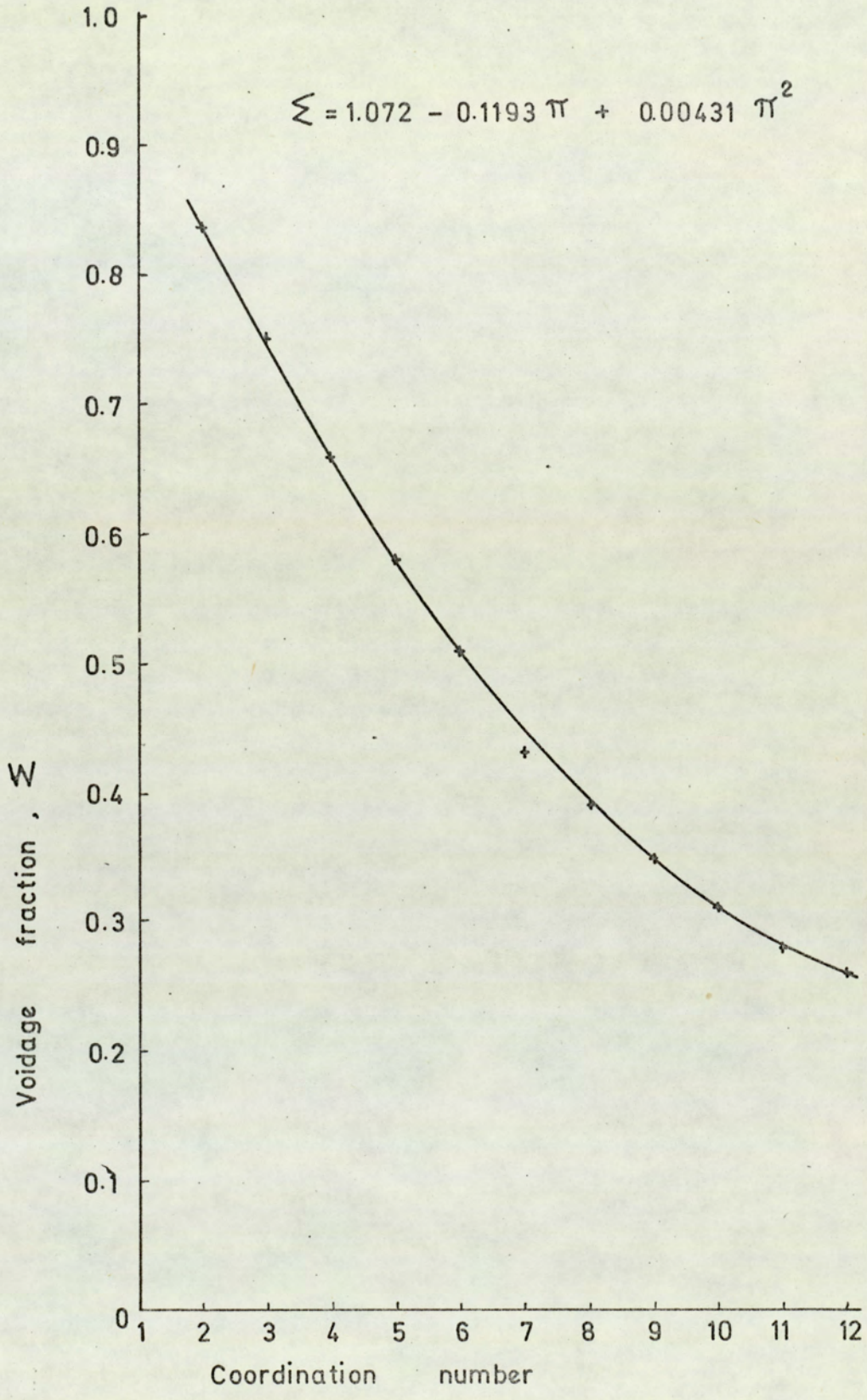

FIG. 7.41 A PLOT OF VOIDAGE AGAINST COORDINATION NUMBER FROM CORRELATED EQUATION (84)

various systems in that isooctane and M.I.B.K droplets attained an efficient close packed arrangement at a smaller fraction of total height than toluene and diethyl carbonate. Thus within a distance of 5-6 mm, or 2-3 drop layers, isooctane and M.I.B.K reached above 80% hold-up which is above the figure for a close packed arrangement of rigid spheres, i.e. 70-75 per cent hold-up (25-30% void volume). The reason for the variation is explainable in terms of the density differences involved in each system.

A high density difference results in the droplets having a higher upward force so that drainage of the continuous phase occurs at a faster rate. Similarly, the greater the free space still available at the zone entry region between the drops, the more rapidly drainage can occur.

This portion of the experimental hold-up curves is defined for the first time in this work as the "Droplet Entry Zone" or "Zone I".

Hartland (72) has reported a similar phenomena in a 'two dimensional' flocculation zone in which there was a greater void space between droplets on entry.

Similarly Jeffreys et al (80) reported unusual behaviour of the droplets at the droplet entry section to the wedge formed

in their settler.

A typical hold-up profile is shown in Figure 7.38 in which the lines AB and AB_1 represent the first zone (Drop Entry Zone). The point B or B_1 at the end of drop entry zone is easily detected in the plots of the experimental results, Figures 7.35 to 7.40, albeit, not as a point but as a sharp change in gradient occurring over about 5 per cent of hold-up. Point B in Figure 7.38 moves in the direction of B_1 consequent upon the following changes in operating parameters,

a) Increase of density difference of the system.

b) Increase of flow rate,

c) Decrease of inlet drop size.

Since the actual slope of the line AB, defined as Zone I, cannot be measured accurately, the exact location of point A is questionable. Numerous hold-up determinations with different systems in this section, however inaccurate, gave values in the range of 25-40 per cent.

Hold-up measurements below the flocculation zone gave results varying from 3-5 per cent, corresponding to a flow rate just sufficient to form a monolayer, to 20-22 per cent at maximum flocculation zone heights attained at flow rates of $V_d = 0.8$ ml. $cm^{-2}.sec^{-1}$. Since the flocculation zone is

packed distinctly denser than that below the bed, greater than 20 per cent hold-up is necessary in the first layer. Moreover, rigid spheres having a packing arrangement with one drop touching 3-4 other drops, would produce around 60 per cent void volume (84). Therefore, the location of point A representing the hold-up at the first layer must be around 30-40 per cent hold-up.

In Figure 7.40 the variation of hold-up with bed height for the different systems indicate that the lines showing the first zone (AB) commence at 0.70; 0.62; 0.47 and 0.30 for the systems M.I.B.K, isooctane, toluene and diethyl carbonate respectively. However, from the theoretical considerations given above and the packing arrangement studies of rigid spheres(84), their true location should be at 0.40 fractional hold-up.

The first region, represented by the line AB in Figure 7.38, is represented, for all systems, by the following general Equation,

$$\phi_1 = m_1 \left(\frac{h}{H}\right) + C_1 \qquad (7.9)$$

where (m_1) is the slope of line AB and (C_1) the ordinate of intersection (point A).

Difficulty arises in determining the actual location of point A by experimentation, so that the particular solution

of this Equation would be inaccurate, with (m_1) the slope and (C_1) the intercept varying between wide limits.

The mid-section of the hold-up profile, corresponding to BC in Figure 7.38, is almost linear between hold-ups of 70% to 90%. This region can be represented by an equation similar to Equation 7.9,

$$\phi_2 = m_2 x + C_2 \qquad (7.10)$$

The range of fractional bed height, x and values of m_2 and C_2 are shown in Table 7.5.1. The region extends from the end of the first region up to approximately 0.9 fractional bed height, as shown in Figure 7.40, but there are distinct differences between the systems. The level of hold-up at the same fractional bed height increases in the order, diethyl carbonate, toluene, M.I.B.k., isooctane, that is in order of increasing $\Delta\rho$.

Since the top of the flocculation zone is the bulk dispersed phase the hold-up profile for the third region, which commences at point C, must terminate at point D ($\phi = 1$ and $x = 1$). Clearly an extension of line BC will not pass through $x = 1$, the profile for all systems showing asharp up-turn at approximately $x = 0.9$. Therefore because of the distinctly different behaviour of the droplets near the interface it is necessary to consider the zone above $x = 0.9$ as a separate

third region. Line CD can be represented by the equation,

$$\phi_3 = m_3 x + C_3 \qquad (7.11)$$

restricted to the range of $x = 0.9$ to $x = 1.0$.

TABLE 7.5.1

SLOPES AND CONSTANTS OF THE EQUATIONS

FOR VERTICAL HOLD-UP PROFILES

(For Equations 7.9, 7.10 and 7.11)

	System			
	Toluene	Isooctane	Diethyl carbonate	M.I.B.K.
x_1	0.16	0.08	0.18	0.11
x_2	0.92	0.93	0.93	0.93
m_1	1.33	3.45	1.85	1.45
c_1	0.295	0.615	0.47	0.70
m_2	0.235	0.065	0.127	0.128
c_2	0.715	0.91	0.74	0.85
m_3	6.70	0.37	1.5	0.37
c_3	0.19	0.64	0	0.64

7.6 Change of drop size in the flocculation zone

An attempt was made to determine the change in mean drop size between entry into the zone and the coalescing interface since this is indicative of the degree of inter-droplet coalescence. Such data can be interpreted in terms of the ratio of drop size at any level to that at the inlet, d_h/d_{12} which is one of the basic parameters in the derivations of equations using number and material balances, as illustrated in the coalescence models in Section 4.4 (79, 80).

Unfortunately the results obtained were not particularly accurate mainly because drops at the interface which had already taken part in one or more inter-droplet coalescences tended to grow by further coalescences at the expense of the new arrivals as described for monolayers. Furthermore deformation of the larger drops made it difficult to calculate equivalent drop diameters. Typical data which is considered to be reliable for the system isooctane-water is included in Appendix 9 and plotted in Figure 7.42.

With the system toluene-water, smaller sized droplets formed a thicker band at the periphery of the columns; since these adhered to the walls and persisted for long periods they tended to confuse the count. When the camera was focused inside the column, blurred images were obtained so that few drops were measurable. Thus to obtain a reliable result, involving a count of 40 drops 2-3 cm high, required 7 to 10 photographs which was not practicable. In addition droplets near the wall in monolayers

and shallow beds were found to be involved in more interdroplet coalescences. Hence a reasonably true representation of the flocculation zone was probably not obtainable from side photp-graphs with the column design employed. Clearer images were generally obtained with isooctane droplets due to,

a. A high density difference

b. A reduced tendency to wet the glass walls.

Reproducible results were achieved with this system.

The data in Figure 7.42 clearly confirms the observations made visually that smaller drops became involved in more interdrop coalescences. Increases in drop size by factors of 2 and 3 were observed with mean inlet drop sizes of 0.28 cm and 0.08 cm respectively but no significant increase occured with 0.43 cm drops.

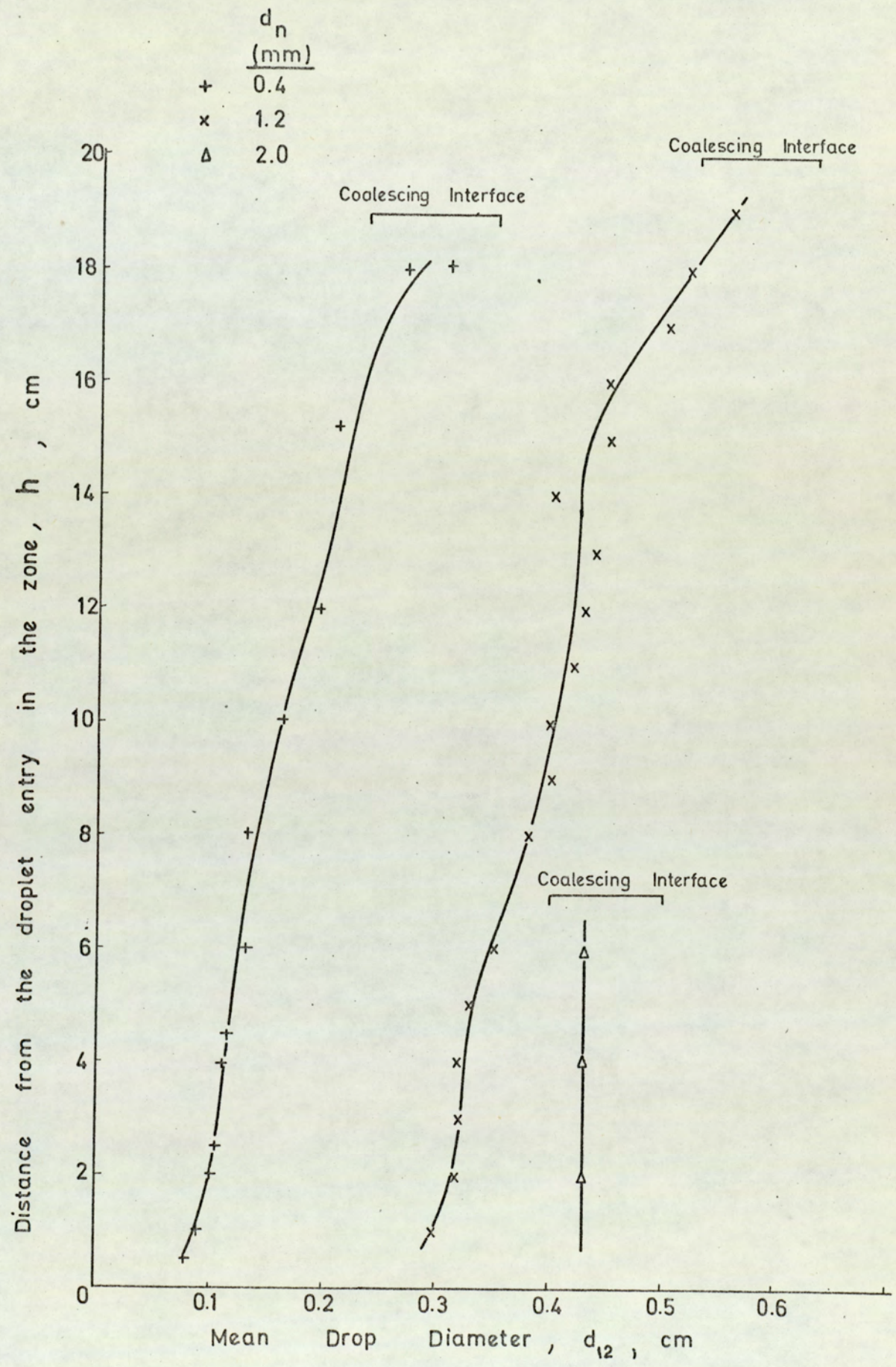

FIG. 7.42 EFFECT OF INTERDROPLET COALESCENCE ON MEAN DROP SIZE IN THE ZONE

Figure 7.42.a Distortion of droplets in a flocculation zone formed in the 6 inch column.
(System M.I.B.K.-water, d_n =1.2 mm.
Lower edge is the droplet entry, hold-up after 1-2 drops $\simeq$ 0.90)

7.7 Droplet residence time in the flocculation zone

7.7.1 Single drop rest times at a plane interface

A limited number of single drop rest times were determined for toluene droplets at a plane interface formed in the 6 inch and 9 inch columns. The results are tabulated in Appendix 7.

The main objective of this part of the work was to provide data for comparison with the residence times measured in monolayers and flocculation zones. Secondly the results enabled a check to be maintained on contamination of system materials, since any significant build-up would result in different mean values in repeat experiments. In the event even the limited study undertaken served to illustrate how very difficult it is to obtain reproducible rest time results and tended to reinforce doubts as to the applicability of laboratory single drop interface mean rest time data to drop swarms in pilot plant or industrial settlers.

The accuracy of the measurements was possibly not of a high order of magnitude with regard to drop diameter since drops were formed at the tip of the nozzle by using a standard syringe. However two fixed points approximately 30 cm apart were marked on the column wall and only those drops which travelled this distance within $\pm$ 0.1 seconds of a certain time

were accepted for coalescence time readings. In this way consistency of the terminal velocity was the criterion that each drop studied from a given injection had the same diameter. The temperature varied between 19.5 and 16 °C on different days but during any experiment remained within 1°C.

The results indicate that there was no significant difference between mean and half life coalescence time. Drops of the smallest diameter (0.9mm) gave distinctly lower times i.e $t_{\frac{1}{2}}$ = 1.1 secs, t_m = 1.2 secs than the four larger sizes. Drops of 1.8 mm had $t_{\frac{1}{2}}$ and t_m = 1.7 seconds but there was no significant difference between the other three sizes (having regard to the accuracy of measurement of about $\mp$0.1 seconds) Reproducibility cannot be produced within $< \mp$0.1 seconds.

Actual rest times were about three times less than rest times calculated from Lawson's Equation (19). This large difference arose because only the first coalescence time was recorded in this investigation. In addition of course very close temperature control was impracticable in this equipment and the use of terminal velocity to guarantee the uniformity of droplet sizes may not be as accurate a method as a micro-syringe.

It was observed that changing the distance of fall and the bulk dispersed phase static head above the interface had no

significant effect on rest times. Distance of fall varied between 15 and 60 cm, less than 15 cm being impracticable because of the need to attain the drops terminal velocity.

A miscellany of other observations are given below, for the sake of completeness,

i. Occasionally a drop arriving at the interface had a rotational motion about its mid-vertical axis. No reason was apparent for this and attempts to reproduce the effect by using different methods of drop formation at the nozzle tip were unsuccessful.

ii. Drops arriving at the interface exhibited in the main a radial motion towards the column wall. This was most noticeable in the size range 0.18 to 0.36 cm but almost completely absent with the smallest drops 0.09 cm. The largest 0.48 cm droplets exhibited this phenomena only to a limited extent.

iii. Removal of a certain amount of material from the interface, reduced the coalescence time.

iv. In the presence of small patches of visible scum at the interface, coalescence times were considerably reduced i.e. to less than 1 second, irrespective of drop diameter.

v. The arrival of a second drop within 6 cm of a drop resting at the interface resulted in increased stability of the drop in 90% of the instances observed.

vi. Impact of a second drop with a drop already resting at the interface resulted in increased stability of the second drop.

vii. Coalescence behaviour was not noticeably affected by vibrations created by other equipment and personnel in the laboratory. This may have been due to the substantial construction of the equipment used.

viii. No difference in mean rest time was observed between drops which arrived at the interface in the centre of the 9 inch column and those near to the column wall. Drops which approached closely to the wall, i.e. so as to rest on the curved portion of the meniscus, generally exhibited larger rest times. Drops which actually came into contact with the wall behaved erratically dependent upon wall condition.

As was discussed in Sections 2 and 4, these observations confirm the wide range of factors affecting the coalescence time of a single drop at a plane interface. However the individual effect of each does not appear to exceed 0.5 seconds whereas deterioration of the interface may cause an increase of up to 30 seconds in coalescence time. The presence of minor impurities is therefore the largest source of deviations in reported rest time data.

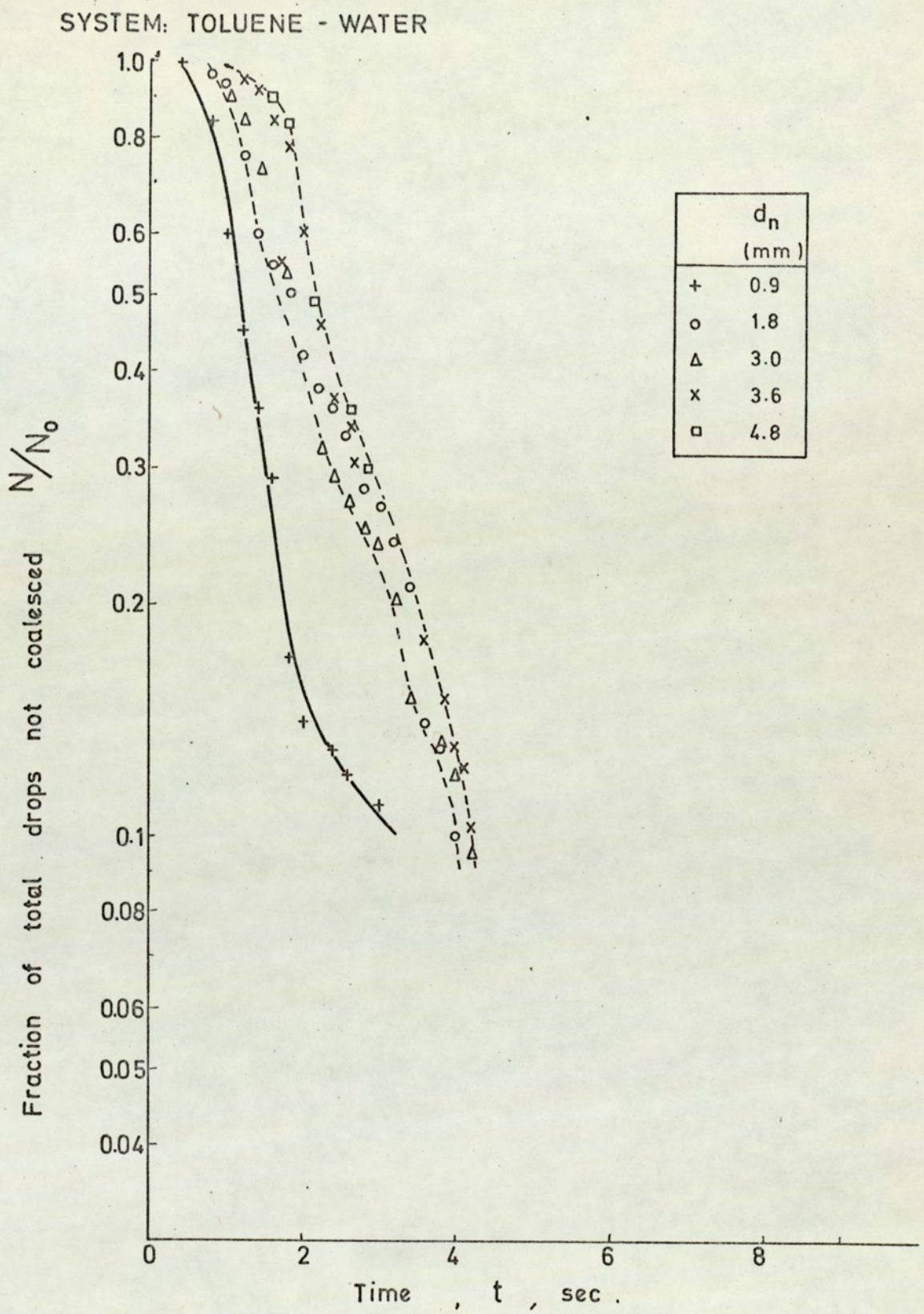

FIG. 7.43 COALESCENCE TIME OF A SINGLE DROP AT A PLANE INTERFACE

7.7.2. Residence times in monolayers

Residence times of a drop in a monolayer were measured using a stopwatch. For identification purposes coloured drops were generated from a syringing assembly and resided in a swarm of uncoloured droplets.

Residence time distribution data are included in Appendix 7. Monolayer residence time data was in fact only collected for the toluene-water system to avoid repetition of the work of Topplis (76). This was considered necessary in order to bridge the gap between flocculation zone and monolayer residence times in the same equipment. The averaged residence times, obtained from 70-110 coloured drops, are plotted against the mean inlet drop diameter in Figure 7.44. Average rest times for a drop at a plane interface are also shown in this Figure. Single drop at a plane interface times show an increase with drop diameter over the range 0.09 cm to 0.3 cm, but then apparently attain an almost constant level, no drop size effect is apparent in the monolayer data which is approximately constant at about 2 seconds. No firm conclusion is possible from the limited, though time consuming data, however.

There is a wider distribution of monolayer data indicative of the more complicated environment. For example the difficulty of obtaining a true monolayer due to the tendency for piling of the drops in 2-3 layers at the column walls and for higher turbulence in the mid-section, have already been described in Section 7.1.

SYSTEM: TOLUENE - WATER

6" Column

+ Single drop

o Monolayer

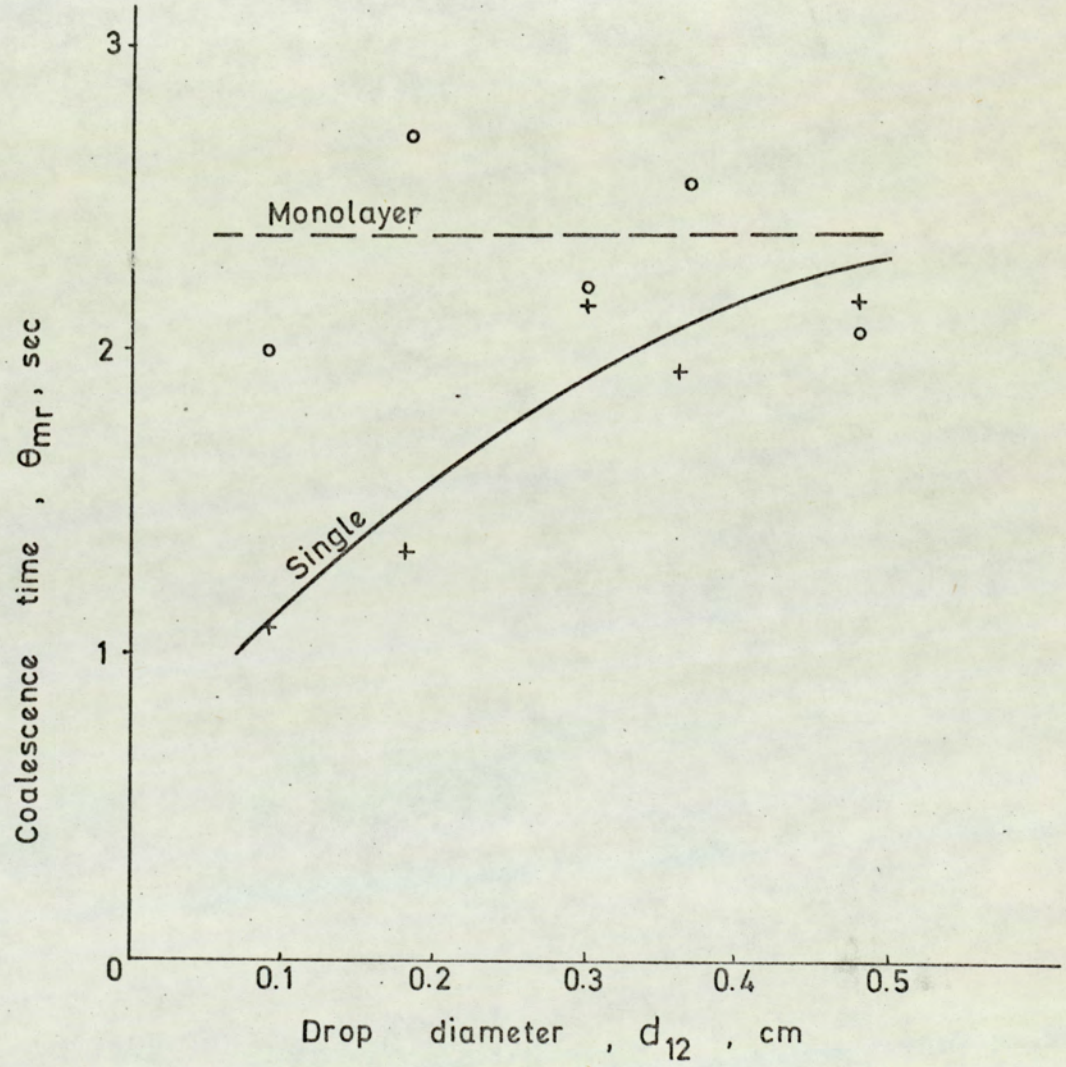

FIG. 7.44 TENTATIVE PLOT SHOWING THE VARIATION OF COALESCENCE TIME WITH DROP DIAMETER FOR ⓐ SINGLE DROP AT PLANE INTERFACE AND ⓑ IN A MONOLAYER

7.7.3. Residence Time in multilayers

The residence time of drops in the flocculation zone was measured in a similar way to those in monolayers. The distribution of residence times for various bed heights are given in Appendix 7.

'Red Oil' dye was used to colour a drop but was found to reduce the interfacial tension at concentrations above 28 mg per litre e.g. a very dark colour corresponding to a concentration of about 35 mg per litre reduced the interfacial tension of toluene to 28 dyne cm^{-1}. Drops containing such a high concentration of dye took part in a series of interdroplet coalescences unlike the undyed drops in the swarm, but when the colour lightened as a result of interdroplet coalescence, the incident was greatly reduced. As a point of interest, when a very dark red drop was injected into the column, after travelling about 50 per cent of the flocculation zone height it formed an elongated thread and moved rapidly through the interstices of the other droplets to the bulk interface where it coalesced immediately. This was due to reduced interfacial tension permitting distortion of the drop in a media of relatively rigid droplets.

Therefore, particular attention was paid to dye concentration and change of system material.

To obtain residence time distribution data, the toluene phase was generally distilled.

The results of residence time measurements are shown in Table 7.7.1 and are plotted in Figures 7.45 and 7.46.

The plot of H/θ against dispersed phase superficial velocity being almost linear. The residence times versus flow rate are shown in Figure 7.45 but further experimental points are required to produce a conclusion regarding the effect of drop size. This is not practicable in the large columns, because of the large amount of the distilled material required.

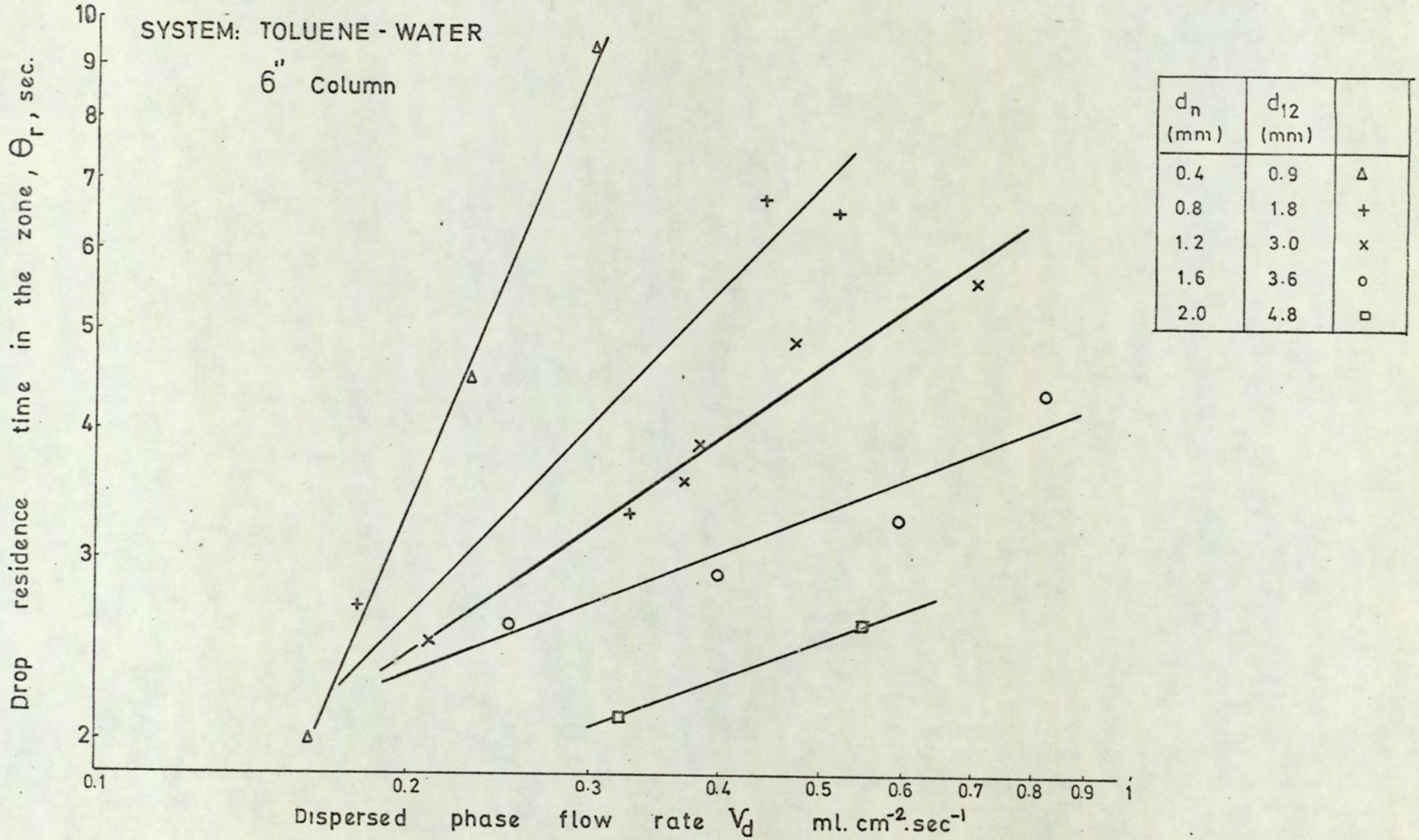

d_n (mm)	d_{12} (mm)	
0.4	0.9	Δ
0.8	1.8	+
1.2	3.0	x
1.6	3.6	o
2.0	4.8	□

FIG. 7.45 MEAN DROP RESIDENCE TIME IN A FLOCCULATION ZONE VERSUS DISPERSED PHASE SUPERFICIAL VELOCITY

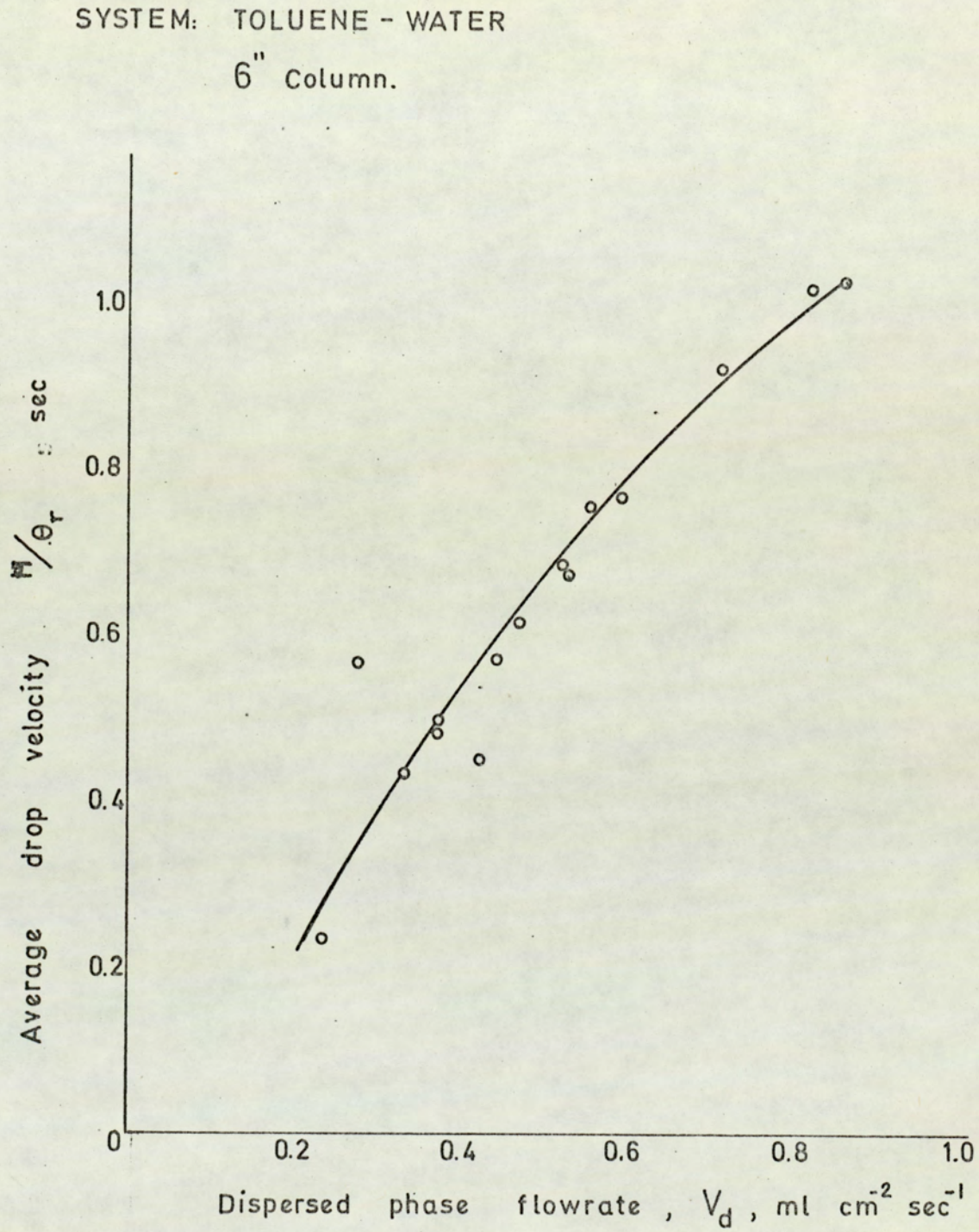

FIG. 7.46 AVERAGE DROP VELOCITY IN FLOCCULATION ZONES AGAINST SUPERFICIAL VELOCITY

TABLE 7.7.1

MEASURED MEAN RESIDENCE TIMES IN THE FLOCCULATION ZONE,

MONOLAYER AND PLANE INTERFACE

System : Toluene-water, 6-inch column

V_d ml.cm^{-2}.sec.	H cm	d_{12} cm.	θ_{rm} sec.	N_t	Nd.d %
single	Plane	0.09	1.2	100	-
0.110	Monolayer	0.09	2.0	107	17.8
0.230	2.2	0.09	4.5	86	19.0
0.275	3.5	0.09	9.8	90	16.7
Single	Plane	0.18	1.7	100	-
0.140	Monolayer	0.18	2.7	92	8.7
0.335	1.9	0.18	3.2	118	8.4
0.440	3.5	0.18	6.7	85	11.7
0.520	4.7	0.18	6.5	95	8.4
Single	Plane	0.30	2.0	100	-
0.160	Monolayer	0.30	2.2	94	5.4
0.370	2.0	0.30	3.7	95	6.3
0.374	2.0	0.30	5.8	103	5.8
0.470	2.6	0.30	4.9	99	4
0.530	2.8	0.30	3.9	104	8.7
0.705	4.5	0.30	5.6	98	13.2
0.860	6.0	0.30	10.1	72	5.7
Single	Plane	0.36	1.9	100	-
0.180	Monolayer	0.36	2.6	102	4.9
0.420	1.9	0.36	2.9	92	4.4
0.590	3.0	0.36	3.3	79	-
0.820	4.2	0.36	4.4	92	-
Single	Plane	0.48	2.1	-	-
0.210	Monolayer	0.48	2.1	103	11.8
0.550	2.2	0.48	2.6	86	7.0

7.7.4. Average velocity of drops in the multilayer

Incremental residence times were measured for isooctane drops in a 24 cm zone by timing them between 2 cm and subsequently 4 cm invervals.

The results are plotted in Figure 7.47, in which the ordinate is the cumulative time necessary to travel each incremental distance and the abscissa is the cumulative distance from droplet entry. The dotted lines represent the minimum and maximum incremental times recorded in 10-14 measurements and the solid lines the average values.

This plot demonstrates that, with the exception of travel through the ends of the column, the average velocity of an isooctane drop was practically constant.

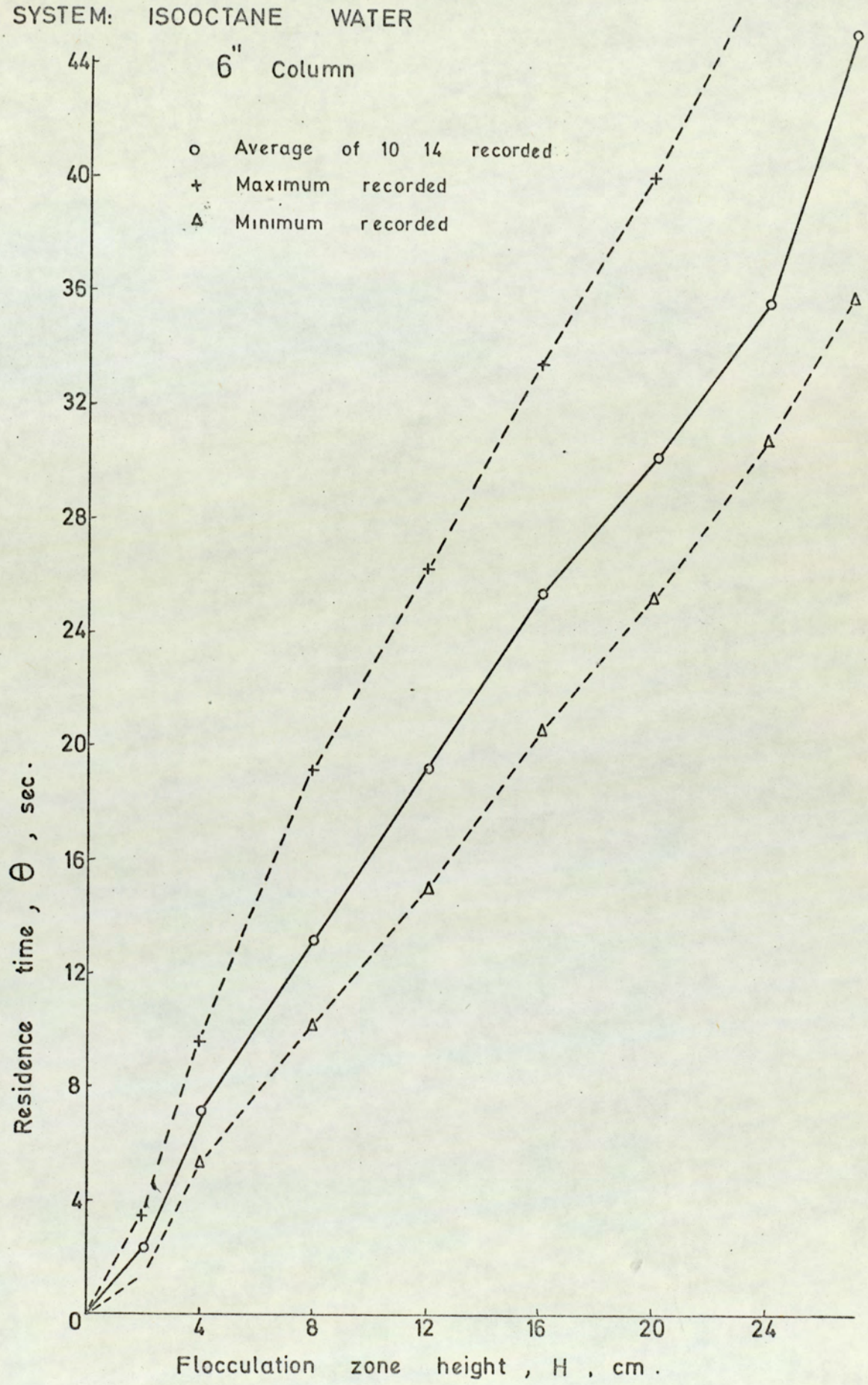

FIG. 7.47 INCREMENTAL RESIDENCE TIME OF DROPS IN A FLOCCULATION ZONE

8. DISCUSSION OF RESULTS

The results obtained have been discussed in detail in Section 7. Therefore this Section is limited to a discussion of the understanding of the mechanisms of phase separation in drop swarms gained from this study. The limitations of the investigation are also reviewed as a basis for future work.

As described in Section 7 the flocculation zone height invariably increased with a decrease in mean inlet drop size and this is in agreement with other published data (5). However for a single drop coalescing at a plane interface a decrease in drop size has been reported to generally result in a decrease in rest time. It is logical to assume that the controlling factor in the separation of a drop swarm is the rate of coalescence with the interface and therefore, if the behavior of individual drops followed that of a single drop, zone height would vary directly with drop diameter. From observations made during the release of a continuous stream of single drops to the interface it is proposed that the rate of coalescence of a single drop under such conditions may be expressed as,

$$\text{Rate of coalescence} = \frac{\text{Volume of dispersed phase coalesced}}{\text{Coalescence time} \times \text{Area of coalescing interface}}$$

$$R = \frac{v_d}{t_{\frac{1}{2}} \cdot A} \qquad (8.1)$$

The following terms may be substituted in this expression assuming a rigid, spherical drop,

Volume of dispersed phase (single drop coalesced) $V_d = \frac{\pi}{6} d^3$

Area of coalescing interface (62), $A = \pi r_f^2$

where $r_f = \left(\frac{3v}{4}\right)^{2/3} \cdot \left(\frac{2 \Delta\rho g}{\sigma}\right)^{1/2}$

or $A \propto d^2$

Hence Equation 8.1 may be expressed,

$$R = \frac{K. d}{t_{\frac{1}{2}}} \qquad (8.2)$$

In order to evaluate R from this expression it is necessary to insert a relationship giving $t_{\frac{1}{2}}$ in terms of drop diameter. Data from models has been rearranged in the required form in Table 8.1. The last column in Table 8.1. gives the derived relationship between R and d from Equation 8.2. However insertion of the experimental correlation,

$$t_{\frac{1}{2}} \propto d^n \qquad (2.9)$$

gives an additional expression for R.

Clearly a considerable discrepancy exists between the relationships for R obtained from film drainage models. Nevertheless from the single drop experimental data,

$$R \propto \frac{1}{d^{n-1}} \qquad (8.3)$$

TABLE 8.1

RELATION BETWEEN COALESCENCE TIME, $t_{\frac{1}{2}}$ RATE, R, AND DROP DIAMETER, d.

Model	$t_{\frac{1}{2}}$	$R = K.d/t_{\frac{1}{2}}$
UNIFORM FILM:		
Gillespie and Rideal (7)	d^5	$K \cdot 1/d^4$
Charles and Mason (8)	d	K
Elton and Picknett (11)	d^2	$K. 1/d$
Princen (12)	d^3	$K. 1/d^2$
Hartland (14)	d	K
NON-UNIFORM FILM:		
Charles and Mason (8)	$1/d$	$K\ d^2$
Hartland (62)	$1/d$	$K\ d^2$
Frankel and Mysels (10)	d^2	$K. 1/d$
Jeffreys and Hawksley (13)	$1/d^3$	$K. d^4$
Hartland (43)	d	K
EXPERIMENTALLY MEASURED:		
Table 2.3, Section 2.2.2	d^n where n varies approximately 1 to 3	$K. 1/d^{n-1}$

On this basis an increase in drop diameter should result in a decrease in coalescence rate that is an increase in zone height. In fact in this work the reverse was found to be the case. Thus it appears doubtful whether single drop rest time data can be applied to the prediction of flocculation zone heights.

In any event coalescence in a flocculation zone cannot be described by any equation as simple as Equation 8.2 because of restrictions placed upon the rate of continuous phase film drainage by the presence of neighbouring droplets. Some support for this is provided by the work of Smith et al (5) who observed that an increase in the number of droplets at an interface resulted in an increase in the coalescence time. Conversely however with viscous systems Hartland et al (72) observed that an increase in the number of droplets in a monolayer decreased the coalescence time, in accordance with the reduction in arc length. Further work is therefore required, along the lines followed by Topliss (76), to determine the effect of physical properties.

In a drop swarm however the effect of the drops beneath the monolayer, in increasing the buoyancy force and promoting drop distortion must also be considered (72).

Continuous phase drainage in the flocculation zone occurs countercurrent to the drop motion. This has been demonstrated by Hartland (72) and in a small column Allak (81) has observed a substantial flow near the walls. In a close packed static

bed of spheres each intersticial volume is bounded by four surfaces and its vertices are in the form of a tetrahedron. It can be demonstrated that only one of the surfaces always tends to the horizontal. Therefore in a single interstice the rate of radial to horizontal flow area is of the order of 3 : 1. Moreover due to buoyancy the droplet immediately below each individual close-packed arrangement will tend to restrict the lower horizontal flow area. It follows from this that in a static bed of spherical droplets, continuous phase will tend to flow radially towards the walls. In a coalesing environment however, each drop-drop or drop-interface coalescence creates a void which is subsequently filled by other droplets and this process imparts a random turbulence onto the continuous phase motion.

As discussed in Section 7.,and demonstrated in Figure 7.34, no correlation proved possible between zone height and physical properties. Earlier, as reviewed in Section 4, Smith et.al (5) were able to produce such a correlation. Their work however did not extend to values of drop diameter < 0.25 mm. As can be seen from Figure 7.29 above this diameter all flocculation zone heights, with the exception of M.I.B.K. which gave poorest agreement in their work, begin to approach the same value.

One limitation of the present work is that a single aqueous continuous phase was employed throughout. Since film drainage

is evidently a controlling mechanism it would be desirable to vary the continuous phase to obtain a range of system viscosities, and moreover extend the study to viscous systems. Similarly the lowest limit of interfacial tension studied was 9.8 dynes cm^{-1} and this should be extended to 3 dynes cm^{-1}. The difficulty in doing this will be to maintain $\Delta\rho$ constant and for work in large columns the best approach may be to employ a binary system containing different concentrations of equilibriated solute (101).

A further limitation is that the range of drop sizes employed, viz 0.7 mm to 0.48 mm, though at the lower end of the 'primary dispersion' range did not extend into the 'transition region'. Thus it would be of interest to repeat some of the work with drops in the size range 0.1 mm to 0.5 mm. Drops in this range are less deformable and furthermore, from observations with single coloured drops reported in Section 7.7., a greater incidence of interdrop coalescence is to be expected. Unfortunately however there is also an increased tendency to adhere to the column walls. It would also be useful to perform work with a preset distribution of drop sizes e.g. 50% at 0.7 mm and 50% at 0.15 mm as a first step towards a complete analysis of coalescence behaviour in settlers associated with agitated vessels.

As it was described in Section 7, counter-current flow of the continuous phase was found to have no significant effect on

other than the first 5% of the flocculation zone. Nevertheless it would be of interest to repeat some of the work with co-current flow, as is often used in gravity settlers, since the increased turbulence in the zone could result in increased interdrop coalescence.

9. PROPOSED MODELS FOR A FLOCCULATION ZONE

9.1 Introduction

As discussed in Section 4.4, numerous models have been reported for flocculation zones (41, 78, 79, 80) based upon predicted, or experimentally determined, single drop mean rest times. Their aim was to extend accumulated data to the case of swarms of drops encountered in commercial equipment. All these models have relied upon assumptions i.e. that the droplets in the heterogeneous zone are rigid and spherical, and that their packing efficiencies are constant throughout the band. Experimental findings in this work confirm earlier observations that these assumptions are invalid. Therefore an improved analysis must take into account the difference between the real situation and those involved in single drop-interface or drop pair coalescence studies.

The purpose of this model is to describe the flocculation zone and the mechanism of coalescence on the basis of the results discussed earlier, that,

(a) The dispersed phase hold-up varies throughout the bed.

(b) The residence time of a drop in a specific bed is constant about a wide distribution mean value.

(c) The bed height is dependent upon the dispersed phase flow rate and inlet drop sizes.

The drops in the flocculation zone progress by replacement. That is the volume vacated by any drop upon coalescing at the interface is occupied by the next one in the queue so that drops

below this layer change their position. Some drops adhere around the walls of the column and remain there for long periods of time so that, an observation via the walls, the whole bed gives the impression of a core of droplets moving within a stationary annulus 2 to 3 droplets thick; the motion of this inner core is intermittent movement over distances equivalent to the mean drop diameter at the interface. The general appearance of the bed motion is hence that of a plug flow. Moreover it was shown, by injecting coloured drops into the bed, that they did not deviate individually from plug flow throughout most of the bed height. Deviations from plug flow were observed at the two ends of the flocculation zone as illustrated by Allak (81) and in the present investigation. However, it has been found, as discussed in Section 7.5.2., that these end sections did not exceed 25% of the total bed height, being lower in the majority of the cases. It is envisaged that the behaviour of the bed as a whole is similar to a homogeneous fluid flow. The system is incompressible and at steady state the bed height is constant or does not vary beyond practical limits.

9.2 DESCRIPTION OF THE MODELS

Accepting resemblance of the flocculation zone to a homogeneous fluid, either of the following three flow mechanisms can be visualised;

(a) It is assumed that the entry zone of the flocculation band

forms an imaginary inexhaustible reservoir of the dispersed phase liquid; any number of small channels emanate from this reservoir such that in any horizontal plane their total cross sectional area is equal to the fractional hold-up multiplied by the area of the column cross section. These channels are considered to extend straight up to the interface and thence into the bulk dispersed phase. A diagramatic sketch of this is shown in Figure 9.2. A channel in the zone is represented by a dotted line.

(b) Similar to (a), but jets not channels are assumed to be formed in the zone fed from the reservoir; the diameter of any one jet is not constant with time but varies according to the periodicity and magnitude of oscillation. The jets extend straight up to the interface and a droplet upon breaking from this jet, merges into the bulk interface. The process as a whole is the reverse of drop formation from a jet (87). Jet heights can be assumed equivalent to zone height. This mechanism is illustrated in Figure 9.1.

(c) The whole flocculation zone is assumed to resemble a conduit within which the droplets move in continuous flow. This conduit has an area at each level proportional to hold-up (or inversely proportional to void space). Therefore the point velocity in the bed is dependent upon the

hold-up and the distance from entry. This is demonstated in Figure 9.2. The effective area is drawn by analogy with the hold-up profile and D_e, the equivalent cross sectional diameter therefore varies throughout the zone.

These three models of the flocculation zone are described further in Sections 9.2.1 to 9.2.3. Mechanism (c) is actually derived from the first two, that is the channels or jets are all combined to give the average flow.

9.2.1. CHANNELS IN THE ZONE

This has been shown in Figure 9.2.

An imaginary channel is shown by a dotted line, starting with a narrow cross section and diverging in a similar manner to drop size increase throughout the zone. The effect which drop-drop coalescence has upon the channels within the bed is visualised in terms of the instantaneous touching of two channels at any level so that a portion of the dispersed phase may be transferred from one to the other. Upon this one channel cross section would increase at the expense of the other. Because of this horizontal transfer, the total amount of dispersed phase at any level remains unaffected, that is the horizontal hold-up remains constant. If drop drop coalescence occurs between two drops at different levels it is reflected in both levels. In summary whilst drop-drop coalescence affects the cross sectional area of each individual channel; it does not affect the total cross

sectional area at any level. The divergence of a channel is analagous to the drop size increase shown in Figure 9.4. The number of channels is proportional to the number of droplets arriving per unit area per unit time. The smaller the inlet drop size for a constant dispersed phase flow, the larger will be the number of the channels; for a given volumetric flowrate the same linear velocity will therefore obtain in all the channels. This will result in a smaller Reynolds number in the small diameter channels and hence increased friction.

9.2.2. JETS IN THE ZONE

Jets are assumed in the zone instead of diverging channels, but again an imaginary inexhaustible reservoir, is assumed to feed the jets and so maintain continuity. A drop coalescing with the bulk dispersed phase is analagous to a drop forming from the tip of this jet. Thus, flocculation zone height corresponds to a jet length as shown in Figure 9.2. and jet velocity is analogous to the drop velocity in the zone.

Data on the variation of jet length with Reynolds number for drop formation in the nozzle against, L/d_n, dimensionless jet length, is reproduced in Figure 9.3. (87). Data from the present study viz, dimensionless flocculation zone height, H/d_n versus drop Reynolds number with mean inlet drop diameters of approx. 0.1 cm. are plotted in Figure 9.4. The relative magnitudes of the Reynolds numbers in these two plots differ between 1 - 10

and 500 - 1500 for the dimensionless zone height and jet length respectively. This arises from the large difference in velocities involved in the two cases and also because the drop velocity is taken as the superficial velocity of the dispersed phase whereas clearly it will be some multiple of this. Nevertheless there is a marked resemblance between the general appearance of the curves; for all the systems except toluene, zone height curves match the jet lengths curves closely over the rising sections. Data were not available for higher values of toluene but it is anticipated that with higher flow rates the bed heights would increase more sharply resulting in a closer resemblance to the curves for the other systems. The descending portions of the curves in Figure 9.3. are not comparable to the experimental dimensionless zone height curves since in this range the column would be flooded. A comparison of the variation of bed height with jet length may be worthy of further study. In the event the dependency of flocculation zone height upon drop Reynolds number suggests that zone behaviour does resemble that of a homogeneous fluid .

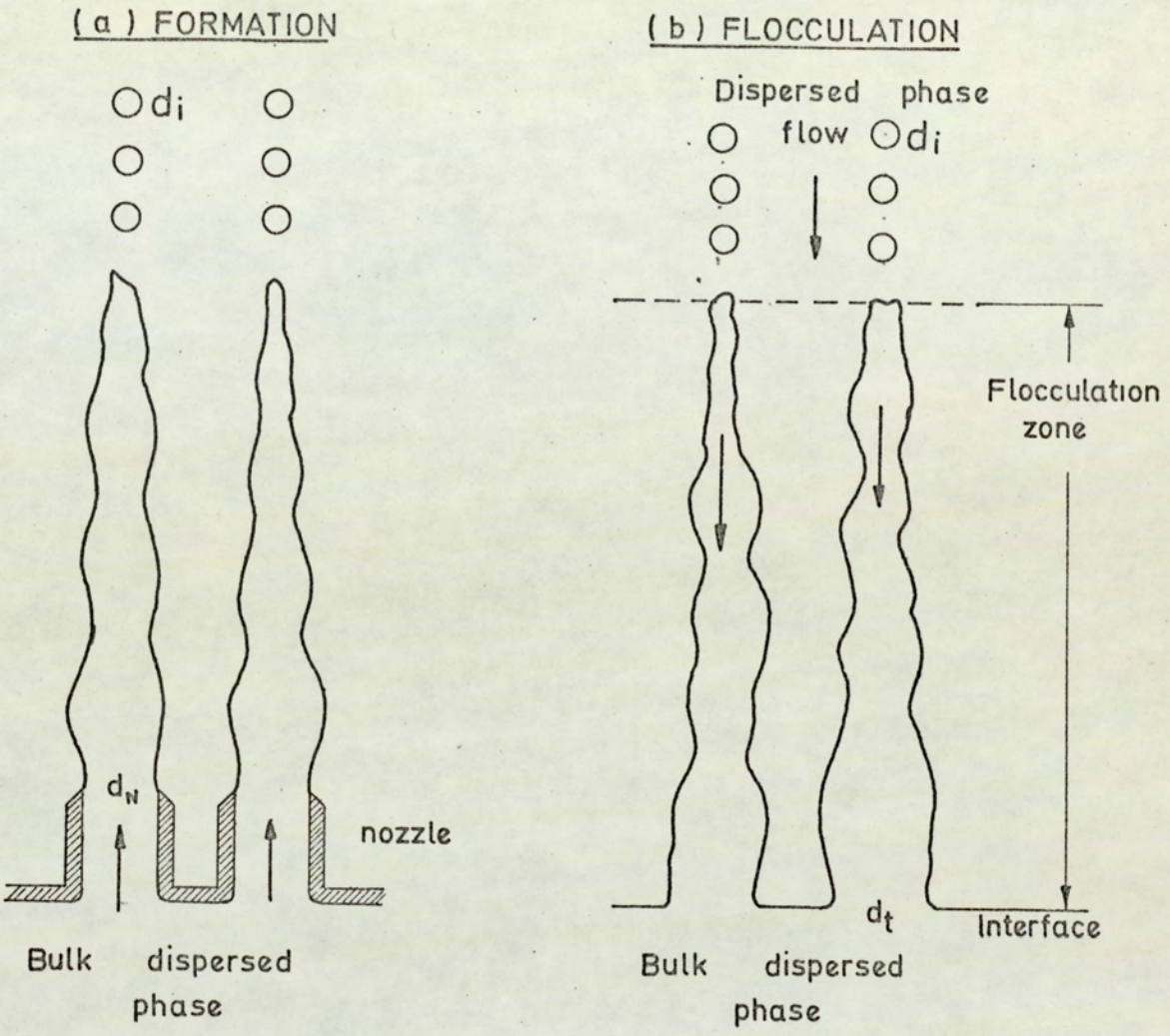

FIG. 9.1 THE ANALOGY BETWEEN DROPLET FORMATION FROM SHARP EDGED NOZZLES AND COALESCENCE OF THE DROPLETS IN A FLOCCULATION ZONE.

FIG. 9.2 DIAGRAMMATIC REPRESENTATION OF

a. DIVERGENT CHANNELS AND THREE CONSTITUENT ZONES IN A FLOCCULATION BAND .

b. IMAGINARY CONDUIT

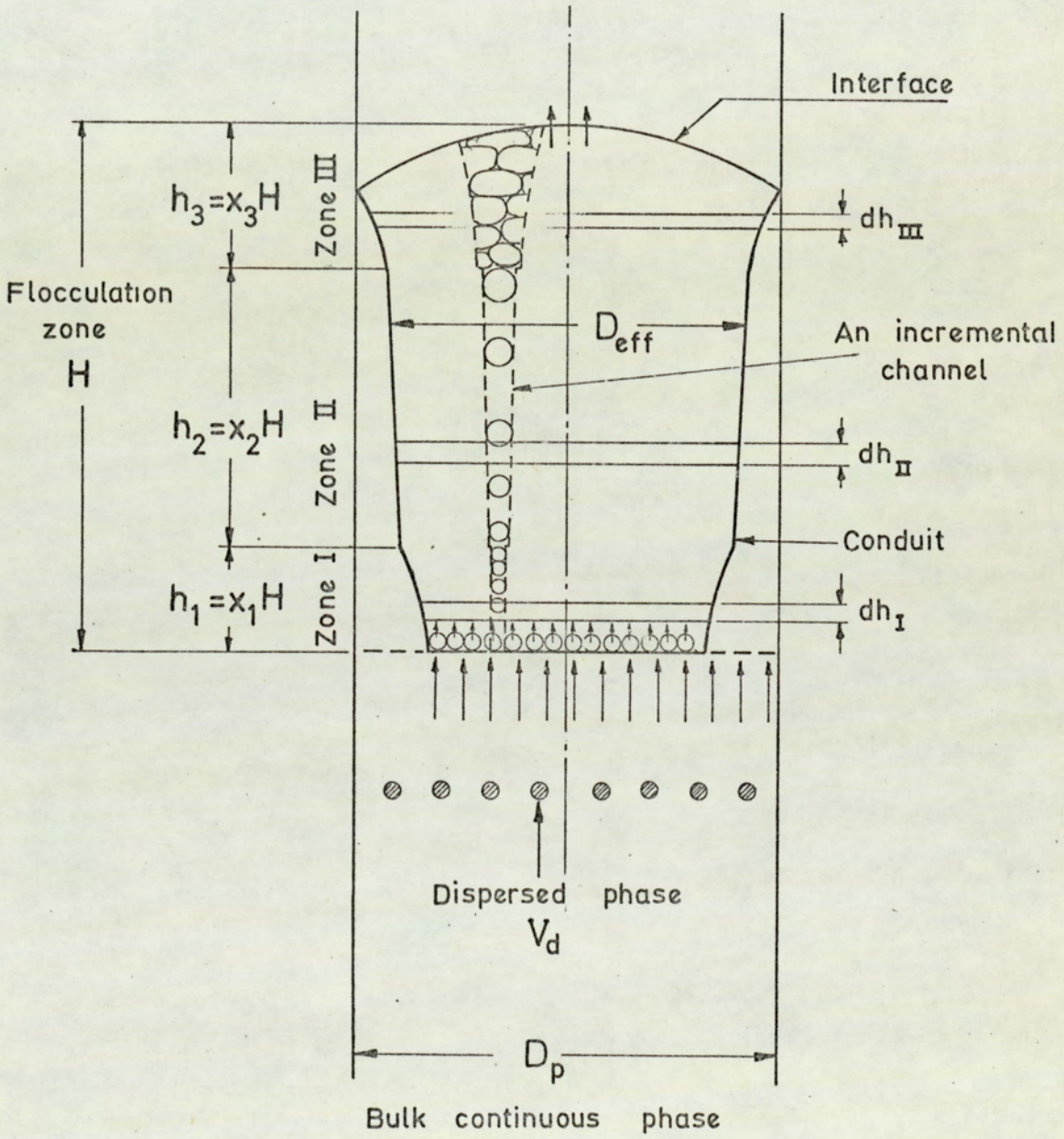

Zone: I : Drop entry zone.

Zone II: Mid zone

Zone III: Interface zone.

System: Heptane injected in water

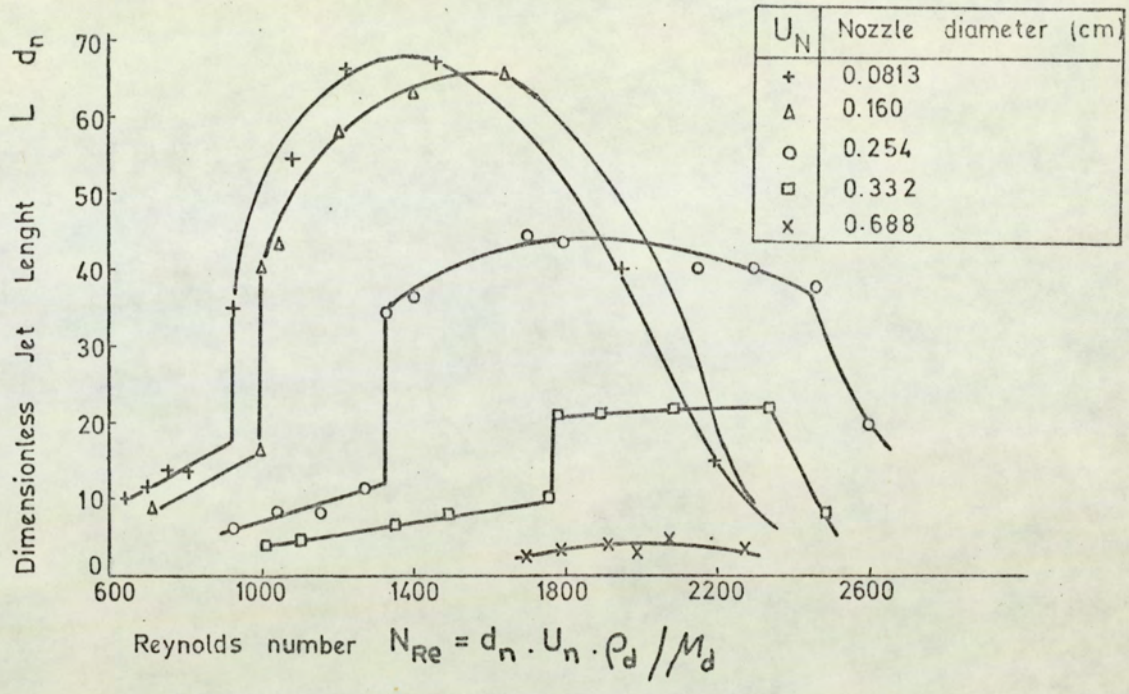

FIG. 9.3 EFFECT OF NOZZLE DIAMETER ON DIMENSIONLESS JET LENGTH (87)

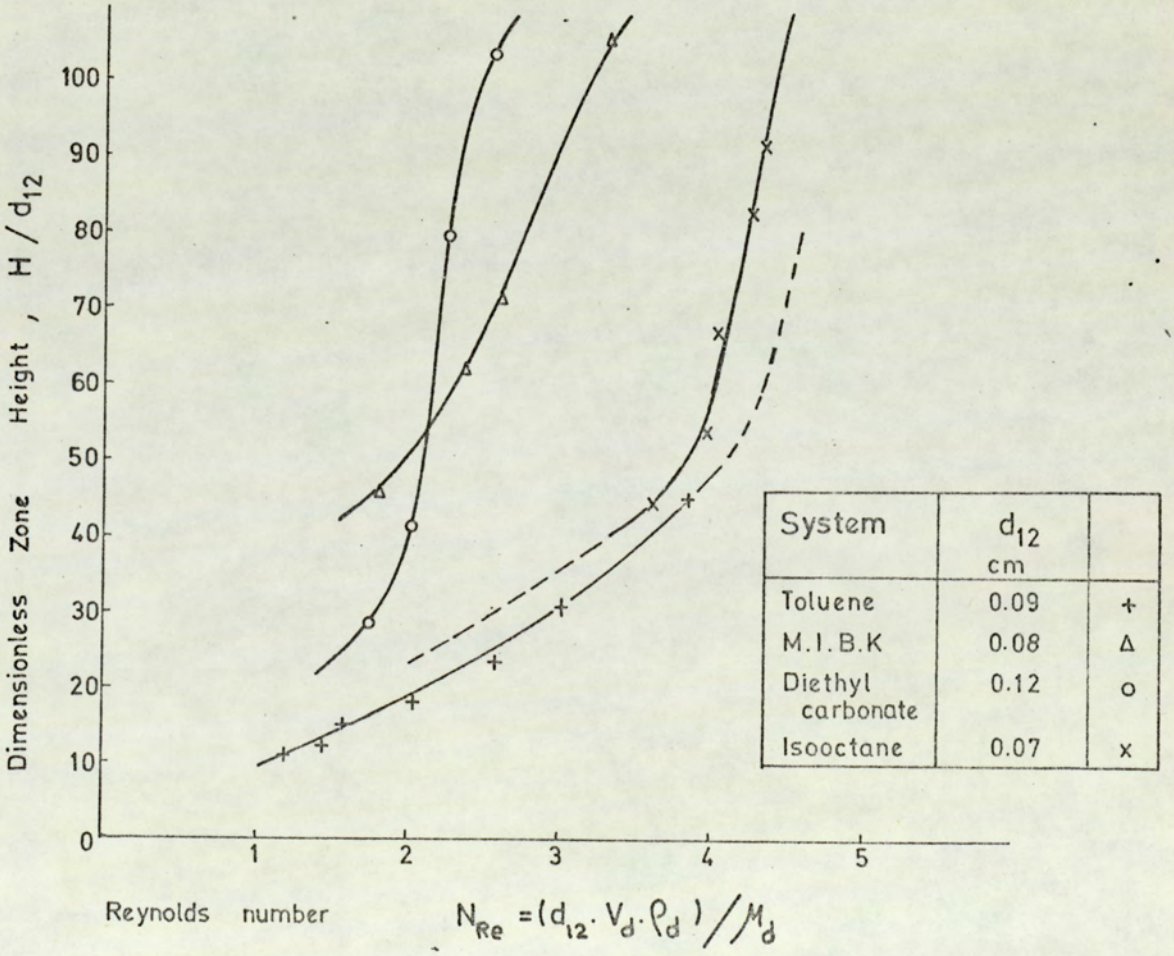

FIG. 9.4 EFFECT OF INLET DROP DIAMETER ON DIMENSIONLESS ZONE HEIGHT (6" Column)

9.2.3. Overall Conduit

At steady state, the flocculation zone height is constant or does not vary beyond practical limits, and the system is incompressible. In addition continuity of dispersed phase flow is assumed in the flocculation zone even though it exists throughout in the form of discrete droplets separated by films of continuous phase of varying thickness. The volume of continuous phase separating the droplets in any cross section is a function of the hold-up and this area is not available for flow of the dispersed phase. Thus, for the average volumetric flow rate of the dispersed phase at any axial position, there is available an effective cross sectional area equal to the cross sectional area of the column less the void areas between the drops which are occupied by the continuous phase.

On this basis, the point dispersed phase velocity in the flocculation zone at any height is given by,

$$u = \frac{V_v}{A_e} \qquad (9.1)$$

or, by defining,

$$A_e = \frac{\pi}{4} D_p^2 \, \phi \qquad (9.1.a.)$$

$$u = \frac{V_v}{\frac{\pi}{4} D_p^2 \, \phi} \qquad (9.2)$$

$$u = \frac{V_d}{\phi} \qquad (9.3)$$

where,

V_v = Dispersed phase volumetric flow rate ($ml.sec.^{-1}$)

V_d = Dispersed phase superficial velocity ($ml.cm.^{-2}sec.^{-1}$)

ϕ = Dispersed phase fractional hold-up.

With a plug flow, a droplet velocity within the bed will represent the dispersed phase velocity. Thus, a droplet point velocity may be written,

$$\frac{dh}{d\Theta} = u \qquad (9.4)$$

where,

h = the position from the bed entry

Θ = the residence time in the bed.

Combing the Equations 9.3 and 9.4 to eliminate (u),

$$\frac{dh}{d\Theta} = \frac{V_d}{\phi} \qquad (9.5)$$

The boundary conditions are at the entry to the bed, $\Theta = 0$; $h = 0$ and at the interface, $\Theta = \Theta_r$; $h = H$, the total flocculation zone height. Hence, on integration of Equation 9.5,

$$\int_{\Theta=0}^{\Theta=\Theta_r} d\Theta = \int_{h=0}^{h=H} \frac{\phi}{V_d}\, dh \qquad (9.6)$$

At steady conditions, for a constant flow rate, (V_d = constant), the bed will have a constant height, H. The hold-up, $\emptyset$, has been found experimentally to vary along the bed and an emprical general relation could be represented by straight line plots of fractional hold-up vs fractional zone height, x, viz,

$$\emptyset = mx + c \qquad (9.7)$$

For zone I:

$$\emptyset_1 = \left[m_1 \left(\frac{h}{H}\right) + c_1 \right]_{h=0}^{h=x_1H} \qquad (9.8)$$

For zone II:

$$\emptyset_2 = \left[m_2 \left(\frac{h}{H}\right) + c_2 \right]_{h=x_1H}^{h=x_2H} \qquad (9.8.a)$$

For zone III:

$$\emptyset_3 = \left[m_3 \left(\frac{h}{H}\right) + c_3 \right]_{h=x_2H}^{h=H} \qquad (9.8.b)$$

In order to evaluate Equation 9.8, 9.8.a, 9.8.b or 9.11 it is clearly necessary to determine the limits of x, and the values of the constants m and c, experimentally in each case.

By dividing the total residence time of a drop in the dispersion band into three consequetive zones and subsequent the respective hold-up relations, the following equations are obtained.

$$\theta_r = \theta_1 + \theta_2 + \theta_3 \qquad (9.9)$$

where,

θ_1, θ_2 and θ_3 are the residence time in zone I, II and III respectively.

Hence, Equation 9.6 becomes,

$$\theta_r = \frac{1}{V_d}\left[\int_{h=0}^{h=x_1H} \left(m_1 \frac{h}{H} + c_1\right) dh + \int_{h=x_1H}^{h=x_2H} \left(m_2 \frac{h}{H} + c_2\right) dh + \int_{h=x_2H}^{h=H} \left(m_3 \frac{h}{H} + c_3\right) dh\right] \qquad (9.10)$$

which on integration and simplification, yields,

$$\frac{V_d \Theta_r}{H} = \left(\frac{m_1 - m_2}{2}\right) x_1^2 + \left(\frac{m_2 - m_3}{2}\right) x_2^2 +$$

$$+ (c_1 - c_2)\, x_1 + (c_2 - c_3)\, x_2$$

$$+ (c_2 - c_3)\, x_2 + \frac{m_3}{2} = K \qquad (9.11)$$

or

$$\frac{V_d \Theta_r}{H} = K \qquad (9.12)$$

9.3 Verification of overall liquid conduit model

Knowing the emprical values for hold-up in each zone, Equations 9.8 - 9.8b as shown in Table 9.2, the residence time (Θ_r) can be calculated for any system from Equation 9.11 for a given dispersed phase flow rate, producing a total bed height H. Calculated and experimentally determined residence time data is plotted in Figure 9.5.

Residence times calculated by Equation 9.11, using values of bed height between 1.9 and 2.2 cm, flow rates between 0.23 and 0.83 $ml.cm.^{-2}sec.^{-1}$ are compared with experimentally determined residence time in Table 9.2.

Considering the wide distribution of measured residence times, the derived formula for calculating residence time in the zone appears to be reasonably satisfactory, on the basis of statistically calculated 1.02 distribution coefficient and 99% correlation in Appendix 8.

Further work to verify the validity of Equation 9.11 is recommended in Section 11.2.

TABLE 9.2

CALCULATED, θ_r, AND EXPERIMENTALLY DETERMINED, θ_{mr}, MEAN RESIDENCE TIME OF DROPLETS IN THE FLOCCULATION ZONE

System: Toluene-water

Column: 6-inch : K =,0.774

Dispersed phase flow rate	Zone Height	Residence Time		Mean inlet drop diam.
		Calculated	Measured	
V_d	H	θ_r	θ_{mr}	d_{12}
ml.cm.$^{-2}$sec.	cm.	sec.	sec.	cm.
0.230	2.2	7.5	4.5	0.09
0.275	3.5	6.1	9.8	0.09
0.335	1.9	4.4	3.2	0.18
0.440	3.5	6.1	6.7	0.18
0.520	4.7	6.9	6.5	0.18
0.370	2.0	4.2	3.7	0.30
0.374	2.0	4.1	5.8	0.30
0.470	2.6	4.3	4.9	0.30
0.530	2.8	4.1	3.9	0.30
0.705	4.5	4.9	5.6	0.30
0.860	6.0	5.4	10.1	0.30
0.420	1.9	3.5	2.9	0.36
0.590	3.0	3.9	3.3	0.36
0.820	4.2	3.9	4.4	0.36
0.550	2.2	3.1	2.6	0.48

TABLE 9.2 (continued)

System: Isooctane-water

Column: 6-inch K= 0.938

V_d ml.cm.$^{-2}$sec.$^{-1}$	H cm.	θ_r sec.	θ_{mr} sec.	d_{12} cm.
0.550	18	36.6	30.8	0.28
0.490	12	26.4	23.0	0.28

System: Diethylcarbonate-water

Column: 6-inch K = 0.822

0.710	22	27.9	25.4	0.35
0.420	8	13	15.7	0.35

SYSTEM: TOLUENE - WATER

6" Column

	d_n (mm)	d_{12} (mm)
□	0.4	0.9
△	0.8	1.8
+	1.2	3.0
×	1.6	3.6
⬠	2.0	4.8

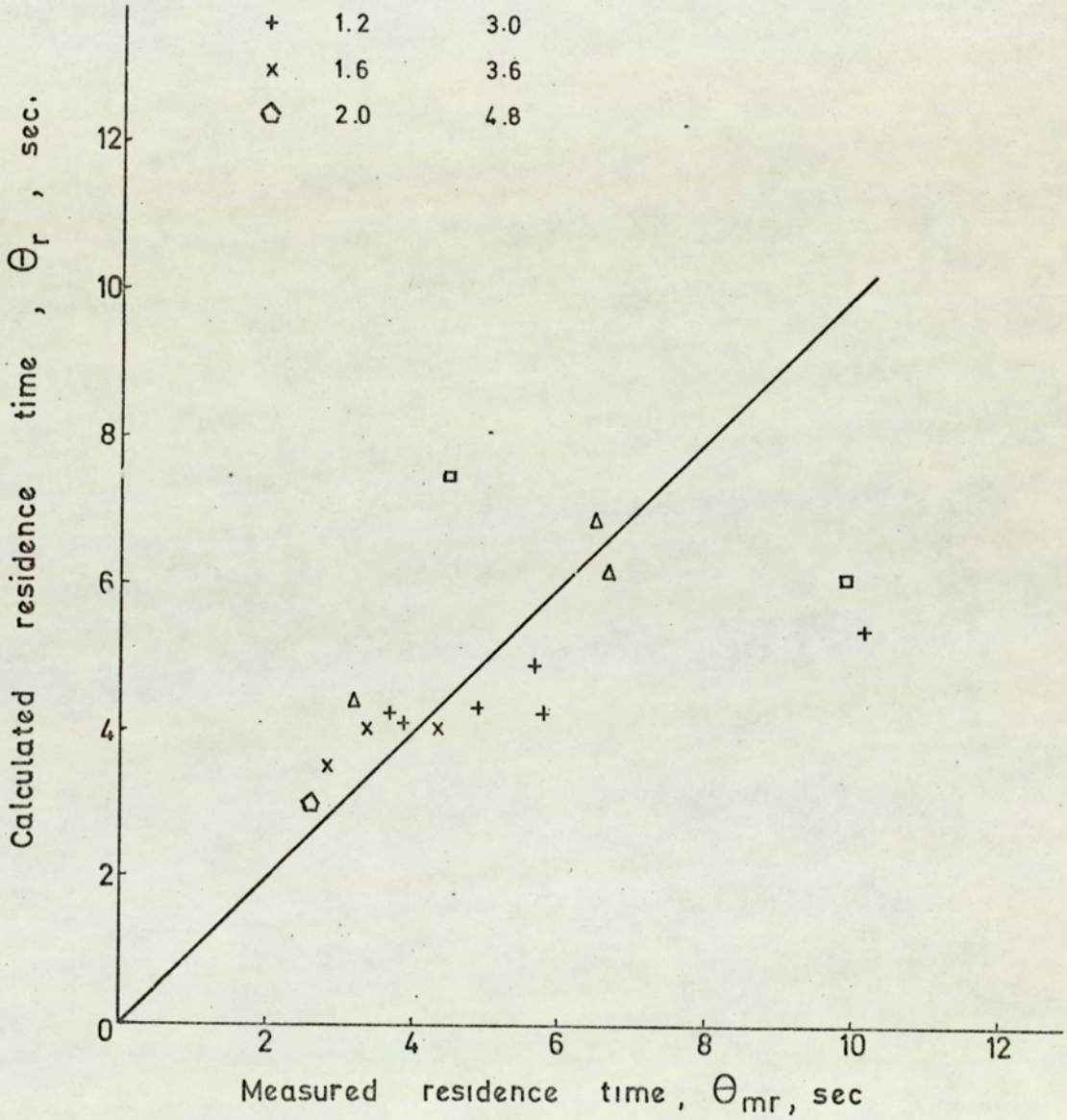

FIG. 9.5 COMPARISON OF MEASURED MEAN DROP RESIDENCE TIMES IN A FLOCCULATION ZONE WITH DATA CALCULATED FROM EQUATION

9.4. Discussion

Equation 9.11 gives a relationship between dispersed phase flow rate, V_d, flocculation zone height, H., drop residence time and K, a constant characteristic of the system and describing the hold-up through the dispersion band,

$$H = \frac{V_d \Theta_r}{K}$$

By itself this does not have much value in the design of a settler unless it is used in scale-up. The use of residence time data in the design of settlers is not new (77, 80, 80), but this simple calculation using an emprical hold-up equation demonstrates its validity. This suggests that point velocity of a drop applies in practice in swarms of droplets, e.g. in a flocculation zone, in a similar way to other areas below the zone. The result demonstrates the significance of hold-up in the flocculation zone. Obviously closer packing of droplets tends to promote drop to drop coalescence. Therefore, it can be concluded that drop-drop coalescence improves the overall coalesence rate as found in other investigations.

It has been illustrated that there is some resemblence between the ratios jet length : nozzle diameter and flocculation zone height : drop diameter. The concept of jets and channels has been introduced to consider factors involved in the flocculation zone in a similar way to in drop formation

and to offer an approach for mathematical treatment trials that may be taken up in further work.

10. A PRELIMINARY ATTEMPT TO EVALUATE THE RESIDENCE TIME DATA BY ANALOGY WITH SEDIMENTATION AND FLUIDIZATION

The fluidization of droplets in a layer in the vicinity of a coalescing interface was assumed by Lee and Lewis (78), as reviewed in Section 4.4. For this the continuous phase must have a sufficient downward velocity, Vc given by,

$$V_c = \frac{1 - \phi}{\phi} \quad V_d \qquad (10.1)$$

The fluidization velocity of Richardson and Zaki (83) was written,

$$V_c = V_t \, (1 - \phi)^n \qquad (10.2)$$

From these Equations, and with certain assumptions, they derived the equation given earlier in Section 4.4.3.a.

An alternative derivation, based upon the residence time in the flocculation zone is described below.

From Equation 10.1 and 10.2, the terminal velocity,

$$V_t = \frac{1}{\phi \, (1 - \phi)^{n-1}} \quad V_d \qquad (10.3)$$

Thus the fluidization model of Lee and Lewis (78) may be applicable within that range of conditions for which values of terminal velocity in the flocculation zone calculated from Equation 10.3 are in agreement with those determined experimentally.

In the present investigation residence times of the droplets were determined as described in Section 7.7, and H/θ vs V_d is given for the system toluene-water in Figure 7.46. This data covered a range of mean inlet drop sizes from 0.09 to 0.48 cm and a total zone height of 2 to 6 cm. The relationship is not linear but with slight sacrifice of accuracy may be written,

$$\frac{H}{\theta} \simeq m V_d \qquad (10.4)$$

Moreover, the motion of drops in a flocculation zone of 24 cm (isooctane water system) was, with the exception of the inlet and exit sections, essentially constant as shown in Figure 7.47.

These experimental results lend support to an assumption that a flocculation zone has a terminal velocity approximating to that of the constituent drops. Thus an average drop terminal velocity, equal to H/θ, may be considered as the zone terminal velocity, V_t. If the fluidized bed model is valid this is also equal to the terminal velocity of a fluidized bed and Equation 10.3, becomes,

$$\frac{H}{\theta} = m V_d = \frac{V_d}{\phi (1 - \phi)^{n-1}} \qquad (10.5)$$

Thus, the slope m = 1.25 of the straight line, approximated from

Figure 7.46,

$$m = \frac{1}{\phi\,(1-\phi)^{n-1}} = 1.25 \qquad (10.6)$$

Lee and Lewis (78) used a value for n given in the correlation by Richardson and Zaki (83),

$$n = 2.7\,k^{0.16} \qquad (10.7)$$

$$k = \frac{\pi}{6}\left(\frac{d_s}{d_p}\right)^3 \qquad (10.8)$$

where d_s = diameter of a sphere with the same volume as the distorted particle

d_p = the diameter of a circle of the same area as the projected profile of the particle, when lying in its most stable position.

As a first approximation it can be assumed that $d_s/d_p \simeq 0.5$, on the basis that the drops are elipsoidal with the ratio of minor: major axis equal to 0.5 which is a not unreasonable description of drops near the interface in a flocculation zone. From Equation 10.7 this yields a value of $n \simeq 1.75$. Substitution of this value in Equation 10.6 and solving for hold-up gives $\phi \simeq 0.30$ which is a very low value except for positions $<$ 10 mm for the droplet entry zone. If average hold-up in the flocculation zone is of the order of 0.30 then the model of Lee and Lewis is valid. However, since this is

not in agreement with the experimental data the correlation of Richardson and Zaki, using values of n determined for solid particles, cannot be applied. This is only to be expected since the droplets in a flocculation zone not to possess a similar freedom to particles in solid-liquid fluidization because of the considerably lower voidage.

As an alternative, taking an average hold-up value for the flocculation zone, to estimate the power n which may be applicable from Equation 10.6, gives $n \simeq 1$ for a hold-up, $\phi = 0.80$. Thus, n in Equation 10.2, correlated by Richardson and Zaki, might be applicable to liquid-liquid flocculation zones with $n \simeq 1$. Furthermore, Steinour (110) evaluated a shape factor, k, for the sedimentation of solid particles in a continuous media of the form,

$$k = \frac{\phi}{1 - \phi} \quad 10^{-1.82\,\phi} \qquad (10.9)$$

which was also derived as a correction factor from Stokes velocity for solid particles. This correction factor is identical with Equation 10.8, which is also a correction factor for fluidized beds studied by Richardson and Zaki (83). Thus it would be possible to use Steinour's correction factor, Equation 10.9, in Richardson and Zaki's correlation for power, n, given in Equation 10.7. Equation 10.7 would then become,

$$n = 2.7 \left(\frac{\phi}{1 - \phi}\right) \times 10^{-1.82\,\phi} \qquad (10.10)$$

Now, for an average flocculation zone hold-up, $\phi = 0.80$, Equation 10.10 gives $n \simeq 0.38$.

Using this value of n in Equation 10.6 gives $m \simeq 2$ which is more comparable with the experimental value of $m = 1.25$. In this way a shape correction factor may be determined to permit the fluidization/sedimentation analogy to be used to predict the flocculation zone heights but only when the minimum fluidization velocity is exceeded. This was never reached in this work, except possibly in the drop entry region, and thus the Conduit Model proposed in Section 9 is more realistic.

11. CONCLUSIONS

The main conclusions drawn from this investigation are as follows,

a. The separation of dispersions in continuous flow involved the formation of a flocculation zone comprising 3 distinct sections. Different droplet behaviours and packing efficiencies were observed in each section.

In the first; 'droplet entry' region rigid drop behaviour pertained and fractional hold-up varied between 0.25 and 0.75. This region extended some 10 to 15 mm from the inlet plane; in it drops moved randomly but the incidence of interdroplet coalescence was small.

The second region constituted the major proportion of the total height and in it a gradual change in hold-up was observed which was characteristic for each system. Droplet deformation and interdrop coalescence was evident.

The third region was turbulent and extended to the bulk dispersed phase interface. The fractional hold-up was of the order of 0.90, droplets underwent maximum distortion, and there was a high incidence of interdrop coalescence.

b. Measured hold-up profiles for each section could be represented by straight line plots of fractional

hold-up vs fractional zone height, viz,

$$\phi = mx + C \qquad (7.9 \text{ to } 7.11)$$

For the entry sections m had a value between 1.33 to 1.85; for the mid-sections m was lower, in the range of 0.06 to 0.24 and was dependent upon the ratio of $g\Delta\rho/\sigma$. Higher values of m pertained in the third section viz 0.37 to 1.5. The value of the constant C was 0.30 to 0.70, 0.70 to 0.90 and 0 to 0.64 for each section respectively.

c. The total flocculation zone heights have been correlated by the following equations,

For the toluene-water system,

$$H = (-3.33d_{12} + 3)\, D_p^{(-0.41d_{12} - 0.09)} V_d^{1.16}\, d_{12}^{-0.62}$$

or,

$$H = 3.28\, d_{12}^{-.062}\, V_d^{1.24} \qquad (7.5)$$

For the diethylcarbonate-water system,

$$H = 15.20\, d_{12}^{-1.56}\, V_d^{1.88} \qquad (7.5a)$$

For the M.I.B.K.-water system,

$$H = 25.0\, d_{12}^{-0.15}\, V_d^{1.43} \qquad (7.5b)$$

For the isooctane-water system,

$$H = 7.65\, d_{12}^{-1.54}\, V_d^{2.80} \qquad (7.5c)$$

d. For inlet drops having a mean diameter between 0.07 to 0.48 cm, the effect of system physical properties upon flocculation zone height could be correlated by the equation,

$$H = a \left(\frac{d_{12}\, g\, \Delta\rho}{\sigma} \right)^{n} \qquad \text{(Table 7.6)}$$

with a and n being constants specific for each system.

e. Countercurrent flow of the continuous phase had no significant effect upon zone heights. Agreement between the results obtained in the 6 inch and 9 inch columns also indicated that wall effects were not significant compared with the 3 inch column.

f. By assuming the overall motion of the flocculated drops to resemble a diverging conduit, the cross sectional area of which can be described in terms of the emprical hold-up equations a model has been proposed leading to the following equation for residence time,

$$\theta_r = K \frac{V_d}{H} \qquad (9.12)$$

Good agreement was obtained between this equation and experimentally determined residence times.

An alternative fluidized bed, or sedimentation, model may be applicable to the zone provided a suitable drop shape correction factor is derived, albeit within an operating range never reached in this work.

12. RECOMMENDATIONS FOR FURTHER WORK.

12.1. AS AN EXTENSION TO THIS STUDY

1. Since inlet drop size has a profound effect upon flocculation zone characteristics, it would be worthwhile extending the experimentation to include a range of smaller drop sizes. It should cover drops between 1 mm. and 0.1 mm. in diameter in either the 6 inch or, preferably, the 9 inch column. This will entail modification of the photographic procedures, because of the increased opacity of the dispersions, or the use of alternative drop analysis techniques e.g. light transmission.

2. The effects of a distribution of drop sizes about a selected mean could also be studied by the insertion of special distributor plates in which the orifice diameters vary in the ratios 1 : 2 : 3.

3. In order to verify the theories regarding film drainage in the flocculation zone (81), inverted systems could be used to obtain different values of continuous phase viscosity. The study of lower interfacial tension systems, e.g. $\leqslant 3$ dynes cm^{-1}, would be of practical value.

4. Although countercurrent phase flow made no significant difference to the flocculation zone, the effects of co-current phase flow, which often exists in external vertical gravity

settlers, should be verified.

5. The techniques described by Allak (81) could be used to advantage to study drop shapes within the relatively unrestricted flocculation zones in the 9 inch column. These are of fundamental importance to the film drainage processes.

12.2. OTHER STUDIES.

1. Drop residence time data, and hence velocity profiles, should be obtained both as a means of verifying film drainage theories (81) and because of their practical value e.g. in the evaluation of K in Equation 9.11. This work would be better performed in smaller diameter columns so that a wider range of pure systems could be studied without great expense or tedious repurification. However smaller initial drop sizes should be used to reduce the ratio of drop: column diameter to diminish wall effects and also to enable thick zones to be produced.

2. The effects of varying flocculation zone geometry can be studied in a settler constructed in the form of a truncated cone. This is a common shape in both extraction column end-sections and certain gravity settlers but there is no quantitative basis for design. The effect of varying interfacial area could be conveniently studied in this one settler merely by altering the level of the interface.

APPENDICES

1. Physical properties of liquid-liquid systems
2. Rotameter calibration
3. Flocculation zone heights- Tables 1-6
4. Distributor design- Table 7
5. Typical inlet drop size distributions - Tables 8-11
6. Dispersed phase hold-up- Tables 12-18
7. Residence time in the flocculation zone- Tables 19-21
8. Distribution coefficient calculations
9. Variation of drop size in the zone
10. LaPlace drop diameter calculations

APPENDIX 1

PHYSICAL PROPERTIES OF LIQUID-LIQUID SYSTEMS

The following physical properties have been taken from International Critical Tables, except interfacial tensions which have been measured by Wilhelmy's method.

Interfacial tension - Dynes/cm

System		Temperature
Toluene - water	35.9	23°C
M.I.B.K. - water	9.8	22°C
Isooctane - water	51.1	23°C
Diethyl carbonate - water	13.1	22°C

Viscosity - centipoise

Toluene	0.58	20.6°C
M.I.B.K.	0.62	21.3°C
Isooctane	0.51	25°C
Diethylcarbonate	0.82	25°C

Density - gm/cc.

Liquid		
Toluene	0.864	20°C
M.I.B.K.	0.80	20°C
Isooctane	0.693	20°C
Diethylcarbonate	0.976	20°C

APPENDIX 1 (Continued)

Materials were purchased to the grades and specifications given below:-

Toluene

Technical grade

Boiling Point Range	109 - 112°C more than 95%
Wt. per ml.	0.860 - 0.866 at 20°C.

Methyl-isobutyl ketone

Minimum Assay ketone	97%
Boiling Range	95% distils between 114°-117°C.
Refractive index	1.3945-1.3963
Free acid	1 ml. $\frac{N}{1}$ %
Non-volatile matter	0.01% max.

Isooctane

Boiling Range 95%	98-99.5°C.
Refractive index 20°C	1.390-1.392

Diethyl carbonate

Minimum Assay	98%
Boiling Range 95% min.	123-127°C
Chloride (Cl) max	0.01%

Decon 75 Concentrate, used for cleaning, was obtained from Medical Pharmaceutical Developments Limited.

APPENDIX 1 (Continued)

Laboratory distilled toluene was collected from 110-112°C. boiling fraction range.

Purchased technical grade toluene - boiling point fractional analysis

---

Boiling point range °C	% Volume
less than 86	0.54
86 - 99.5	0.40
99.5 - 103.0	0.60
103.0 - 104.0	0.54
104.0 - 106.0	0.47
106.0 - 108.0	1.08
108.0 - 109.0	2.00
109.0 - 110.0	5.40
110.0 - 112.0	88.50
more than 112	0.47
	100.00

APPENDIX 2

ROTAMETER CALIBRATION

Rotameter Mfg. Co.

Rotameter No.18 Reading	Flow Rate, lit./min.			
	Toluene	Isooctane	Diethyl carbonate	M.I.B.K
32	2.20	2.44	2.04	2.26
65		3.66		
66	3.30			3.39
68			3.06	
97	4.40	4.88	4.08	4.52
126	5.50	6.10	5.10	5.65
153	6.60	7.32	6.12	6.78
180	7.70	8.54	7.14	7.91
206	8.80	9.76	8.16	9.04
232	9.90	10.98	9.18	10.17
257	11.0	12.23	10.20	11.30

Rotameter No,14 Reading	
15	0.33
20	0.40
30	0.50
40	0.65
50	0.77
60	0.90
70	1.05
80	1.20
90	1.33
100	1.50
110	1.65
130	2.00
150	2.35
180	2.95
200	3.35

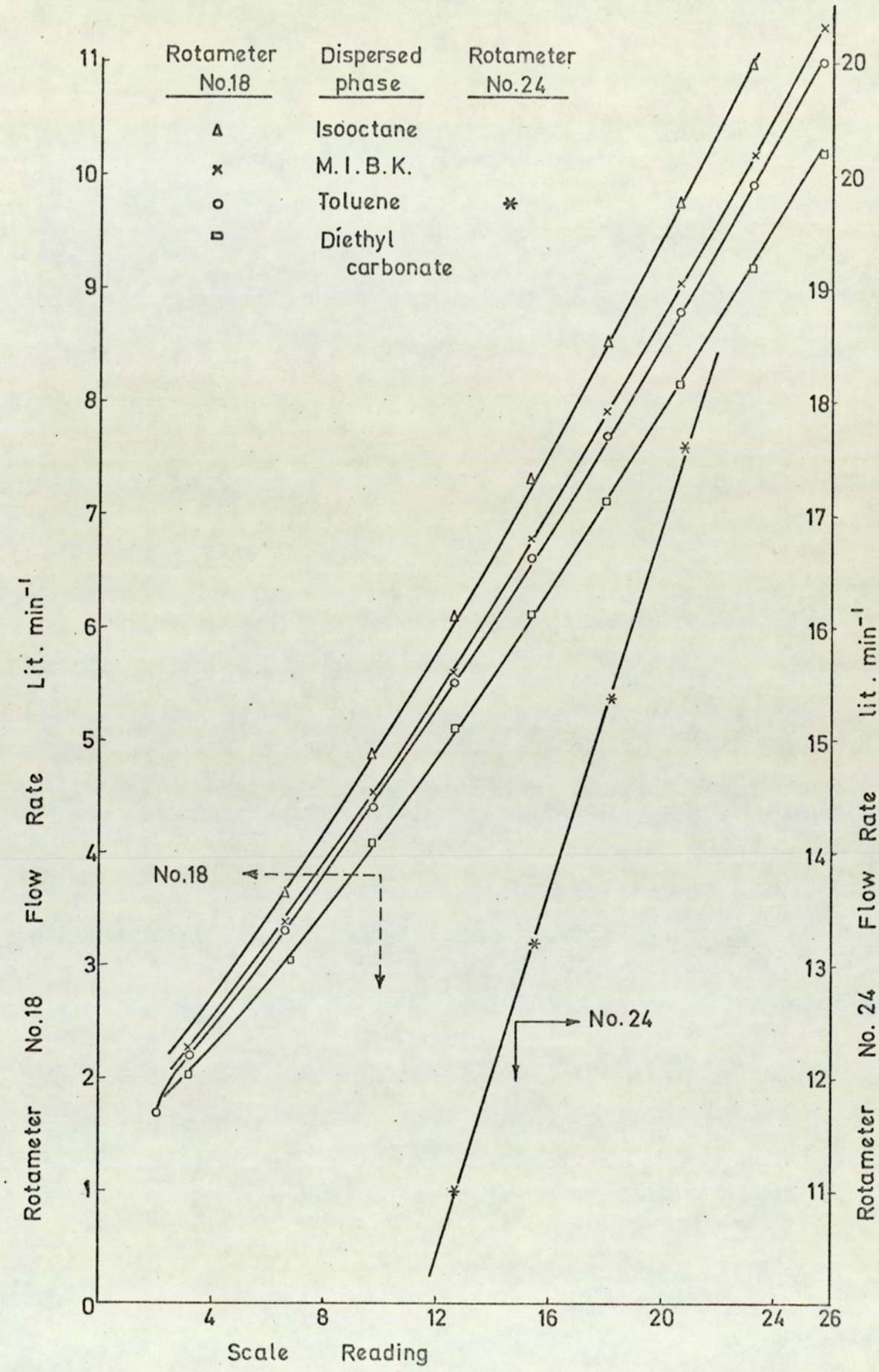

FIG. A.2.1 CALIBRATION CHART OF ROTAMETERS.

APPENDIX 3

FLOCCULATION ZONE HEIGHTS

Table 1. Toluene-water system

9-inch column

d_n = 1.2 mm.

Rot.18	V lit.min.$^{-1}$	V_d Ml.cm^{-2} sec.	H mm.
8.0	3.80	0.168	8
9.2	4.25	0.198	10
9.1	4.22	0.187	11
12.0	5.30	0.235	14
15.8	6.70	0.300	17

d_n = 1.6 mm.

7.0	3.45	0.153	7
8.0	3.80	0.169	8
9.0	4.25	0.188	9
11.9	5.20	0.230	12
15.2	6.50	0.288	14
18.5	7.85	0.348	16
20.6	8.80	0.390	18
23.6	10.10	0.448	21

d_n = 2.0 mm.

10.1	4.60	0.204	7
12.0	5.30	0.234	9
17.0	7.25	0.323	11
20.6	8.80	0.390	12
23.0	9.90	0.438	15
13.0*	11.30	0.500	19
15.4*	13.20	0.584	21
20.0*	16.85	0.745	25

* Rotameter No.24

APPENDIX 3 (Continued)

Table 2. Toluene-water system

6 inch column

d_n = 0.4 mm.

Rot. 18	V lit.min.$^{-1}$	V_d ml.cm.$^{-2}$sec.$^{-1}$	H mm.
17.0*	0.96	0.090	10
23.0*	1.17	0.109	11
27.0*	1.25	0.117	14
2.0	1.65	0.157	15
2.8	2.10	0.196	21
4.0	2.45	0.228	28
6.0	3.10	0.289	42

* Rotameter No.7

d_n = 0.8 mm.

2.0	1.65	0.154	10
2.5	1.95	0.182	10
3.0	2.10	0.196	13
4.3	2.55	0.238	16
6.0	3.10	0.290	19
7.0	3.45	0.322	23
9.0	4.20	0.391	31
12.0	5.30	0.495	44
13.6	5.85	0.545	54

d_n = 1.2 mm.

2.0	1.65	0.154	9
2.4	1.85	0.172	10
2.9	2.05	0.191	10
4.3	2.55	0.238	13
6.2	3.15	0.294	17
8.8	4.10	0.382	20
12.0	5.30	0.494	26
15.2	6.50	0.606	38
16.4	7.00	0.654	39
19.0	8.10	0.755	55

APPENDIX 3 (Continued)

Table 2. (Continued)

d_n = 1.6 mm.

Rot.18	V lit.min.$^{-1}$	V_d ml.cm.$^{-2}$sec.$^{-1}$	H mm.
2.4	1.85	0.172	8
3.0	2.10	0.196	9
4.0	2.45	0.226	10
6.0	3.10	0.289	13
8.0	3.80	0.354	16
10.4	4.70	0.438	21
13.6	5.90	0.550	28
17.4	7.40	0.690	35
19.0	8.10	0.755	42

d_n = 2.0 mm.

3.0	2.10	0.196	8
5.0	2.70	0.252	10
6.5	3.30	0.308	12
8.0	3.80	0.354	13
9.5	4.35	0.403	16
12.0	5.25	0.491	19
14.0	6.05	0.563	22
17.4	7.35	0.686	25
19.2	8.30	0.818	33

APPENDIX 3 (Continued)

Table 3. Toluene-water system

3 inch column

d_n = 0.4 mm

Rot.14	V	V_d	H
	lit.min.$^{-1}$	ml.cm.$^{-2}$sec.$^{-1}$	mm.
1.0	0.20	0.082	12
1.3	0.28	0.110	14
2.0	0.35	0.128	16
3.0	0.50	0.203	22
3.4	0.55	0.224	26
4.0	0.65	0.250	33
4.5	0.75	0.281	36
5.0	0.80	0.305	40
5.5	0.85	0.322	46

d_n = 0.8 mm

2.0	0.35	0.136	11
2.3	0.40	0.156	12
2.5	0.45	0.175	14
3.0	0.50	0.195	16
4.0	0.65	0.253	18
5.1	0.80	0.312	21
6.0	0.90	0.350	26
7.0	1.05	0.408	32
8.1	1.20	0.467	41
10.0	1.50	0.585	48

d_n = 1.2 mm

2.0	0.35	0.136	10
2.5	0.40	0.175	11
3.0	0.50	0.195	12
3.5	0.60	0.230	14
5.0	0.75	0.292	16
5.5	0.85	0.332	19
6.8	1.00	0.390	21
8.5	1.25	0.487	28
10.5	1.55	0.605	36

APPENDIX 3 (Continued)

Table 3. (Continued)

d_n = 1.6 mm

Rot.14	V	V_d	H
	lit.min.$^{-1}$	ml.cm.$^{-2}$sec.$^{-1}$	mm.
2.2	0.42	0.156	9
2.5	0.45	0.175	10
3.0	0.50	0.195	11
3.5	0.60	0.230	14
4.7	0.75	0.293	15
5.5	0.85	0.332	19
7.0	1.05	0.410	22
7.5	1.10	0.430	24
9.0	1.30	0.507	27
10.1	1.55	0.605	34
11.0	1.65	0.645	36
12.5	1.85	0.722	45

d_n = 2.0 mm

2.5	0.45	0.175	9
3.1	0.55	0.215	10
4.0	0.65	0.254	11
5.1	0.80	0.310	13
6.3	0.95	0.371	18
8.1	1.20	0.470	22
9.8	1.45	0.566	27
12.0	1.80	0.704	31

APPENDIX 3 (Continued)

Table 4. Diethyl carbonate-water system

6 inch column

d_n = 0.4 mm

Rot.18	V lit.min.$^{-1}$	V_d ml.cm.$^{-2}$sec^{-1}	H mm.
23.0*	1.30	0.123	35
29.0*	1.50	0.142	50
1.5	1.70	0.161	95
2.5	1.90	0.180	125
3.0	2.00	0.189	140
3.5	2.15	0.203	180
4.0	2.30	0.218	210

* Rotameter No.7

d_n = 1.2 mm

2.0	1.75	0.165	25
4.4	2.40	0.230	40
6.8	3.10	0.290	61
9.0	3.80	0.360	96
10.4	4.30	0.400	112

d_n = 1.6 mm

2.0	1.75	0.165	17
4.0	2.30	0.217	22
6.0	2.85	0.269	36
8.0	3.50	0.330	48
10.0	4.15	0.392	68
12.0	4.85	0.459	80
13.0	5.20	0.490	96

APPENDIX 3 (Continued)

Table 5. Methyl-isobutyl ketone-water system

6 inch column

d_n = 0.4 mm

Rot.18	V lit.min.$^{-1}$	V_d ml.cm.$^{-2}$sec.$^{-1}$	H mm.
2.0	1.90	0.180	37
4.0	2.50	0.236	50
5.4	2.90	0.274	61
7.0	3.50	0.330	85
8.2	4.00	0.368	110
10.2	4.75	0.445	180

d_n = 0.8 mm

2.0	1.90	0.180	23
4.0	2.50	0.236	42
6.0	3.20	0.300	73
8.0	3.90	0.375	103
10.0	4.70	0.440	140
13.0	5.80	0.545	190
13.5	6.10	0.570	230

d_n = 1.6

2.0	1.90	0.180	27
4.0	2.50	0.236	32
6.0	3.20	0.300	40
8.0	3.90	0.375	55
11.0	5.00	0.470	90
14.0	6.30	0.590	130
16.0	7.05	0.660	150
18.6	7.90	0.740	175

APPENDIX 3 (Continued)

Table 5. (Continued)

d_n = 2.0 mm

Rot.18	V	V_d	H
	lit. in.$^{-1}$	ml.cm.$^{-2}$ sec.$^{-1}$	mm.
4.0	2.50	0.236	35
6.0	3.20	0.302	60
8.1	3.95	0.373	80
10.0	4.70	0.444	105
12.0	5.40	0.510	145
14.0	6.20	0.585	170
16.0	7.10	0.670	190

APPENDIX 3 (Continued)

Table 6. Isooctane-water system

6 inch column

Rot.18	V lit.min.$^{-1}$	V_d ml.cm.$^{-2}$sec.$^{-1}$	H mm.
d_n = 0.4 mm			
1.5	2.0	0.189	31
2.0	2.2	0.208	38
2.5	2.3	0.218	47
3.0	2.4	0.227	63
4.0	2.8	0.264	85
4.5	2.9	0.274	105
5.0	3.1	0.293	120
5.5	3.2	0.302	160
6.0	3.4	0.321	170
6.0	3.4	0.321	210
d_n = 1.2 mm			
6.0	3.50	0.330	25
8.0	4.20	0.397	37
10.4	5.10	0.467	55
12.0	5.80	0.544	75
13.0	6.20	0.580	85
14.0	6.70	0.628	105
15.0	7.05	0.660	210
d_n = 2.0 mm			
8.0	4.20	0.397	20
10.0	5.00	0.472	25
12.0	5.80	0.548	33
13.0	6.20	0.585	45
15.0	7.00	0.670	55
15.1	7.10	0.680	65
16.0	7.60	0.726	75
18.0	8.50	0.802	90

APPENDIX 4

DISTRIBUTOR DESIGN

The sizes of holes in the distributor plates were estimated initially from the Hayworth's correlated equation (88),

$$V_p + 9.68\,(10^{-10})\,\frac{V_d^{\frac{2}{3}}\,\rho\,d\,V_n^2}{\Delta\rho} = \frac{4.92\,(10^{-9})\,\sigma\,d_n}{\Delta\rho} + \frac{4.95\,(10^{-4})\,d^{1.12}\,V_n^{0.547}\,\mu_c^{0.279}}{\Delta\rho^{1.5}}$$

A number of 1/16th inch thick removeable brass plates with up to 120 holes were fabricated and tested. Finally plates for the 6 and 9 columns in this work comprised 450 holes on 3/16th inch triangular pitch; five distributor plates having 0.4, 0.8, 1.2, 1.6 and 2.0 mm diameter holes were used.

The hole positions were marked first, then pressed and subsequently drilled to produce orifices.

Predicted drop diameters against flow rates through 450 orifices for various systems are given in Table 7.

APPENDIX 4 (Continued)

Table 7. Predicted drop diameters

Flow rate lit. min^{-1}	Predicted Drop Diameter, mm.							
	1	1.5	2	2.5	3	4	6	8
Toluene;								
at d_n = 0.4	1.7	1.3	1.1	0.9	0.6	-	-	-
d_n = 0.8	4.6	4.3	3.9	3.4	3.0	2.8	1.9	-
d_n = 1.2	5.5	5.4	5.3	5.2	5.0	4.7	4.0	3.4
d_n = 1.6	6.1	6.1	6.1	6.1	6.0	5.9	5.7	5.5
d_n = 2.0	6.4	6.4	6.4	6.4	6.3	6.3	6.3	6.2
Iso octane;								
at d_n = 0.4	2.0	1.5	1.2	1.0	0.8	-	-	-
d_n = 1.2	4.4	4.5	4.4	4.3	4.3	4.2	3.8	3.1
d_n = 2.0	5.7	5.8	5.8	5.8	5.8	5.8	5.7	5.7
M.I.B.K;								
at d_n = 0.4	1.7	1.2	1.0	0.7	0.6	-	-	-
d_n = 1.2	4.2	4.2	4.2	4.1	4.1	4.0	3.4	3.0
d_n = 1.6	4.3	4.4	4.5	4.6	4.7	4.8	4.6	4.3
d_n = 2.0	4.4	4.6	4.8	4.9	5.0	5.0	5.0	4.9
Diethyl Carbonate								
at d_n = 0.4	2.3	1.7						
d_n = 1.2	-	-	-	-	-	-	5.5	4.6
d_n = 1.6	-	-	-	-	-	-	-	8.0

APPENDIX 5

TYPICAL INLET DROP SIZE DISTRIBUTIONS

Table 8. M.I.B.K-water system

6 inch column

d_n = 0.4 mm.
V_d = 0.47

d_e	n	nd	nd^2	nd^3
0.59	6	3.54	2.07	1.23
0.65	8	5.20	3.36	2.19
0.71	20	14.20	10.00	7.20
0.77	12	9.24	7.19	5.50
0.83	6	4.98	4.14	3.42
0.88	14	12.32	10.90	9.50
0.94	6	5.64	5.28	5.04
1.00	2	2.00	2.00	2.00
1.06	2	2.12	2.24	2.38
	76	59.24	47.18	38.46

$d_{12} = \frac{59.24}{76} = 0.78$ mm; $d_{32} = \frac{38.46}{47.18} = 0.81$ mm

d_n = 0.4 mm.
V_d = 0.2

1.18	4	4.72	5.60	6.60
1.23	2	2.46	3.02	3.90
1.30	18	23.40	30.02	3.96
1.35	2	2.70	2.64	4.92
1.41	8	11.28	15.84	25.20
1.47	8	11.76	20.00	25.60
1.53	2	3.06	4.68	7.20
1.59	6	11.54	15.12	24.06
1.65	4	6.60	10.84	18.00
1.71	8	13.68	22.48	40.00
1.77	2	3.54	6.28	11.20
1.82	2	3.64	6.60	12.02
1.88	4	7.52	7.04	25.28
	70	105.90	151.16	207.74

$d_{12} = \frac{151.16}{105.9} = 1.42$mm; $d_{23} = \frac{207.74}{151.16} = 1.38$ mm

APPENDIX 5 (Continued)

Table 8 (Continued)

$d_n = 1.2$
$V_d = 0.58$

d_e	n	nd	nd^2	nd^3
2.4	6	14.4	34.0	83.0
2.5	4	10.0	25.0	62.5
2.6	6	15.6	40.6	105.3
2.7	1	2.7	7.3	19.7
2.8	4	11.2	47.0	132.0
2.9	6	17.4	33.7	97.8
3.0	2	6.0	18.0	54.0
3.1	1	3.1	9.6	29.8
3.2	2	6.4	20.5	65.6
3.3	4	13.2	43.6	140.4
3.4	4	13.6	47.2	157.2
3.5	2	7.0	24.5	45.8
	42	120.6	351.0	993.1

$d_{12} = \frac{120.6}{42} = 2.87$ mm; $d_{23} = \frac{993.1}{351.0} = 2.83$ mm.

$d_n = 1.6$
$V_d = 0.45$

2.8	2	5.6	15.6	44.0
3.0	3	9.0	27.0	81.0
3.2	15	48.0	153.6	491.0
3.3	2	6.6	21.8	71.8
3.4	3	10.2	34.8	118.0
3.6	6	21.6	71.8	280.2
3.7	3	10.1	41.1	151.8
	34	111.1	365.7	1237.8

$d_{12} = \frac{111.1}{34} = 3.27$ mm; $d_{23} = \frac{1237.8}{365.7} = 3.38$ mm.

APPENDIX 5 (Continued)

Table 8. (Continued)

$d_n = 2.0$ $V_d = 0.25$

d_e	n	nd_e
4.4	2	8.8
4.5	6	27.0
4.9	12	58.8
5.2	14	72.8
5.6	3	16.8
5.8	5	29.0
5.9	1	5.9
	43	219.1

$$d_{12} = \frac{219.1}{43} = 5.06 \text{ mm}$$

APPENDIX 5 (Continued)

Table 9. Diethyl carbonate-water system

6 inch column

$d_n = 0.4$
$V_d = 0.17$

d_e	n	nd	nd^2	nd^3
1.1	7	7.7	8.47	9.31
1.2	5	6.0	7.20	8.65
1.3	6	7.8	10.14	13.20
1.4	7	9.8	12.72	19.18
1.5	7	10.5	18.75	23.66
1.6	4	6.4	10.24	16.40
1.7	3	5.1	8.67	14.73
1.8	3	5.4	9.72	17.49
1.9	2	3.8	6.22	13.72
	44	62.1	92.13	136.34

$d_{12} = \frac{62.1}{44} = 1.41$ mm; $d_{23} = \frac{136.34}{92.13} = 1.48$ mm.

$d_n = 0.4$
$V_d = 0.13$

1.2	1	1.3	1.69	2.20
1.4	1	1.4	1.96	2.74
1.5	4	6.0	9.00	15.52
1.6	8	12.8	20.48	32.80
1.7	4	6.8	11.56	19.64
1.8	5	9.0	16.20	29.15
1.9	6	11.4	21.66	41.16
2.0	4	8.0	16.00	32.00
2.1	3	6.3	13.23	27.78
	36	63.0	111.78	222.99

$d_{12} = \frac{63.0}{36} = 1.75$ mm; $d_{23} = \frac{222.99}{111.78} = 2.0$ mm.

APPENDIX 5 (Continued)

Table 9 (Continued)

d_n = 1.6 mm
V_d = 0.48

d_e	n	nd_e
4.5	6	27.0
4.6	5	23.0
4.8	3	14.4
5.0	14	70.0
5.1	2	10.2
	30	144.6

$d_{12} = \frac{114.6}{30} = 4.82$ mm;

d_n = 1.2
V_d = 0.37

d_e	n	nd_e
2.9	3	8.7
3.2	3	9.6
3.3	6	19.8
3.4	5	17.0
3.5	6	21.0
3.7	2	7.4
3.9	2	7.8
4.2	6	25.2
4.3	3	12.9
	36	129.4

$d_{12} = \frac{129.4}{36} = 3.6$ mm.

APPENDIX 5 (Continued)

Table 10. Iso octane-water system

6 inch column

d_n = 1.2 mm

V_d = 0.72

d_e	n	nd_e
2.4	8	19.2
2.5	15	37.5
2.7	14	37.8
2.8	7	19.6
3.0	5	15.0
3.1	7	21.7
3.3	7	23.1
3.7	1	3.7
	64	177.6

$d_{12} = \frac{177.6}{64} = 2.76$ mm;

V_d =

d_e	n	nd_e
2.0	1	2.0
2.2	2	4.4
2.3	1	2.3
2.4	5	12.0
2.6	10	26.0
2.7	6	16.2
2.9	31	89.9
3.0	8	24.0
3.2	1	3.2
3.4	1	3.4
	66	183.4

$d_{12} = \frac{183.4}{66} = 2.78$ mm.

d_n = 2.0 mm

V_d = 0.34

4.2	12	50.4
4.4	3	13.2
4.6	4	18.4
4.7	8	37.6
4.8	4	19.2
5.0	5	25.0
5.2	16	83.2
5.3	8	42.4
	60	289.4

$d_{12} = \frac{289.4}{60} = 4.82$ mm;

V_d = 0.9

2.4	3	7.2
2.7	3	8.1
2.9	7	20.3
3.0	8	24.0
3.2	16	51.2
3.3	11	36.3
3.4	16	54.4
3.6	4	14.4
3.7	2	7.4
3.9	1	3.9
	71	227.2

$d_{12} = \frac{227.2}{71} = 3.2$ mm

APPENDIX 5 (Continued)

Table 10 (Continued)

d_n = 0.4 mm
V_d = 0.35

d_e	n	nd_e	nd_e^2	nd_e^3
0.6	2	1.2	0.72	0.44
0.7	9	5.6	4.41	3.08
0.8	11	8.8	7.04	6.63
0.9	12	10.8	9.72	8.75
1.0	9	9.0	9.00	9.00
1.1	1	1.1	1.21	1.33
1.2	2	2.4	1.44	3.46
	44	39.3	33.54	32.69

$d_{12} = \frac{39.3}{44} = 0.89$ mm; $d_{23} = \frac{32.69}{33.54} = 0.98$ mm.

APPENDIX 5 (Continued)

Table 11. Toluene-water system

6 inch column

d_n = 0.4 mm.
V_d = 0.26

d_e	n	nd_e
0.65	6	3.30
0.83	29	19.10
1.00	24	24.00
1.16	15	17.40
1.32	2	2.64
1.50	4	6.00
	80	72.44

$d_{12} = \frac{72.44}{80} = 0.91$ mm;

V_d = 0.3

d_e	n	nd_e
0.60	3	1.80
0.67	12	8.05
0.74	17	12.60
0.81	13	11.50
0.89	19	16.90
0.96	4	3.84
1.04	9	9.36
1.20	4	4.80
	81	68.85

$d_{12} = \frac{68.85}{81} = 0.85$ mm.

---

d_n = 1.2 mm
V_d = 0.65

2.4	3	7.2
2.6	2	5.2
2.7	6	16.2
2.8	12	33.6
2.9	5	14.5
3.0	9	27.0
3.1	17	52.7
3.2	7	22.4
3.3	6	19.8
3.4	2	6.8
	69	205.2

$d_{12} = \frac{205.2}{69} = 2.97$ mm;

d_n = 1.6 mm
V_d = 0.62

2.7	1	2.7
2.9	2	5.8
3.0	3	9.0
3.2	2	6.4
3.3	4	13.2
3.5	13	45.5
3.6	8	28.8
3.7	11	40.7
3.8	5	19.0
4.0	3	12.0
	52	183.1

$d_{12} = \frac{183.1}{52} = 3.52$

APPENDIX 5 (Continued)

Table 11 (Continued)

d_n = 1.2
V_d = 0.72

d_e	n	nd	nd^2	nd^3
2.1	2	4.2	8.8	18.6
2.6	7	18.2	47.4	123.0
2.8	7	19.6	54.8	154.0
2.9	8	23.2	67.3	195.0
3.0	14	42.0	126.0	278.0
3.3	8	26.4	87.1	288.0
3.6	3	10.8	39.0	140.1
	49	144.4	430.4	1196.7

$d_{12} = \frac{144.4}{49} = 2.95$ mm; $d_{23} = \frac{1196.7}{430.4} = 2.78$ mm.

d_n = 1.2 mm
V_d = 0.72

2.4	4	9.6	23.2	55.2
2.5	2	5.0	12.5	31.2
2.6	2	5.2	13.5	35.6
2.8	6	16.8	46.8	132.0
2.9	6	17.4	49.2	150.8
3.0	2	6.0	18.0	54.0
3.1	4	12.4	38.4	119.2
3.2	4	12.8	41.0	131.2
3.3	6	19.8	65.4	240.0
3.4	4	13.6	46.4	157.2
3.6	2	7.2	26.0	93.4
	42	125.8	380.4	1199.8

$d_{12} = \frac{125.8}{42} = 3.0$ mm; $d_{23} = \frac{1199.8}{380.4} = 3.15$ mm.

APPENDIX 5 (Continued)

Table 11. (Continued

d_n = 0.8 mm
V_d = 0.42

d	n	nd	nd^2	nd^3
1.2	1	1.2	1.44	1.73
1.4	3	4.2	5.88	8.22
1.5	6	9.0	13.50	20.28
1.6	3	4.8	7.68	12.30
1.8	3	5.4	9.72	17.49
1.9	3	5.7	10.83	20.58
2.0	8	16.0	32.00	64.00
2.1	5	10.5	22.05	46.30
2.2	1	2.2	4.84	10.65
2.3	2	4.6	10.58	24.34
2.4	1	2.4	5.76	13.82
2.5	2	5.0	12.50	31.20
	38	71.0	135.78	270.92

$d_{12} = \frac{71.0}{38} = 1.87$ mm; $d_{23} = \frac{270.92}{135.78} = 2.06$ mm.

d_n = 0.4
V_d = 0.17

1.0	1	1.0	1.00	1.00
1.1	2	2.2	2.42	2.66
1.2	6	7.2	8.64	10.38
1.3	17	22.1	28.70	37.40
1.4	21	29.4	41.10	57.50
1.5	4	6.0	9.00	13.52
1.6	3	4.8	7.68	12.30
1.7	2	3.4	5.78	9.82
1.8	3	5.4	9.72	17.49
	59	81.5	114.04	162.07

$d_{12} = \frac{81.5}{59} = 1.38$ mm; $d_{23} = \frac{162.07}{114.04} = 1.42$ mm.

APPENDIX 5 (Continued)

Table 11 (Continued)

$d_n = 1.6$

$V_d = 0.42$

d_e	n	nd_e
2.6	7	18.2
3.0	3	9.0
3.3	12	39.6
3.7	13	48.1
4.1	14	57.4
4.4	16	70.4
4.8	3	14.4
5.2	3	15.6
5.5	4	22.0
	75	294.7

$$d_{12} = \frac{294.7}{75} = 3.94 \text{ mm.}$$

APPENDIX 6

DISPERSED PHASE HOLD-UP IN FLOCCULATION ZONE

Table 12. Change of hold-up at a particular point with syringing time using 9 mm. bore glass tube

System: Toluene-water, at $h/_H$ = 0.5; H = 28 mm; d_n = 1.6 mm.

Duration of syringing time seconds	Dispersed phase Hold - up %	Arithmetic mean	Deviation of mean from min.	max.	overall
5	68, 69, 72, 75, 77	72	-4	+5	-8
7	70, 71, 75, 77, 77	75	-4	+3	-5
8	77, 78, 80, 80, 82	80	-3	+2	0
9	77, 80, 81, 82, 82	80	-3	+2	0
10	80, 80, 81, 82, 83	81	-2	+2	+1
12	79, 81, 81, 83, 84	81	-3	+3	+1
14	80, 83, 85, 85, 87	84	-4	+3	+4
16	81, 84, 84, 87, 87	84	-3	+3	+4
18	80, 82, 86, 86, 88	84	-4	+4	+4
20	81, 84, 84, 88, 89	85	-4	+4	+5
25	80, 85, 87, 87, 89	85	-5	+4	+5
30	84, 86, 86, 88, 88	86	-2	+2	+6
		977			

Overall mean of average of each group $= \frac{977}{12} = 80\%$

Overall mean of the average of the groups between 8 to 20 seconds of syringe $= \frac{499}{6} = 83\%$

Deviation from overall mean for 8 to 20 seconds in hold-ups ∓ 3

APPENDIX 6 (Continued)

DISPERSED PHASE HOLD-UP IN FLOCCULATION ZONE

Table 13. Vertical hold-up profile of flocculation zone of M.I.B.K. - water system

6 inch column

d_n = 1.2 mm. V_d = 0.64 ml. cm^{-2}. sec^{-1}

H mm	h mm	x = h/H	ø
230	8	0.04	0.77
230	15	0.065	0.83
230	25	0.11	0.84
196	57	0.29	0.84
196	57	0.29	0.88
210	57	0.27	0.88
220	57	0.26	0.86
230	57	0.25	0.89
240	57	0.24	0.88
170	77	0.46	0.89
170	77	0.46	0.86
195	77	0.40	0.89
172	79	0.46	0.88
230	75	0.33	0.89
258	88	0.34	0.90
258	88	0.35	0.89
230	95	0.41	0.91
258	113	0.44	0.94
230	130	0.57	0.91
250	160	0.64	0.94
250	185	0.74	0.96
255	230	0.98	0.96
Below the bed			0.22

APPENDIX 6 (Continued)

Table 14. Vertical hold-up profile of flocculation zone of Diethyl carbonate - water system 6 inch column

d_n = 1.2 mm. V_d = 0.590 ml. cm^{-2}. sec^{-1}

H mm	h mm	$x = h/H$	ϕ
195	10	0.051	0.562
195	10	0.051	0.413
195	30	0.154	0.725
195	30	0.154	0.698
195	60	0.308	0.73
193	98	0.507	0.74
168	135	0.81	0.82
168	153	0.87	0.87
176	153	0.91	0.91
188	178	0.95	0.80
188	178	0.95	0.82
195	188	0.96	0.91
195	188	0.96	0.82
Below the bed			0.19

APPENDIX 6 (Continued)

Table 15. Vertical hold-up profile of flocculation zone of isooctane - water system

6 inch column

d_n = 1.2 mm. ; V_d = 0.78 ml. cm^{-2}. sec^{-1}

H mm	h mm	$x = h/H$	ϕ
260	10	0.038	0.71
260	12	0.038	0.832
280	23	0.082	0.908
280	23	0.082	0.875
270	23	0.085	0.883
290	33	0.114	0.915
290	33	0.114	0.915
280	44	0.179	0.927
280	44	0.179	0.931
287	66	0.230	0.923
287	66	0.230	0.921
305	100	0.328	0.908
305	100	0.328	0.932
305	128	0.420	0.930
305	128	0.420	0.933
300	159	0.530	0.948
300	159	0.530	0.950
295	188	0.634	0.945
295	188	0.634	0.939
295	218	0.740	0.960
295	218	0.740	0.958
Below the bed			0.21

APPENDIX 6 (Continued)

Table 16. Vertical hold-up profile of flocculation zone of Toluene - water system

6 inch column

d_n = 1.6 mm ; H = 20 mm.
V_d = 0.394 ml. cm^{-2}. sec^{-1}.

h mm	$x = h/H$	ϕ
18	0.90	0.89
15	0.75	0.85
13	0.65	0.79
10	0.50	0.77
7	0.35	0.72
5	0.25	0.64
3	0.15	0.42
Below bed		0.11

d_n = 1.2 mm. ; H = 25 mm
V_d = 0.450 ml. cm^{-2}. sec^{-1}.

h mm	$x = h/H$	ϕ
22	0.88	0.89
19	0.76	0.86
16	0.64	0.80
12	0.48	0.76
10	0.40	0.69
8	0.23	0.64
5	0.20	0.57
3	0.12	0.41
Below the bed		0.14

d_n = 1.6 mm. ; H = 30 mm.
V_d = 0.680 ml. cm^{-2}. sec^{-1}.

32	0.92	0.91
30	0.86	0.88
28	0.80	0.87
23	0.77	0.79
17	0.49	0.72
12	0.34	0.69
6	0.17	0.60
Below bed		0.14

d_n = 1.2 mm. ; H = 30 mm.
V_d = 0.590 ml. sm^{-2}. sec^{-1}

28	0.93	0.91
24	0.80	0.88
20	0.67	0.83
15	0.50	0.79
9	0.30	0.73
7	0.23	0.62
5	0.17	0.65
Below the bed		0.16

APPENDIX 6 (Continued)

Table 16. (Continued)

d_n = 1.6 mm. ; H = 49 mm
V_d = 0.820 ml.cm^{-2}.sec^{-1}.

h mm	$x = h/H$	ϕ
44	0.90	0.92
42	0.86	0.88
39	0.80	0.86
34	0.69	0.85
30	0.61	0.78
26	0.53	0.75
18	0.37	0.72
14	0.29	0.69
10	0.20	0.60
5	0.10	0.42
Below bed		0.20

d_n = 1.2 mm. ; H = 40 mm.
V_d = 0.720 ml.cm^{-2}. sec^{-1}.

h mm	$x = h/H$	ϕ
37	0.92	0.92
33	0.83	0.89
30	0.75	0.87
25	0.63	0.84
22	0.55	0.79
15	0.37	0.73
10	0.25	0.65
5	0.12	0.46
Below the bed		0.19

d_n = 0.4 mm. ; H = 32mm
V_d = 0.25 ml.cm^{-2}.sec^{-1}

28	0.87	0.91
24	0.75	0.89
20	0.63	0.84
18	0.56	0.82
12	0.38	0.75
9	0.28	0.70
7	0.22	0.66
4	0.12	0.48
Below the bed		0.15

d_n = 0.8 mm. ; H = 28 mm.
V_d = 0.42 ml.cm^{-2}.sec^{-1}.

23	0.83	0.90
18	0.65	0.85
15	0.55	0.82
11	0.40	0.78
7	0.25	0.70
4	0.15	0.55
Below the bed		0.14

d_n = 0.4 mm. ; H = 25mm
V_d = 0.22 ml.cm^{-2}.sec^{-1}.

21	0.84	0.90
17	0.68	0.87
12	0.48	0.82
7	0.28	0.74
5	0.20	0.64
Below the bed		0.14

d_n = 0.4 mm. ; H = 15 mm.
V_d = 0.18 ml.cm^{-2}.sec^{-1}.

12	0.80	0.86
9	0.60	0.81
6	0.40	0.74
3	0.20	0.63

APPENDIX 6 (Continued)

Table 17. Vertical hold-up profile of flocculation zone of toluene - water system

3 inch column

d_n = 0.4 mm. ; H = 21 mm. V_d = 0.140 ml.cm^{-2}. sec^{-1}.			d_n = 0.8 mm. ; H = 24 mm V_d = 0.20 ml.cm^{-2}.sec^{-1}.		
h mm	h/H	ϕ	h mm	h/H	ϕ
17	0.81	0.89	21	0.88	0.88
15	0.71	0.86	19	0.79	0.86
13	0.62	0.80	14	0.59	0.78
11	0.52	0.71	10	0.42	0.74
8	0.38	0.64	6	0.25	0.67
5	0.24	0.48	3	0.13	0.47
Below the bed		0.11	Below the bed		0.13
d_n = 0.4 mm. ; H = 33 mm. V_d = 0.28 ml.cm^{-2}. sec^{-1}.			d_n = 0.8 mm. ; H = 33 mm. V_d = 0.41 ml.cm^{-2}. Sec^{-1}.		
29	0.88	0.91	29	0.88	0.89
26	0.79	0.89	24	0.73	0.84
23	0.70	0.85	20	0.61	0.80
20	0.61	0.80	15	0.45	0.73
15	0.45	0.76	11	0.33	0.71
11	0.33	0.68	7	0.21	0.64
7	0.21	0.60	3	0.09	0.41
3	0.09	0.36			
Below the bed		0.17	Below the bed		0.19
d_n = 0.4 mm. ; H = 39 mm V_d = 0.30 ml.cm^{-2}. sec^{-1}.			d_n = 0.8 mm. ; H = 51 mm. V_d = 0.62 ml.cm^{-2}. sec^{-1}.		
34	0.87	0.92	47	0.92	0.91
30	0.77	0.88	45	0.88	0.89
26	0.67	0.84	41	0.80	0.86
21	0.54	0.81	37	0.73	0.85
17	0.44	0.71	33	0.65	0.82
12	0.33	0.72	26	0.51	0.77
8	0.32	0.64	21	0.41	0.75
4	0.30	0.51	16	0.31	0.71
Below the bed		0.21	13	0.26	0.68
			9	0.18	0.61
			6	0.09	0.35
			Below the bed		0.19

APPENDIX 6 (Continued)

Table 17. (Continued)

d_n = 1.6 mm. ; H = 21 mm.
V_d = 0.39 ml.cm^{-2}. sec^{-1}.

h mm	x = h/H	ø
19	0.90	0.89
17	0.81	0.83
13	0.62	0.78
11	0.52	0.73
8	0.38	0.66
5	0.24	0.59
Below the bed		0.14

d_n = 1.2 mm. ; H = 25 mm.
V_d = 0.41 ml.cm^{-2}. sec^{-1}.

h mm	x = h/H	ø
21	0.84	0.89
18	0.72	0.84
13	0.52	0.77
9	0.36	0.71
6	0.24	0.62
3	0.12	0.51
Below the bed		0.15

d_n = 1.6 mm. ; H = 33 mm.
V_d = 0.610 ml.cm^{-2}. sec^{-1}.

30	0.91	0.90
26	0.79	0.86
22	0.67	0.80
19	0.57	0.77
15	0.45	0.73
10	0.30	0.61
7	0.21	0.55
Below the bed		0.17

d_n = 1.2 mm. ; H = 34 mm.
V_d = 0.60 ml.cm^{-2}. sec^{-1}.

29	0.85	0.91
25	0.74	0.86
21	0.62	0.79
16	0.47	0.74
11	0.32	0.71
8	0.24	0.51
4	0.12	0.30
Below the bed		0.17

d_n = 1.6 mm. ; H = 45 mm.
V_d = 0.79 ml.cm^{-2}. sec^{-1}.

40	0.89	0.90
37	0.82	0.86
32	0.71	0.84
29	0.65	0.80
25	0.56	0.78
21	0.47	0.74
17	0.38	0.66
12	0.27	0.64
9	0.20	0.56
6	0.14	0.50
Below the bed		0.21

APPENDIX 6 (Continued)

Table 18. Vertical hold-up profile of flocculation zone of toluene - water system

9 inch column

d_n = 1.6 mm. ; H = 20 mm.
V_d = 0.61 ml. cm^{-2}. sec^{-1}.

h	h/H	ø
18	0.90	0.94
15	0.75	0.88
12	0.60	0.83
9	0.45	0.76
7	0.35	0.66
6	0.30	0.54
3	0.15	0.38
Below the bed		0.14

d_n = 1.6 mm. ; H = 16 mm.
V_d = 0.43 ml.cm^{-2}. sec^{-1}.

12	0.75	0.87
9	0.56	0.72
6	0.37	0.55
3	0.19	0.29
Below the bed		0.12

d_n = 1.2 mm. ; H = 22 mm.
V_d = 0.64 ml.cm^{-2}. sec^{-1}.

19	0.88	0.84
14	0.64	0.80
12	0.55	0.66
10	0.46	0.64
8	0.36	0.56
4	0.18	0.32
Below the bed		0.18

APPENDIX 7

RESIDENCE TIME IN THE FLOCCULATION ZONE

Table 19. SUMMARY OF RESIDENCE TIMES

System : Toluene - water

Column : 6 inch

d_{12} cm	V_d ml. $cm^{-2}.sec^{-1}$	H cm	θ_{mr} sec.
0.09	0.230	2.2	4.5
0.09	0.275	3.5	9.8
0.18	0.335	1.9	3.2
0.18	0.440	3.5	6.7
0.18	0.520	4.7	6.5
0.30	0.370	2.0	3.7
0.30	0.374	2.0	5.8
0.30	0.470	2.6	4.9
0.30	0.530	2.8	3.9
0.30	0.705	4.5	5.6
0.30	0.860	6.0	10.1
0.36	0.420	1.9	2.9
0.36	0.590	3.0	3.3
0.36	0.820	4.2	4.4
0.48	0.550	2.2	2.6

System : Isooctane - water

Column : 6 inch

0.28	0.550	18	30.8
0.28	0.490	12	23.0

System : Diethyl carbonate - water

Column : 6 inch

0.35	0.710	22	27.9
0.35	0.420	8	13

APPENDIX 7 (Continued)

Table 20. SINGLE DROP REST-TIME AT A PLANE INTERFACE FORMED IN THE 6" COLUMN

System : TOLUENE-WATER Temp. 18 ± 1.5°C., First step

t sec.	Number of drops coalesced at orifice dia. 1/64"	1/32"	3/64"	1/16"	5/64"
0.4-0.6	2	1	-	1	-
0.6-0.8	12	2	1	2	1
0.8-1.0	26	4	4	2	4
1.0-1.2	15	19	6	8	-
1.2-1.4	9	14	9	2	5
1.4-1.6	7	5	21	8	5
1.6-1.8	12	5	22	6	14
1.8-2.0	3	8	11	18	19
2.0-2.2	3	4	8	23	17
2.2-2.4	-	2	2	8	1
2.4-2.6	1	3	2	2	13
2.6-2.8	1	5	2	4	1
2.8-3.0	-	1	1	2	4
3.0-3.2	1	3	4	1	2
3.2-3.4	-	3	5	1	1
3.4-3.6	-	7	-	2	1
3.6-3.8	-	1	1	3	-
3.8-4.0	-	3	3	1	1
More than 4.0	8	10	2	6	11
n	100	100	100	100	100
$t_m = \frac{nt}{n} =$	1.2	1.7	2.0	2.1	2.1 sec.
$t_{\frac{1}{2}} =$	1.1	1.7	1.9	2.1	2.1 sec
	7.1	9.2	10.2	11.4	13.0 cm. sec

Table21. RESIDENCE TIME DISTRIBUTION IN THE ZONE - Toluene-water system, 6 inch column

Inside brackets, (*), show number of drop-drop coalescence.

d_n = 0.4 mm	d_m = 1.6 mm
V_d = 0.110 ml.cm^{-2}.sec^{-1}.	V_d = 0.59 ml.cm^{-2}.sec^{-1}.
H = monolayer	H = 3 cm

θ	n	nθ	θ	n	nθ
0.7	1	0.7	1.4	2	2.8
1.0	4	4.0	1.6	1	1.6
1.1	1	1.1	1.8	1	1.8
1.2	11 (3)	13.2	2.0	4	8.0
1.3	9	11.7	2.1	2	6.3
1.4	14 (4)	19.6	2.2	6	13.2
1.5	8	12.0	2.3	6	13.8
1.6	5 (1)	8.0	2.4	1	2.4
1.7	5 (1)	8.5	2.5	1	2.5
1.8	9 (2)	16.2	2.6	3	7.8
1.9	10 (1)	19.0	2.7	6	16.2
2.1	1	2.1	2.9	1	2.9
2.2	2	4.4	3.0	7	21.0
2.4	4 (2)	9.6	3.1	4	12.4
2.6	3 (1)	7.8	3.2	7	22.4
2.9	1	2.9	3.3	2	6.6
3.1	3	9.3	3.4	6	20.4
3.4	1	3.4	3.5	2	7.0
3.5	1	3.5	3.9	1	3.9
3.6	2	7.2	4.6	1	4.6
3.7	2	7.4	4.8	1	4.8
4.0	7 (2)	28.0	5.3	3	15.9
4.3	1	4.3	5.6	1	5.6
5.1	1	5.1	6.2	4	24.8
6.1	1	6.1	6.3	1	6.3
	107 (19)	213.1	6.6	3	19.8
			7.1	1	7.1
				79	261.9

$\theta_{mr} = \frac{213.1}{107} = 2.0$ sec.

% inter drop coal. = 17.8

$\theta_{mr} = \frac{261.9}{79} = 3.3$ sec.

% drop-drop coal. = Not recorded

APPENDIX 7 (Continued)

Table 21. (Continued)

d_n = 1.2 mm
V_d = 0.160 ml.cm^{-2}sec^{-1}
H = monolayer

θ	n	nθ
0.8	1	0.8
1.0	1	1.0
1.2	3	3.6
1.3	1	1.3
1.5	7 (1)	10.5
1.6	6	9.6
1.7	7	11.9
1.8	11 (2)	19.8
1.9	11	20.9
2.0	9	18.0
2.1	8	16.8
2.2	1	2.2
2.3	1	2.3
2.5	1 (1)	2.5
2.7	3	2.7
2.9	1	2.9
3.2	3 (1)	9.6
3.3	1	3.3
3.6	1	3.6
3.8	1	3.8
4.0	1	4.0
4.2	1	4.2
4.3	3	12.9
4.7	2	9.4
4.8	1	4.8
5.2	2	10.4
5.3	1	5.3
5.6	1	5.6
5.7	1	5.7
	94 (5)	208.4

$\theta_{mr} = \frac{208.4}{94} = 2.22$ sec.

% drop-drop coal. = 5.4

d_n = 1.2 mm
V_d = 0.370 ml.cm^{-2}sec^{-1}
H = 2.0 cm

θ	n	θn
1.4	1	1.4
1.6	1	1.6
1.8	1	1.8
1.9	4	7.6
2.0	3	6.0
2.1	2	4.2
2.4	2	4.8
2.5	1 (1)	2.5
2.6	3	7.8
2.7	2	5.4
2.8	1	2.8
3.1	3	9.3
3.2	3 (1)	9.6
3.3	9 (2)	29.7
3.4	3	10.2
3.5	12	42.0
3.6	1	3.6
3.7	4 (1)	14.8
3.8	1 (1)	3.8
3.9	5	19.5
4.0	1	4.0
4.2	2	8.4
4.3	1	4.3
4.6	3	13.8
4.8	3	14.4
4.9	8	39.2
5.0	5	25.0
5.1	1	5.1
5.3	1	5.3
5.6	5	28.0
5.9	1	5.9
6.2	1	6.2
6.6	1	6.6
	95 (6)	354.6

$\theta_{mr} = \frac{354.6}{95} = 3.73$ sec.

% drop-drop coal. = 6.3

APPENDIX 7 (Continued)

Table 21. (Continued)

d_n = 1.2 mm
V_d = 0.47 ml.cm^{-2}sec^{-1}
H = 2.6 cm.

θ	n	nθ
1.9	1	1.9
2.3	1	2.3
2.5	3	7.5
2.6	1	2.6
2.7	1	2.7
2.8	3	8.1
3.0	2	6.0
3.2	1	3.2
3.3	1	3.3
3.5	1	3.5
3.8	3	11.4
3.9	1	3.9
4.1	2	8.2
4.3	6 (1)	25.8
4.4	2	8.8
4.5	2	9.0
4.6	2	9.2
4.7	4 (1)	18.8
4.8	5	24.0
4.9	1	4.9
5.0	3	15.0
5.1	11 (1)	56.1
5.2	5	26.0
5.3	6 (1)	31.8
5.4	1	5.4
5.5	2	11.0
5.6	1	5.6
5.7	4	22.8
5.8	1	5.8
5.9	3	17.7
6.0	2	12.0
6.1	1	6.1
6.2	8	49.6
6.4	1	6.4
6.6	2	13.2
6.7	1	6.7
6.9	1	6.9
7.3	2	14.6
7.6	1	7.6
	99 (4)	485.4

$\theta_{mr} = \frac{485.4}{99} = 4.9$ sec

d_n = 1.2 mm
V_d = 0.374 ml.cm^{-2}sec.$^{-1}$
H = 2.0 cm

θ	n	nθ
1.6	1	1.6
1.8	3	5.4
2.0	1	2.0
2.1	7	14.7
2.2	4	8.8
2.3	4	9.2
2.5	1	2.5
2.6	1	2.6
2.8	1 (1)	2.8
3.1	1	3.1
3.3	1	3.3
3.5	5 (1)	17.5
3.6	1	3.6
3.7	6	22.2
3.8	7	26.6
3.9	2	7.8
4.0	4	20.0
4.1	11 (2)	45.1
4.2	1	4.2
4.3	6	25.8
4.4	6	26.4
4.5	1	4.5
4.7	1	4.7
4.8	1	4.8
4.9	7 (1)	34.3
5.1	1	5.1
5.2	1	5.2
5.3	1	5.3
5.4	1	5.4
5.5	2 (1)	11.0
5.9	1	5.9
6.1	1	6.1
6.3	1	6.3
6.4	1	6.4
6.5	1	6.5
6.8	1	6.8
7.1	1	7.1
7.4	4	29.6
7.8	1	7.8
	103 (6)	397.5

$\theta_{mr} = \frac{397.5}{103} = 4.0$ sec

APPENDIX 7 (Continued)

Table 21. (Continued)

d_n = 0.8 mm	d_n = 0.8 mm
V_d = 0.335	V = 0.14
H = 1.9	H = monolayer

θ	n	nθ	θ	n	nθ
1.3	1	1.3	0.8	1	0.8
1.5	1	1.5	1.0	1	1.0
1.6	2	3.2	1.1	6 (1)	6.6
1.7	2	3.4	1.2	1	1.2
1.8	4	7.2	1.3	1	1.3
1.9	11 (1)	20.9	1.4	3	4.2
2.0	13 (2)	26.0	1.5	11 (1)	16.5
2.1	13 (2)	27.3	1.6	11 (1)	17.6
2.2	9 (1)	19.8	1.7	7	11.9
2.3	7	16.1	1.8	3	5.4
2.4	7 (1)	16.8	1.9	4	7.6
2.5	2	5.0	2.0	1	2.0
2.6	1	2.6	2.1	2	4.2
2.7	1	2.7	2.3	1	2.3
2.9	1	2.9	2.4	1 (1)	2.4
3.0	1	3.0	2.6	2	5.2
3.1	5	15.5	3.0	1	3.0
3.2	4 (1)	12.8	3.1	1	3.1
3.3	4	13.2	3.3	1	3.3
3.4	6 (1)	20.4	3.5	5 (1)	17.5
3.5	3	10.5	3.7	2	7.4
3.7	2	7.4	3.9	3	11.7
3.8	2	7.6	4.0	1	4.0
3.9	1	3.9	4.2	3	12.6
4.0	3	12.0	4.4	1	4.4
4.1	1	4.1	4.5	6 (2)	27.0
4.3	1 (1)	4.3	4.7	2	9.4
4.5	1	4.5	4.8	5 (1)	24.0
4.8	3	14.4	5.1	1	5.1
4.9	1	4.9	5.2	2	10.4
5.0	1	5.0	5.3	1	5.3
5.3	1	5.3	6.2	1	6.2
5.4	1	5.4		92 (8)	244.6
5.8	1	5.8			
6.4	1	6.4			
	118 (10)	323.1			

$\theta_{mr} = \frac{323.1}{118} = 3.24$ sec.

% drop-drop coal. = 8.4

$\theta_{mr} = \frac{244.6}{92} = 2.67$ sec.

% drop-drop coal. = 9%

APPENDIX 7 (Continued)

Table 21. (Continued)

d_n = 1.2 mm
V_d = 0.53 ml.$cm^{-2}sec^{-1}$
H = 2.8 cm

θ	n	nθ
1.3	1 (1)	1.3
1.6	1	1.6
1.7	1	1.7
2.1	1	2.1
2.2	3 (1)	6.6
2.3	2 (1)	4.6
2.4	5	12.0
2.5	6	15.0
2.6	1	2.6
2.7	1	2.7
2.8	1	2.8
2.9	2	5.8
3.0	4	12.0
3.1	2	6.2
3.2	1	3.2
3.3	1	3.3
3.4	1	3.4
3.5	4	14.0
3.6	1	3.6
3.7	5 (1)	18.5
3.9	4	15.6
4.0	12 (1)	48.0
4.1	10 (2)	41.0
4.2	6	25.2
4.3	2	8.6
4.4	2	8.8
4.5	4	18.0
4.6	1	4.6
4.7	2	9.4
4.8	1	4.8
4.9	1	4.9
5.0	2	10.0
5.2	2 (1)	10.4
5.4	3	16.2
5.6	1	5.6
6.9	1	6.9
6.4	2 (1)	12.8
6.6	1	6.6
6.9	1	6.9
7.5	1	7.5
7.8	1	7.8
	104 (9)	402.6

θ_{mr} = 3.87 sec

d_n = 1.2 mm
V_d = 0.705
H = 4.5 cm

θ	n	nθ
2.1	1	2.1
2.5	1	2.5
2.8	1 (1)	2.8
3.1	1	3.1
3.3	3 (1)	9.9
3.5	4	14.0
3.7	1	3.7
3.8	4 (1)	15.2
3.9	1	3.9
4.0	1	4.0
4.2	1	4.2
4.3	1	4.3
4.4	1	4.4
4.5	2	9.0
4.7	9 (3)	42.3
4.8	2	9.6
4.9	3	14.7
5.0	2	10.0
5.1	1	5.1
5.2	2	10.4
5.3	1	5.3
5.4	4	21.6
5.6	3 (1)	16.8
5.8	6	34.8
5.9	1	5.9
6.1	4	24.4
6.2	2	12.4
6.3	13 (2)	81.9
6.4	1	6.4
6.5	4 (1)	26.0
6.6	2	13.2
6.7	5 (2)	33.5
6.8	1	6.8
7.1	1	7.1
7.5	2 (1)	15.0
7.7	2	15.4
7.8	3	23.4
8.1	1	8.1
9.1	1	9.1
	98 (13)	542.3

$\theta_{mr} = \frac{542.3}{98}$ = 5.62 sec.

APPENDIX 7 (Continued)

Table 21. (Continued)

d_n = 1.6 mm V_d = 0.420 ml.cm^{-2}sec^{-1} H = 1.9 cm			d_n = 1.6 mm V_d = 0.18 ml.cm^{-2}sec^{-1} H = monolayer		
θ	n	nθ	θ	n	nθ
1.1	1	1.1	0.8	1	0.8
1.3	1	1.3	1.0	1	1.0
1.5	3	4.5	1.1	4	4.4
1.6	4	6.4	1.2	2	2.4
1.7	1	1.7	1.4	7 (1)	9.8
1.8	2	3.6	1.5	2	3.0
1.9	1 (1)	1.9	1.6	1	1.6
2.0	6	12.0	1.7	5 (1)	8.5
2.1	8	16.8	1.8	8	14.4
2.2	7	15.4	1.9	11	20.9
2.3	5	11.5	2.0	12	24.0
2.4	3	7.2	2.1	9	18.9
2.5	9 (2)	22.5	2.2	1	2.2
2.6	3	7.8	2.3	4	9.2
2.7	4	10.8	2.4	1	2.4
2.8	3	8.4	2.5	1 (1)	2.5
2.9	3	8.7	2.7	2	5.4
3.0	4	12.0	2.9	1	2.9
3.1	4	12.4	3.0	3	9.0
3.2	2	6.4	3.3	1	3.3
3.5	1	3.5	3.5	4 (1)	14.0
3.7	1	3.7	3.6	1	3.6
4.2	1	4.2	4.0	1	4.0
4.4	1	4.4	4.1	4	16.4
4.6	2	9.2	4.2	1	4.2
5.1	4	20.4	4.3	1	4.3
5.3	1	5.3	4.4	1 (1)	4.4
5.7	1	5.7	4.7	1	4.7
5.9	3 (1)	17.7	5.0	2	10.0
6.1	1	6.1	5.5	1	5.5
6.8	1	6.8	5.7	2	11.4
7.4	1	7.4	5.9	1	5.9
	92 (4)	266.8	6.3	4	25.2
			6.9	1	6.9
				102 (5)	267.1
$\theta_{mr} = \frac{266.8}{92} = 2.9$			θ_{mr} = 2.61 sec.		
% drop-drop coal. = 4.5			% drop-drop coal. = 4.9		

APPENDIX 7 (Continued)

Table 21. (Continued)

d_n = 2.0 mm
V_d = 0.55 ml.cm^{-2}sec^{-1}
H = 2.2 cm

θ	n	θn
1.1	2	2.2
1.2	3	3.6
1.3	1	1.3
1.5	6 (1)	9.0
1.6	4	6.4
1.7	1	1.7
1.8	1	1.8
1.9	1	1.9
2.0	1	2.0
2.1	1	2.1
2.2	1	2.2
2.3	1 (1)	2.3
2.4	7	16.8
2.5	7	17.5
2.6	8 (1)	20.8
2.7	7	18.9
2.8	6 (2)	16.8
2.9	3	7.7
3.0	1 (1)	3.0
3.2	3	9.6
3.4	1	3.4
3.5	5	17.5
3.8	3	11.4
4.1	1	4.1
4.4	1	4.4
4.5	1	4.5
4.7	1	4.7
5.4	1	5.4
5.7	5	5.7
6.2	1	6.2
6.6	1	6.6
	86 (6)	221.5

$\theta_{mr} = \frac{221.5}{86} = 2.58$ sec

% drop-drop coal. = 7

d_n = 2.0 mm
V_d = 0.21 ml.cm^{-2}sec^{-1}
H = monolayer

θ	n	nθ
0.9	1	0.9
1.0	1	1.0
1.1	6	6.6
1.2	7 (3)	8.4
1.3	1	1.3
1.4	2 (1)	2.8
1.5	2	3.0
1.6	7 (1)	11.2
1.7	4	6.8
1.8	6 (1)	10.8
1.9	12	22.8
2.0	12	24.0
2.1	13 (4)	27.3
2.2	3	6.6
2.3	2	4.6
2.4	2	4.8
2.5	1	2.5
2.6	5 (1)	13.0
2.7	3	8.1
2.8	1 (1)	2.8
2.9	1	2.9
3.0	1	3.0
3.3	1	3.3
3.6	2	7.2
4.0	2	8.0
4.3	1	4.3
4.6	1	4.6
4.9	1	4.9
5.5	2	11.0
	103 (12)	218.3

θ_{mr} = 2.13 sec

% drop-drop coal. = 12.2

APPENDIX 7 (Continued)

Table 21. (Continued)

d_n = 0.8 mm
V_d = 0.440 ml.cm^{-2}sec^{-1}
H = 3.5 cm

θ	n	nθ
2.9	1	2.9
3.4	3 (1)	10.2
3.6	1	3.6
3.8	1 (1)	3.8
4.3	1	4.3
4.4	1	4.4
4.5	2	9.0
4.6	6 (1)	27.6
4.7	4	18.8
4.8	2	9.6
4.9	1	4.9
5.0	4 (1)	20.0
5.3	2	10.6
5.4	1	5.4
5.5	1 (1)	5.5
5.9	1	5.9
6.2	1	6.2
6.4	1 (1)	6.4
6.5	4	26.0
6.7	2	13.4
7.0	1	7.0
7.2	2	14.4
7.4	3	22.2
7.6	2	15.2
7.7	4	30.8
7.8	8 (1)	62.4
7.9	7 (2)	55.3
8.0	2 (1)	16.0
8.1	3	24.3
8.3	3	24.9
8.4	1	8.4
8.5	1	8.5
8.7	1	8.7
8.8	1	8.8
8.9	1	8.9
9.2	1	9.2
9.3	1	9.3
9.5	2	19.0
9.6	1	9.6
	85 (10)	561.4

$\theta_{mr} = \frac{561.4}{85} = 6.73$ sec.

% drop-drop coal. = 11.7

d_n = 0.8 mm
V_d = 0.520 ml.cm^{-2}sec^{-1}
H = 4.7 cm

θ	n	nθ
3.7	1	3.7
4.0	1	4.0
4.2	1	4.2
4.4	2	8.8
4.6	5 (1)	23.0
4.7	2	9.4
4.8	2	9.6
4.9	1	4.9
5.0	3	15.0
5.1	1	5.1
5.3	1	5.3
5.5	1	5.5
5.6	3 (1)	16.8
5.8	1 (1)	5.8
5.9	1 (1)	5.9
6.0	1	6.0
6.2	4	24.8
6.3	3 (1)	18.9
6.4	6	38.4
6.5	3	19.5
6.6	4 (1)	26.4
6.7	3	20.1
6.8	6 (2)	40.8
6.9	3	20.7
7.0	3	21.0
7.1	3	21.3
7.2	3	21.6
7.3	4	29.2
7.5	7	52.5
7.6	4	30.4
7.9	3	23.7
8.0	1	8.0
8.1	1	8.1
8.2	1	8.2
8.8	2	17.6
9.4	4	37.6
	95 (8)	620.8

$\theta_{mr} = \frac{620.8}{95} = 6.5$ sec.

% drop-drop coal. = 8.4

APPENDIX 7 (Continued)

Table 21. (Continued)

d_n = 1.2 mm V_d = 0.860 ml.cm^{-2}sec^{-1} H = 6 cm			d_n = 1.6 mm V_d = 0.82 ml.cm^{-2}sec^{-1} H = 4.2 cm		
θ	n	nθ	θ	n	nθ
5.3	1	5.3	1.6	1	1.6
6.5	1	6.5	1.8	1	1.8
6.7	1	6.7	1.9	3	5.7
6.9	1	6.9	2.0	3	6.0
7.3	3	21.9	2.1	3	6.3
7.4	1	7.4	2.2	3	6.6
7.5	2	15.0	2.3	5	11.5
7.7	1	7.7	2.5	2	5.0
8.2	1	8.2	2.6	1	2.6
8.4	1	8.4	2.7	1	2.7
8.5	1	8.5	2.9	2	5.9
8.7	4 (1)	32.8	3.0	1	3.0
8.8	2	17.6	3.3	2	6.6
9.1	3	27.3	3.4	1	3.4
9.3	2	27.6	3.6	1	3.6
9.4	1 (1)	9.4	3.7	1	3.7
9.7	1	9.7	3.8	1	3.8
9.8	1	9.8	2.9	2	7.8
10.0	1	10.0	4.0	1	4.0
10.1	1	10.1	4.1	5	20.5
10.2	2	20.4	4.2	8	33.6
10.3	2	20.6	4.3	7	30.1
10.4	3	31.2	4.4	4	17.6
10.5	1	10.5	4.5	2	9.0
10.6	2	21.2	4.6	1	4.6
10.7	2	21.4	4.7	1	4.7
10.8	3 (1)	32.4	4.8	1	4.8
10.9	2	21.8	4.9	1	4.9
11.0	1	11.0	5.2	2	10.4
11.1	6 (1)	66.6	5.4	2	10.8
11.2	3	33.3	5.6	1	5.6
11.3	1	11.3	5.7	1	5.7
11.4	3	34.2	5.8	5	29.0
11.5	3	34.5	5.9	1	5.9
11.6	2	23.2	6.1	1	6.1
11.7	1	11.7	6.3	1	6.3
11.9	1	11.9	6.4	1	6.4
12.1	1	12.1	7.0	3	21.0
12.4	1	12.4	7.2	5	35.0
12.5	1	12.5	7.4	1	7.4
12.9	1	12.9	8.0	2	16.0
			8.3	1	8.3
			9.4	1	9.4
	72 (4)	723.9		92	403.6
θ_{mr} = 10.1 sec			θ_{mr} = 4.41 sec.		

APPENDIX 7 (Continued)

Table 21. (Continued)

d_n = 0.4 mm
V_d = 0.275 $ml.cm^{-2}sec^{-1}$
H = 3.5 cm

θ	n	nθ
5.4	1	5.4
6.1	1 (1)	6.1
6.6	1	6.6
6.8	3 (1)	20.4
7.2	1 (1)	7.2
7.4	2	14.8
7.6	5 (1)	38.0
7.8	1	7.8
8.1	2	16.2
8.3	3	24.9
8.4	4 (1)	33.6
8.5	4	34.0
8.6	1	8.6
8.7	1	8.7
8.9	1 (1)	8.9
9.0	1	9.0
9.1	3	27.3
9.3	4 (1)	37.2
9.4	9 (1)	84.6
9.5	7 (1)	66.5
9.6	1	9.6
9.7	2 (1)	19.4
9.9	2	19.8
10.0	5 (1)	50.0
10.2	2	20.4
10.4	1	10.4
10.6	1	10.6
10.8	2	21.6
11.2	1	11.2
11.3	2 (1)	22.6
11.5	3	34.5
11.7	5 (2)	58.5
12.0	4 (1)	48.0
12.1	1	12.1
12.4	1	12.4
12.6	1	12.6
12.8	1	12.8
	90 (15)	852.3

$\theta_{mr} = \frac{852.3}{90} = 9.47$

% drop-drop coal. = 16.7

d_n = 0.4
V_d = 0.230
H = 2.2

θ	n	nθ
1.5	1	1.5
1.8	1 (1)	1.8
2.1	4	8.4
2.6	1	2.6
2.7	1 (1)	2.7
2.8	1	2.8
3.0	9 (2)	27.0
3.1	1	3.1
3.2	3	9.6
3.4	5 (1)	17.0
3.5	1	3.5
3.8	3 (1)	11.4
3.9	1	3.9
4.1	1	4.1
4.3	3 (1)	12.9
4.6	2	9.2
4.8	8 (3)	38.4
4.9	2	9.6
5.0	2	10.0
5.1	12 (2)	61.2
5.2	8 (2)	41.6
5.3	1	5.3
5.5	1	5.5
5.6	3 (1)	16.8
5.7	1	5.7
5.8	1	5.8
6.3	2	12.6
6.4	1 (1)	6.4
6.8	3	20.4
7.1	1	7.1
8.2	1 (1)	8.2
9.1	1	9.1
	86 (17)	384.2

$\theta_{mr} = \frac{384.2}{86} = 4.5$ sec.

% drop-drop coal. = 19

APPENDIX 8

CALCULATION OF CORRELATION COEFFICIENT
MEASURED AND CALCULATED RESIDENCE TIMES

x	y			
θ_{mr}	θ_c	$\theta_{mr}\theta_c$	θ^2_{mr}	θ^2_c
4.5	7.5	33.73	20.25	56.25
9.8	6.1	59.80	96.04	37.21
3.2	4.4	14.08	10.24	19.36
6.7	6.2	41.51	44.89	38.44
6.5	6.9	44.90	42.25	47.61
3.7	4.2	15.50	13.69	17.64
5.8	4.1	23.80	33.64	16.81
4.9	4.3	21.06	24.01	18.49
3.9	4.1	15.96	15.21	16.81
5.6	4.9	27.40	31.36	24.01
10.1	5.4	54.50	102.00	29.16
2.9	3.5	10.15	8.41	12.25
3.3	3.9	12.88	10.89	15.21
4.4	3.9	17.12	19.36	15.21
2.6	3.1	8.06	6.76	9.61
77.9	72.5	400.45	478.98	374.07

$n\sum xy = 15 \times 400.45 = 600.68$

$x\sum y = 77.9 \times 72.5 = 5647.75$

$n\sum xy - \sum x \quad y = -5047.07$

$n\sum x^2 = 15 \times 478.98 = 718.47$

$(\sum x)^2 = (77.9)^2 = 6068.41$

$n\sum x^2 - (\sum x)^2 = -5249.94$

$n\sum y^2 = 15 \times 374.07 = 561.10$

$(\sum y)^2 = (72.5)^2 = 5256.25$

$n\sum y^2 - (\sum y)^2 = -4595.15$

Correlation Coefficient; $r = \dfrac{-5047.07}{\left[(-5249.94)(-4595.15)\right]^{0.5}}$

" " $= \dfrac{-5047.07}{4911.5} = -1.02$

$\therefore \quad r = -1.02$

APPENDIX 9

Table 22. Variation of drop size in the zone

Isooctane - water system.

6 inch column

Distance from entry h	Mean drop size, d_h, cm at d_n = 0.4		d_n = 1.2		d_n = 2.0 mm	
cm	d_h	d_h/d_{12}	d_h	d_h/d_{12}	d_h	d_h/d_{12}
0	0.08	1	0.28	1	0.43	1
0.5	0.08	1	-		-	
1.0	0.09	1.12	0.30	1.08	-	
2.0	0.10	1.25	0.32	1.14	0.43	1
2.5	0.11	1.37	-	1.22	-	
3.0	-		0.34	1.18	-	
4.0	0.11	1.37	0.32	1.14	0.43	1
4.5	0.11	1.37	-		-	
5.0	-		0.33	1.18	-	
6.0	0.13	1.62	0.35	1.25	0.43	1
8.0	0.13	1.62	0.38	1.36	*	
9.0	-		0.40	1.43		
10.0	0.16	2.00	0.40	1.43		
11.0	-		0.42	1.50		
12.0	2.0	2.50	0.43	1.54		
13.0	-		0.44	1.57		
14.0	-		0.40	1.43		
15.3	2.2	2.74	0.45	1.61		
16.0			0.45	1.61		
17.0			0.50	1.79		
18.0	2.7	3.38	0.52	1.86		
19.0	*		0.56	2.00		
20.0			*			

* Coalescing interface level

APPENDIX 10.

Table 23. Variation of flocculation zone height with Laplace diameter at $V_d = 0.3$

$\frac{d^2 g \Delta \rho}{\sigma}$	Zone height, H, cm. Toluene	Isooctane	Diethyl carbonate	M.I.Bk
0.038	3.2			
0.150	2.1			
0.340	1.6			
0.600	1.2			
0.050		16.0		
0.230		3.3		
0.530		1.2		
0.020			46.0	
0.084			16.0	
0.034			3.8	
0.180				8.2
0.760				7.0
1.800				5.6
3.00				5.0

NOMENCLATURE

Symbols have the following meanings except where specifically indicated in the text.

Symbols

a, a_o, b, c, e	=	a constant in the correlation equations of this work
c_1, c_2, c_3	=	vertical hold-up profile equations constants
D	=	column inside diamater, cm.
D_e	=	equivalent cross sectional diameter of conduit model (Section 9)
d	=	drop diameter
d_{12}	=	mean drop diameter
d_{32}	=	mean volume - surface drop diameter
d_n	=	orifice hole diameter on the distributor plates
g	=	acceletation due to gravity
H	=	total flocculation zone height
h	=	distance in the flocculation zone from the droplet entry
K	=	a constant derived from the flocculation zone hold-up vertical profile equations as in Equation 9.11

m_1, m_{2D}, m_3,	=	droplet entry, mid-section and interface zone linear relationship slopes respectively
t	=	coalescence time , sec.
$t_{1/2}$	=	half-life coalescence time, sec.
t_m	=	mean coalescence time , sec.
u	=	drop point velocity in the zone cm. sec^{-1}
V_n	=	linear velocity in the orifice holes and nozzles , cm $sec.^{-1}$
V_d	=	dispersed phase superficial velocity in the column, ml. cm^{-2} sec^{-1}
V_v	=	volumetric flow rate in the column, lit. min^{-1}
x	=	fractional bed height, h/H
v_d	=	drop volume
$\Delta\rho$	=	phases density difference $gm/_{cm^3}$
σ	=	interfacial tension, dyne cm^{-1}
μ	=	phase viscosities , poise
ϕ	=	fractional dispersed phase hold-up

Subscripts

c	=	continuous phase
d	=	dispersed phase

REFERENCES

1. JEFFREYS, G.V., and DAVIES, G.A., "Recent Advances in Liquid-liquid Extraction" Edited by Hanson, C., Pergaman Press, Oxford, N.Y. etc., (1971)

2. BIKERMAN, J.J., "Surface Chemistry", 2nd Edition, Academic Press, Inc., N.Y. (1958).

3. KINTNER, R.C., Advances in Chem.Eng., Vol.4, Drew, T.B., Hooper, J.W. Jr., and Vermeulen, T., Academic Press, (1963).

4. GAL-OR, B., KLINZING, G.E., TAVLARIDES, L.L., Ind. and Eng. Chem., V. 61, No.2, p.2, (1969).

5. SMITH, D.V., and DAVIES, G.A., The Canad. J. Chem.Eng., V.48, p.628 (1970).

6. WEBSTER, A.M., "Webster's Elementary Dictionary", American Book Co., N.Y., (1941).

7. GILLESPIE, T., and RIDEAL, E.K., Trans. Faraday Soc., 52, p.173, (1956).

8. CHARLES, G.E., and MASON, S.G., J. Colloid Sci., 15, p.236 (1960).

REFERENCES (continued)

9. CHAPPELEAR, D.C., J. Colloid. Sci., 16, p.186 (1961)

10. FRANKEL, S.P. and MYSELS, K.S., J. Phys. Chem., 66 p.190, (1962).

11. ELTON, G.A. and PICKNETT, R.G., Proceedings of the 2nd International Congress on Surface Activity Vol.1, p.288, p.307, Butterworths, London, (1957)

12. PRINCEN, H.M., J. Colloid Sci., 18, p.178, (1963)

13. JEFFREYS, G.V., and HAWKSLEY, J.L., A.I. Ch. E.J., 11, p.413, (1965)

14. HARTLAND, S., Chem. Eng. Sci., 22, p.1675, (1967)

15. REYNOLDS, O., Chem. News, 44, p.211, (1881)

16. MAHAJAN, L.D., Phil. Mag., 10, p.283,(1930)

17. LAWSON, G.B., Chem. and Proc. Eng., V.48, No.5, p.45, (1967)

18. BROWN, A.H., and HANSON, C., British Chem. Eng., 11, No.7, p.695, (1966)

19. LAWSON, G.B., Ph.D. Thesis, University of Manchester, (1967)

20. DAVIES, G.A., JEFFREYS, G.V., and SMITH, D.V., I.S.E.C., Hague, (1971)

21. LANG, S.B. and WILKE, C.R., Ind. Eng. Chem. Fundam., V.10, No.3, p.329, (1971)

22. COCKBAIN, E.G. and McROBERTS, T.S., J. Colloid Sci., 8, p.440, (1953)

23. HODGSON, T.D., and LEE, J.C., J. Colloid Interface Sci., 30, 94 (1969)

24. HODGSON, T.D., and WOODS, D.R. J. Colloid Interface Sci., 30, 429, (1969)

25. WATANABE, T., and KUSUI, M., Bull. Chem. Soc. Japan, 31, p.236, (1958)

26. JEFFREYS, G.V., and LAWSON, G.B., Trans. Instn. Chem. Engrs., V.43, T.294, (1965)

27. NEILSEN, L.E., WALL, R., and ADAMS, G., J. Colloid Sci., 13, p.441, (1958)

28. MacCAY, G.D.M., and MASON, S.G., J. Colloid Sci., 18, p.674, (1963)

29. MIZRAHI, J., and BARNEA, E., British Chem. Eng., V.15, 4, p.497, (1970)

30. REHBINDER, P.A., and WENSTROM, E.K., Kolloid - Z., 53, 145, (1930)

31. JEFFREYS, G.V., and HAWKSLEY, J.L., J. Applied Chem., 12, p.329, (1962)

32. KONNECKI, H.G., Z. Phys. Chem., 211, p.208, (1959)

33. SHEDULKO, A., Z. Electrochem., 61, p.222, (1957)

34. CHARLES, G.E., and MASON, S.G., J. Colloid Sci., V.15, p.105, (1960)

35. WARK, J.W., and COX, A.B., Nature, 136, p.182, (1935)

36. LINTON, M. and SUTHERLAND, K.L., J. Colloid Sci., 11, p.391, (1956)

37. BROWN, A.H., and HANSON, C., Trans. Farad. Soc., 61, p.1754, (1965)

38. JACKSON, R., The Chem. Eng., May 1964, C.E. 107

39. DAVIES, G.A., JEFFREYS, G.V. and ALI, F.A., Can. J. Chem. Eng., V.48, p.328, (1970)

40. ALLAN, R.S. and MASON, S.G., Trans. Farad. Soc., 57, p.2027, (1961)

41. SMITH, D.V., Ph. D. Thesis, University of Manchester, (1969)

42. HARTLAND, S., Can. J. Chem. Eng., 47, p.221, (1969)

43. HARTLAND, S., J. Colloid Sci., 26, p.383, (1968)

44. LANG, S.B., PhD. Thesis, University of California, (1962)

45. LANG, S.B., WILKE, C.R., Ind. Eng. Chem., Fund. 10, 329, (1971)

46. HARTLAND, S., Trans. Instn. Chem. Engrs., 45, T.102, (1967)

47. HARTLAND, S., Trans. Instn. Chem. Engrs., 45, T.109, (1962)

48. ROBINSON,D., and HARTLAND, S., The Chem. Eng. J., v.1, p. 22, (1970).

49. HERSHEY, A.V., Physic. Rev., 56, p.204, (1939)

50. GROOTHIUS, H., ZWIDERWEG, F.J., Chem. Eng. Sci., 12, p.288, (1960)

51. SAWITOWSKI, H., "Recent Advances in Liquid- Liquid Extraction", edited by Hanson, C., Pergamon Press, Oxford, (1971)

52. LONGSDAIL, D.H., THORNTON, J.D., PRATT, H.R.C., Trans. Inst. Chem. Eng., 35, p.301, (1957)

53. SMITH, A.R., CASWELL, J.E., LARSON, P.P. and CAVERS, S.D., Can. J. Chem. Eng., 41, 150, (1963)

54. HEERTJES, P.M. and de NIE, L.H., I.S.E.C. Hague, paper No.128, (1971)

55. STERMLING, C.V. and SCRIVEN, L.E., A.I. Ch. E.J., 5, p.514, (1959)

56. HARTLAND, S., Trans. Instn. Chem. Engs., V.46, p. T.275, (1968).

57. KATALINIC, M., Nature, 136, p.916, (1935)

58. KOMASAWA, I., and OTAKE, T., J. Chem. Eng. Japan, V.3, No.2, (1970).

59. SMITH, D.V., M.Sc. Thesis, Univ. of Manchester, (1966)

60. HARTLAND, S., Trans. I. Chem. Eng., 1967, 45, p. T.97, (1967)

61. BASHFORTH, F. and ADAMS, J.C., An Attempt to test the Theories of Capillary Action, Cambridge Univ. Press, (1883). Cited in reference 1.

62. HARTLAND, S., Chem. Eng. J., 1, p.67, (1970)

63. ALLEN, R.S., CHARLES, G.E. and MASON, S.G., J. Colloid Sci., 16, p.150, (1961)

64. Van den TEMPEL, Rec. Trav. Chim., 72, p.419, (1953)

65. DERJAGUIN, B.V. and KUSSAKOV, Acta Physio. Chim., (1939), 10, p.25. Cited in Reference (1).

66. STEFAN, J., Cited in Reference (8).

67. REYNOLDS, O., Cited in Reference (8)

68. GUNN, R., Science, 150, p.695, (1965)

69. PARK. R.W., and CROSBY, E.J., Chem. Eng. Sci., 20, p.39, (1965)

70. SCHEELE, G.F. and LENG, D.E., Chem. Eng. Sci., 26, p.1867, (1971)

71. SCHROEDER, R.R., and KINTNER, R.C., A.I. Ch. E.J., 11, p.5, (1965)

72. ROBINSON, J., and HARTLAND, S., I.S.E.C., Paper no.56, (1971)

73. MATEJICEK, A., SIVOKOVA, M. and EICHLER, J., Collection Czechoslav. Chem. Commun., V.36, p.35, (1971)

74. McAVOY, R.M. and KINTNER, R.C., J. Colloid Sci., 20, p.188, (1965)

75. MURDOCH, P.G. and LENG, D.E., Chem. Eng. Sci., 26, p.1881, (1971)

76. TOPLISS, J.A., 1st Ch. Eng. Dept. Research Symposium, May, (1970)

77. RYAN, A.D., DALEY, F.L. and LOWRIE, R.S., Chem. Eng. Prog., 55, p.70, (1959)

78. LEE, J.C. and LEWIS, G., Inst. of Chem. Eng. Symposium on Liquid Extraction, Newcastle, (1967)

79. JEFFREYS, G.V., DAVIES, G.A. and PITT, K., Inst. Chem. Eng. Symposium, Newcastle, (1967)

80. JEFFREYS, G.V., DAVIES, G.A. and PITT, K., A.I. Ch. E.J., V.16, No.5, pp. 823-831, (1970)

81. ALLAK, A., JEFFREYS, G.V. and DAVIES, G.A., Paper to be presented in 4th CHISA Congress, Czechoslovakia, (1972)

82. MEISSNER, H.P. and CHERTOW, B., Ind. Eng. Chem., 38, p.856, (1946)

83. RICHARDSON, J.F. and ZAKI, W.N., Trans. Instn. Chem. Engrs., V.32, p.35, (1954)

84. RIDGWAY, K., and TARBUCK, K.J., British Chem. Eng., 12, p.137, (1967)

85. HAUGHEY, D.P. and BEVERIDGE, G.S.G., Chem. Eng. Sci., 22, p.715, (1967)

86. HAUGHEY, D.P. and BEVERIDGE, G.S.G., Chem. Eng. Sci., 21, p.905, (1966)

87. MEISTER, B.J., and SCHEELE, G.F., A.I. Ch. E.J., 15, p.689, (1969)

88. TREYBAL, R.E., "Liquid-Extraction", 2. Ed. McGraw Hill, N.Y., (1963)

89. MUMFORD, C.J., British Chem. Eng., 13, No.7, p.337, (1968)

90. DAVIS, M.W., HICKS, T.E. and VERMEULEN, T., Chem. Eng. Prog., 50, 4, p.188, (1954)

91. L.M.T.S., Lurgi Gasellschaft, Frankfurt am Main

92. I.M.I. Institute for Research and Development, Israel, U.S. Patent 3489526

93. HANSON, C., and KAYE, D.A., Brit. Pat. Appl. 44707/63

94. LUGSDAIL, D.H., and LOWES, L., Recent Advances in Liquid - Liquid Extraction, Ed. C. Hanson, Pergamon (1971), 146

95. MAREK, J. and MISEK, T., Soc. of Chem. Ind., Conference on Solvent Extraction, London, 27th March, (1969)

96. MISEK, T., Coll. Czech., Chem. Comm. 28, p.426, (1963)

97. MUMFORD, C.J., Ph.D. Thesis, Univ. of Aston in Birmingham, (1970)

98. AL-HEMIRI, A.A.A., Univ. of Aston in Birmingham, unpublished work, (1972)

99. JEFFREYS, G.V. and MUMFORD, C.J., 3rd Chisa Congress, Marianska Lazne, September, (1969)

100. DAVIES, J.T., RICHIE, J.M. and SOUTHWOOD, D.C., Trans. Instn. Chem. Engs., 38, p.331, (1960)

101. ARNOLD, D.R., unpublished work, University of Aston in Birmingham, (1972)

102. THOMAS, R.J. and MUMFORD, C.J., I.S.E.C., Hague, Paper No.50, (1971)

103. GODSMARK, J.S., EVANS, R.J. and CURTICE, R., Final year projects Ch. E. Dept., University of Aston in Birmingham, (1969)

104. MORGAN, P.W., "Condensation Polymers by Interfacial and Solution Methods", Interscience Publishers, N.Y., London, (1965)

105. McCOY, B.J., and MADDEN, A.J., Chem. Eng. Sci., V.24, p.416, (1969)

106. RASNICK, W., Paper presented at 3rd Chisa Congress, September, (1969)

107. Van HEUVEN, J.W. and BEEK, W.J., I.S.E.C., Hague, Paper No.51, (1971)

108. SCOTT, G., Chemistry Dept., University of Aston in Birmingham, Private Communication, (1970)

109. BEVINGTON, J.C., "Radical Polymerization", Academic Press, London, N.Y., (1961)

110. STEINOUR, H.H., Ind. Eng. Chem., V.36, No.7, p.618, (1944)

111. GONDO, S. and KUSUNOKI, K., Hydrocarbon Processing, September, p.209, (1969)

112. KINTNER, R.C., I.S.E.C. Hague, Session 3A, Chairman Comments, (1971)